The genetic dissection of mycobacterial infection

Tania Di Pietrantonio

Department of Human Genetics
McGill University, Montreal

Submitted August 2010

A thesis submitted to McGill University in partial fulfilment of the requirements of the degree of Doctor of Philosophy

ABSTRACT

The host response to mycobacterial infection is highly variable. A role for host and bacterial factors in this variability is well established, although it is not known whether these factors act independently of each other or whether infection outcome results from a joint effect of host and pathogen. To address this question, the present thesis concurrently examined the effect of genetically controlled host and bacterial factors using a mouse model of infection. A panel of recombinant congenic (RC) mouse strains and their A/J and C57BL/6J inbred progenitors were infected with virulent *Mycobacterium tuberculosis* or the attenuated *M. bovis* Bacille Calmette Guérin (BCG) Russia and Pasteur strains. A joint effect of host and pathogen on the course of mycobacterial infection was observed at both the phenotypic and genetic level. In the A/J and C57BL/6J mouse strains, pathogen-associated factors had a major impact on biological phenotypes (pulmonary replication, lung histopathology) as well as mechanistic phenotypes (pulmonary transcription of *Ifng*, *Il12b*, *Il4* and chemokine genes) with the host genetic background modulating the magnitude of these responses. At the genetic level, a comparative analysis of the pulmonary and splenic counts of BCG Russia and BCG Pasteur in the RC strains revealed that mycobacterial infection is under the control of both generic and strain-specific genetic effects. A locus on chromosome 1 indistinguishable from *Nramp1* controlled early BCG Pasteur and early and late BCG Russia infection in a spleen-specific manner. Loci impacting on the counts of BCG Russia but not BCG Pasteur were identified on chromosome 13 for the spleen and on chromosome 11 for the lung and spleen at the late phase of infection. *M. tuberculosis* infection was also under distinct genetic control in the RC strains, further demonstrating that genetic control of mycobacterial infection is adapted to the infecting mycobacterial strain. A strong genetic effect detected on chromosome 10 was linked with early death following *M. tuberculosis* infection. Analysis conditional on this locus identified a set of genetic control elements on chromosomes 2, 4, and 13. Together, these studies provide compelling evidence for strong specificity of the host response to the infecting pathogen.

RÉSUMÉ

La réponse de l'hôte aux infections par des mycobactéries est hautement variable. Des facteurs de l'hôte et de la bactérie ont un rôle à jouer dans cette variabilité bien qu'on ne sache pas si ces facteurs agissent indépendamment ou si le résultat de l'infection découle d'un effet combiné de l'hôte et du pathogène. Pour répondre à cette question, la présente thèse a évalué l'impact de facteurs de l'hôte et du pathogène sous contrôle génétique à l'aide d'un modèle murin d'infection. Un panel de souches de souris congéniques recombinantes (CR) et leurs progéniteurs consanguins A/J et C57BL/6J furent infectés avec du *Mycobacterium tuberculosis* virulent ou les souches atténuées *M. bovis* Bacille Calmette Guérin (BCG) Russie et Pasteur. Un effet combiné de l'hôte et du pathogène sur le déroulement de l'infection mycobactérienne fut observé autant aux niveaux phénotypiques que génétiques. Chez les souches A/J et C57BL/6J, des facteurs associés au pathogène ont eu un impact majeur sur les phénotypes biologiques (réplication au niveau du poumon, histopathologie pulmonaire) de même que sur les phénotypes mécanistes (transcription de *Ifng*, *Il12b*, *Il4* et de gènes de chimiokines dans le poumon), alors que le fond génétique modulait la magnitude de ces réponses. Au niveau génétique, une analyse comparative des comptes pulmonaires et spléniques de BCG Russie et BCG Pasteur chez les souches CR a révélé que l'infection par des mycobactéries est sous le contrôle d'effets génétiques génériques de même que spécifiques à la souche. Dans la rate, un locus sur le chromosome 1 qui ne pouvait être discriminé de *Nramp1* a contrôlé l'infection précoce par BCG Pasteur et l'infection précoce et tardive par BCG Russie. Dans la phase tardive d'infection, des locus influençant les comptes de BCG Russie mais non de BCG Pasteur ont été identifiés sur le chromosome 13 pour la rate et sur le chromosome 11 pour la rate et le poumon. L'infection par *M. tuberculosis* était également sous contrôle génétique distinct chez les souches CR, ce qui démontre à nouveau que le contrôle génétique d'infections mycobactériennes est adapté à la souche de mycobactérie qui infecte. Un important effet génétique détecté sur le chromosome 10 fut lié à une mortalité précoce suite à une infection par *M. tuberculosis*. Une analyse conditionnelle à ce locus a identifié un ensemble

d'éléments de contrôle génétique sur les chromosomes 2, 4 et 13. Globalement, ces études relèvent la forte spécificité de la réponse de l'hôte au pathogène qui infecte.

PREFACE

The work described in Chapter 3 of this thesis has been published as follows:

Di Pietrantonio, T.; Hernandez, C.; Girard, M.; Verville, A.; Orlova, M.; Belley, A.; Behr, M.A.; Loredo-Osti, JC.; and Schurr E. Strain-specific differences in the genetic control of two closely related mycobacteria. PLoS Pathog 2010; 6:e1001169.

At the time of thesis submission, Chapter 2 was submitted for review.

Related manuscripts for which I made a valued contribution but that are not included as part of this thesis, have been published as follows:

Gallant, C.; **Di Pietrantonio, T.**; and Schurr, E. Genetics of susceptibility to tuberculosis. In: Tuberculosis. Sharma S.K. and Mohan (eds). Jaypee Brothers Medical Publishers Ltd. 2009.

Di Pietrantonio, T. and Schurr, E. Mouse models for the genetic study of tuberculosis susceptibility. Brief Funct Genomic Proteomic. 2005; 4:277-92.

Belley, A.; Alexander, D.; **Di Pietrantonio, T.**; Girard, M.; Jones, J.; Schurr, E.; Liu, J.; Sherman, D.R.; and Behr, M.A. Impact of methoxymycolic acid production by Mycobacterium bovis BCG vaccines. Infect Immun. 2004; 72: 2803-9.

Di Pietrantonio, T.; Gallant, C.; and Schurr, E. Host Genetics of Tuberculosis Susceptibility. MJM. 2003; 7:113-122.

Mira, M.T.; Alcais, A.; **Di Pietrantonio, T.**; Thuc, N.V.; Phuong, M.C.; Abel, L.; and Schurr E. Segregation of HLA/TNF region is linked to leprosy clinical spectrum in families displaying mixed leprosy subtypes. Genes Immun. 2003; 4:67-73.

CONTRIBUTION OF AUTHORS

Chapter 2: All experiments described in this chapter were planned and performed by me. Dr. Marianna Orlova helped with organ harvesting for the RNA extraction. Dr. Jose Correa contributed to the two-way ANOVA analysis and provided helpful suggestions for the manuscript. Dr. Marcel Behr participated in interpretation of results and provided a critical reading of the final version of the manuscript. Dr. Erwin Schurr designed the study and supervised the execution of the experiments. Dr. Jose Correa, Dr. Erwin Schurr, and I participated in the writing of the manuscript.

Chapter 3: Manon Girard, Annie Verville and I phenotyped all mice for the lung and spleen bacillary load. Dr. Marianna Orlova provided additional help when required. Carmen Hernandez and Dr. J C. Loredo-Osti developed the statistical models and contributed to the data analysis. Dr. Adam Belley provided the recombinant BCG Russia and BCG Pasteur bacteria. Dr. Marcel Behr performed a critical reading of the manuscript. Dr. Erwin Schurr designed the study and supervised the execution of the experiments. Dr. J C. Loredo-Osti, Dr. Erwin Schurr, and I participated in the writing of the manuscript.

Chapter 4: All experiments included in this chapter were planned and performed by me. Carmen Hernandez and Dr. J C. Loredo-Osti contributed to the data analysis. Dr. Erwin Schurr designed the study and supervised the execution of the experiments. Dr. J C. Loredo-Osti, Dr. Erwin Schurr and I and participated in the writing of the manuscript.

TABLE OF CONTENTS

LIST OF FIGURES

Chapter 1

Chapter 2

Chapter 3

Chapter 4

LIST OF TABLES

Chapter 1

Chapter 2

Chapter 3

ABBREVIATIONS

AcB	Recombinant congenic mouse strain containing C57BL/6J-derived chromosomal segments on an A/J genetic background
Adam17	a disintegrin and metallopeptidase domain 17
ALOX5	5-lipoxygenase
ANOVA	Analysis of Variance
ATPase	adenosine triphosphatase
BcA	Recombinant congenic mouse strain containing A/J-derived chromosomal segments on a C57BL/6J genetic background
BCG	Bacille Calmette Guérin
CCL	chemokine (C-C motif) ligand
CCR	chemokine (C-C motif) receptor
CFP-10	culture filtrate protein 10-kDa
CFU	colony forming units
CI	confidence intervals
CX3CL1	chemokine (C-X3-C motif) ligand 1
CX3CR1	chemokine (C-X3-C motif) receptor 1
CXCL	chemokine (C-X-C motif) ligand
CXCR	chemokine (C-X-C motif) receptor
DU	duplication
ESAT-6	early secreted antigenic target 6-kDa
GWA	genome-wide-association
GWL	genome-wide-linkage
Hsmtb1	hypersusceptibility to mycobacterium tuberculosis 1
Icsbp	interferon consensus sequence-binding protein 1
Ifi75	interferon-gamma-induced protein 75
IFN‑g (*Ifng*)	interferon-gamma
IFN‑gR	interferon-gamma receptor
Igh	immunoglobulin heavy chain
IL-12 (*Il12*)	interleukin-12
IL-4 (*Il4*)	interleukin-4
IL-4Rα	interleukin-4 receptor α
iNOS (*Nos2*)	inducible nitric oxide synthetase
Ipr1	intracellular pathogen resistance 1
IRF-8 (*Irf8*)	interferon regulatory factor 8
IRGM	immunity-related guanosine triphosphatase M
LSM	least square mean
LOD	logarithm of odds
LRG-47	interferon inducible protein
LSP	large sequence polymorphism
LXA_4	lipoxin A_4
Map2k2	mitogen-activated protein kinase kinase 2

Mmp11	matrix metallopeptidase 11
MST	median survival time
MHC	major histocompatibility complex
MTC	*M. tuberculosis complex*
Mknk2	MAP kinase-interacting serine/threonine kinase 2
Nramp1 (*Nramp1*)	natural resistance-associated macrophage protein 1
PGE_2	prostaglandin E_2
PGL-tb	phenolic glycolipid
Pip5k1c	phosphatidylinositol-4-phosphate 5-kinase, type 1 gamma
Pklr	pyruvate kinase
pks1-15	polyketide synthase
PMN	polymorphonuclear
QTL	quantitative trait locus
RC	recombinant congenic
RCS	recombinant congenic strain
RD	region of difference
RR	relative risk
SDP	strain distribution pattern
sigK	sigma factor K
Slc	solute carrier
SNP	single nucleotide polymorphism
sst1	susceptibility to tuberculosis 1
STAT-1	signal transducer and activator of transcription 1
STAT-6 (*Stat6*)	signal transducer and activator of transcription 6
Stk11	serine/threonine kinase 11
Smtb1	susceptibility to mycobacterium tuberculosis 1
Tace	TNF-α-converting enzyme
tbs	tuberculosis severity
TCR	T cell receptor
Th1	T helper 1
Th2	T helper 2
Timp3	tissue inhibitor of metalloproteinase 3
TLR	toll-like receptor
TM	transmembrane
TNFRI	tumor necrosis factor α type I receptor
TNFRII	tumor necrosis factor α type II receptor
TNF-α (*Tnfa*)	tumor necrosis factor α
Trl	tuberculosis resistance locus

ACKNOWLEDGMENTS

First and foremost, I would like to thank my supervisor, Erwin Schurr, for his guidance, encouragement, and patience. I will always be grateful for his support and mentorship.

I am especially thankful for the statistical input and help provided by Dr. J C. Loredo-Osti and Carmen Hernandez. Much of this work would not have been possible without them. Special thanks must also be given to Dr. Jose Correa for his help with the statistical analysis. I would also like to thank Dr. Kenneth Morgan and Mary Fujiwara for their invaluable advice.

I am thankful to Dr. Marcel Behr for providing scientific insight throughout my PhD studies. I also thank Dr. Pilar Domenech for help with the experimental design of *M tuberculosis* infection; Fiona McIntosh and Vlad Kamenski for their technical assistance; Dr. Michael Reed for his scientific input, and all members of the Behr and Reed labs for their helpful advice and discussions.

I also thank my advisory committee members, Drs. Danielle Malo and Danuta Radzioch, for their helpful suggestions.

I would like to thank the past and present members of the Schurr lab-Andrea, Annie, Audrey, Caroline, Charlie, Elsa, Leah, Louis, Manon, Marianna, and Marcelo-with whom I have fostered many great friendships. Special thanks must also be given to Annie, Manon, and Marianna for all the help they have provided throughout the years.

I am grateful to my friends-Athena, Arthur, George, Jerome, Milly, Paris, Sandra and Vanessa-for their valued friendships and support throughout the years.

Most importantly, I would like to thank my mom, dad and sister, Mary. I would not have made it this far without their love and encouragement.

OBJECTIVES AND RATIONALE

The factors controlling the development of mycobacterial disease are complex. While it is generally accepted that *Mycobacterium* spp. and host genetic factors interact to define the outcome of infection, studies rarely take into account the combined effect of both host and pathogen. Most comparative studies of mycobacterial immunity and pathogenesis focus on changes on the course of infection depending on either host or pathogen only and rarely take into account joint effects of both organisms. In mouse genetic studies for example, a large number of backcross or F2 animals are usually infected with one strain of *M. tuberculosis* and host genetic factors that control the infection are mapped. Likewise, in pathogen-centered studies, one set of inbred mice is infected with a panel of mycobacterial strains and differences in virulence are assessed. These studies have greatly increased our insight into mycobacterial pathogenesis and the genetic basis of tuberculosis susceptibility. Yet, these studies do not address to what extent the discovered characteristics are representative of host-pathogen interactions in a situation where a large number of genetically diverse hosts are exposed to varied strains of *M. tuberculosis*. This highlights the fundamental biological question to what extent host responsiveness following exposure to an infectious agent is dependent on the genetic background of the host and the genetic background of the infectious agent. To address this question, the present thesis concurrently examined the effect of genetically determined host and bacterial factors using a mouse model of infection. This study used three mycobacterial strains of varying virulence together with a panel of recombinant congenic mouse strains or their progenitors to model the natural variation across *M. tuberculosis* isolates and human populations. The underlying hypothesis was that closely related mycobacteria experience general and specific aspects of host responsiveness which are decisive for the overall outcome of infection.

The following specific aims were pursued:

(1) To investigate the joint impact of host and mycobacterial genome variability in two inbred mouse strains, A/J and C57BL/6J, infected with *M. tuberculosis* H37Rv or the Russia and Pasteur strains of *M. bovis* Bacille Calmette Guérin (BCG).

(2) To identify aspects of pathogenesis that are characteristic of a specific host and pathogen combination by comparing the host genetic control of different strains of *M. bovis* BCG in a recombinant congenic mouse model

(3) To dissect the host genetic control of a fully virulent strain of *M. tuberculosis*

CHAPTER 1
Introduction and Literature Review

Tuberculosis is a major global health concern. Statistics by the World Health Organization estimate that over 2 billion individuals are latently infected with *Mycobacterium tuberculosis*, the causative agent of tuberculosis. In 2008, there were an estimated 11.1 million prevalent cases and 1.8 million people died of the disease [1]. Of the 9.4 million incident cases reported that year, the majority occurred in Asia (55%) and Africa (30%), with India, China, South Africa, Nigeria and Indonesia having the largest numbers of new cases [1]. The threat of tuberculosis persists despite multidrug therapy, the existence of global tuberculosis control programmes, and the established use of the *M. bovis* Bacille Calmette Guérin (BCG) vaccine. While effective at preventing tuberculosis in young children [2,3], the efficacy of BCG against adult tuberculosis is variable, ranging from 80% to no protection from clinical disease [4]. Variable efficacy with BCG results from a combination of host genetic, demographic, and environmental factors as well as the existence of different strains of BCG [5].

M. tuberculosis is transmitted by the respiratory route. The bacilli are ingested by macrophages in the lung where they are either killed or replicate to a limited extent [6]. This triggers the release of pro-inflammatory cytokines. Infected dendritic cells migrate to the peripheral lymph nodes where they sensitize $CD4^+$ and $CD8^+$ T-cells to initiate an acquired immune response [7,8]. Primed T-cells migrate back to the lung where they initiate granuloma formation via the secretion of tumor necrosis factor α (TNF-α) and gamma-interferon (IFN-γ) [9]. Cell-mediated immunity develops within 2 to 6 weeks and generally helps to contain the infection. In approximately 5% of cases, the cellular immune response is not effective and primary infection progresses to active disease. Of the 95% who contain the primary infection, an additional 5% will develop reactivation tuberculosis within the course of their lifetime. Infrequently, the pathogen disseminates and forms small miliary lesions or life-threatening meningitis as seen predominantly in children and immune-compromised individuals [10-12]. In most immune-competent adult patients, tuberculosis manifests as a pulmonary

disease. Cavitary lesions develop in the lung and the patient becomes infectious, spreading disease by speaking, coughing and sneezing (Figure 1) [13].

Progression from latent infection to clinical disease in a subset of infected persons involves a combination of host, bacterial and environmental factors. Several lines of evidence support the importance of host genetic factors in tuberculosis susceptibility. These include the geographic and ethnic clustering of tuberculosis cases [14,15], increased concordance rates of tuberculosis in monozygotic compared to dizygotic twins [16], genetic variants identified as risk factors for tuberculosis, and documented cases of Mendelian predisposition to tuberculosis (reviewed in [17,18]). Genetic differences among *M. tuberculosis* strains are also increasingly recognized. Informative mutations in the form of large sequence polymorphisms (LSPs) and single nucleotide polymorphisms (SNPs) have identified families of genetically diverse *M. tuberculosis* strains that vary in their geographical distribution and potentially differ in their ability to transmit and cause disease [19,20]. Several environmental risk factors such as alcoholism, malnutrition, homelessness, and comorbidities such as HIV also contribute to disease outcome [21]. Tuberculosis is of particular importance in HIV-infected individuals, with 1.4 million incident cases and 500 000 deaths reported in 2008 [1].

Studies in humans have played a key role in our understanding of the complex aspects of tuberculosis susceptibility. While intriguing, these studies cannot exclude confounding environmental factors. In this regard, mouse models are ideal to investigate host and pathogen factors involved in susceptibility to mycobacterial disease. This chapter describes how experiments in the mouse have elucidated mechanisms of host immunity and bacterial pathogenesis that could not have been identified by human studies alone.

1.1 Mouse Models of Mycobacterial Infection

The long-standing history of the mouse as an experimental tool for tuberculosis research dates as early as 1882 with Robert Koch's discovery of *M. tuberculosis*.

The mouse was among the animal species used by Koch to fulfill the so-called "Koch's postulates", whereby tubercle bacilli were isolated from diseased tissue, propagated in culture, and used to elicit disease in naive animals [22]. Today, mouse models present several advantages for the study of tuberculosis. Studies of anti-tuberculosis immunity can be performed in the mouse where many aspects of human immunity are accurately reproduced [23]. Pathogenesis studies take advantage of the uniform response in inbred mouse strains to investigate the molecular basis of *M. tuberculosis* virulence. Characterization and quantification of host response phenotypes is facilitated by the large assortment of immunological and biochemical reagents available for murine studies. Mice can be bred at will and repeatedly tested, which increases the accuracy of phenotypic estimates. The uniform environment under which strains are kept and the controlled exposure to the pathogen also minimize experimental variability.

Two major genetic approaches can be applied in the mouse to identify genetic factors affecting the host response to mycobacterial infection. In the reverse genetics approach, genetically engineered mice with targeted mutations (gene knockout or knock-in) are infected to determine the role of the corresponding gene [24]. In the forward genetics approach, the differential susceptibility of inbred, recombinant, congenic or mutant strains is investigated using standard mouse crosses. Quantitative trait locus (QTL) analysis of informative F2 or backcross progeny determines if genes impacting on phenotype expression are linked to the location of polymorphic markers, such as microsatellites and SNPs, distributed throughout the genome. Candidate genes or chromosomal regions identified through these studies can be validated using genetically engineered or congenic mice [25]. Congenic strains are produced by transferring a defined chromosomal segment from a donor strain onto a recipient background through marker-assisted backcrossing [26,27].

Recombinant inbred and recombinant congenic strains can also be used to transform the genetic complexity of tuberculosis susceptibility into distinct

chromosomal effects that can be independently studied. Recombinant inbred strains are obtained from successive brother-sister breeding of selected F1 mice derived from two inbred strains. An approximately equal proportion of genome from the two progenitors is contained within each strain [28]. If a double backcross is performed before inbreeding, recombinant congenic strains are produced. Each recombinant congenic strain contains discrete chromosomal segments of donor genome (12.5%) on a recipient genetic background (87.5%). These strains differ from congenic strains in that marker-assisted selection is not performed during their derivation [29]. Congenic segments within the genome of each strain are localized by genotyping once strains are considered inbred. Since extensive genetic data already exists for these strains, mapping a phenotypic trait does not require additional genotyping. Alternatively, if strains producing phenotypes outside the range of the progenitors are identified, the discordant strains can be outcrossed to generate F2 mice which can be used for further mapping [30]. The AcB/BcA strain set used in the present thesis was derived from A/J and C57BL/6J progenitors [31] (Figure 2).

1.2 *Mycobacterium bovis* BCG

BCG strains are attenuated derivatives of virulent *M. bovis* that are used as anti-tuberculosis vaccines. Attenuated vaccines retain sufficient immunogenicity to induce protective immunity while maintaining a low level of virulence. Since it is attenuated, BCG is often used in the laboratory to study general aspects of the host response to mycobacterial infection.

1.2.1 The evolution of BCG vaccines

All BCG vaccines originated from an ancestral BCG strain developed by Albert Calmette and Camille Guérin at the Pasteur Institute in Lille, France. The history of BCG begins in 1908 with "lait Nocard", a strain of *M. bovis* isolated from the milk of a cow with tuberculosis mastitis and brought to Calmette and Guérin for pathogenesis studies. Initially a virulent strain, cultivation on glycerinated potato medium containing bile [32] had caused a progressive decrease in its virulence [33].

Recognizing the implications of attenuation for vaccine development, Calmette and Guérin maintained this bacterium in bile-containing culture medium for 13 years [34] before the first BCG vaccine trial in 1921. Vaccination with BCG was well-tolerated and reportedly protective against tuberculosis [35]. Beginning in 1924, cultures were distributed to different countries for local vaccine production. Selective adaptation by repeated culturing caused variation in the bacterium such that unique strains emerged from each vaccine laboratory. The resulting strains were named after the laboratory, city, or country from which they were derived (Figure 3) [36,37].

Genetic alterations coinciding with the attenuation and evolution of BCG vaccines have been uncovered. Insight into the genetic basis of BCG attenuation was first obtained from studies involving subtractive hybridization [38] and whole-genome microarrays [39]. Among the deletions identified, only the region of difference 1 (RD1) was absent from all the BCG strains studied but present in virulent strains of *M. bovis* and *M. tuberculosis* [38-40]. RD1 encodes the T cell antigens ESAT-6 (early secreted antigenic target 6-kDa) and CFP-10 (culture filtrate protein 10-kDa) [41,42] as well as the ESX-1 secretion system for their export [43,44]. Disruption of RD1 in *M. tuberculosis* diminished virulence in a mouse model [45] while restoration of RD1 in BCG partially reversed attenuation [40], indicating that loss of RD1 contributed to the original attenuation of BCG. All BCG daughter strains have also accrued a SNP in the *Crp* gene encoding the cAMP-receptor protein, which affects the DNA-binding domain of the protein [46].

Additional deletions were either identified in subsets of strains or restricted to individual BCG strains [39]. These deletions corresponded well with historical records of strain dissemination and enabled the reconstruction of a molecular phylogeny for BCG [47]. In addition, recently identified tandem duplication events have refined the framework for the BCG evolutionary scheme and now divide the vaccines into four duplication 2 (DU2) groups and the duplication 1 (DU1) group (Figure 2). The DU1 duplication is specific to BCG Pasteur while DU2 exists in

one of four configurations (I to IV) in all BCG strains. The first DU2 duplication (DU2-I) occurred in the early BCG strains Russia, Moreau, and Japan. BCGs Birkhaug and Sweden contain a second configuration of the DU2 duplication, termed DU2-II, and are grouped accordingly. The DU2-III group consists of the BCG strains Prague, Glaxo, Mérieux, and Denmark (alias Danish). Members of the DU2-IV group include BCG Pasteur, which contains the DU1 and DU2-IV duplication, and the BCGs Tice, Montreal (alias Frappier), Connaught, and Phipps [46].

BCG Russia is considered the most ancient BCG strain. Aside from RD1, only the *Rv3698* orthologue (RDRussia) was deleted from BCG Russia [48]. The high degree of genome conservation results in part from the lack of RecA-mediated recombination due to an insertion mutation in the *recA* gene (recA_D140*) [49]. BCG Russia and the other DU2-I members also contain duplicate copies of the IS6110 transposable element [50]. The additional IS6110 insertion has recently been localized to the promoter region of *phoP* [46]. The *phoP* gene encodes a transcriptional regulator in the PhoP-PhoR two-component signal transduction system and may have implications for virulence [51,52]. A number of BCG strains have independently incurred deletions that have been shown to affect PhoP-PhoR function, at least in the case of BCG Prague. [46,53]. This suggests that the PhoP-PhoR regulon contributes to mycobacterial virulence and is not essential for *in vitro* growth.

Additional deletions, duplications, and frameshift mutations have been described for the other BCG strains (Figure 2). BCG Montreal and BCG Pasteur are members of the DU2-IV group [46] and share a number of genetic alterations. Deletion of the RD2 region causes a lack of MPB64 antigen [38,54] in both strains. These strains are also low producers of the antigenic proteins MPB70 and MPB83 due to a start codon mutation in the sigma factor K (*sigK*) regulatory gene [55]. A SNP in the *mmaA3* gene also results in the inability of both strains to synthesize a lipid cell wall constituent known as methoxymycolic acids [56]. A SNP located in

the *Crp* gene of these strains affects the cAMP binding site of CRP, leading to a non-functional protein [57]. BCG Montreal and BCG Pasteur also share a common nRD18 deletion [58] which potentially inactivates the SigI protein through the in-frame fusion of *sigI* (*Rv1189*) with *Rv1191* [46]. Mutations affecting genes that encode transcriptional regulators and antigens may modify the overall immunogenicity and virulence of individual BCG strains. Differences between the Montreal and Pasteur strains of BCG include the loss of RD14, which is specific to BCG Pasteur, and the deletion of RDFrappier and RD8 (equivalent to RD15 in Brosch *et al*. [46]), which occurred in BCG Montreal but not BCG Pasteur [39,48]. Seminal genetic studies in the mouse were performed with BCG Montreal and are discussed in the following section.

1.2.2 Forward Genetic Studies of BCG Infection

Innate susceptibility to BCG infection is determined by the extent of bacterial replication in the spleen during the first three weeks of infection. Inbred strains are either permissive (e.g. B10.A, C57BL/6, BALB/c) or resistant (e.g. C3H/HeCr, A/J, DBA/2) to BCG replication after a low dose intravenous infection (1-5 x 10^4 bacteria) [59]. Susceptibility is inherited as a simple recessive trait that maps to a locus, *Bcg*, on proximal chromosome 1 [60-62]. *Bcg* co-localized with two other loci, *Ity* and *Lsh*, which control susceptibility to infection with *Salmonella typhimurium* and *Leishmania donovani* respectively [62,63]. *Ex vivo* infection experiments demonstrated that macrophages were responsible for the phenotypic expression of the *Bcg*/*Ity*/*Lsh* locus [64]. A positional cloning approach identified *Nramp1* [natural resistance-associated macrophage protein 1, alias solute carrier family 11 member 1 (*Slc11a1*)] as the gene underlying this locus. *Nramp1* encodes an integral membrane protein containing 12 putative transmembrane (TM) domains. Susceptibility to infection among inbred strains is associated with a single Gly169Asp (G169D) substitution in the predicted TM4 region of Nramp1 [65]. The G169D mutation impairs protein folding and maturation, causing absence of Nramp1 expression in the membrane compartment of susceptible macrophages [66]. Validation that *Nramp1* and *Bcg*/*Ity*/*Lsh* are allelic

was provided by transgenic mouse studies. Genetic disruption of *Nramp1* made an otherwise resistant mouse strain susceptible to infection with all three infectious agents [67]. Likewise, transfer of the resistant *Nramp1*^{G169} allele onto a susceptible background restored resistance [68]. *Nramp1*-mediated resistance has also been observed for other species of *Mycobacterium* including *M. paratuberculosis* [69], *M. avium* [70], *M. intracellulare* [71], *M. smegmatis* [72], and *M. lepraemurium* [73] but not *M. tuberculosis*. Studies have indicated that mice with loss- or gain-of-function alleles at *Nramp1* are as resistant to *M. tuberculosis* as their wild-type counterparts [74,75]. The interplay between *Nramp1* function, specific pathogen encoded factors and host range of *Nramp1* genetic action is still poorly understood.

The Nramp1 protein is expressed in the tertiary granules of neutrophils and in the lysosomal membrane of macrophages and monocytes [76,77]. In macrophages, Nramp1 is rapidly recruited to the membrane of phagosomes containing engulfed particles or bacteria [76,77]. Nramp1 functions as a pH-dependent, metal efflux transporter that pumps divalent cations such as Fe^{2+} and Mn^{2+} out of the phagosomal space [78,79]. Nramp1-mediated depletion of the Fe^{2+} and Mn^{2+} ions restricts intracellular replication by (a) depriving the bacteria of nutritionally essential metals, (b) enhancing bactericidal activity or (c) antagonizing bacterial survival functions [18]. During BCG infection, Nramp1 recruitment to the membrane of BCG-containing phagosomes abrogates the ability of BCG to block phagosome-lysosome fusion, thereby causing increased vacuolar acidification and decreased intracellular replication [80].

In inbred mice, allelic variation at the *Nramp1* gene is strictly correlated with susceptibility to low dose BCG infection [81]. The *Mus spretus* and BXH-2 strains represent notable examples where the action of *Nramp1* modifier loci is observed. BXH-2 is a recombinant inbred strain derived from C3H/HeJ (*Nramp1*^{G169}) and C57BL/6J (*Nramp1*^{D169}) progenitors. Despite a fixed *Nramp1*^{G169} resistance allele, BXH-2 strains have an increased susceptibility to BCG infection [82].

Modulation of *Nramp1*-dependent BCG replication is caused by a defect in the interferon regulatory factor 8 (*Irf8*) gene [alias interferon consensus sequence-binding protein 1 (*Icsbp*)], which encodes a transcriptional co-regulator for IFN-responsive genes. The IRF-8 protein of BXH-2 mice contains a loss-of-function Arg294Cys (R294C) substitution. In F2 mice homozygous for the $Irf8^{C294}$mutation, BCG replication in the spleen is increased relative to mice of the same *Nramp1* genotype carrying an $Irf8^{R294}$ allele [83]. BXH-2 mice are also highly susceptible to infection with *M. tuberculosis* [84].

The wild-derived *Mus spretus* (SPRET/EiJ) mouse strain harbours a resistant $Nramp1^{G169}$ allele yet displays an intermediate level of susceptibility to BCG infection relative to resistant and susceptible laboratory strains. Detection of novel gene effects is greatly facilitated in crosses between *M. spretus* and the *M. musculus* laboratory strains, due to the considerable phylogenetic divergence between these two species [85]. A genome-wide scan of an informative (C57BL/6J × SPRET/EiJ) x C57BL/6J backcross was performed to identify loci that modify the $Nramp1^{G169}$ advantage of SPRET/EiJ mice. In addition to *Nramp1*, single marker effects were detected on chromosomes 4 and X in male mice and on chromosomes 9 and 17 in female mice. The chromosome 17 locus identified in females overlaps the major histocompatibility complex (MHC) and interacts strongly with *Nramp1* [86].

1.2.3 *Reverse Genetic Studies of BCG Infection*

BCG replication is bi-phasic in the spleen following a low dose intravenous infection. The early, non-immune phase is controlled by the *Nramp1* gene [60]. The late phase is associated with T-cell mediated immunity and results in either complete elimination of the bacteria or persistent infection in susceptible strains [87]. Studies involving genetically modified mice have contributed substantially to our understanding of the cell types and molecules involved in the curative phase of BCG infection. The importance of cell-mediated immunity during BCG infection has been determined from studies involving RAG-1-deficient mice,

which lack mature B and T cells. RAG-1$^{-/-}$ mutant mice succumb within 60 days of infection with 10^6 bacteria, whereas inoculation of control mice produces a nonlethal, self-limiting infection [88].

Mice with deletions affecting different T cells subsets have been used to determine the relative contribution of each T cell type. T helper 1 (Th1) and Th2 cells express a T cell receptor (TCR), composed of α and β chains, and a CD4 co-receptor. Cytotoxic T lymphocytes express an α/β TCR and a CD8 co-receptor [89]. Mice deficient in the β chain of the TCR are therefore devoid of both $CD4^+$ and $CD8^+$ T cells [90]. These mice develop a fatal BCG infection and succumb within 60 days of infection with $>10^6$ BCG bacteria [88]. Priming of $CD4^+$ and $CD8^+$ T-cell occurs through the interaction of the α/β TCR with antigen presented in the context of MHC class II and class I molecules, respectively [91]. The importance of $CD4^+$ and $CD8^+$ T cells can therefore be assessed using mice with a deletion in the MHC class II and class I molecules. Mice deficient in MHC class II molecules died of BCG infection by day 60, demonstrating a protective role for $CD4^+$ T cells. β2-microglobulin knockout mice lacking MHC class I molecules survived less than one year, suggesting a potential involvement of $CD8^+$ T cells in BCG immunity [92]. The role of γδ T cells, which contain a unique TCR composed of γ and δ chains [93-95], has also been investigated using gene-deleted mice. TCRδ$^{-/-}$ mice successfully controlled BCG infection, although the bacterial load was slightly higher than control mice [88]. These findings indicate that immunity in the late phase of BCG infection is mediated mostly by $CD4^+$ T cells with the contribution of $CD8^+$ T cells.

Th2 cells produce interleukin-4 (IL-4) [96], which has a limited role in anti-mycobacterial immunity [97]. Th1 cells, in contrast, are potent producers of IFN-γ [96] which is essential for protection against intracellular bacteria [98]. IFN-γ is also produced by $CD8^+$ T lymphocytes and by NK cells [99]. Mice deficient in IFN-γ have 10- to 100-fold more bacteria in the lung, liver, and spleen compared to wild-type controls. These mice succumb to a high intravenous dose of BCG (10^7)

within 9 weeks [100]. Similarly, mice with a targeted deletion of the gene encoding the IFN-γ receptor (IFN-γR) die within 7-9 weeks of infection [101]. Rapid mortality is also observed in mice deficient in TNF-α responsiveness, possibly due to a defect in the recruitment and activation of mononuclear cells. Mice devoid of TNF-α succumb within 8 to 12 weeks of BCG infection whereas TNF-α type I receptor (TNFRI)-deficient mice die within 5 weeks [102]. Together, these results show that TNF-α and IFN-γ play a central role in immunity against BCG.

Activation of Th1 cells is regulated by the production of IL-12 [103]. Bioactive IL-12p70 is composed of a 35-kDa and 40-kDa chain (p35 and p40 respectively) [104]. The p40 subunit of IL-12 can also heterodimerize with a p19 chain to form IL-23, which has overlapping activity with IL-12 [105]. Lack of IL-23p19 did not impact on bacterial growth in mice infected with BCG [106]. IL-12p35-deficient mice also controlled and cleared BCG infection, although the bacterial burden was slightly elevated compared to wild-type mice [107]. In the absence of IL-12p35, IL-23 compensated for IL-12 to reduce the bacterial load [106]. In mice devoid of both IL-12 subunits, BCG infection was chronic but not lethal following intravenous inoculation with 10^6 bacteria [107]. Deletion of IL-12p40 was associated with a decrease in both IFN-γ and TNF-α levels [108], suggesting that IL-12p40 contributes to the regulation of the host immune response to BCG.

1.3 *Mycobacterium tuberculosis*

The majority of immunological and biochemical studies investigating the host response to mycobacteria in the mouse use avirulent or attenuated strains of mycobacteria. However, it is known that host responses to these bacteria can differ in critical aspects from the corresponding responses directed against fully virulent strains of *M. tuberculosis*.

1.3.1 The M. tuberculosis *Pathogen*

Tuberculosis in humans is caused primarily by *M. tuberculosis*. *M. tuberculosis* is a member of the *M. tuberculosis* complex (MTC), which also includes tuberculosis-causing pathogens such as *M. bovis*, *M. canetti* and *M. africanum* as well as avirulent microbes such as BCG [109-111]. Members of the MTC typically share over 99.9% nucleotide identity, yet they differ characteristically in pathogenicity and host tropism [112,113]. *M. tuberculosis*, *M. canetti* and *M. africanum* represent the most ancestral lineages of the MTC and have been isolated predominantly from humans [114]. Human-adapted members of the MTC can be further subdivided into six major lineages, which are each associated with a particular geographical region. These include the East-Asian, Euro-American, Indo-Oceanic, East-African-Indian, and West-African-1 and -2 lineages. East-Asian strains include, but are not confined to, the Beijing family of strains [115]. *M. tuberculosis* strains of the Beijing genotype are the most widely studied, due to their high prevalence in Asia [116-119] and Russia [120,121] and their association with drug resistance [122] [120,123,124]. The West African lineages 1 and 2 correspond to strains that are traditionally referred to as *M. africanum* subtype 1 [115]. *M. africanum* subtype 2 is associated with East Africa and is considered a sublineage of *M. tuberculosis* [109,125]. Strains of the Euro-American lineage predominate in Europe and the Americas but are also found in regions of Africa and the Middle East [115]. The Euro-American lineage includes the *M. tuberculosis* clinical isolates CDC1551 and HN60, the Haarlem strains and the laboratory strains H37Rv, H37Ra, and Erdman [126-128].

1.3.2 Infection and Immunity

Experimental *M. tuberculosis* infection in mice is usually performed by intravenous injection or aerosol exposure. Intravenous infection delivers mycobacteria through the bloodstream and causes hematogenous seeding to the liver (95%), spleen (4%), and lungs (0.1%) [23]. Aerosol infection deposits the bacteria directly into the lungs, with extrapulmonary dissemination occurring after

initial lung colonization [129]. Pulmonary exposure with *M. tuberculosis* is more pathogenic than intravenous infection, even when numbers of blood-borne bacteria in the lung are similar to those implanted directly by aerosol [130]. Respiratory infection therefore requires lower doses of *M. tuberculosis* to cause significant pathology.

Following inhalation, bacilli are deposited into the lower airways and alveolar tissue where they infect alveolar macrophages. Once in the lung parenchyma, bacilli invade and replicate within resident tissue macrophages. Infected macrophages release cytokines such as TNF-α and chemokines that together initiate a local inflammatory response [131]. Dendritic cells sampling the airway and alveolar tissue are also infected by *M. tuberculosis* and migrate to the lung draining lymph node [7,8]. In the lymph nodes, dendritic cells prime naive $CD4^+$ T cells into Th1 cells in the presence of polarizing cytokines such as IL-12 [132]. Naive $CD8^+$ T cells are also activated to become cytotoxic T lymphocytes. Inflammatory signals from the lung direct the effector $CD4^+$ and $CD8^+$ T cells back through the circulation and into the site of infection where they secrete IFN-γ. IFN-γ activates the macrophages to kill or limit intracellular replication of *M. tuberculosis* and upregulates the expression of chemokines. The chemokine gradient recruits monocytes/macrophages, effector $CD4^+$ and $CD8^+$ T cells, and B lymphocytes to the site of infection. These cells aggregate with the infected macrophages to form a granuloma [131].

Granuloma formation is the hallmark of infection with *M. tuberculosis*. It functions mainly to contain the bacilli and prevents further spread of infection. The architecture of the granuloma also facilitates cellular interactions that are necessary for effector $CD8^+$ T cell functions, macrophage activation, and cytokine production. The cellular organization of the granuloma differs between humans and mice. Macrophages of the human granuloma are centrally located with a surrounding rim of lymphocytes whereas macrophages of the murine granuloma are arranged as sheets adjacent to lymphocytic aggregates (Figure 4) [133]. In the

mouse, granuloma formation begins after 2-3 weeks of infection. At this time, the granuloma structure includes T lymphocytes, macrophages, and neutrophils. By 4-5 weeks post-infection, the granuloma has increased in size and neutrophils are less abundant. B lymphocytes have also migrated to the site of granuloma formation and form densely packed clusters. At 5-6 weeks, lymphocyte numbers stabilize and the granuloma is established. If bacterial growth is not contained, cellular influx continues. Lesions become dominated by neutrophils and a necrotizing pathology develops, causing early death. Although necrosis within the lung granulomata of humans is common, necrosis in the murine granuloma is only visible if there is overwhelming *M. tuberculosis* replication. It is rarely observed in mice that successfully control infection [131].

Virulent *M. tuberculosis* induces necrosis of the macrophage as a strategy to escape host defence mechanisms and to promote bacterial dissemination. Non-pathogenic mycobacteria stimulate apoptosis instead, resulting in containment and killing of bacteria as well as the priming of antigen-specific T cell responses [134]. Lipoxin A_4 (LXA_4) and prostaglandin E_2 (PGE_2) are arachidonic metabolites that exert polar effects on mycobacteria-induced macrophage death [135]. LXA_4 produced during *M. tuberculosis* infection negatively regulates expression of pro-inflammatory molecules such as IL-12, IFN-γ and inducible nitric oxide synthetase (iNOS, alias NOS2) [136] and decreases antigen presentation by dendritic cells [137]. Accumulation of LXA_4 suppresses apoptosis and promotes necrosis. Absence of LXA_4 in macrophages through the loss of the 5-lipoxygenase (ALOX5) enzyme caused decreased microbial replication and preferentially induced apoptosis [138]. LXA_4 antagonizes the effect of PGE_2 [135]. Expression of PGE_2 is greater in macrophages infected with avirulent bacteria as compared to virulent *M. tuberculosis*. Upregulation of PGE_2 during infection with avirulent mycobacteria was associated with death by apoptosis [135]. In studies using *M. tuberculosis*-infected macrophages, treatment with exogenous PGE_2 repaired the damaged plasma membrane and reduced death by necrosis [138].

Avirulent and virulent strains of mycobacteria also differ in their ability to manipulate processes linked to autophagy. Macrophages perform autophagy to destroy engulfed bacteria. During autophagy, infected phagosomes are sequestered within an autophagosome, which is then delivered to a lysosome to eliminate the invading pathogen [139-141]. The autophagy pathway is triggered by avirulent mycobacteria, resulting in bacterial elimination. *M. tuberculosis* inhibits autophagy, which enables it to reside and replicate within the immature phagosome [142,143]. Experimental induction of autophagy in *M. tuberculosis*-infected mouse macrophages resulted in increased phagosomal acidification, enhanced colocalization of autophagy effector proteins with the phagosome, and reduced intracellular survival of mycobacteria [144], consistent with a role for autophagy in reduced bacterial pathogenesis. Increased autophagy has been linked to expression of IFN-γ and the interferon inducible protein LRG-47 (alias immunity-related guanosine triphosphatase M, IRGM), a molecule recruited to the *M. tuberculosis*-containing phagosome [144,145]. The autophagic response to *M. tuberculosis* is also induced by Toll-like receptor 4 (TLR4) [146] but is inhibited by the Th2 cytokines IL-4 and IL-13 [147].

1.3.3 Forward Genetic Studies of M. tuberculosis *Infection*

Beginning with observations by Long and Vogt in the 1940s [148], a number of studies quickly established that inbred mouse strains differed in their inherent susceptibility to tuberculosis [149-152]. Lynch and colleagues speculated that the "gradation" observed across mouse strains argued for "existence of a number of genes, with different combinations or frequencies characterizing the different strains". In 1965, they demonstrated, through interbreeding and backcrossing experiments between Swiss and C57BL strains, that genetic factors influenced the response of mice to infection with *M. tuberculosis* [153]. F1 hybrids between the two strains exhibited overdominance, with F1 mice surviving longer than either parent strain. Informative backcross (F1 × C57BL) progeny resolved into two populations, resistant or susceptible, suggesting a major gene effect segregating in

this cross. Thus, the authors concluded that susceptibility to tuberculosis in the mouse was a complex trait under multigenic control.

Susceptibility of the mouse to *M. tuberculosis* is defined as early death caused by progressive lung disease and/or uncontrolled bacterial replication. Inbred mouse strains have been classified as susceptible (e.g. A/J, C3H, CBA, DBA/2, I/St, 129/Sv) or resistant (e.g. A/Sn, BALB/c, C57BL/10, C57BL/6) to tuberculosis based on their survival time [154-157]. Initially, *M. tuberculosis* growth is similar in the lungs of susceptible (A/J, CBA, DBA/2) and resistant (C57BL/6) strains. In a low dose aerosol model, replication is rapid during the first month and is eventually stabilized (1-5 months) in both resistant and susceptible mice. This control eventually subsides in susceptible strains and bacterial replication resumes, resulting in widespread tissue damage and premature death [155,158-160]. Resistant C57BL/6 mice continue to restrict bacterial growth and limit massive tissue injury although they ultimately succumb to infection. At the time of death, lung pathology differs considerably between susceptible and resistant strains. Pulmonary lesions in C57BL/6 mice display large lymphocytic aggregates which penetrate the granuloma. Lesions in susceptible mice (A/J, CBA, DBA/2, C3H/HeJ) contain large foamy macrophages, degenerating neutrophils, and a few dispersed lymphocytes and are often necrotic [160-164].

The I/St mouse strain is particularly susceptible to *M. tuberculosis* infection compared to A/Sn mice with regard to survival time, bacterial load, lung pathology and body weight loss [157]. The genetic basis for the differential susceptibility of I/St and A/Sn was investigated by whole genome scanning using weight loss as a proxy for tuberculosis susceptibility. Initial mapping studies in an informative (A/Sn × I/St) × I/St backcross indicated that weight loss induced by intravenous *M. tuberculosis* H37Rv infection was controlled by two major loci on chromosomes 3 and 9 and two suggestive loci on chromosomes 8 and 17 in female mice [165]. Suggestive loci in male mice were localized to chromosomes 5 and 10. A limited genome scan using weight loss and survival time as

quantitative phenotypes in (A/Sn × I/St) F2 mice confirmed the loci that mapped to chromosome 3 (designated tuberculosis severity 1, *tbs1*), chromosome 9 (*tbs2*) and chromosome 17 in proximity to the H-2 complex [166]. The effect of the H-2 locus has been attributed to a coding mutation in the *Tnfa* gene of the susceptible I/St strain. This polymorphism results in a larger secretion of TNF-α, which is speculated to contribute to the susceptibility of I/St mice by increasing lung pathology [167]. The genes responsible for the *tbs1* and *tbs2* loci remain unknown.

The genetic control of susceptibility to tuberculosis is complex in C3H strains [168]. The C3HeB/FeJ strain is exquisitely susceptible to *M. tuberculosis*, with a much shorter survival time (3.5-4 weeks) following intravenous infection relative to other susceptible C3H substrains [169]. Premature death in C3HeB/FeJ mice is associated with progressive lung disease characterized by increased bacterial loads, extensive pneumonitis, and necrotic lesions. Classical linkage studies in (C3HeB/FeJ × C57BL/6J) F2 mice intravenously infected with *M. tuberculosis* Erdman identified a major locus on chromosome 1 designated *sst1* (for susceptibility to tuberculosis 1) [170]. Congenic C3HeB/FeJ mice bearing a resistant C57BL/6J-derived allele of *sst1* (C3H.B6-*sst1*) survived two times longer and had a 50-100 fold lower pulmonary bacterial burden compared to the parental C3HeB/FeJ strain. Explanted bone-marrow derived macrophages from C3H.B6-*sst1* mice had an enhanced ability to restrict intracellular replication of *M. tuberculosis* and induced apoptosis following infection, whereas phagocytes from C3HeB/FeJ died by necrosis. A positional cloning strategy identified intracellular pathogen resistance 1 (*Ipr1*) as a strong candidate for *sst1*. *Ipr1* encodes the IFN-induced protein 75 (Ifi75), a putative transcriptional regulator. *M. tuberculosis* infection induced expression of *Ipr1* in the lungs of C3H.B6-*sst1* mice and other C3H strains but not in susceptible C3HeB/FeJ mice. Restoration of a full-length *Ipr1* in C3HeB/FeJ mice limited *M. tuberculosis* replication in the lungs of mice and in macrophages infected *in vitro*, confirming that *Ipr1* was the gene underlying *sst1* [169].

Resistance and susceptibility alleles of *sst1* are not sufficient to confer full protection or susceptibility in congenic mice, indicating that genes outside of *sst1* also contribute to the phenotype of the C3HeB/FeJ and C57BL/6J parental strains. The existence of additional loci controlling survival to tuberculosis was investigated using mice from *sst1*-adjusted crosses. A genome-wide scan in (C3H.B6-*sst1* × C57BL/6J) F2 hybrids identified four loci which mapped to chromosomes 7, 12, 15 and 17 [171]. The effect of the chromosome 17 locus, which overlaps the H-2 complex, was further examined using C57BL/10J strains bearing different H-2 haplotypes. The C57BL/10J (H-2^b) and C57BL.Br (H-2^k) strains, representing C57BL/6J and C3HeB/FeJ mice respectively, differed in survival time. Mice harbouring the H-2^k haplotype succumbed more rapidly to infection, indicating that the C3HeB/FeJ-associated haplotype is linked to increased susceptibility. Positional candidates for the chromosome 12 locus include the immunoglobulin heavy chain (*Igh*) locus, which is polymorphic between C57BL/6J and C3HeB/FeJ strains. The loci on chromosomes 12 and 17 may therefore reflect differences in acquired immunity that influence survival to infection [171]. The molecular identities of the loci on chromosomes 7 and 15 are currently unknown. A second whole genome scan where the effect of the susceptible *sst1* allele was fixed also detected the chromosome 7 locus. This study identified a role for the chromosome 7 locus in the control of intracellular *M. tuberculosis* replication *in vivo*. Importantly, combining resistant C57BL/6J-derived alleles at the *sst1* and chromosome 7 loci on a C3HeB/FeJ-susceptible background significantly reduced lung pathology and lengthened survival following *M. tuberculosis* infection [172].

A genetic study of tuberculosis susceptibility/resistance was also performed using susceptible DBA/2J and resistant C57BL/6J mouse strains. A genome-wide scan for loci affecting survival time following intravenous *M. tuberculosis* H37Rv infection was conducted in (C57BL/6J × DBA/2J) F2 hybrids. Two significant loci were detected on chromosomes 1 and 7, designated tuberculosis resistance locus 1 (*Trl-1*) and *Trl-3* respectively. A third suggestive locus was identified on

chromosome 3 (*Trl-2*). Homozygosity for C57BL/6J-derived alleles was associated with resistance at each locus [173]. A second genome scan analyzed pulmonary replication in (C57BL/6J × DBA/2J) F2 mice 90 days following low dose aerosol infection. Strong linkage was detected on chromosome 19 (*Trl-4*) and suggestive linkages were localized to the *Trl-3* region as well as chromosomes 5 and 10. A strong additive effect was detected between *Trl-3* and *Trl-4* such that F2 mice homozygous for one parental allele at both loci had lung bacillary loads comparable to that parental strain [159]. The genetic effect of *Trl-3* and *Trl-4* was further investigated using congenic strains. Transfer of a C57BL/6J-derived, *Trl-3* chromosome 7 segment onto a DBA/2J genetic background (D2.B6-Chr7) increased resistance to *M. tuberculosis* infection as evidenced by the decreased pulmonary load and longer survival time. In contrast, D2.B6-Chr19 congenic mice harbouring a C57BL/6J-derived, *Trl-4* chromosome 19 segment did not have an altered resistance to *M. tuberculosis* infection relative to DBA/2J mice [174]. This finding suggests that the effect of *Trl-4* involves genetic interactions with other unknown loci, further illustrating the genetic complexity of susceptibility to tuberculosis.

1.3.4 Reverse Genetic Studies of M. tuberculosis *Infection*

Gene-targeted mice have been used extensively to study the involvement of different molecules and cell types during *M. tuberculosis* infection (Table I). Until recently, B lymphocytes were generally not considered important for anti-tuberculosis immunity, despite their abundance in tuberculous granulomas [175]. This followed from the observation that B cell-deficient mice ($IgM^{-/-}$) controlled pulmonary bacterial replication during a low dose aerosol infection, even though fewer macrophages, neutrophils and $CD8^+$ T cells were recruited to the lung [176,177]. A role for B cells in *M. tuberculosis* infection was reconsidered, given that mice lacking B cells have increased bacterial counts following a high dose aerosol or intravenous challenge [178,179]. High dose aerosol infection of B cell-deficient mice caused early mortality and severe lung pathology, characterized by enhanced neutrophil accumulation [178]. These results suggested a role for B cells in the

modulation of neutrophil expansion or their migration to the lung. In support of this hypothesis, a vaccine model using mice with impaired B lymphocyte development and function demonstrated that B cell deficiency causes early neutrophil migration to the site of BCG injection. Ingestion of BCG bacilli by neutrophils rather than macrophages led to a lower number of IFN-γ-producing $CD4^+$ T cells, which ultimately decreased protection by vaccination [180].

Activation of $CD4^+$ T cells by MHC class II molecules is essential for the control of *M. tuberculosis* infection. Mice deficient in CD4 or MHC class II molecules had severely depleted levels of IFN-γ early in infection which caused premature death of both types of mutant strains [181]. Mice devoid of class II MHC molecules displayed a greater susceptibility to tuberculosis than mice lacking class I MHC molecules, demonstrating that $CD4^+$ T cell responses are dominant to $CD8^+$ T cell mediated immunity in the control of infection [182]. A role for $CD8^+$ T cells in anti-tuberculosis immunity was initially investigated using β2-microglobulin deficient mice, which proved to be highly susceptible [183]. Studies involving a combination of knockout mice later demonstrated that β2-microglobulin deficient mice were more susceptible than $CD8\alpha^{-/-}$ mutant mice [184] and the heightened susceptibility of β2-microglobulin deficient mice was attributed to an overload of iron [185]. Mice lacking CD8α were nonetheless susceptible, indicating that $CD8^+$ T cells also contribute to immunity against *M. tuberculosis* [184]. A survey of mice deficient in αβ or γδ T cells or in the MHC class I and class II molecules further confirmed that protective anti-tuberculosis immunity involves primarily $CD4^+$ and $CD8^+$ αβ T cells and showed that mice devoid of γδ T cells were as resistant to infection as wild-type controls [182]. Other studies have provided evidence for a dose-dependent contribution of γδ T cells. For example, mice lacking γδ T cells were shown to control lower doses of *M. tuberculosis* administered intravenously but succumbed to a high dose infection [186]. A second study also observed mortality following a high dose challenge. Death was speculated to result from an exaggerated granulomatous response [187], outlining a potential role for γδ T cells in the control of cell trafficking.

The rapid progression and death of mice lacking IFN-γ has provided indirect evidence that Th1-polarized $CD4^+$ cells are more important than Th2 effector cells. Bacterial replication is essentially unrestricted in *Ifng* gene-deleted mice, and although granulomas develop, they become quickly necrotic [188]. Macrophage activation is defective in IFN-γ-deficient mice and expression of *Nos2* is low [100,188], such that these mice cannot produce the reactive nitrogen intermediates necessary for the destruction of intracellular bacteria. However, the susceptibility of iNOS-deficient mice is less severe than mice lacking IFN-γ, IFN-γR1, or the IFN-responsive, signal transducer and activator of transcription 1 (STAT-1) molecule, suggesting that there are iNOS-independent mechanisms of protection. A proposed alternative pathway involves LRG-47, a phagosomal protein involved in autophagy. A deficiency in LRG-47 caused early mortality similar to that of IFN-γR1 knockout mice, outlining a role for LRG-47 in defence against *M. tuberculosis* infection [189].

Additional evidence for Th1-cell mediated protection against *M. tuberculosis* arose from studies involving IL-12 knockout mice. Mouse strains with a double disruption of IL-12p35 and IL-12p40 (IL-12p70-deficient) were susceptible to a low dose aerosol *M. tuberculosis* infection and succumbed within 10 weeks. IL-12p70-deficient mice did not mount Th1 and cytotoxic T cell responses, resulting in severe lung pathology. These mutant mice exhibited greater susceptibility to *M. tuberculosis* compared to mice lacking only one of the two subunits [107]. Mice lacking the IL-12p40 subunit were more susceptible than IL-12p35$^{-/-}$ mutant mice, as evidenced by increased bacterial burden, reduced IFN-γ production, and decreased survival time [190,191]. Mice devoid of the IL-12p40 subunit also had aberrant dendritic cell migration to the lung draining lymph node, causing reduced T cell activation [192]. IL-12p35-deficient mice were able to generate antigen-specific IFN-γ responses but had a reduced ability to control bacterial replication and died within 20 weeks of infection [107,190]. Since IL-12p70 is absent in mice lacking the IL-12p35 subunit, production of IFN-γ-

secreting cells was dependent upon IL-23 (heterodimer of IL-12p40 and IL-23p19) [193]. This follows from the finding that IL-23p19 deficiency alone did not impact on IFN-γ T cell responses whereas double IL-12p35 and IL-23p19-deficient mice were unable to generate IFN-γ-producing cells. Although absence of IL-23p19 did not alter disease progression or mycobacterial growth, double IL-12p35 and IL-23p19-deficient mice were as susceptible as mice lacking IL-12p40, owing to a loss of the IFN-γ-producing cellular response. IL-23p19 is therefore important for IFN-γ production and mycobacterial resistance only in the absence of IL-12p35. A deficiency IL-23p19 also caused a substantial reduction in the number of IL-17-secreting T cells, although the absence of IL-17 had minimal effects on tuberculosis resistance [193].

Because Th1 cells antagonize Th2 cell functions, the absence or reduction of Th1 immunity in IFN-γ- and IL-12p40-deficient mice was proposed to cause increased Th2 cell activation and IL-4 production. In both mutant strains however, a lack of mycobacterial-specific Th1 immunity did not trigger a Th2 response and IL-4 levels were not increased [188,191], suggesting that the increased susceptibility of these mice is caused by a defective Th1 response and not by an increased Th2 response. Generation of a Th2 response involves signalling by IL-4. IL-4 binds the IL-4 receptor on T cells, which activates the STAT-6 pathway and induces transcription of Th2 cytokine genes [194,195]. A progressive increase in IL-4 production has been detected in both resistant C57BL/6J mice and the more susceptible BALB/c strain during *M. tuberculosis* infection [196,197]. However, reverse genetic studies involving mice of either genetic background have provided conflicting results. Resistance to tuberculosis was not altered in IL-4 deficient mice of a C57BL/6J background [198,199]. Similarly, absence of the alpha chain of the IL-4 receptor (IL-4Rα) in C57BL/6J mice did not impact on tuberculosis susceptibility [200]. By contrast, genetic disruption of *Il4* on a BALB/c background increased resistance to *M. tuberculosis* infection, as evidenced by the lower bacterial burdens following intranasal infection [201]. A 100-fold reduction in pulmonary counts was also observed in response to intratracheal infection with

M. tuberculosis [202]. However, genetic inactivation of *Stat6* on a BALB/c background did not affect resistance to *M. tuberculosis* infection [200]. These results together suggest that IL-4 has mildly detrimental effects on tuberculosis resistance in BALB/c mice, although the contribution of IL-4 remains to be confirmed in C57BL/6J.

TNF-α is essential for macrophage activation and for the formation and maintenance of granulomas. Mice devoid of TNF-α or TNFRI are highly susceptible to *M. tuberculosis* infection. Absence of TNF-α following a low aerosolized dose of *M. tuberculosis* caused mortality within 35 days [203]. There were 10^5 fold more bacteria detected in TNF-$\alpha^{-/-}$ mutant mice compared to wild-type controls. Mice lacking the TNFRI had a mean survival time of 20 days following an intravenous dose of *M. tuberculosis* (5 x 10^5 bacteria) and had 50- to 100-fold more bacilli than wild type mice [204]. Mice devoid of both the TNF-α type II receptor (TNFRII) and TNFRI also succumbed within 28 days of aerosol infection and had larger bacterial burdens compared to control mice [205]. TNF-α synergizes with IFN-γ to induce production of iNOS [206-208]. iNOS expression was delayed in TNFRI$^{-/-}$ mice [204] but not in TNF-$\alpha^{-/-}$ mutant mice [203], suggesting alternate signalling in the absence of TNF-α. The granulomatous response following *M. tuberculosis* infection was also defective in both TNF-α and TNFRI-deficient mice. Although a few activated macrophages were present, lymphocyte co-localization with the macrophages was impaired, resulting in disorganized granuloma formation [203,204]. Chemokine induction was also delayed in TNF-α-deficient mice, outlining a role for TNF-α in the regulation of chemokine expression [209].

Chemokines are small chemotactic cytokines that mediate the migration of leukocytes from the blood into tissues. There are four chemokine subfamilies designated CC, CXC, C, and CX3C based on the number of amino acids that separate their first two cysteine residues. Chemokines signal through G protein coupled receptors expressed on the surface of leukocytes. Receptors that interact

with CC chemokines are called CCR1-11 whereas those that bind CXC chemokines are designated CXCR1-5 [210]. The chemokines and receptors relevant to this thesis are presented in Table II. Chemokines are divided into two major groups. Homeostatic chemokines are often constitutively expressed and participate in immune surveillance by recruiting lymphocytes and dendritic cells to the secondary lymphoid organs where the stimulation of naive lymphocytes occurs [211]. Inflammatory chemokines are produced in response to inflammatory signals and mediate the recruitment of effector cells to the site of infection [210]. Leukocytes switch from constitutive receptors to inflammatory receptors as a result of cell activation and polarization. For example, immature dendritic cells express CCR5 and CCR1 before the uptake of antigen. Upon maturation, dendritic cells downregulate CCR5 and CCR1 expression and upregulate receptors such as CCR7, which directs the migration of dendritic cells to lymph nodes for the priming of T cells [212]. Naive T cells also express CCR7 whereas activated T lymphocytes express CCR1, CCR2, CCR5, CXCR3 and CXCR5, causing migration of activated T cells from the lymph nodes to the site of inflammation [213]. Monocyte trafficking to establish populations of tissue macrophages is mediated by an unknown constitutive receptor while the recruitment of macrophages and monocytes into inflamed tissue is orchestrated by CCR2 and CCR5 [214,215]. Despite this knowledge, the requirement and function of individual chemokine receptors and their ligands during *M. tuberculosis* infection has been difficult to determine, owing to a redundancy in both the chemokines and their receptors. Studies utilizing genetically modified mice have provided some insight into the roles of these molecules in anti-tuberculosis immunity.

CCL19 and CCL21 are homeostatic chemokines secreted by stromal cells in the paracortical T-cell zones of the secondary lymphoid organs. CCL21 is also expressed by the high endothelial venules and the lymphatic endothelium [216-218]. Both CCL19 and CCL21 signal through CCR7 to home naive T cells and dendritic cells to the secondary lymphoid organs [216-218]. Recent evidence has indicated that *M. tuberculosis* infection induces production of CCL19 and another

homeostatic chemokine, CXCL13, in the lungs of mice. Lung granulomas have also been suggested to contain areas resembling ectopic lymphoid follicles, together prompting the study of homeostatic chemokines during *M. tuberculosis* infection [219]. Absence of the CCR7 receptor did not affect control of a low dose tuberculosis infection in mice and caused no significant difference in survival or lung bacillary loads [219,220]. At a higher dose however, mice lacking CCR7 succumbed significantly earlier than CCR7-sufficient mice and had larger pulmonary burdens. Dendritic cell migration from the lung to the lymph node was impaired in CCR7-deficient mice, consistent with a role for CCR7 in the trafficking of dendritic cells [220]. The spatial arrangement of lymphocytes was also defective within the pulmonary granulomas of $CCR7^{-/-}$ mice, suggesting a role for CCR7 in the organization of the granuloma [219]. To further investigate the involvement of CCR7 in tuberculosis infection, mice lacking expression of the CCR7 ligands CCL19 and CCL21 were challenged with *M. tuberculosis*. Like CCR7, CCL19 and CCL21 were shown to be important for the migration of *M. tuberculosis*-infected dendritic cells from the lung to the draining lymph node. Since CCL19 and CCL21 were also involved in the generation of IFN-γ-producing T cells and their accumulation in the lung, their absence caused altered granuloma formation and diminished control of bacterial replication [221].

CXCL13 is a homeostatic chemokine produced by follicular dendritic cells and other stromal cells within the B-cell area of the secondary lymphoid organs. CXCL13 binds CXCR5 and directs homing of CXCR5-expressing lymphocytes to the follicular areas of the secondary lymphoid organs [222]. Mice deficient in CXCL13 expression have defective B cell trafficking [223,224] and lack peripheral lymph nodes [225]. $CXCL13^{-/-}$ mice challenged with *M. tuberculosi*s were able to accumulate an equivalent number of activated T cells in the lungs as their wild-type counterparts, due to alternate priming of IFN-γ-producing T cells within the spleens of mutant mice. However, a defect in the spatial organization of effector lymphocytes within the granuloma minimized the interaction of lymphocytes with infected myeloid cells, limiting phagocyte activation, and reducing the control of

bacterial growth in CXCL13$^{-/-}$ mice [221]. CXCL13 is therefore considered essential for the localization of T lymphocytes and macrophages within the granuloma, although it is not required for the generation of IFN-γ responses.

Expression of the CC chemokines CCL2, CCL3, CCL7, and CCL12 has been reported in mice following *M. tuberculosis* infection [226-228]. Murine macrophages infected with *M. tuberculosis* also express CCL4 and CCL5 [131]. The CCR1 receptor binds several of these chemokines, including CCL3, CCL5, and CCL7 and is present on leukocytes such as neutrophils, monocytes, eosinophils, and lymphocytes [229]. Yet, CCR1-deficient mice are indistinguishable from wild-type mice in their ability to control *M. tuberculosis* infection, with comparable bacterial burdens and normal granuloma formation [230]. CCR5 may compensate for the absence of CCR1, given that CCL3, CCL4, and CCL5 are also ligands for CCR5.

CCR5 is expressed on macrophages, granulocytes, CD8^{+} and Th1 CD4^{+} lymphocytes, and immature dendritic cells [231,232]. As in CCR1$^{-/-}$ mice, a deficiency in CCR5 did not impact on survival, pulmonary bacterial loads, or on number and size of granulomas following a low dose of aerosolized *M. tuberculosis* [233]. However, there was increased infiltration of T lymphocytes into the lungs of *Ccr5* gene-deleted mice. It was suggested that enhanced targeting of dendritic cells to the lymph node occurs in the absence of CCR5, resulting in a higher number of primed T lymphocytes [234]. In mice lacking the CCL5 ligand however, increased bacterial growth and impaired granuloma formation were observed in response to *M. tuberculosis* infection, potentially resulting from a decreased recruitment of macrophages, monocytes, and T cells [235]. Conflicting results between CCL5- and CCR5-deficient mice may reflect a redundancy in ligand specificity: CCL5 can bind CCR1 and CCR3 whereas CCR5 can be bound by up to eight ligands [236].

The CCR2 receptor binds CCL2 [237], CCL7 [238,239], CCL8 [240], CCL12 [241], and CCL13 [242,243] and is expressed on monocytes [214,244], macrophages [214,245,246], dendritic cells [247] and activated T lymphocytes [244]. Mice deficient in CCR2 are susceptible to moderate and high intravenous doses of *M. tuberculosis* (3.3-8 x 10^5 bacteria) and die early following infection, with 100-fold more bacteria in their lungs relative to wild-type animals [226]. By contrast, bacterial burdens in $CCR2^{-/-}$ mice were comparable to control mice during a low dose aerosol infection, and mutant mice did not succumb [228]. In both instances, macrophage recruitment to the lungs was reduced. Although the smaller number of macrophages was insufficient to control higher doses, it was enough to contain a lower dose of *M. tuberculosis*, suggesting that the immune response is more robust than required in the low dose model. Transgenic mice that constitutively express CCL2 (MCP-1), the major ligand for CCR2, were also shown to be more susceptible to tuberculosis than wild-type animals [248]. This result suggests either that constitutive binding of CCL2 to the CCR2 receptor causes desensitization of the receptor or that the concentration gradient of CCL2 is lost due to overexpression of the protein, resulting in a decreased migration of leukocytes to the site of infection. In mice lacking CCL2, a slightly diminished resistance to *M. tuberculosis* infection was observed, with only a transient increase in pulmonary bacterial growth and fewer macrophages migrating to the lungs [249,250]. The relative resistance of $CCL2^{-/-}$ mice compared to $CCR2^{-/-}$ mice may be explained by the functional redundancy existing among the chemokines that bind CCR2.

Expression of the IFN-γ inducible chemokines CXCL9 and CXCL10 has been detected following the *ex vivo* infection of murine macrophages with *M. tuberculosis* [227,251]. A deficiency in CXCL10 caused a delay in T cell migration to the lymph nodes, although no apparent defect in cellular migration to the lung was observed [131]. CXCL9, CXCL10 and CXCL11 signal through the CXCR3 receptor, which is expressed primarily on the surface of B cells, NK cells, dendritic cells, and activated T cells, particularly $CD4^+$ Th1 cells [252,253]. Absence

of CXCR3 in mice of a C57BL/6J background transiently impaired granuloma formation following a low dose of aerosolized *M. tuberculosis* H37Rv, causing a reduction in granuloma size, number and density. The early defect in granuloma formation was attributed to a decrease in the recruitment of cells signalling through CXCR3. However, $CXCR3^{-/-}$ C57BL/6J mice did not have altered survival or bacterial growth [254]. This finding contrasts a recent study which investigated CXCR3-deficiency in mice of a BALB/c or C57BL/6J background infected with a moderate dose of aerosolized *M. tuberculosis* Erdman. Both BALB/c and C57BL/6J *Cxcr3* gene-deleted mice exhibited a superior resistance to *M. tuberculosis* infection, characterized by lower bacterial burdens in the spleens of BALB/c mice and in the lungs of C57BL/6J and BALB/c mice. Mice devoid of CXCR3 also contained a higher number of $CD4^+$ T lymphocytes in the lung [255].

The chemokine receptor CX3CR1 and its ligand, fractalkine (CX3CL1), direct the migration of monocytes and T cells from the bloodstream into infected tissue [256]. Survival, lung bacillary load, and granuloma formation following a low dose of *M. tuberculosis* was monitored in mice lacking CX3CR1. Differences between $CX3CR1^{-/-}$ mutant mice and wild type controls were not observed, indicating that CX3CR1 does not have an essential role in the control of *M. tuberculosis* infection [257].

1.3.5 Pathogen Comparative Studies in the Mouse

While most genetic studies of host responsiveness in the mouse focus on host genes that result in differential responses towards the same mycobacterial strain, recent comparative studies have identified marked differences in the virulence of *M. tuberculosis* strains. Virulence is defined as the ability of bacteria to cause disease, a property that is investigated in terms of changes induced in the host. In the mouse, it is measured by pathogen-induced mortality, tissue bacillary load, and histopathology [258]. Based on these parameters, *M. tuberculosis* strains of the Beijing lineage were found to be more virulent than strains of the Somali and

Haarlem genotype families as well as *M. canetti*. Specifically, Beijing strains were associated with accelerated bacterial multiplication, more pronounced lung pathology, extensive pneumonia and earlier death compared to the other strains [259]. Beijing isolates also generated non-protective immune responses characterized by delayed *Ifng* transcription as well as early but transient *Tnfa* and *Nos2* transcription. Conversely, *M. canetti* strains evoked an early and effective immune response that was associated with extended survival. Importantly, vaccination with BCG conferred significantly less protection against bacteria of the Beijing lineage relative to the other strains [259].

The HN878 isolate, another member of the Beijing family of strains, displayed enhanced virulence in an independent pathogen comparative study. In comparison to two Euro-American clinical isolates (CDC1551, HN60) and two laboratory strains (H37Rv, Erdman), HN878 was associated with non-protective immunity characterized by the accumulation of macrophage deactivating cytokines such as IL-11 and IL-13 and a decrease in proinflammatory cytokines such as TNF-α, IL-1β, IL-12, and IFN-γ [260-262]. HN878 was also shown to induce production of the type 1 interferons (α and β), which have been associated with earlier mortality in mice [262,263]. The "hypervirulent" phenotype of HN878 and other Beijing strains has been partly attributed to the production of a phenolic glycolipid (PGL-tb) molecule [264]. Most *M. tuberculosis* strains lack expression of PGL-tb due to a seven-base pair deletion in the polyketide synthase (*pks1-15*) gene [265,266]. Experiments in a mouse model have indicated that Beijing strains synthesizing PGL-tb evoke a delayed and less robust immune response compared with isogenic variants not producing this molecule. Specifically, absence of PGL-tb caused an increased induction of TNF-α, IL-6 and IL-12 whereas overexpression of PGL-tb or treatment with purified PGL-tb resulted in a reduced production of these cytokines [264].

In another pathogen comparative study, the CH isolate of the East African-Indian lineage was shown to induce less IL-12p40 and greater IL-10 production *in vitro*

relative to CDC1551 and H37Rv. Strains of the East African-Indian lineage are characterized by the loss of RD750 [115], which encompasses the *Rv1519* and *Rv1520* genes [267]. Complementation of CH with *Rv1519* did not impact on IL-12p40 secretion but reversed the IL-10 stimulatory effect, suggesting this deletion contributes to immune subversion by CH strains [268]. Together, these studies demonstrate that bacterial components may alter the virulence of a strain by modifying host defence mechanisms. The implication of these observations for the present thesis is that host responses to mycobacteria can be modulated by the expression of strain specific bacterial factors.

1.3.6 Host Pathogen Associations in Mycobacterial Disease

The course and severity of *M. tuberculosis* infection depends on a complex interplay between host defence mechanisms and bacterial virulence factors that avoid or modify these responses. An emerging new area of research combines host and pathogen genetic strategies in the same experimental system to study host-pathogen interactions. This approach concurrently investigates the *in vivo* function of a particular bacterial virulence factor and host gene by combining bacterial and mouse mutants. This strategy was used to confirm a role for the *katG* gene of *M. tuberculosis* in resistance to host-derived reactive oxygen species [269]. KatG is a catalase-peroxidase-peroxynitritase which is speculated to catabolize peroxides produced through oxidative burst. Mice deficient in the gp91 subunit of NADPH oxidase ($gp91^{phox-/-}$) are incapable of generating reactive oxygen species yet are relatively resistant to *M. tuberculosis* infection [270,271]. Deletion of the *katG* gene produced mutants which were attenuated in C57BL/6J and iNOS-deficient mice but not in $gp91^{phox-/-}$ mice and $gp91^{phox-/-}$ $iNOS^{-/-}$ double knockout mice. These results indicate that KatG detoxifies peroxides produced by the phagocyte NADPH oxidase but is dispensable in its absence [269].

A similar approach was used to identify *M. tuberculosis* genes involved in nitric oxide resistance. A transposon-generated mutant of *M. tuberculosis* with an insertion in *Rv2115c* had increased sensitivity to reactive nitrogen intermediates

in vitro. *Rv2115c* encodes a presumptive proteosomal adenosine triphosphatase (ATPase). *Rv2115c* mutants were attenuated in C57BL/6J mice but displayed intermediate virulence in iNOS$^{-/-}$ mice which are unable to produce nitric oxide. These results suggest an involvement of the bacterial proteasome in resistance against nitrosative stress [272]. In another series of experiments, mice deficient in iNOS and their wild-type controls were infected with virulent *M. tuberculosis* H37Rv or avirulent H37Ra to examine the effects of varying bacterial virulence and host genetic susceptibility. As expected, H37Rv infection of iNOS-deficient mice produced the most severe outcome. These mice developed acute lung injury characterized by neutrophil infiltration and widespread necrosis that ultimately resulted in death. Wild-type mice survived the duration of the experiment although they developed a chronic infection with elevated H37Rv pulmonary burdens. Conversely, iNOS-deficient mice were able to control infection with H37Ra and bacterial counts were low in both mouse strains. The authors concluded that the protective role of iNOS is dependent on *M. tuberculosis* virulence factors that are present H37Rv but absent in H37Ra [273], suggesting that infection outcome is governed by reciprocal effects between host and pathogen. Observations in humans have provided tentative evidence in support of this hypothesis.

An increasing number of human studies indicate that specific strains of *M. tuberculosis* are more prevalent in certain geographical areas [20]. The observation of geographically clustered pathogen populations suggests that particular pathogen strains are preferentially associating with specific human populations, thereby transmitting and causing disease among specific ethnic groups. The six major geographically constrained phylogenetic lineages of *M. tuberculosis* (East-Asian, East-African-Indian, Euro-American, Indo-Oceanic and West-African-1 and -2 lineages) were based largely on isolates from San Francisco [115] and were independently replicated using a Montreal cohort [274]. These geographical associations are highly stable [275] and were likely shaped by human migration and demography [126], suggesting that humans and

M. tuberculosis strains have co-evolved. Co-evolution is defined as reciprocal, adaptive genetic changes between two or more interacting species. Major selective factors for co-evolution and co-adaptation include pathogen infectivity and host resistance [276]. These co-evolutionary selective pressures may also partly explain the geographic variation in BCG vaccine efficacy [4,277]. Although these geographical studies support the notion of co-adaptation, confounding sociological and epidemiological factors cannot be discounted.

Molecular evidence for co-evolution has been obtained from the study of interacting host-pathogen genotypes. The recent association of host and *M. tuberculosis* genotypes in disease development [278] supports the suggestion of co-adaptation and indicates that host-pathogen interactions can influence disease outcome. Specifically, it was shown that disseminated disease occurs more frequently in Vietnamese adults bearing a *TLR2* susceptibility polymorphism infected with strains of the highly prevalent East Asian/Beijing lineage. In a Ghanian study population, an association was noted between pulmonary disease caused by the *M. africanum* strains of the West-African-2 lineage and an exonic non-synonymous variant of the *ALOX5* gene [279]. A variant in the *IRGM* gene was also shown to be protective against *M. tuberculosis* strains of the Euro-American lineage [280], which lack expression of the PGL-tb molecule [115]. The immunomodulatory properties of PGL-tb suggest that non-Euro-American strains may alter IRGM-mediated immune mechanisms via PGL-tb.

Collectively, these findings support the importance of host-pathogen combinations for increased tuberculosis risk and suggest that the host genetic control of tuberculosis varies across *M. tuberculosis* strains. This could partly explain why population-based studies which reflect the natural genetic variation in both the host and pathogen fail to detect strong genetic effects while high heritability is observed in twin studies. A major genetic effect on tuberculosis susceptibility was also identified in a study of a tuberculosis outbreak involving an extended Aboriginal Canadian family [281]. To model gene-environment

interactions, individuals were assigned to risk (liability) classes. Significant evidence for linkage was obtained only when the liability classes were specified, outlining the importance of gene environment interactions. Since the most common environmental factor for any infectious disease is the pathogen, it is reasonable to speculate that at least part of the missing heritability of tuberculosis disease may be explained by pathogen variability and possible host-pathogen genetic fits. This hypothesis was formally tested in the present thesis.

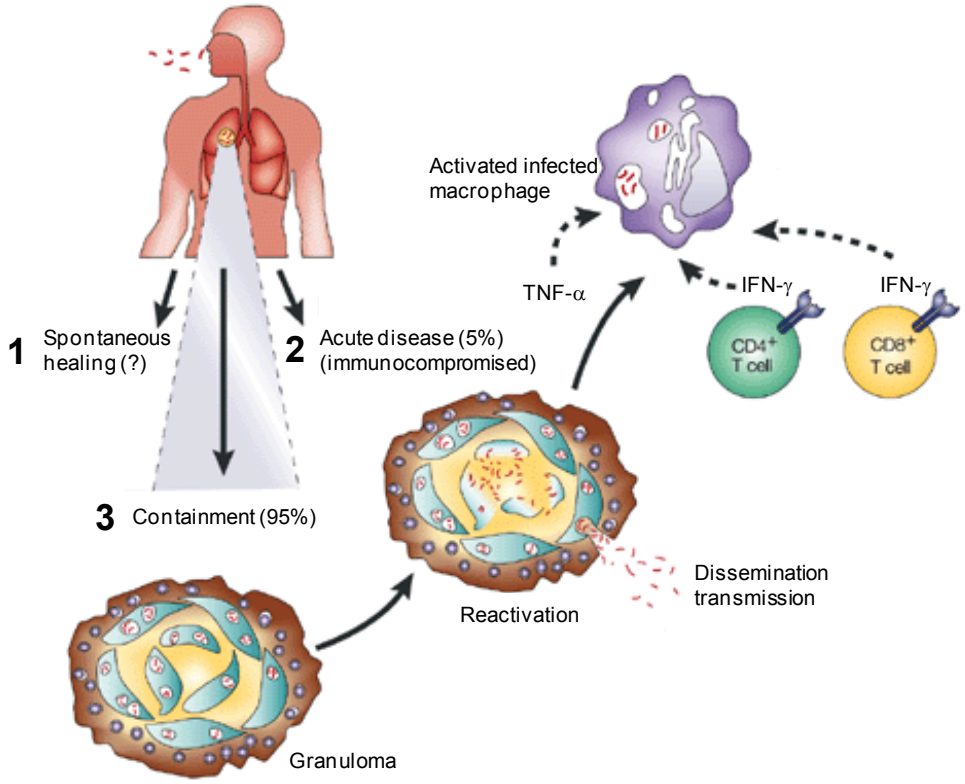

Figure 1. Course of *M. tuberculosis* infection. Exposure to *M. tuberculosis* causes three possible outcomes: (1) Abortive infection resulting in spontaneous healing; (2) Acute disease that develops directly following infection, as seen in immunocompromised individuals; and (3) Containment. Among the 95% of individuals who contain the primary infection, an additional 5% will develop reactivation tuberculosis. The granuloma is the site of bacterial containment and host defense. IFN-γ and TNF-α produced by T cells activate macrophages to exert phagosomal maturation and to produce antimicrobial molecules such as reactive nitrogen and oxygen intermediates. (Adapted by permission from Macmillian Publishers Ltd: Nature Reviews Immunology [13], copyright 2001).

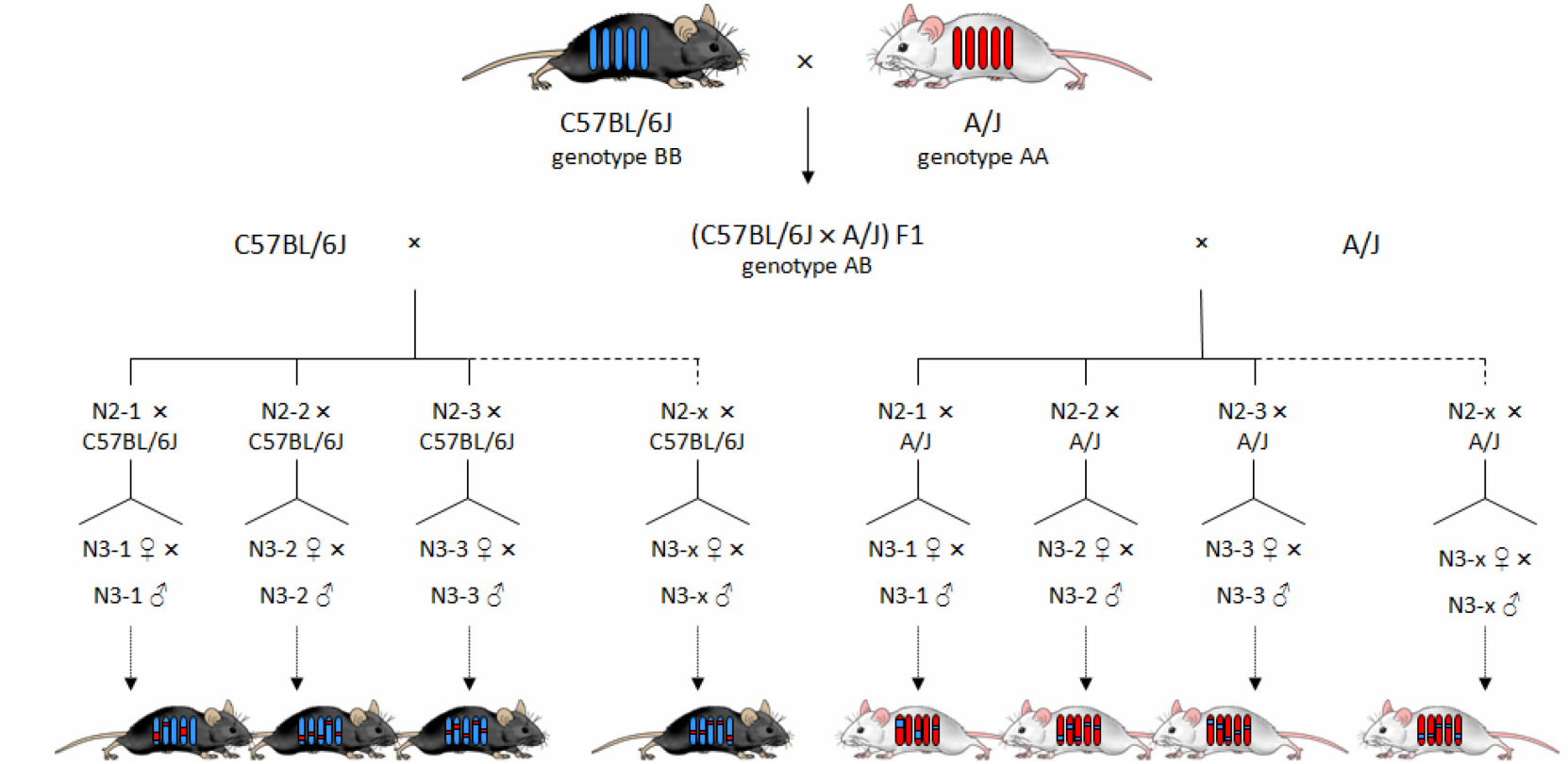

Figure 2. Breeding scheme for recombinant congenic strains. Recombinant congenic strains are derived by successive inbreeding following the double backcross of F1 mice to a receiver strain. The AcB/BcA panel was derived from A/J and C57BL/6J progenitors. Strains of the AcB set [(F1 × A/J) × A/J inbred] contain on average 13.25% of the donor C57BL/6J genome (blue) on the recipient A/J genetic background (red). BcA strains [(F1 × C57BL/6J) × C57BL/6J inbred] carry approximately 13.24% of the donor A/J genome on the C57BL/6J genetic background [31].

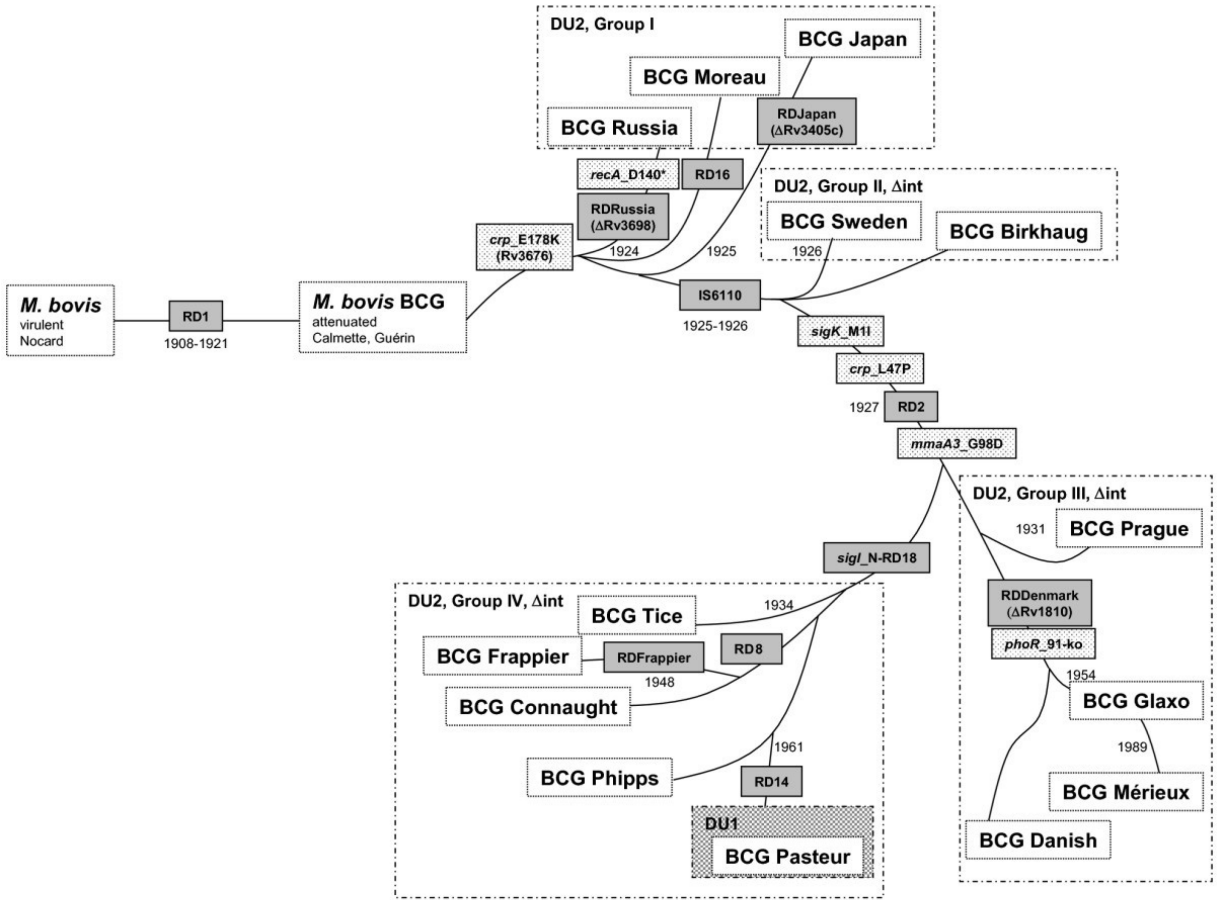

Figure 3. BCG vaccine phylogeny. BCG vaccines are phylogenetic descendants of an ancestral BCG strain originally derived from virulent *M. bovis*. Genetic alterations including deletion of the regions of difference (RD), single nucleotide polymorphisms, and duplications (DU) are depicted. BCG strains are distributed into four groups based on the configuration of DU2. (Adapted from Keller *et al* [49], copyright BioMed Central Publishers 2008).

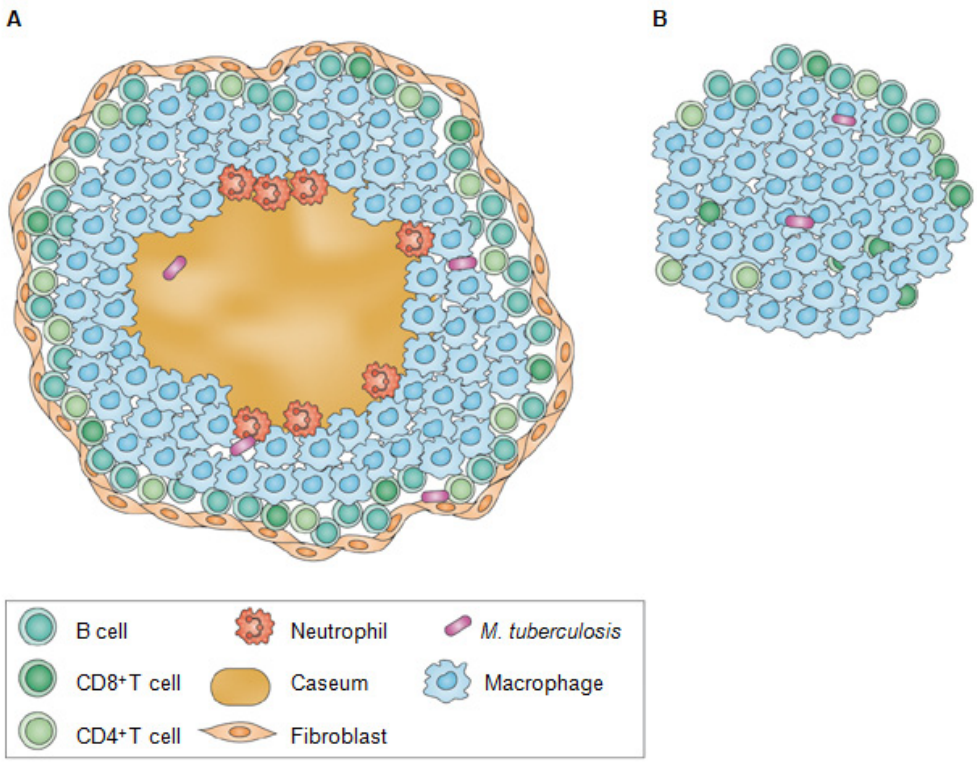

Figure 4. The tuberculous granuloma. (A) The typical human granuloma is composed of epithelial macrophages, neutrophils, and a cuff of lymphocytes (B cells and $CD4^+$ and $CD8^+$ T cells) surrounded by peripheral fibrosis. The center is caseous, a necrotic state consisting of dead macrophages and other cells. (B) The classic murine granuloma consists primarily of macrophages and lymphocytes. This lesion is also observed in humans. (Adapted by permission from Macmillian Publishers Ltd: Nature Reviews Microbiology [133], copyright 2009).

Table 1. Response phenotypes in mouse knockout models infected with *M. tuberculosis*

Knockout Strain	Function	Effect*	References
ADAPTIVE IMMUNITY			
αβ T cells	Cell-mediated immunity	+++++	182
β2-microglobulin	Cell surface expression and stability of MHC class I	+++ (?)	183-185
γδ T cells	Immune surveillance	DD	182,186,187
B cells	Humoral immunity	DD	176-179
$CD4^+$ T cells	Cell-mediated (Th1) and antibody mediated (Th2) immunity	+++	181
$CD8^+$ T cells	Cytotoxicity	++	184
MHC class I	Antigen presentation to CD8+ T cells	++	182
MHC class II	Antigen presentation to CD4+ T cells	++++	181,182
CYTOKINES & CYTOKINE RESPONSIVE ELEMENTS			
IFN-γ	Macrophage activation	+++++	188,189
IFN-γR1	Subunit of the IFN-γ receptor	+++++	189
IL-12p35	Subunit of bioactive IL-12p70	+++	107
IL-12p40	Subunit of bioactive IL-12p70 and IL-23	++++	107,190
IL-12p70	Differentiation of CD4+T cells into Th1 cells; IFN-γ inducing factor	++++	107
IL-23p19	Subunit of bioactive IL-23	0	193
IL-4	Differentiation of CD4+T cells into Th2 cells; B cell activation	0/-	198,201,202
IL-4Rα	Subunit of the IL-4 receptor	0	200
iNOS	Synthesis of reactive nitrogen intermediates	++++(+)	182,189
LRG-47	IFN-g-inducible GTPase	+++++	189
STAT-1	IFN-g receptor signaling molecule	+++++	189
STAT-6	IL-4 receptor signaling molecule	0	200
TNF-α	Macrophage activation	+++++	203
TNFRI	Receptor for TNF-α, member of the TNF receptor superfamily	+++++	204

Table 1. Response phenotypes in mouse knockout models infected with *M. tuberculosis*, continued

Knockout Strain	Function	Effect*	References
CHEMOKINES & CHEMOKINE RECEPTORS			
CCL2	Chemotactic for monocytes, macrophages, dendritic cells and T cells	+	249,250
CCL5	Chemotactic for T cells, monocytes and macrophages	+	235
CCL19/CCL21	Homing of lymphocytes and dendritic cells to secondary lymphoid organs	+	221
CCR1	Receptor for CCL3, CCL5 and CCL7	0	230
CCR2	Receptor for CCL2, CCL7, CCL8, CCL12 and CCL13	DD	226,228
CCR5	Receptor for CCL3, CCL4 and CCL5	0	233
CCR7	Receptor for CCL19 and CCL21	DD	219,220
CXCL10	Chemotactic for T cells, NK cells, and dendritic cells	0	131
CXCL13	Chemotactic for B cells	+	221
CXCR3	Receptor for CXCL9, CXCL10 and CXCL11	0/+	254,255
CX3CR1	Receptor for CX3CL1	0	257

* Effect: + slightly susceptible to +++++ extremely susceptible, 0 no change in susceptibility, 0/+ and 0/- conflicting data obtained from different studies, (?) susceptibility attributed to an overload of iron, ++++(+) level of susceptibility differed between two studies and DD dose dependent

Adapted from Henry Stewart Publications: Briefings in Functional Genomics & Proteomics [282], copyright 2005.

Table 2. Chemokines and their receptors

Name	Scy name	Alternative names	Receptor
CC family			
CCL1	Scya1	I-309, TCA-3	CCR8
CCL11	Scya11	Eotaxin	CCR3
CCL12	Scya12	MCP-5	CCR2
CCL13	Scya13	MCP-4	CCR2, CCR3
CCL17	Scya17	TARC	CCR4
CCL19	Scya19	MIP-3β, ELC, Exodus-3	CCR7
CCL2	Scya2	MCP-1	CCR2
CCL20	Scya20	MIP-3α, LARC, Exodus-1	CCR6
CCL21	Scya21	6Ckine, SLC, Exodus-2, TCA-4	CCR7
CCL3	Scya3	MIP-1α	CCR1, CCR5
CCL4	Scya4	MIP-1β	CCR5
CCL5	Scya5	RANTES	CCR1, CCR3, CCR5
CCL7	Scya7	MCP-3, MARC	CCR1, CCR2, CCR3
CCL8	Scya8	MCP-2	CCR2, CCR3
CCL9	Scya9	MRP-2, CCF18, MIP-1g	Unknown
CXC family			
CXCL1	Scyb1	Gro-α	CXCR2, CXCR1
CXCL10	Scyb10	IP-10	CXCR3
CXCL11	Scyb11	I-TAC	CXCR3
CXCL12	Scyb12	SDF-1α/β	CXCR4
CXCL13	Scyb13	BLC, BCA-1	CXCR5
CXCL15	Scyb15	Lungkine	Unknown
CXCL5	Scyb5	ENA-78, LIX	CXCR2
CXCL8	Scyb8	IL-8	CXCR1, CXCR2
CXCL9	Scyb9	MIG	CXCR3
CX3C family			
CX3CL1	Scyd1	Fractalkine, Neurotactin	CX3CR1

Preface to Chapter 2

Observations in humans suggest that strains of *M. tuberculosis* preferentially associate with specific human populations to cause disease. While these findings support the notion that host and pathogen factors jointly determine the course of *M. tuberculosis* infection, they can also be confounded by unknown factors. In this regard, mouse models are ideal for investigating the contribution of host and pathogen to susceptibility to mycobacterial disease. The A/J and C57BL/6J mouse strains display variation in their response to *M. tuberculosis* and BCG. A/J mice are susceptible to infection with *M. tuberculosis* whereas C57BL/6J mice are resistant. This is in striking contrast to BCG infection, where A/J mice are classically considered resistant and C57BL/6J are susceptible. The disparity in susceptibility of the two mouse strains to the different mycobacteria suggests a reciprocal effect of host and pathogen in the response to infection. In Chapter 2, we jointly examined the effect of host and pathogen genetic variation on common biological and mechanistic phenotypes.

CHAPTER 2
Differential effects of host genetic background and mycobacterial strain on susceptibility to infection

---

Tania Di Pietrantonio[1,2,3], José A. Correa[4], Marianna Orlova[1,2] , Marcel A. Behr[1,3], and Erwin Schurr[1,2,3]

[1] McGill Centre for the Study of Host Resistance, Research Institute of the McGill University Health Centre, Montreal, Quebec, Canada

[2]Department of Human Genetics, McGill University, Montreal, Quebec, Canada

[3]Department of Medicine, McGill University, Montreal, Quebec, Canada

[4]Department of Mathematics and Statistics, McGill University, Montreal, Quebec, Canada

ABSTRACT

The present study examined the differential contribution of host genetic background and mycobacterial strain variability on biological and mechanistic phenotypes of infection. For this purpose, A/J and C57BL/6J mice were infected intravenously with a low dose of *Mycobacterium tuberculosis* H37Rv or the Russia and Pasteur substrains of *Mycobacterium bovis* Bacille Calmette Guérin (BCG). As biological phenotypes we selected the number of pulmonary bacterial counts (CFU) at 1, 3 and 6 weeks post-infection as well as lung histopathology at 6 weeks post infection. Compared to the host genetic background, the mycobacteria exerted a stronger effect on variation in lung CFU, although differences in pulmonary burdens across the three mycobacteria were more pronounced in A/J mice. Changes in lung histopathology were primarily dependent upon the mycobacterial strain. As mechanistic phenotypes, pulmonary transcript levels of select cytokines (*Ifng*, *Il12b*, *Il4*) and 34 chemokines and their receptors were measured. The differences in induction of these immune messenger genes between A/J and C57BL/6J mice were modest and generally failed to reach significance. By contrast, all three mycobacterial strains induced significant variance in a subset of the immune messenger genes that again were more evident in A/J relative to C57BL/6J mice. Hence, in our experimental mouse model mycobacterial variation was the major regulator while host genetic background was an important modulator of host responses. These results demonstrated the importance of considering the joint effects of mycobacterial strain and host genetic background in susceptibility to mycobacterial infections.

INTRODUCTION

Exposure of humans to *Mycobacterium tuberculosis*, the cause of tuberculosis, induces a highly variable response. Among persons exposed to *M. tuberculosis*, only 50-70% become infected, and of those infected only approximately 10% develop clinical disease. There is now clear evidence for the important impact of host genetic factors on this variable response [1-3]. Evidence for an equally important role of *M. tuberculosis* strain variability is emerging (reviewed in [4,5]). However, it is not known if susceptibility to infection and disease is the result of host and pathogen factors acting independently or is the result of joint effects between host genes and the *M. tuberculosis* strain. Although studies have examined the impact of host background and mycobacterial type separately, strategies that focus on the simultaneous analysis of host and mycobacteria in disease expression have been lacking.

We have used well-characterized mouse strains and mycobacteria to study their simultaneous contribution to quantitative measures of host susceptibility. We employed *M. tuberculosis* and two strains of *M. bovis* Bacille Calmette Guerin (BCG): BCG Russia and BCG Pasteur. The most notable genetic differences between *M. tuberculosis* and BCG strains are chromosomal deletions, such as the region of difference 1 (RD1) [6,7]. BCG Russia and BCG Pasteur are the most phylogenetically distant members of the BCG vaccine family. In addition to RD1, Rv3698 (RD Russia) is the only known orthologue to be deleted from BCG Russia [8]. In BCG Russia, the promoter region of the *phoP* gene contains an IS*6110* element [9] which may have implications for virulence. BCG Pasteur lacks this insertion, resulting in a lower expression of *phoP* [9]. Compared to BCG Russia, BCG Pasteur has also three additional chromosomal segments deleted: RD2, n-RD18 and RD14 [10-12].

As hosts, we employed the A/J and C57BL6/J inbred mouse strains. Mice of these strains differ in their response to mycobacteria. Following aerosol or intravenous infection with *M. tuberculosis*, susceptible A/J mice succumb more

rapidly compared to C57BL/6J mice [13,14]. The early death of A/J animals is caused by a progressive interstitial pneumonitis characterized by widespread tissue necrosis and an inability to form cohesive granulomas. In contrast, C57BL/6J mice form functional granulomas and survive for extended periods. Despite these differences, early pulmonary *M. tuberculosis* replication is similar between C57BL/6J and A/J mice [13,15]. A/J and C57BL6/J mice also differ in their innate susceptibility to low dose infection with BCG Montreal [16,17]. The differential susceptibility in early growth of BCG Montreal has been shown to be due to two allelic forms of the *Nramp1* gene [17]. To avoid an overwhelming effect of the *Nramp1* gene on host responses, we did not employ BCG Montreal in our study. In addition, we focused our analysis on pulmonary responses which are less impacted by *Nramp1* [18].

In the present study, the A/J and C57BL/6J mouse strains were infected with a low dose of BCG Russia, BCG Pasteur or *M. tuberculosis* H37Rv and a set of host response phenotypes was characterized in the lungs of both mouse strains in a time-dependent manner. This design permitted the parallel investigation of the host genetic background and the mycobacterial strain on the magnitude and variation of the host responses.

MATERIALS AND METHODS

Animals

A/J and C57BL/6J mice were purchased from the Jackson Laboratory (Bar Harbor, ME) and housed in the rodent facility of the Montreal General Hospital. All animal procedures were performed in accordance with the guidelines outlined by the Canadian Council on Animal Care and approved by the Animal Care Committee of McGill University.

Infection of mice

BCG Russia (ATCC 35740) and BCG Pasteur (ATCC 35734) were transformed with a Hygromycin resistance vector [19]. Recombinant BCG Russia, recombinant BCG Pasteur, and *M. tuberculosis* H37Rv (Pasteur) were grown on a rotating platform at 37°C in Middlebrook 7H9 medium (Difco Laboratories, Detroit, MI) containing 0.05% Tween 80 (Sigma-Aldrich, St. Louis, MO) and 10% albumin-dextrose-catalase (ADC) supplement (Becton Dickinson and Co., Sparks, MD). At early logarithmic phase (OD_{600} = 0.4-0.5), bacterial cultures were sonicated to disperse clumps and diluted accordingly. For intravenous infection, mice were injected with ~3×10^3 colony forming units of *M. tuberculosis* or BCG in the lateral tail vein. Inoculum doses were verified by serial dilution plating on Middlebrook 7H10 agar (Difco Laboratories, Detroit, MI) supplemented with oleic acid-albumin-dextrose-catalase (OADC) enrichment (Becton Dickinson and Co., Sparks, MD). For aerosol infection, BCG Russia and BCG Pasteur cultures were grown to an OD_{650} nm of 0.4 and diluted to 3.5×10^7 CFU/ml. Mice were infected for 10 minutes in an inhalation exposure system (In-Tox Products, Moriaty, NM). At one day post-infection, infectious doses of ~2×10^3 were confirmed by homogenizing lungs in 2 ml of 0.025% Saponin-PBS using large tissue grinders (TYCO Healthcare Group, Mansfield, MA). 200 μL of the homogenate was plated on Middlebrook 7H10 agar (Difco Laboratories, Detroit, MI) supplemented OADC enrichment (Becton Dickinson and Co., Sparks, MD) and BACTEC PANTA PLUS (Becton Dickinson and Co., Sparks, MD).

Pulmonary BCG growth

Infected mice were sacrificed by CO_2 inhalation after 1, 3 and 6 weeks post-infection. Lungs were aseptically removed and placed in 0.025% Saponin-PBS. BCG-infected lungs were homogenized mechanically using a Polytron PT 2100 homogenizer (Brinkman Instruments, Westbury, NY) and lungs infected with H37Rv were disrupted using large tissue grinders (TYCO Healthcare Group, Mansfield, MA). Homogenates were serially diluted tenfold and plated on Middlebrook 7H10 agar containing OADC enrichment and hygromycin B (Wisent Inc., St.-Bruno, QC) or BACTEC PANTA PLUS (Becton Dickinson and Co., Sparks, MD) with our modifications. Bacterial enumeration was performed after a 3 or 6-week incubation at 37°C.

RNA isolation

For the isolation of total cellular RNA, lungs were harvested from control and BCG Pasteur-, Russia-, or H37Rv-infected mice at 1, 3 or 6 weeks post-infection and stored in RNA later (QIAGEN, Mississauga, ON). Lungs were mechanically disrupted and RNA was purified using the RNeasy Mini Kit (QIAGEN, Mississauga, ON) according to the manufacturer's instructions. Genomic DNA was removed during the RNA extraction process using the RNase-free, DNase kit (QIAGEN, Mississauga, ON). The concentration and integrity of all RNA samples was assessed using the NanoDrop ND-1000 spectrophotometer (NanoDrop Technologies, Wilmington, DE) and the Agilent Bioanalyzer 2100 (Agilent Technologies, Palo Alto, CA).

Gene quantification studies

Synthesis of first-strand complementary DNA (cDNA) was performed with 0.5 μg of total RNA using the QuantiTect Reverse Transcription Kit (QIAGEN, Mississauga, ON) as recommended by the manufacturer. QuantiTect Gene Expression Assays for *Ifng*, *Il12b*, *Il4*, and the *Gapdh* endogenous control gene were purchased from QIAGEN (QIAGEN, Mississauga, ON) (Table 1). cDNA

was amplified using Quantitect reagents on the Rotor-Gene 3000 (Corbett Research, Sydney, Australia) as specified.

For multi-gene expression profiling, samples were reverse transcribed with the RT² First Strand Kit (SuperArray Bioscience Corporation, Frederick, MD). cDNA was amplified on the ABI Prism® 7500 (Applied Biosystems, Foster City, CA) using either the Mouse Inflammatory Cytokines and Receptors RT² Profiler PCR Array (APMM-011A) or the Mouse Chemokines & Receptors PCR Array (PAMM-022A) in combination with the RT² Real-Time PCR SYBR Green/ROX Master Mix (SuperArray Bioscience Corporation, Frederick, MD). Of the 84 genes, 34 met our inclusion criteria. These genes were included in both sets of arrays and dissociation assays did not show evidence of cross-hybridization. Using the NormFinder [20] and geNorm [21] algorithms, *Gusb*, *Hprt*, *Hspcb*, *Gapdh*, and *Actb* were determined to be a suitable set of endogenous control genes for normalization.

Histopathology

Mice were euthanized by CO_2, perfused with PBS, and fixed with 10% buffered formalin. Lungs of infected mice were fixed in formalin overnight and preserved in ethanol until they were embedded in paraffin, sectioned and stained with haematoxylin-eosin.

Statistical methods

A two-way analysis of variance (ANOVA) (SAS Institute, Cary, NC) was performed to investigate differences in bacterial replication across time following intravenous infection. An analysis of residuals for this model detected violations of the assumptions of normality and heterogeneity of variance of errors across groups for ANOVA. Thus, CFU values were log-transformed (natural logarithm) and an ANOVA model with unequal variances with residual variances for each combination of mouse or bacterial strain and time was considered [22]. We used the procedure PROC MIXED available in SAS, version 9.2 (SAS Institute Inc., Cary,

NC) to fit the model. Degrees of freedom were adjusted using the Kenward-Roger correction [23] because the groups were unbalanced in the sense that groups did not have the same number of subjects. Pair-wise post-hoc comparisons of means between bacterial strains at each time were performed, where warranted, and p-values were adjusted for multiple testing with the simulation-based adjustment for multiple testing implemented in the SAS %SimTests macro [24] to ensure an overall family-wise error rate (fwer). Differences in the log-transformed pulmonary loads following aerosol infection were statistically examined with the Student's t test for unequal variances. $P<0.05$ was used to indicate statistical significance.

Fold changes of transcript levels between infected and control samples were determined by the $\Delta\Delta C_T$ calculation [25]. Data are presented as the mean fold difference ± S.E.M on a logarithm dualis ($\log_2$) scale, which assumes an optimum PCR efficiency (E) of 2. When applicable, confidence intervals (CI) of 95% were computed with a lower limit $2^{-\Delta\Delta CT - Z\ 1.960\ S.E.M}$ and an upper limit $2^{-\Delta\Delta CT + Z\ 1.960\ S.E.M.}$, where $-\Delta\Delta C_T \pm Z_{1.960}$ S.E.M. denotes the upper and lower confidence limits of the change $\Delta\Delta C_T$, S.E.M. is the standard error of the mean change $-\Delta\Delta C_T$, and $Z_{1.960}$ is the 95th-percentile of the standard normal distribution [26]. Differences in *Ifng*, *Il12b*, and *Il4* expression were analyzed by a two-way ANOVA model (SAS Institute, Cary, NC) with unequal variances. Residual variances for each combination of mouse or bacterial strain and time were considered [22]. We used the procedure PROC MIXED available in SAS, version 9.2 (SAS Institute Inc., Cary, NC) to fit the model. Real-time Superarray data was statistically examined using ANOVA for unequal variances with a Benjamini and Hochberg multiple test correction (GeneSpring GX software, Agilent Technologies, Palo Alto, CA).

RESULTS

To analyze the extent to which mycobacterial strain and host background contribute to susceptibility, we used C57BL/6J and A/J mice and *M. tuberculosis*, BCG Russia or BCG Pasteur as host and mycobacterial variants, respectively. Mice were intravenously infected with a low dose (~3×10^3 bacilli) of bacteria and multiple phenotypic traits of infection were measured at various times post-infection. Since the ability of mycobacteria to replicate in the lungs is a critical indicator of host susceptibility to infection, pulmonary bacterial loads were compared in mice of both strains at 1, 3, and 6 weeks post-infection by two-way ANOVA. The kinetics of lung CFU were significantly different for *M. tuberculosis*, BCG Russia, and BCG Pasteur in both A/J and C57BL/6J mice (Figure 1). In A/J animals, the log CFU of the three strains of bacteria were significantly different [$F(2,15) = 97.20$, $P<0.001$], and CFU changed with time [$F(2,13.3) = 34.39$, $P<0.001$]. In addition, an interaction between bacterial strain and time [$F(4,11.6) = 21.75$, $P<0.001$] indicated that differences in bacillary burdens were more pronounced at particular time points. *Post hoc* testing revealed that at all three time points, *M. tuberculosis* CFU were greater than BCG Pasteur ($P_{Adj}=0.019$, $P_{Adj}<0.001$, and $P_{Adj}<0.001$ at weeks 1, 3, and 6 respectively) and BCG Russia counts ($P_{Adj}=0.019$, $P_{Adj}=0.002$, and $P_{Adj}=0.019$ at weeks 1, 3, and 6 respectively). Significant differences between the pulmonary loads of BCG Pasteur and BCG Russia were identified at the 6 week time point only ($P_{Adj}<0.001$). Likewise, in the C57BL/6J mouse strain, lung CFU of *M. tuberculosis*, BCG Russia, and BCG Pasteur differed significantly [$F(2,17.5) = 40.20$, $P<0.001$]. Again, time after infection had strong impact on CFU yielding an F ratio of $F(2,10.6) = 17.39$, $P<0.001$. An interaction between time and CFU [$F(4,13.1) = 10.00$, $P<0.001$] demonstrated that differences between bacterial CFU varied with time. By *post hoc* testing, significant differences in the pulmonary loads were observed at the 6 week time point only, with BCG Pasteur having lower counts than *M. tuberculosis* ($P_{Adj}<0.001$) and BCG Russia ($P_{Adj}=0.001$). When the host component in the contribution to lung CFU was analysed, the mouse strains did not differ significantly in the extent of

BCG Russia or BCG Pasteur pulmonary replication (Figure 1). However, a mouse strain effect was observed in *M. tuberculosis* proliferation [$F(1,18.3) = 12.62$, $P=0.002$] where pulmonary loads were significantly larger in A/J mice (least square mean [LSM] of $\log_{10}$CFU=3.96, standard error [SE]=0.14) compared to C57BL/6J animals (LSM of $\log_{10}$CFU=3.13, SE=0.20) and there was a significant effect of time [$F(2,13.5) = 13.56$, $P<0.001$]. The results indicated that differences in mycobacterial burdens were maximal at the 6 week time-point and were more pronounced in the A/J strain.

Unlike BCG Russia or *M. tuberculosis*, BCG Pasteur was consistently associated with low bacillary counts in the lungs of both mouse strains. This raised the question if the low pulmonary burden of BCG Pasteur reflected the inability of BCG Pasteur to home in the lung following intravenous infection, or if BCG Pasteur had a general limited capacity to multiply in lungs. To test the ability of Pasteur to replicate in the lung, bacilli were directly implanted into the lung by aerosol. Using a high dose aerosol infection model (~2 $x10^3$ bacilli), the counts of BCG Pasteur and BCG Russia were compared at the 6 week time point. BCG Pasteur still had smaller pulmonary burdens in both the A/J ($P= 0.001$) and C57BL/6J ($P= 5.7 \times 10^{-5}$) mice (Figure 2), suggesting a low ability of BCG Pasteur to thrive in the lung. In addition, a difference in BCG Russia pulmonary loads was observed between the mouse strains ($P= 0.009$) with C57BL6/J mice displaying higher CFUs. This was in contrast to *M. tuberculosi*s that reached higher bacterial counts in the lungs of A/J mice following intravenous infection (Figure 1). These results demonstrated that differences in pulmonary bacterial counts reflect a different ability of the three bacterial strains to grow in lungs, and this difference was significantly dependent on the mouse strain.

The histological trait of lung pathology was examined in infected A/J and C57BL/6J mice and revealed marked differences, particularly due to the infecting bacterial strain. At 6 weeks, inflammatory lesions consisted predominantly of mononuclear cells including macrophages and lymphocytes. A few epitheloid

cells were observed in BCG Pasteur- and BCG Russia-infected animals, but were more numerous during *M. tuberculosis* infection. *M. tuberculosis* infection caused pulmonary vascular congestion and thickening of the vascular walls, which did not occur in response to BCG (data not shown). A few microgranulomas were observed among the BCG-infected animals, but these were characteristically smaller and much less developed compared to granulomas seen with *M. tuberculosis*. The overall lung involvement was also much reduced during BCG infection, with visibly normal lung parenchyma and only a few isolated lesions. Lesions collectively occupied less than 10% of the lung volume during BCG infection, while up to 30% of the lung tissue was involved during *M. tuberculosis* infection. Although inflammation was relatively mild in response to both strains of BCG, lesions appeared less extensive during BCG Russia infection, particularly in the A/J mouse strain (Figure 3). BCG-induced lesions in A/J mice were intraparenchymal or perivascular and dominated by lymphocytes admixed with macrophages. The extent of granulomatous involvement was slightly smaller compared to C57BL/6J animals. The cellular distribution was mainly peribronchovascular and perivascular in the C57BL/6J strain, although a few parenchymal lesions were observed. Lungs of A/J and C57BL/6J mice infected with *M. tuberculosis* were indistinguishable despite differences in bacterial loads.

Next, we investigated if and to what extent the kinetics of pulmonary *Ifng* transcript levels differed in either A/J or C57BL/6J mice between the mycobacterial strains following intravenous infection (Figure 4). In A/J mice, we identified an effect of bacteria on *Ifng* production [$F(2,10.7) = 127.30$, $P<0.001$]. Time yielded an F ratio of $F(2,12.4) = 45.71$, $P<0.001$, and the interaction was significant [$F(4,9.56) = 16.42$, $P<0.001$] indicating that bacteria-specific effects varied with time. As shown by *post-hoc* analysis, *M. tuberculosis* induced significantly more *Ifng* than BCG Pasteur ($P_{Adj}=0.004$, $P_{Adj}<0.001$, and $P_{Adj}=0.015$ at weeks 1, 3, and 6 respectively) and BCG Russia ($P_{Adj}=0.002$, $P_{Adj}<0.001$, and $P_{Adj}=0.002$ at weeks 1, 3, and 6 respectively). A difference

between BCG Pasteur and BCG Russia was detected at the 3 week time-point only (P_{Adj}<0.001). In C57BL/6J mice, expression of *Ifng* also differed significantly across the three mycobacterial strains [F(2,11.5) = 34.08, P<0.001] and across time [F(2,11.2) = 28.44, P<0.001] with a significant interaction between the two effects [F(4,8.93) = 6.06, P=0.012]. *Post-hoc* tests showed that *Ifng* levels induced by *M. tuberculosis* were larger than BCG Pasteur at weeks 1 and 6 post-infection (P_{Adj}=0.002 and P_{Adj}=0.041, respectively) and BCG Russia at weeks 3 and 6 post-infection (P_{Adj}<0.001 and P_{Adj}=0.045, respectively). BCG Pasteur and BCG Russia differed at the 3 week time-point only (P_{Adj}=0.012). Differences in *Ifng* expression attributable to the bacterial strain were therefore detected in both strains of mice (Figure 4). As a next step, *Ifng* levels for each mycobacterial strain were compared between the two strains of mice. Differences in *Ifng* transcriptional levels between A/J and C57BL/6J mice were only observed for BCG Russia [F(1,16.4) = 23.54, P<0.001] with C57BL/6J mice producing more *Ifng* than A/J mice. The effect of time was also significant [F(2,10.2) = 13.90, P=0.001]. During BCG Pasteur and *M. tuberculosis* infection, *Ifng* transcript levels did not vary significantly between A/J and C57BL/6J mice. These results showed that mycobacterial strain was the major determining factor of *Ifng* transcript levels while the host genetic background had only a minor modulating impact.

The pulmonary transcript levels of *Il12b* and *Il4* were next measured. Bacterial-related differences in *Il12b* induction were significant in both A/J and C57BL/6J mice (Figure 5). *Post hoc* analysis in both mouse strains revealed that *M. tuberculosis* induced significantly more *Il12*b than the two BCG strains whereas differences between BCG Russia and BCG Pasteur were not significant. Hence, while the mycobacterial strain had a large impact on *Il12b* production in both A/J and C57BL6/J mice, this effect was mainly due a strong induction of *Il12b* by *M. tuberculosis*. Unlike *Il12b*, pulmonary *Il4* expression was negatively correlated with infection by the three mycobacterial strains (Figure 6). Two-way ANOVA detected a significant effect of bacterial strain on *Il4* expression in both

A/J and C57BL/6J mice. However, *post hoc* analysis did not identify specific differences between bacteria except that in C57BL/6J mice BCG Pasteur significantly downregulated *Il4* more than did *M. tuberculosis* (P_{Adj}=0.034). Regarding mouse strain-specific effects, an impact of the host genetic background on pulmonary *Il12b* and *Il4* transcription was either absent or of modest magnitude (Figure 5 and 6).

Transcriptional levels of 34 chemokine and chemokine-related genes were profiled by real-time PCR in response to *M. tuberculosis*, BCG Russia and BCG Pasteur in A/J and C57BL/6J mice at 3 and 6 weeks post-infection. One-way ANOVA analyses comparing the two mouse strains were performed for each mycobacterium and at each time point. Unexpectedly, no significant differences in chemokine transcript levels were detected between A/J and C57B/6J mice. Hence, subsequent analyses were focused on the extent of differential gene expression across the three strains of mycobacterial strains in the two mouse strains and at each time point. The magnitude of the transcriptional response was shown to be the largest during *M. tuberculosis* infection, while BCG Russia had a lagged expression for most of the genes tested. Expression differences across the three mycobacterial strains were more pronounced in the A/J mouse strain. Among the genes that were significantly up- or down-regulated, 12 and 11 genes were differentially expressed at 3 and 6 weeks, respectively (Summary: Tables 2 and 5; Complete data set: Tables 3 and 4). In C57BL6/J mice, differences in induction related to the mycobacterial strain were observed for 7 genes at 3 weeks and for 3 genes at 6 weeks (Summary: Tables 2 and 5; Complete data set: Tables 6 and 7). These results demonstrated that the magnitude of the difference in cytokine and chemokine levels following mycobacterial infection is critically dependent on the host background.

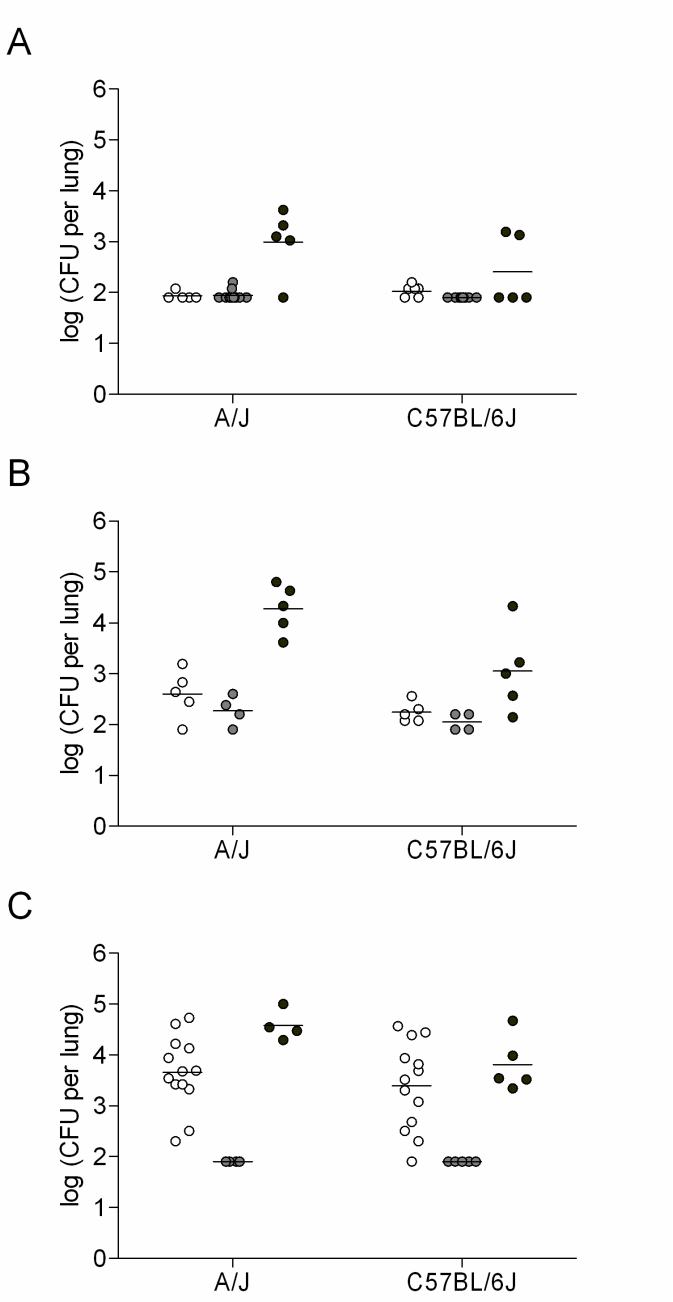

Figure 1. Pulmonary bacterial counts of BCG Russia, BCG Pasteur, and *M. tuberculosis* in the A/J and C57BL/6J mouse strains. The number of bacteria (log_{10}CFU) in the lungs of individual A/J and C57BL/6J mice was quantified at 1 week (A), 3 weeks (B), and 6 weeks (C) following intravenous infection with a low dose (~3×10^3 bacilli) of BCG Russia, BCG Pasteur or *M. tuberculosis*. Bars indicate the mean log_{10}CFU for the group. White, BCG Russia; grey, BCG Pasteur; black, *M. tuberculosis*.

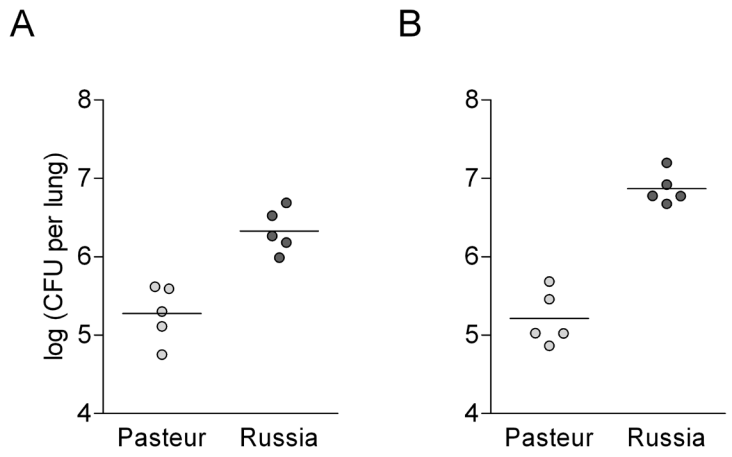

Figure 2. Pulmonary loads of BCG Pasteur and BCG Russia in A/J and C57BL/6J mice following a high dose aerosol infection. The bacterial counts (log_{10}CFU) of BCG Pasteur (light grey) or BCG Russia (dark grey) were determined in the lungs of A/J (A) and C57BL/6J (B) mice at 6 weeks following a high dose (~2 $\times 10^3$ bacilli) aerosol infection. Bars are representative of the mean log_{10}CFU for the group.

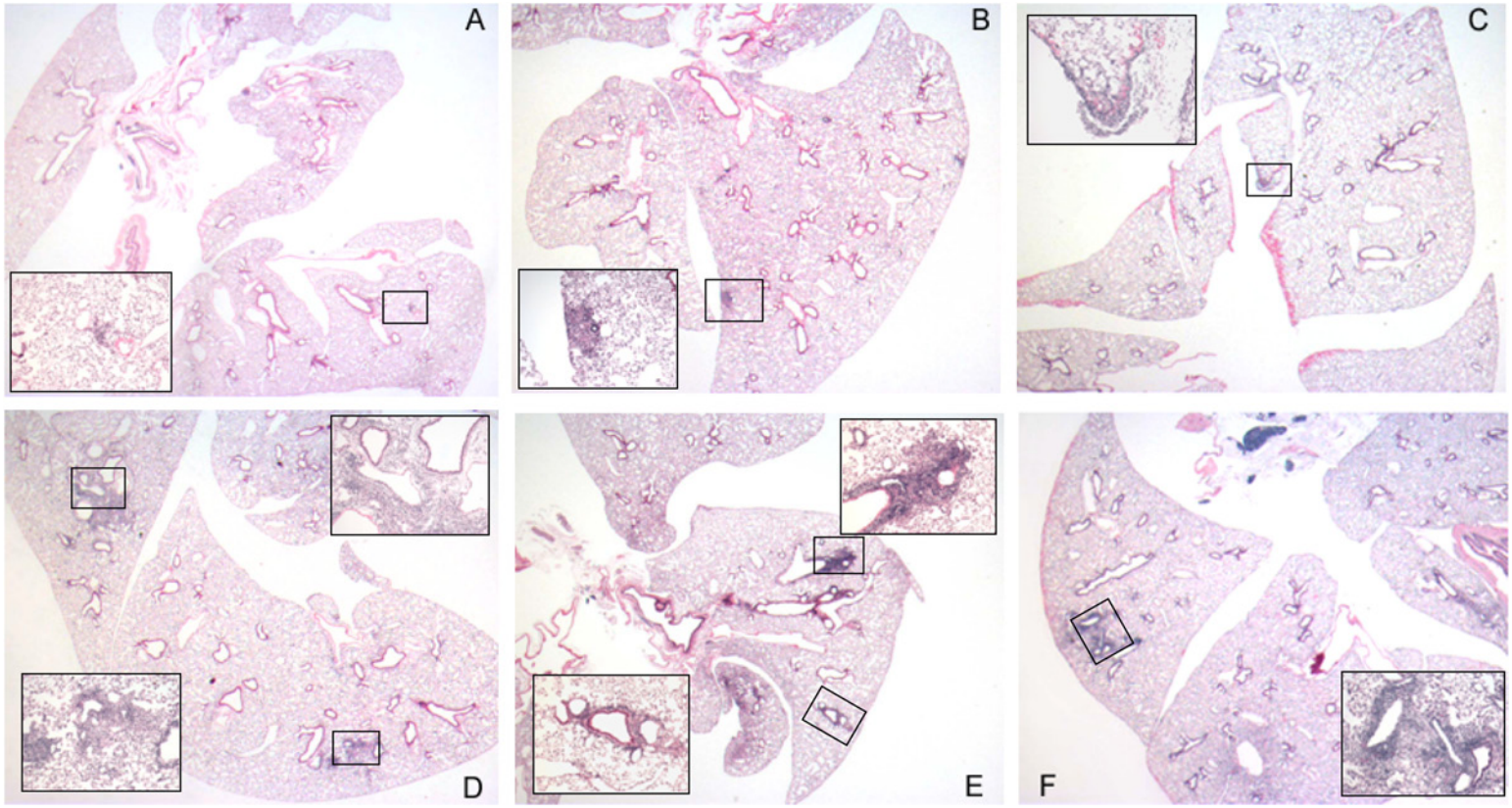

Figure 3. Cellular infiltration in the lungs of A/J and C57BL/6J mice following mycobacterial infection. Mice of the A/J (A, B, C) and C57BL/6J (D, E, F) strains were infected intravenously with a low dose of BCG Russia (A, D), BCG Pasteur (B, E) or *M. tuberculosis* (C, F) and histological analysis of the lungs was performed at 6 weeks post-infection. Lung sections were stained with hematoxylin and eosin. Lesions are boxed. Representative results of four mice per group are shown (1× magnification; inset: 10× magnification).

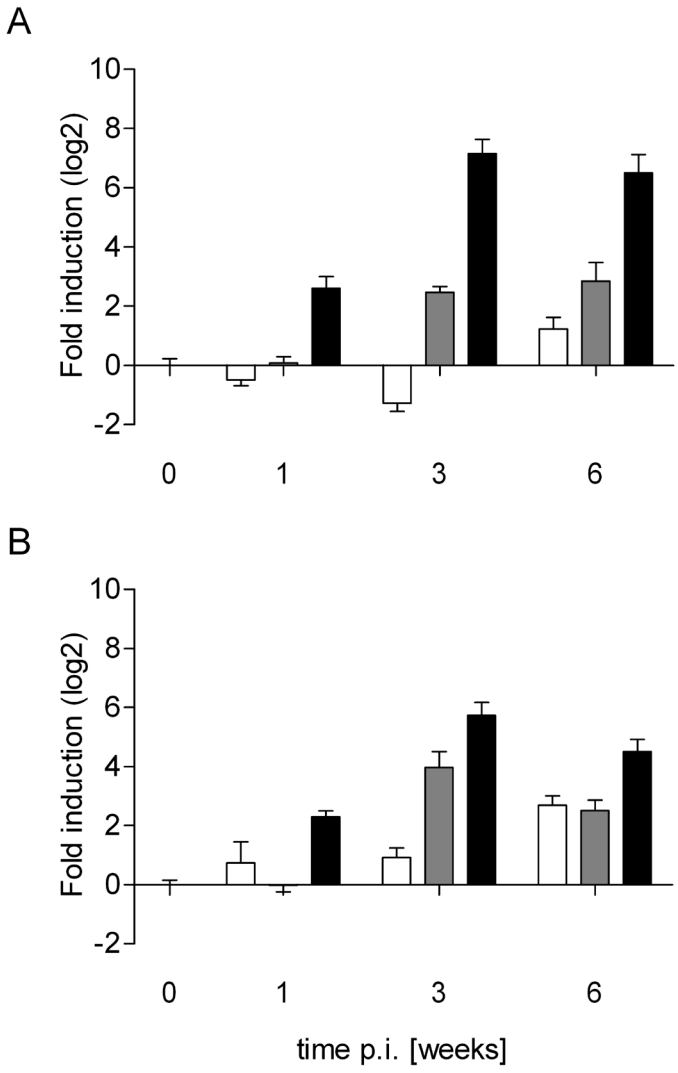

Figure 4. Pulmonary *Ifng* transcript levels in the A/J and C57BL/6J mouse strains following mycobacterial infection. Induction of *Ifng* transcription by BCG Russia (white), BCG Pasteur (grey) and *M. tuberculosis* (black) was compared in the A/J (A) and C57BL/6J (B) mouse strains at 1, 3, and 6 weeks of a low dose intravenous infection. Fold induction (log_2) is the ratio of *Ifng* expression in infected mice (n=4) relative to uninfected mice (n=4). Error bars represent SEM.

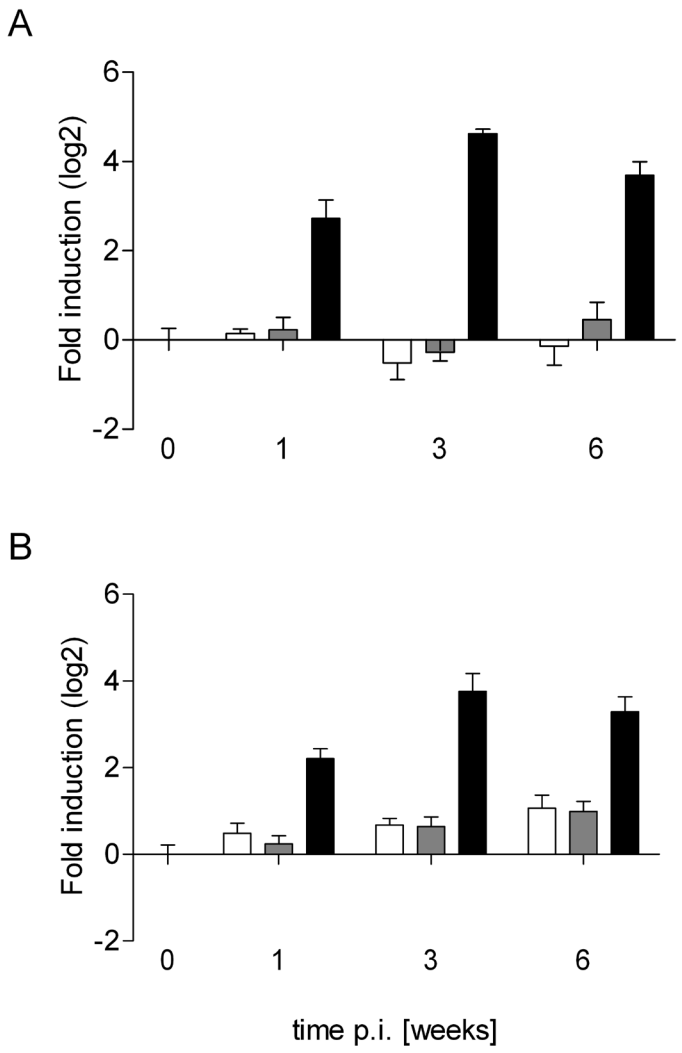

Figure 5. Pulmonary transcription of *Il12b* in the A/J and C57BL/6J mouse strains infected with BCG Russia, BCG Pasteur or *M. tuberculosis*. Induction of *Il12b* during a low dose intravenous infection with the three bacterial strains was compared in A/J (A) and C57BL/6J (B) mice at 1, 3, and 6 weeks by two-way ANOVA. In the A/J strain, there was a significant difference in the levels of *Il12b* transcription induced by the three mycobacterial strains (effect of bacterial strain: $F(2,11.9) = 138.49$, $P<0.001$). The effect of time was nonsignificant [$F(2,11.9) = 0.78$, $P > 0.05$], but there was a significant interaction between the two effects [$F(4,8.15) = 6.50$, $P=0.012$]. Bacterial-specific effects on *Il12b* transcription were also observed in C57BL/6J animals [$F(2,16) = 31.12$, $P<0.001$]. There was a significant effect of time [$F(2,16.6) = 5.32$, $P=0.017$] but the interaction was nonsignificant. Data represents the fold change (log_2) of *Il12b* transcription in infected (n=4) relative to uninfected (n=4) mice + SEM. White, BCG Russia; grey, BCG Pasteur; black, *M. tuberculosis*.

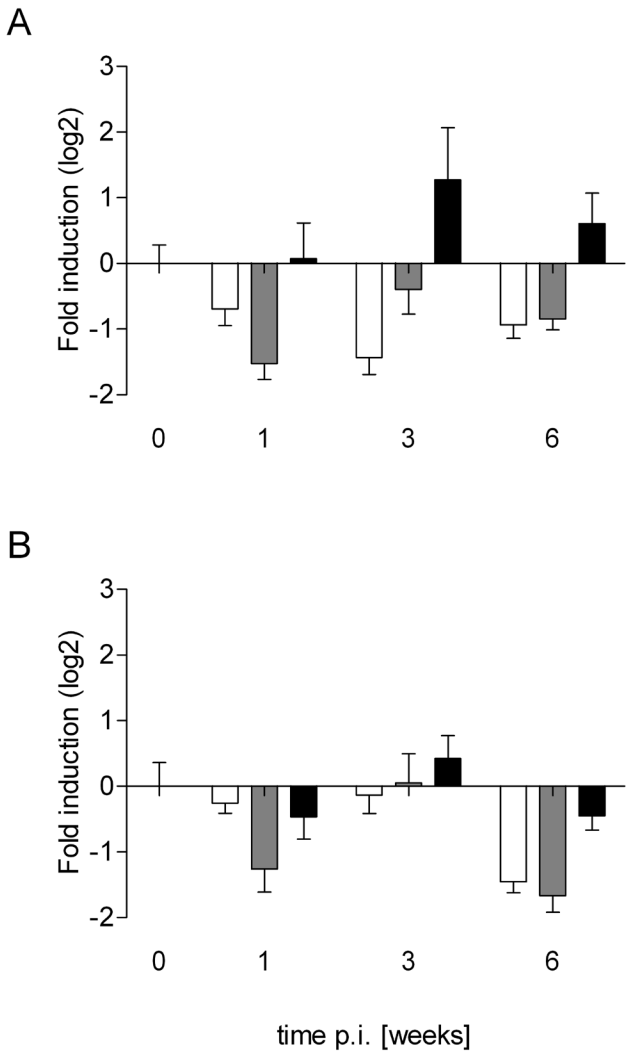

Figure 6. Transcript levels of *Il4* in the lungs of A/J and C57BL/6J mice following infection with BCG Russia, BCG Pasteur or *M. tuberculosis*. The extent of pulmonary *Il4* transcription was determined at 1, 3, and 6 weeks following a low dose intravenous infection with the three mycobacterial strains. Two-way ANOVA detected a significant effect of bacteria on *Il4* expression in A/J mice (A) [$F(2,15.7) = 9.33$, $P=0.002$]. Although *Il4* production did not vary significantly with time [$F(2,15.4) = 1.25$, $P>0.05$], the interaction between the two factors was significant [$F(4,17) = 3.40$, $P=0.032$]. In C57BL/6J mice (B), the magnitude of *Il4* downregulation also differed significantly across the bacterial strains [$F(2,13.6) = 3.84$, $P=0.048$]. The effect of time was considerable [$F(2,11.6) = 10.32$, $P=0.003$], although the interaction was nonsignificant. Data is presented as a fold change of *Il4* transcription in infected (n=4) relative to uninfected (n=4) mice + SEM. White, BCG Russia; grey, BCG Pasteur; black, *M. tuberculosis*.

Table 1. Qiagen Gene Expression Assays

Gene name	Sequence	Primer/Probe
Ifng		
Mm_Ifng_FAM_1	GCCAAGTTTGAGGTCAACA	Forward primer
Mm_Ifng_FAM_1	ATCAGCAGCGACTCCTTT	Reverse primer
Mm_Ifng_FAM_1	TCCAGCGCCAAGCATT	Probe
Il12b		
Mm_Il12b_FAM_1	CTGAAGTGTGAAGCACCAAA	Forward primer
Mm_Il12b_FAM_1	ACAGAGACGCCATTCCACAT	Reverse primer
Mm_Il12b_FAM_1	AGAGCAGTAGCAGTTCC	Probe
Il4		
Mm_Il4_FAM_1	CT*CTAGTGTTCTCATGGA	Forward primer
Mm_Il4_FAM_1	CTTTCAGTGATGTGGACTTGG	Reverse primer
Mm_Il4_FAM_1	CTCTTTCGG*GCTTTTC	Probe
Gapdh		
Mm_Gapd_FAM_1	AACGGATTTGGCCGTATTG	Forward primer
Mm_Gapd_FAM_1	CGTGAGTGGAGTCATACTGGAA	Reverse primer
Mm_Gapd_FAM_1	AAAGTGGAGATTGTTGC	Probe

* signifies a Super-G superbase

Table 2. Summary of genes differentially expressed across mycobacteria at week 3

	Adjusted p-value	
	A/J	C57BL/6J
Genes identified in A/J and C57BL/6J		
Ccl20	0.0374	0.0481
Ccl4	0.0057	0.0211
Ccl5	0.0057	0.0211
Cxcl10	0.0057	0.0211
Genes specific to A/J		
Ccl1	0.0132	-[a]
Ccl12	0.0057	-
Ccl2	0.0330	-
Ccl7	0.0195	-
Ccl8	0.0087	-
Ccr5	0.0195	-
Cx3cl1	0.0067	-
Cxcl11	0.0287	-
Cxcl9	0.0057	-
Cxcr3	0.0105	-
Tnf	0.0105	-
Genes specific to C57BL/6J		
Ccl11	-	0.0481
Ccl19	-	0.0324
Ccr9	-	0.0479
Cxcl5	-	0.0481
Il18	-	0.0385

[a] non-significant

Table 3. Pulmonary gene induction three weeks following mycobacterial infection in A/J mice

Gene	BCG Russia	BCG Pasteur	*M. tuberculosis*	Adjusted p-value
Ccl1	-3.19 (-7.27, -1.40)	1.01 (-2.38, 2.40)	3.63 (1.54, 8.55)	**0.0132** [a]
Ccl11	-1.48 (-2.34, 1.08)	-1.35 (-2.01, 1.10)	-1.58 (-3.27, 1.31)	- [b]
Ccl12	-4.40 (-6.24, -3.10)	-1.55 (-4.02, 1.67)	4.95 (3.86, 6.36)	**0.0057**
Ccl17	-1.21 (-1.66, 1.14)	-1.04 (-1.37, 1.26)	1.53 (1.01, 2.30)	-
Ccl19	-1.58 (-2.20, -1.13)	1.14 (-1.22, 1.57)	1.61 (1.11, 2.35)	0.0067 [c]
Ccl2	1.68 (-1.17, 3.30)	2.09 (-1.35, 5.90)	6.48 (4.08, 10.30)	**0.0330**
Ccl20	1.95 (-1.04, 3.97)	3.25 (1.67, 6.35)	5.65 (2.58, 12.38)	**0.0374**
Ccl4	-1.57 (-1.81, -1.35)	1.50 (-1.47, 3.30)	4.63 (3.69, 5.80)	**0.0057**
Ccl5	-1.83 (-2.61, -1.28)	1.53 (-1.20, 2.82)	4.89 (3.34, 7.16)	**0.0057**
Ccl7	-1.35 (-1.80, -1.01)	1.33 (-2.25, 4.00)	9.80 (4.78, 20.11)	**0.0195**
Ccl8	-1.78 (-3.21, 1.01)	-1.02 (-2.49, 2.41)	6.89 (3.60, 13.19)	**0.0087**
Ccl9	-2.38 (-6.90, 1.22)	-1.70 (-3.78, 1.31)	1.20 (-1.10, 1.59)	-
Ccr1	-1.10 (-1.78, 1.47)	1.01 (-1.86, 1.90)	1.73 (1.33, 2.26)	0.0287
Ccr2	-1.17 (-2.02, 1.47)	-1.50 (-3.50, 1.56)	1.32 (-1.60, 2.77)	-
Ccr4	-1.12 (-1.77, 1.40)	-1.66 (-2.85, 1.03)	-1.20 (-1.59, 1.10)	-
Ccr5	-1.29 (-1.88, 1.13)	1.08 (-1.65, 1.92)	3.19 (2.23, 4.57)	**0.0195**
Ccr7	-1.76 (-2.44, -1.27)	-1.85 (-2.61, -1.31)	-1.78 (-2.86, -1.11)	-
Ccr9	-1.10 (-1.38, 1.15)	-1.33 (-1.56, -1.13)	1.38 (-1.01, 1.92)	0.0283
Cx3cl1	-1.19 (-1.80, 1.28)	-1.63 (-2.25, -1.18)	-2.18 (-3.09, -1.54)	**0.0067**
Cxcl1	1.65 (1.07, 2.53)	1.28 (-1.41, 2.30)	2.67 (1.14, 6.21)	-
Cxcl10	-1.62 (-3.37, 1.29)	2.98 (-1.03, 9.08)	16.48 (9.26, 29.33)	**0.0057**
Cxcl11	1.41 (-1.15, 2.30)	2.47 (-1.45, 8.85)	11.12 (6.00, 20.60)	**0.0287**
Cxcl12	1.33 (1.05, 1.70)	1.13 (-1.10, 1.39)	-1.89 (-2.64, -1.35)	0.0075
Cxcl13	-1.88 (-8.54, 2.42)	-1.95 (-8.87, 2.33)	1.32 (-2.54, 4.40)	-
Cxcl15	2.47 (1.12, 5.42)	1.52 (-1.15, 2.64)	1.85 (-1.03, 3.51)	-
Cxcl5	71.53 (38.51, 132.87)	61.60 (28.84, 131.58)	32.69 (18.79, 56.88)	-
Cxcl9	-1.67 (-5.20, 1.87)	4.72 (1.16, 19.17)	37.33 (11.95, 116.65)	**0.0057**
Cxcr3	-1.86 (-2.69, -1.29)	-1.49 (-3.03, 1.35)	2.63 (1.85, 3.73)	**0.0105**
Il16	1.12 (-1.43, 1.79)	-1.65 (-3.49, 1.28)	-1.22 (-1.57, 1.06)	0.0236
Il18	-1.65 (-2.89, 1.06)	-1.65 (-2.67, -1.02)	1.65 (1.08, 2.51)	0.0105
Il1a	-1.48 (-2.73, 1.25)	1.21 (-1.30, 1.91)	-1.32 (-1.72, -1.02)	0.0330
Il8rb	1.24 (-1.44, 2.22)	2.13 (1.50, 3.03)	1.07 (-1.49, 1.70)	-
Tnf	-2.01 (-2.72, -1.49)	-1.21 (-2.00, 1.36)	2.15 (1.64, 2.80)	**0.0105**
Tnfrsf1a	1.15 (-1.14, 1.51)	1.06 (-1.20, 1.35)	-1.51 (-1.72, -1.33)	0.0070

[a] Bold type indicates genes that differ significantly across the mycobacterial strains with a fold change >2 in at least one mycobacterial strain

[b] non-significant

[c] Genes with a fold change < 2 that differ significantly across the mycobacterial strains

Table 4. Pulmonary gene induction three weeks following mycobacterial infection in C57BL/6J mice

Gene	BCG Russia	BCG Pasteur	*M. tuberculosis*	Adjusted p-value
Ccl1	1.44 (-1.51, 3.13)	6.72 (2.48, 18.18)	6.45 (2.74, 15.20)	- [a]
Ccl11	-1.19 (-2.06, 1.45)	2.14 (1.51, 3.04)	1.73 (1.11, 2.70)	**0.0481** [b]
Ccl12	2.93 (-1.28, 11.02)	1.58 (-2.51, 6.29)	4.04 (1.89, 8.62)	-
Ccl17	1.27 (-1.20, 1.92)	1.90 (1.28, 2.81)	1.78 (1.46, 2.16)	-
Ccl19	1.41 (1.12, 1.79)	1.91 (1.46, 2.49)	2.16 (1.60, 2.91)	**0.0324**
Ccl2	1.41 (-1.07, 2.12)	2.42 (1.87, 3.14)	2.38 (1.23, 4.63)	-
Ccl20	2.10 (-1.05, 4.64)	1.06 (-1.62, 1.83)	3.86 (2.46, 6.05)	**0.0481**
Ccl4	1.04 (-1.18, 1.27)	2.27 (1.81, 2.86)	1.88 (1.56, 2.28)	**0.0211**
Ccl5	1.12 (-1.47, 1.84)	3.03 (2.16, 4.26)	3.15 (2.21, 4.49)	**0.0211**
Ccl7	2.30 (1.33, 3.97)	3.19 (2.27, 4.48)	5.59 (3.22, 9.70)	-
Ccl8	3.40 (1.27, 9.10)	2.89 (1.31, 6.38)	5.32 (2.35, 12.02)	-
Ccl9	-1.82 (-2.57, -1.29)	-1.65 (-3.71, 1.36)	1.03 (-1.21, 1.29)	0.0271 [c]
Ccr1	1.22 (-1.31, 1.95)	-1.79 (-2.95, -1.09)	-1.57 (-2.74, 1.11)	0.0479
Ccr2	1.21 (-1.05, 1.55)	-1.50 (-2.30, 1.02)	-1.82 (-2.57, -1.29)	0.0092
Ccr4	1.66 (1.14, 2.42)	1.29 (1.09, 1.54)	-1.39 (-1.73, -1.11)	0.0211
Ccr5	1.25 (1.03, 1.52)	1.42 (1.07, 1.88)	1.75 (1.14, 2.68)	-
Ccr7	-1.11 (-1.81, 1.46)	-1.09 (-1.78, 1.51)	-1.55 (-1.88, -1.29)	-
Ccr9	2.70 (1.89, 3.85)	1.24 (-1.11, 1.70)	1.72 (1.17, 2.54)	**0.0479**
Cx3cl1	-1.14 (-1.90, 1.48)	1.24 (-1.15, 1.78)	-1.13 (-1.42, 1.11)	-
Cxcl1	1.56 (1.04, 2.33)	1.46 (-1.03, 2.20)	1.47 (-1.10, 2.39)	-
Cxcl10	1.83 (-1.06, 3.53)	9.52 (5.46, 16.58)	13.74 (8.31, 22.72)	**0.0211**
Cxcl11	4.98 (1.75, 14.19)	16.72 (10.20, 27.40)	14.29 (4.56, 44.79)	-
Cxcl12	1.10 (-1.13, 1.36)	1.34 (1.04, 1.72)	1.03 (-1.33, 1.40)	-
Cxcl13	2.73 (-1.30, 9.71)	1.19 (-1.46, 2.06)	2.54 (1.67, 3.87)	-
Cxcl15	1.07 (-1.43, 1.65)	-1.48 (-2.48, 1.13)	-1.69 (-2.73, -1.05)	0.0092
Cxcl5	7.08 (2.23, 22.44)	2.08 (-1.58, 6.87)	1.06 (-2.24, 2.53)	**0.0481**
Cxcl9	3.69 (1.20, 11.36)	25.57 (9.93, 65.85)	25.99 (12.03, 56.16)	-
Cxcr3	1.06 (-1.72, 1.91)	1.92 (1.31, 2.82)	2.18 (1.63, 2.93)	-
Il16	-1.42 (-1.86, -1.09)	1.03 (-1.23, 1.31)	-1.75 (-2.12, -1.45)	0.0479
Il18	2.03 (1.32, 3.14)	-1.19 (-2.11, 1.50)	1.04 (-1.21, 1.32)	0.0385
Il1a	-1.12 (-1.44, 1.15)	-1.43 (-1.80, -1.14)	-1.04 (-1.47, 1.36)	-
Il8rb	-1.74 (-3.15, 1.04)	-2.40 (-4.16, -1.39)	-3.63 (-8.35, -1.57)	-
Tnf	1.23 (-1.36, 2.05)	1.72 (1.22, 2.41)	1.50 (-1.09, 2.46)	-
Tnfrsf1a	1.09 (-1.25, 1.47)	1.07 (-1.20, 1.37)	-1.09 (-1.54, 1.29)	-

[a] non-significant

[b] Bold type indicates genes that differ significantly across the mycobacterial strains with a fold change >2 in at least one mycobacterial strain

[c] Genes with a fold change < 2 that differ significantly across the mycobacterial strains

Table 5. Summary of genes differentially expressed across mycobacteria at week 6

	Adjusted p-value	
	A/J	C57BL/6J
Genes identified in A/J and C57BL/6J		
Ccr1	0.0370	0.0068
Ccr2	0.0342	0.0232
Genes specific to A/J		
Ccl5	0.0481	-[a]
Ccl8	0.0401	-
Ccr5	0.0401	-
Ccr9	0.0342	-
Cxcl10	0.0401	-
Cxcl15	0.0342	-
Cxcl5	0.0481	-
Cxcl9	0.0401	-
Cxcr3	0.0076	-
Genes specific to C57BL/6J		
Ccl19	-	0.0183

[a] non-significant

Table 6. Pulmonary gene induction six weeks following mycobacterial infection in A/J mice

Gene	BCG Russia	BCG Pasteur	*M. tuberculosis*	Adjusted p-value
Ccl1	1.10 (-1.81, 2.20)	1.54 (-2.25, 5.37)	2.29 (-1.61, 8.45)	- [a]
Ccl11	-1.44 (-2.09, 1.01)	-2.14 (-3.23, -1.42)	-1.96 (-4.03, 1.04)	-
Ccl12	2.59 (1.51, 4.44)	2.26 (1.60, 3.21)	3.35 (2.43, 4.61)	-
Ccl17	-1.12 (-1.90, 1.53)	1.08 (-1.26, 1.46)	1.08 (-1.32, 1.54)	-
Ccl19	1.38 (-1.20, 2.29)	1.08 (-1.39, 1.62)	1.95 (1.32, 2.88)	-
Ccl2	2.40 (1.08, 5.34)	3.94 (1.52, 10.19)	6.31 (3.83, 10.39)	-
Ccl20	1.37 (-1.45, 2.73)	2.59 (1.21, 5.55)	2.37 (1.17, 4.78)	-
Ccl4	1.55 (-1.21, 2.89)	5.31 (2.30, 12.27)	5.05 (3.72, 6.85)	-
Ccl5	1.37 (-1.14, 2.16)	2.57 (1.57, 4.20)	4.37 (2.91, 6.55)	**0.0481** [b]
Ccl7	3.30 (2.12, 5.13)	3.74 (1.99, 7.03)	7.96 (3.83, 16.52)	**-**
Ccl8	3.70 (1.60, 8.55)	3.80 (2.32, 6.23)	7.79 (4.38, 13.84)	**0.0401**
Ccl9	1.19 (-1.90, 2.69)	1.06 (-1.80, 2.01)	1.27 (-1.02, 1.66)	**-**
Ccr1	1.62 (-1.04, 2.73)	2.31 (1.61, 3.32)	-1.03 (-1.32, 1.24)	**0.0370**
Ccr2	1.20 (-1.35, 1.94)	2.99 (1.82, 4.91)	-1.16 (-2.47, 1.84)	**0.0342**
Ccr4	1.26 (-1.55, 2.47)	1.13 (-1.42, 1.83)	1.03 (-1.31, 1.40)	**-**
Ccr5	1.25 (-1.36, 2.14)	3.45 (2.41, 4.96)	2.21 (1.43, 3.41)	**0.0401**
Ccr7	-1.60 (-2.21, -1.16)	-1.21 (-1.55, 1.06)	-2.03 (-3.49, -1.18)	**-**
Ccr9	-2.03 (-3.18, -1.29)	1.37 (1.13, 1.66)	1.15 (-1.16, 1.54)	**0.0342**
Cx3cl1	-1.64 (-2.24, -1.20)	-1.20 (-1.65, 1.14)	-1.92 (-2.68, -1.37)	**-**
Cxcl1	1.47 (-1.00, 2.16)	2.10 (1.28, 3.45)	1.59 (-1.22, 3.08)	**-**
Cxcl10	2.11 (-1.20, 5.34)	6.47 (1.98, 21.20)	14.40 (8.65, 23.96)	**0.0401**
Cxcl11	1.20 (-2.42, 3.47)	7.24 (2.22, 23.57)	10.15 (5.94, 17.34)	**-**
Cxcl12	-1.25 (-1.58, 1.01)	-1.00 (-2.10, 2.09)	-1.54 (-1.88, -1.26)	**-**
Cxcl13	1.02 (-3.93, 4.09)	-1.42 (-7.53, 3.72)	1.35 (-2.78, 5.08)	**-**
Cxcl15	1.41 (-1.14, 2.28)	2.69 (1.62, 4.45)	1.08 (-1.80, 2.11)	**0.0342**
Cxcl5	11.46 (2.97, 44.23)	72.71 (41.32, 127.94)	8.96 (4.10, 19.62)	**0.0481**
Cxcl9	4.56 (1.09, 19.04)	19.31 (4.93, 75.68)	42.74 (16.11, 113.40)	**0.0401**
Cxcr3	1.19 (-1.15, 1.65)	2.07 (1.64, 2.60)	3.24 (2.60, 4.04)	**0.0076**
Il16	-1.25 (-2.10, 1.34)	1.77 (1.08, 2.91)	-1.20 (-1.71, 1.19)	0.0342 [c]
Il18	1.53 (-1.09, 2.56)	1.14 (-1.59, 2.06)	1.27 (-1.22, 1.96)	-
Il1a	-1.08 (-1.74, 1.50)	-1.75 (-2.73, -1.12)	-1.83 (-2.36, -1.41)	0.0342
Il8rb	1.05 (-1.35, 1.49)	1.40 (-1.34, 2.62)	-1.38 (-2.26, 1.19)	-
Tnf	1.19 (-1.48, 2.08)	1.93 (1.57, 2.38)	1.67 (1.27, 2.19)	-
Tnfrsf1a	-1.18 (-1.50, 1.07)	1.13 (-1.13, 1.44)	-1.41 (-1.73, -1.15)	0.0076

[a] non-significant

[b] Bold type indicates genes that differ significantly across the mycobacterial strains with a fold change >2 in at least one mycobacterial strain

[c] Genes with a fold change < 2 that differ significantly across the mycobacterial strains

Table 7. Pulmonary gene induction six weeks following mycobacterial infection in C57BL/6J mice

Gene	BCG Russia	BCG Pasteur	*M. tuberculosis*	Adjusted p-value
Ccl1	2.93 (1.01, 8.52)	5.02 (1.41, 17.85)	13.11 (5.01, 34.30)	- [a]
Ccl11	1.20 (-1.17, 1.68)	-1.15 (-1.65, 1.26)	-1.62 (-5.52, 2.10)	-
Ccl12	3.23 (-1.02, 10.64)	3.07 (-1.01, 9.57)	2.86 (1.13, 7.23)	-
Ccl17	1.76 (-1.07, 3.29)	1.02 (-2.08, 2.18)	1.28 (-2.07, 3.39)	-
Ccl19	1.21 (-1.10, 1.62)	1.14 (-1.43, 1.85)	2.86 (1.79, 4.57)	**0.0183** [b]
Ccl2	3.08 (1.89, 5.01)	2.61 (1.61, 4.22)	3.23 (1.42, 7.37)	-
Ccl20	2.92 (1.69, 5.04)	2.99 (1.88, 4.74)	8.20 (4.37, 15.38)	-
Ccl4	1.21 (-1.20, 1.76)	1.41 (1.06, 1.88)	2.40 (1.36, 4.26)	-
Ccl5	2.25 (1.59, 3.16)	2.08 (1.33, 3.25)	3.09 (2.07, 4.60)	-
Ccl7	4.84 (3.08, 7.60)	5.30 (3.44, 8.14)	4.31 (1.85, 10.01)	-
Ccl8	7.30 (3.43, 15.56)	8.19 (3.63, 18.50)	5.31 (1.47, 19.11)	-
Ccl9	-1.59 (-2.22, -1.14)	-1.74 (-2.66, -1.14)	1.00 (-1.18, 1.18)	-
Ccr1	-2.01 (-3.26, -1.23)	1.13 (-1.40, 1.78)	-2.07 (-5.13, 1.20)	**0.0068**
Ccr2	-1.68 (-2.31, -1.23)	1.44 (1.07, 1.93)	-2.59 (-10.64, 1.59)	**0.0232**
Ccr4	1.11 (-1.12, 1.38)	1.14 (-1.17, 1.51)	-1.08 (-1.40, 1.19)	-
Ccr5	1.31 (-1.05, 1.79)	1.97 (1.23, 3.15)	-1.02 (-5.08, 4.85)	-
Ccr7	-1.57 (-2.50, 1.01)	-1.01 (-1.82, 1.78)	-1.77 (-3.97, 1.27)	-
Ccr9	1.08 (-1.36, 1.58)	1.98 (1.37, 2.86)	1.01 (-3.91, 3.96)	-
Cx3cl1	-1.04 (-1.52, 1.40)	-1.10 (-1.53, 1.25)	-1.03 (-1.75, 1.66)	-
Cxcl1	1.58 (1.30, 1.93)	2.62 (1.58, 4.35)	-1.40 (-4.82, 2.46)	-
Cxcl10	5.91 (2.58, 13.51)	7.14 (3.50, 14.58)	9.69 (5.74, 16.36)	-
Cxcl11	8.99 (3.90, 20.69)	7.45 (2.20, 25.23)	5.97 (1.99, 17.88)	-
Cxcl12	1.12 (-1.13, 1.42)	1.25 (-1.06, 1.65)	1.20 (-1.56, 2.24)	-
Cxcl13	2.14 (1.49, 3.08)	2.85 (1.59, 5.11)	7.22 (2.47, 21.07)	-
Cxcl15	-1.04 (-1.57, 1.47)	1.21 (-1.29, 1.89)	-2.93 (-12.99, 1.52)	-
Cxcl5	4.83 (1.51, 15.43)	11.71 (4.97, 27.57)	-1.64 (-5.94, 2.22)	-
Cxcl9	19.24 (7.14, 51.80)	30.82 (10.11, 94.00)	16.42 (4.42, 61.01)	-
Cxcr3	1.45 (-1.15, 2.42)	2.12 (1.38, 3.26)	2.63 (1.88, 3.68)	-
Il16	-1.28 (-1.69, 1.03)	-1.35 (-1.87, 1.03)	-1.65 (-3.12, 1.14)	-
Il18	1.26 (-1.11, 1.75)	1.90 (1.06, 3.40)	-1.05 (-1.43, 1.29)	-
Il1a	-1.10 (-1.39, 1.14)	-1.48 (-2.29, 1.04)	-1.44 (-4.23, 2.04)	-
Il8rb	-5.03 (-8.87, -2.86)	-2.50 (-5.29, -1.18)	-6.48 (-14.76, -2.84)	-
Tnf	1.07 (-1.54, 1.75)	1.22 (-1.70, 2.52)	2.49 (1.37, 4.55)	-
Tnfrsf1a	-1.07 (-1.44, 1.27)	1.03 (-1.25, 1.33)	-1.40 (-2.47, 1.25)	-

[a] non-significant

[b] Bold type indicates genes that differ significantly across the mycobacterial strains with a fold change >2 in at least one mycobacterial strain

DISCUSSION

Analysis of functional host phenotypes in the mouse has demonstrated that bacteria of different *M. tuberculosis* lineages cause a range of immunological and pathological effects [27,28]. Specifically, the Beijing group of strains produce a phenolic glycolipid (PGL-tb) molecule that has been associated with a less effective immune response and increased mortality in mice [29]. Differences in the magnitude of the inflammatory response have also been observed in response to infection with BCG substrains [30]. Moreover, different strains of BCG induce different levels of protective tuberculosis immunity in mice and vary in the incidence of adverse effects in human studies [31,32]. These studies show an association between mycobacterial genetic variation and host immune responses. On the other hand, it has been clearly established that genetically distinct inbred mice and humans differ dramatically in their susceptibility to mycobacterial infections. In humans, it has recently been shown that susceptibility to infection with *M. tuberculosis* is under genetic control and is strongly impacted by a locus on chromosome 11 [2,3]. A number of additional genes modulate the risk of developing clinical tuberculosis in infected persons, including the *NRAMP1* gene [33,34]. The mouse orthologue of the latter gene was previously identified as the major determinant of innate susceptibility to infection in the spleen with *M. bovis* BCG Montreal [17]. In addition, variable susceptibility of inbred strains of mice to *M. tuberculosis* has been linked to a number of loci [35-41]. Taken together, these data establish that genetic variability of both mycobacterial strains and murine or human hosts strongly impact on different aspects of host susceptibility to mycobacterial infection. However, there is a lack of studies that have systematically analysed, in parallel, the joint contribution of both host and mycobacterial strain on host responses.

A consistent finding of our experiments was that all infectious phenotypes were more sensitive to variation of the mycobacterial strain than host background. Given the very small number of mycobacterial and host strains, this may be at least partly a result of the larger genetic variability among the three mycobacterial

strains as compared to the more closely related A/J and C57BL/6J mice. By including wild-derived mice or mice with known genetic defects in such comparisons, by studying a later phase of infection, or by changing the mode and dose of infection, the relative impact of host genetic background vs bacterial strain may well have been different. Despite such limitations, our data are consistent with the view that the major effect on host responses is due to the type of mycobacterial strain while the host genetic background is the modulator of responsiveness. Yet, even in our study with a dominant impact of mycobacterial strain on the studied phenotypes, it became clear that a comparison of the mycobacterial strains for both pulmonary CFU burden and mechanistic phenotypes (*Ifng* and chemokine transcript levels) had more discriminatory power in A/J mice as compared to C57BL/6J mice. This highlights problems that can be encountered when studies employing the same mycobacterial strain are compared in different hosts.

Across mycobacterial strains there was poor correlation between bacterial counts and *Ifng* transcript levels. For example, at the 3 week time point bacterial burdens are similar between Pasteur and Russia while the level of pulmonary *Ifng* is strikingly different; a general effect that is even more pronounced at the 6 week time point (Figure 4). The ability of BCG Russia to avoid triggering an *Ifng* response is clearly part of its ability to expand to high pulmonary loads. In contrast, *M. tuberculosi*s triggers a strong *Ifng* response but requires substantially higher levels of *Ifng* to control replication. Our data show a striking difference in the ability of the three mycobacterial strains to induce *Ifng* transcription, especially when the number of bacilli in the lungs is taken into account. Then the strongest inducer of *Ifng* transcripts is BCG Pasteur followed by *M. tuberculosi*s while BCG Russia is distinguished by its pronounced ability to avoid triggering an *Ifng* response. However, once *Ifng* is produced, BCG Russia appeared exquisitely sensitive to its action while *M. tuberculosis* is significantly more refractory to *Ifng* microbicidal action.

The important finding of our study is the demonstration of differential effects of host genetic background and pathogen strain on commonly used phenotypic traits of mycobacterial susceptibility. By necessity this invokes differences in the pathogenesis, either quantitative or qualitative, between different host-pathogen strain combinations. Given that both lung CFU and the wide array of mechanistic phenotypes we studied showed evidence for significant joint mycobacteria-host effects, it seems likely that similar effects are also seen in human populations. This opens the question if the search for protective correlates of tuberculosis should be focused on mechanistic phenotypes that show little sensitivity to host-pathogen variability or if different host-pathogen combinations invoke different protective correlates. Similarly, if a large numbers of persons are exposed to an array of *M. tuberculosis* strains it is possible that among the persons who develop tuberculosis some are susceptible to all strains while others are susceptible to specific subsets of *M. tuberculosis* strains. Such a hypothetical scenario would provide a straightforward biological explanation why *M. tuberculosis* strains are preferentially associated with distinct human populations [42,43]. If correct, differential host-mycobacteria effects should become a focus of future research aimed at identifying determinants of the flow of *M. tuberculosis* through exposed populations.

ACKNOWLEDGEMENTS

We gratefully acknowledge the technical assistance of Manon Girard, Fiona McIntosh, Vlad Kamenski, and Annie Verville. We thank Lydia Ouadi for expert histological support and Athena Kalyvas for help with the histology figures. We also thank Adam Belley for providing the BCG Russia and BCG Pasteur as well as Pilar Domenech for providing the *M. tuberculosis* H37Rv (Pasteur).

References

1. Baghdadi JE, Orlova M, Alter A, et al. An autosomal dominant major gene confers predisposition to pulmonary tuberculosis in adults. *J Exp Med.* Jul 10 2006;203(7):1679-1684.

2. Cobat A, Gallant CJ, Simkin L, et al. High heritability of antimycobacterial immunity in an area of hyperendemicity for tuberculosis disease. *J Infect Dis.* Jan 1 2010;201(1):15-19.

3. Cobat A, Gallant CJ, Simkin L, et al. Two loci control tuberculin skin test reactivity in an area hyperendemic for tuberculosis. *J Exp Med.* Nov 23 2009;206(12):2583-2591.

4. Gagneux S, Small PM. Global phylogeography of *Mycobacterium tuberculosis* and implications for tuberculosis product development. *Lancet Infect Dis.* May 2007;7(5):328-337.

5. Malik AN, Godfrey-Faussett P. Effects of genetic variability of *Mycobacterium tuberculosis* strains on the presentation of disease. *Lancet Infect Dis.* Mar 2005;5(3):174-183.

6. Pym AS, Brodin P, Brosch R, Huerre M, Cole ST. Loss of RD1 contributed to the attenuation of the live tuberculosis vaccines *Mycobacterium bovis* BCG and *Mycobacterium microti*. *Mol Microbiol.* Nov 2002;46(3):709-717.

7. Lewis KN, Liao R, Guinn KM, et al. Deletion of RD1 from *Mycobacterium tuberculosis* mimics bacille Calmette-Guerin attenuation. *J Infect Dis.* Jan 1 2003;187(1):117-123.

8. Mostowy S, Tsolaki AG, Small PM, Behr MA. The in vitro evolution of BCG vaccines. *Vaccine.* Oct 1 2003;21(27-30):4270-4274.

9. Brosch R, Gordon SV, Garnier T, et al. Genome plasticity of BCG and impact on vaccine efficacy. *Proc Natl Acad Sci U S A.* Mar 27 2007;104(13):5596-5601.

10. Salamon H, Kato-Maeda M, Small PM, Drenkow J, Gingeras TR. Detection of deleted genomic DNA using a semiautomated computational analysis of GeneChip data. *Genome Res.* Dec 2000;10(12):2044-2054.

11. Behr MA, Wilson MA, Gill WP, et al. Comparative genomics of BCG vaccines by whole-genome DNA microarray. *Science.* May 28 1999;284(5419):1520-1523.

12. Mahairas GG, Sabo PJ, Hickey MJ, Singh DC, Stover CK. Molecular analysis of genetic differences between *Mycobacterium bovis* BCG and virulent *M. bovis*. *J Bacteriol.* Mar 1996;178(5):1274-1282.

13. Actor JK, Olsen M, Jagannath C, Hunter RL. Relationship of survival, organism containment, and granuloma formation in acute murine tuberculosis. *J Interferon Cytokine Res.* Oct 1999;19(10):1183-1193.

14. Jagannath C, Hoffmann H, Sepulveda E, Actor JK, Wetsel RA, Hunter RL. Hypersusceptibility of A/J mice to tuberculosis is in part due to a deficiency of the fifth complement component (C5). *Scand J Immunol.* Oct 2000;52(4):369-379.

15. Watson VE, Hill LL, Owen-Schaub LB, et al. Apoptosis in *Mycobacterium tuberculosis* infection in mice exhibiting varied immunopathology. *J Pathol.* Feb 2000;190(2):211-220.

16. Gros P, Skamene E, Forget A. Genetic control of natural resistance to *Mycobacterium bovis* (BCG) in mice. *J Immunol.* Dec 1981;127(6):2417-2421.

17. Vidal SM, Malo D, Vogan K, Skamene E, Gros P. Natural resistance to infection with intracellular parasites: isolation of a candidate for *Bcg*. *Cell.* May 7 1993;73(3):469-485.

18. Di Pietrantonio T, Hernandez C, Girard M, et al. Strain-specific differences in the genetic control of two closely related mycobacteria. *PLoS Pathog.* 2010;6(10):e1001169.

19. Belley A, Alexander D, Di Pietrantonio T, et al. Impact of methoxymycolic acid production by *Mycobacterium bovis* BCG vaccines. *Infect Immun.* May 2004;72(5):2803-2809.

20. Andersen CL, Jensen JL, Orntoft TF. Normalization of real-time quantitative reverse transcription-PCR data: a model-based variance estimation approach to identify genes suited for normalization, applied to bladder and colon cancer data sets. *Cancer Res.* Aug 1 2004;64(15):5245-5250.

21. Vandesompele J, De Preter K, Pattyn F, et al. Accurate normalization of real-time quantitative RT-PCR data by geometric averaging of multiple internal control genes. *Genome Biol.* Jun 18 2002;3(7):RESEARCH0034.

22. Littell RC, Milliken GA, Stroup WW, Wolfinger RD, Schabenberger O. *SAS® for Mixed Models, Second Edition*. Cary, NC, USA: SAS Institute Inc.; 2006.

23. Kowalchuk RK, Keselman HJ, Algina J, Wolfinger RD. The Analysis of Repeated Measurements with Mixed-Model Adjusted F Tests. *Educ Psychol Meas.* Apr 2004;64(2):224-242.

24. Westfall PH. Multiple testing of general contrasts using logical constraints and correlations. *J Am Stat Assoc* 1997;92::299–306.

25. Livak KJ, Schmittgen TD. Analysis of relative gene expression data using real-time quantitative PCR and the 2(-Delta Delta C(T)) Method. *Methods.* Dec 2001;25(4):402-408.

26. Fu WJ, Hu J, Spencer T, Carroll R, Wu G. Statistical models in assessing fold change of gene expression in real-time RT-PCR experiments. *Comput Biol Chem.* Feb 2006;30(1):21-26.

27. Dormans J, Burger M, Aguilar D, et al. Correlation of virulence, lung pathology, bacterial load and delayed type hypersensitivity responses after infection with different *Mycobacterium tuberculosis* genotypes in a BALB/c mouse model. *Clin Exp Immunol.* Sep 2004;137(3):460-468.

28. Lopez B, Aguilar D, Orozco H, et al. A marked difference in pathogenesis and immune response induced by different *Mycobacterium tuberculosis* genotypes. *Clin Exp Immunol.* Jul 2003;133(1):30-37.

29. Reed MB, Domenech P, Manca C, et al. A glycolipid of hypervirulent tuberculosis strains that inhibits the innate immune response. *Nature.* Sep 2 2004;431(7004):84-87.

30. Irwin SM, Goodyear A, Keyser A, et al. Immune response induced by three *Mycobacterium bovis* BCG substrains with diverse regions of deletion in a C57BL/6 mouse model. *Clin Vaccine Immunol.* May 2008;15(5):750-756.

31. Leung AS, Tran V, Wu Z, et al. Novel genome polymorphisms in BCG vaccine strains and impact on efficacy. *BMC Genomics.* 2008;9:413.

32. Liu J, Tran V, Leung AS, Alexander DC, Zhu B. BCG vaccines: their mechanisms of attenuation and impact on safety and protective efficacy. *Hum Vaccin.* Feb 2009;5(2):70-78.

33. Greenwood CM, Fujiwara TM, Boothroyd LJ, et al. Linkage of tuberculosis to chromosome 2q35 loci, including *NRAMP1*, in a large aboriginal Canadian family. *Am J Hum Genet.* Aug 2000;67(2):405-416.

34. Malik S, Abel L, Tooker H, et al. Alleles of the *NRAMP1* gene are risk factors for pediatric tuberculosis disease. *Proc Natl Acad Sci U S A.* Aug 23 2005;102(34):12183-12188.

35. Kramnik I, Dietrich WF, Demant P, Bloom BR. Genetic control of resistance to experimental infection with virulent *Mycobacterium tuberculosis*. *Proc Natl Acad Sci U S A.* Jul 18 2000;97(15):8560-8565.

36. Lavebratt C, Apt AS, Nikonenko BV, Schalling M, Schurr E. Severity of tuberculosis in mice is linked to distal chromosome 3 and proximal chromosome 9. *J Infect Dis.* Jul 1999;180(1):150-155.

37. Mitsos LM, Cardon LR, Fortin A, et al. Genetic control of susceptibility to infection with *Mycobacterium tuberculosis* in mice. *Genes Immun.* Dec 2000;1(8):467-477.

38. Mitsos LM, Cardon LR, Ryan L, LaCourse R, North RJ, Gros P. Susceptibility to tuberculosis: a locus on mouse chromosome 19 (*Trl-4*) regulates *Mycobacterium tuberculosis* replication in the lungs. *Proc Natl Acad Sci U S A.* May 27 2003;100(11):6610-6615.

39. Sanchez F, Radaeva TV, Nikonenko BV, et al. Multigenic control of disease severity after virulent *Mycobacterium tuberculosis* infection in mice. *Infect Immun.* Jan 2003;71(1):126-131.

40. Sissons J, Yan BS, Pichugin AV, Kirby A, Daly MJ, Kramnik I. Multigenic control of tuberculosis resistance: analysis of a QTL on mouse chromosome 7 and its synergism with sst1. *Genes Immun.* Jan 2009;10(1):37-46.

41. Yan BS, Kirby A, Shebzukhov YV, Daly MJ, Kramnik I. Genetic architecture of tuberculosis resistance in a mouse model of infection. *Genes Immun.* Apr 2006;7(3):201-210.

42. Gagneux S, DeRiemer K, Van T, et al. Variable host-pathogen compatibility in *Mycobacterium tuberculosis*. *Proc Natl Acad Sci U S A.* Feb 21 2006;103(8):2869-2873.

43. Reed MB, Pichler VK, McIntosh F, et al. Major *Mycobacterium tuberculosis* lineages associate with patient country of origin. *J Clin Microbiol.* Apr 2009;47(4):1119-1128.

Preface to Chapter 3

In Chapter 2, we showed that genetic variation between the A/J and C57BL/6J mouse strains and among mycobacteria is correlated with differences in the host response to infection. Phenotypic differences were observed across the two mouse strains and the three mycobacteria, suggesting a joint effect of host and pathogen in the course of mycobacterial infection. Host-pathogen specific pathogenesis in turn implies differences in the host genetic control of infection. In the following chapter, we performed a comparative genetic analysis using the A/J- and C57BL/6J-derived recombinant congenic (RC) strains infected with BCG Russia and BCG Pasteur to determine whether the host genetic control of mycobacterial infection is jointly dependent on the host and pathogen. This notion is consistent with the variable efficacy of different BCG vaccines in different human populations as well as with recent studies suggesting co-adaptation of *M. tuberculosis* strains to specific human ethnicities.

CHAPTER 3
Strain-Specific Differences in the Genetic Control of Two Closely Related Mycobacteria

---

Tania Di Pietrantonio[1,2,3], Carmen Hernandez[1], Manon Girard[1], Annie Verville[1], Marianna Orlova[1,2], Adam Belley[1], Marcel A. Behr[1,3], J Concepción Loredo-Osti[4*] and Erwin Schurr[1,2,3*]

[1] McGill Centre for the Study of Host Resistance, Research Institute of the McGill University Health Centre, Montreal, Quebec, Canada

[2]Department of Human Genetics and [3]Department of Medicine, McGill University, Montreal, Quebec, Canada

[4]Department of Mathematics and Statistics, Memorial University of Newfoundland, St Johns, Newfoundland and Labrador, Canada

* Share senior authorship.

ABSTRACT

The host response to mycobacterial infection depends on host and pathogen genetic factors. Recent studies in human populations suggest a strain specific genetic control of tuberculosis. To test for mycobacterial-strain specific genetic control of susceptibility to infection under highly controlled experimental conditions, we performed a comparative genetic analysis using the A/J- and C57BL/6J-derived recombinant congenic (RC) mouse panel infected with the Russia and Pasteur strains of *Mycobacterium bovis* Bacille Calmette Guérin (BCG). Bacillary counts in the lung and spleen at weeks 1 and 6 post infection were used as a measure of susceptibility. By performing genome-wide linkage analyses of loci that impact on tissue-specific bacillary burden we were able to show the importance of correcting for strain background effects in the RC panel. When linkage analysis was adjusted on strain background, we detected a single locus on chromosome 11 that impacted on pulmonary counts of BCG Russia but not Pasteur. The same locus also controlled the splenic counts of Russia but not Pasteur. By contrast, a locus on chromosome 1 which was indistinguishable from *Nramp1* impacted on splenic bacillary counts of both Russia and Pasteur. Additionally, dependent upon BCG strain, tissue and time post infection, we detected 9 distinct loci associated with bacillary counts. Hence, the ensemble of genetic loci impacting on BCG infection revealed a highly dynamic picture of genetic control that reflected both the course of infection and the infecting strain. This high degree of adaptation of host genetics to strain-specific pathogenesis is expected to provide a suitable framework for the selection of specific host-mycobacteria combinations during co-evolution of mycobacteria with humans.

INTRODUCTION

The primary cause of tuberculosis is the human pathogenic bacterium *Mycobacterium tuberculosis*. The host cells of *M. tuberculosis* are macrophages and the bacilli have developed numerous adaptations to survive within these powerful immune effector cells. For example, human pathogenic strains of *M. tuberculosis* inactivate microbicidal superoxide via katalase [1], avoid the detrimental effects of iNOS products [2], skew the anti-mycobacterial response in macrophages towards production of anti-inflammatory molecules [3, 4], and favour necrosis over apoptosis [5-7]. Interestingly, circulating strains of *M. tuberculosis* may differ in their pathogenic potential [8, 9]. Since humans and *M. tuberculosis* have co-evolved over millennia, a question remains if and to what extent *M. tuberculosis* has adapted to genetically distinct hosts. Indeed, two studies conducted in ethnically mixed samples detected a non-random association of *M. tuberculosis* strains with distinct ethnic populations [10, 11]. These observations are supported by the results of several genetic association studies that detected preferential associations between a Toll-like receptor 2 (*TLR2*) polymorphism and tuberculosis meningitis caused by Beijing strains [12], as well as between variants of 5'-lipoxygenase (*ALOX5*) and pulmonary tuberculosis caused by *M. africanum*, but not *M. tuberculosis* [13]. In addition, variants of the immunity-related GTPase M (*IRGM*) were associated with protection from pulmonary tuberculosis due to Euro-American strains of *M. tuberculosis* [14]. Due to the complex interactions of *M. tuberculosis* and humans in exposed populations, it is possible that those results may have been confounded by unrecognized factors. In the absence of independent replication studies, the question of strain specific genetic effects as a consequence of *M. tuberculosis* human co-evolution still awaits testing under carefully controlled conditions.

M. bovis Bacille Calmette-Guerin (BCG) strains are phylogenetic descendants of an ancestral BCG stock originally derived from virulent *M. bovis* through *in vitro* propagation [15-17]. Attenuation of the original BCG stock occurred as a result of deletions in the *M. bovis* genome, specifically the region of difference 1 (RD1)

[18, 19]. Loss of RD1 is common across all BCG strains, although additional genetic alterations have been identified for each strain. BCG Russia and BCG Pasteur are among the most phylogenetically distant BCG strains [15]. Genetic events identified in BCG Russia include the deletion of RD Russia (Rv3698) [20], an insertion mutation in the *recA* gene (recA_D140*) [21], and the presence of an IS*6110* element in the promoter region of the *phoP* gene [15, 22]. BCG Pasteur is characterized by the loss of RD2, nRD18, and RD14 [23-25] as well as a number of single point mutations and duplication events [22, 23, 26, 27]. Phenotypic differences between BCG Pasteur and BCG Russia can therefore be tentatively linked to these known changes in gene content and an unknown number of point mutations. A number of unresolved questions surround the BCG host interplay which is characterized by highly variable host responsiveness. For example, the immunogenicity of the same strain of BCG given to vaccinees of different genetic background can vary tremendously [28, 29] while host responses triggered by different strains of BCG are equally divergent [30]. On a population scale, BCG strains differ in the adverse reactions they trigger [31] and there is evidence that the protective effect of BCG vaccination against tuberculosis meningitis varies among ethnically divergent population groups [32]. Taken together, these data suggest that, similar to tuberculosis susceptibility, host responsiveness may reflect specific host-BCG strain interactions. To test this possibility, we compared the genetic control of closely related strains of BCG in a mouse model of infection.

Recombinant congenic (RC) strains are a set of genetically related inbred strains. In RC strains, discrete chromosomal segments of donor genome (12.5%) are transferred onto a recipient genetic background (87.5%) through a double backcross and corresponding strains are derived by subsequent inbreeding [33]. The AcB/BcA panel used in the present study was derived from a reciprocal double backcross between C57BL/6J and A/J [34], two mouse strains known to differ in their susceptibility to *M. bovis* BCG strain Montreal [35]. Each RC strain is genetically distinct with its own unique genome. The genomes of all RC strains have been mapped extensively and represent frozen replicas of recombinant

progenitor genomes with known genomic boundaries of chromosomal segments derived from the two progenitor strains. A major advantage of RC strains over conventional crosses is that any phenotype can be measured repeatedly in genetically identical mice of a RC strain, greatly improving the accuracy of the phenotypic estimates.

In the present study, 35 distinct AcB/BcA strains were infected with a low dose of either BCG Pasteur or BCG Russia. A genetic analysis of the bacillary counts in the spleen and lungs of these strains identified general, as well as tissue- and BCG strain-specific susceptibility loci for BCG infection. These results demonstrated that the host response to mycobacteria reflects a genetically controlled, joint effect of both host and pathogen. Our findings established strain specific effects of the host-mycobacteria interplay in the absence of selective pressure and, therefore, argue in favour of additional host-mycobacterial adaptation during the co-evolution of humans and mycobacteria.

MATERIALS AND METHODS

Mice and ethics statement

A/J and C57BL/6J mice were purchased from the Jackson Laboratory (Bar Harbor, Maine). Thirty-five independent RC strains originally derived from a reciprocal double backcross between the A/J and C57BL/6J progenitors [34] were purchased from Emerillon Therapeutics Inc. (Montreal, Qc.). All mice were housed in the rodent facility of the Montreal General Hospital. Animal use protocols were approved by the Animal Care Committee of McGill University and are in direct accordance with the guidelines outlined by the Canadian Council on Animal Care.

Bacterial strains

Recombinant BCG Russia (ATCC 35740), and Pasteur (ATCC 35734), were transformed with pGH1, an integrating vector that inserts into the attB site of the mycobacterial genome and that combines a firefly luciferase lux gene cassette, an integrase [int] gene, a MOP promoter, and a hygromycin resistance [Hyg] gene [31]. The pGH1 vector allows for growth on antibiotic-containing media to reduce risk of contamination [36].

Infection of mice

BCG strains were grown on a rotating platform at 37°C in Middlebrook 7H9 medium (Difco Laboratories, Detroit, Mich.) containing 0.05% Tween 80 (Sigma-Aldrich, St. Louis, Mo.) and 10% albumin-dextrose-catalase (ADC) supplement (Becton Dickinson and Co., Sparks, Md.). At an optical density (OD_{600}) of 0.4 to 0.5, bacteria were diluted in phosphate buffered saline (PBS) to 10^5 colony forming units (CFU)/ml. Mice were injected intravenously with 10^3 to 10^4 CFU of BCG in 100µL of PBS. Inoculum doses were confirmed by plating on Middlebrook 7H10 agar (Difco Laboratories, Detroit, Mich.) supplemented with oleic acid-albumin-dextrose-catalase (OADC) enrichment (Becton Dickinson and Co., Sparks, Md.).

BCG load in target organs

Infected mice were sacrificed by CO_2 inhalation after 1 and 6 weeks post-infection. Lungs and spleens were aseptically removed, placed in 0.025% Saponin-PBS, and homogenized mechanically using a Polytron PT 2100 homogenizer (Brinkman Instruments, Westbury, NY). Homogenates were serially diluted tenfold and plated on Middlebrook 7H10 agar supplemented with OADC enrichment and containing hygromycin B (Wisent Inc., St.-Bruno, Qc.). Bacterial enumeration was performed following a six-week incubation at 37°C. For BCG Pasteur infection, a total of 221 and 175 mice were used at the week 1 and 6 time points, respectively. A total of 145 and 189 mice, respectively, were used at 1 and 6 weeks for BCG Russia infection.

Genotyping

Strains of the AcB/BcA panel were genotyped for 625 microsatellite markers spanning the entire genome with an average distance of 2.6 cM [34]. From the 625 markers, six with reassigned marker positions were removed from the current analysis [37].

Statistical analysis

a) Model without genetic background.

The first QTL model considered was the linear model

$$\mathbf{y} = \mathbf{X\beta} + \mathbf{q}_m\xi_m + \mathbf{e}$$

where y represents a vector with the individual total count of bacteria ($\log_{10}$ CFU); $\mathbf{q}_m$ is a vector with each entry being an indicator variable of the genotype BB at the marker position m with ξ_m being its associated effect (major gene effect)**;** $\mathbf{X}$ is a matrix of fixed covariates (a constant and gender in our main model) and its corresponding parameter vector $\boldsymbol{\beta}$; $\mathbf{e}$ is a vector of independent and identically distributed random variables representing the error term with $E(\mathbf{e}) = \mathbf{0}$ and $Var(\mathbf{e}) = \sigma^2\mathbf{I}$. Since a large over-dispersion of the data was observed which

was thought to be the effect of outliers in the data, M-estimates of the parameters and the test statistic were computed at each marker position *m*,

$$t_m = \frac{|\hat{\xi}_m|}{\hat{\sigma}_{\hat{\xi}_m}}$$

The genome-wide corrected p-values were obtained by bootstrap under the hypothesis that there is no major gene, i.e. re-sampling under the reduced model

$$\mathbf{y} = \mathbf{X\beta} + \mathbf{e}$$

Mean confidence bounds at each marker were defined as twice the standard error around the marker's group mean without considering gender effect in the model.

b) Model with genetic background.

Another plausible source of over-dispersion may be a random component omitted in the model. In genetic studies, the natural candidate for this sort of effect is genetic background, i.e., the additive minuscule effect of many genes whose individual contribution is not large enough to be mapped. In order to account for the genetic background, a second linear model of the form

$$\mathbf{y} = \mathbf{X\beta} + \mathbf{Z\gamma} + \mathbf{q}_m\xi_m + \mathbf{e}$$

was employed, i.e., our second model was the mixed model resulting from adding a random component, $\mathbf{Z\gamma}$, to our original model, where $\boldsymbol{\gamma}$ is a random vector associated to the genetic background of each RCS and $\mathbf{Z}$ is the design matrix associating the RCS effect to the phenotype $\mathbf{y}$. The assumptions for this model component were $E(\boldsymbol{\gamma}) = 0$ and $Var(\boldsymbol{\gamma}) = \sigma_{\boldsymbol{\gamma}}^2\mathbf{G}$, with $\sigma_{\boldsymbol{\gamma}}^2 > 0$ being an unknown constant and $\mathbf{G}$ a positive definite-matrix (in fact, a background correlation matrix which is a function of length of the segments identical by descent shared amongst strains) assumed to be known, although a genomic estimate of it was previously obtained. At each marker position *m*, iteratively, estimates of fixed effect parameters and the variance components were obtained under this model and a test statistic of the same form as before

$$t_m = \frac{|\hat{\xi}_m|}{\hat{\sigma}_{\hat{\xi}_m}}$$

was computed. The genome-wide corrected p-values were obtained by bootstrap under the hypothesis that there is no major gene, i.e., re-sampling under the reduced model

$$\mathbf{y} = \mathbf{X}\boldsymbol{\beta} + \mathbf{Z}\boldsymbol{\gamma} + \mathbf{e}$$

Estimation and testing procedure are described in more detail below.

Estimation. Without loss of generality, here we describe the estimation for the mixed model

$$\mathbf{y} = \mathbf{X}\boldsymbol{\beta} + \mathbf{Z}\boldsymbol{\gamma} + \boldsymbol{\varepsilon}$$

where $\mathbf{X}$, $\mathbf{Z}$ are known matrices, $\boldsymbol{\beta}$ is an unknown fixed vector and $\boldsymbol{\gamma}$ and $\boldsymbol{\varepsilon}$ are random vectors with null mean and variance $\sigma_\gamma^2\boldsymbol{\Delta}_1$ and $\sigma^2\mathbf{I}$, respectively. Thus

$$\mathrm{E}(\mathbf{y}) = \mathbf{X}\boldsymbol{\beta} \qquad \text{and} \qquad \mathrm{Var}(\mathbf{y}) = \sigma^2\left(\mathbf{Z}\mathbf{G}\mathbf{Z}'+\mathbf{I}\right) = \sigma^2\boldsymbol{\Sigma}$$

with $\mathbf{G} = \lambda^{-1}\boldsymbol{\Delta}_1$ and $\lambda = \dfrac{\sigma^2}{\sigma_\gamma^2}$. Given $\mathbf{G}$ (which means λ is known), the BLUE of $\boldsymbol{\beta}$ and the BLUP of γ can be written as

$$\tilde{\boldsymbol{\beta}} = (\mathbf{W}'\mathbf{W})^{-}\mathbf{W}'\mathbf{v} \quad \text{and} \quad \tilde{\boldsymbol{\gamma}} = \mathbf{G}\mathbf{Z}'\boldsymbol{\Sigma}^{-\frac{1}{2}}(\mathbf{v} - \mathbf{W}\boldsymbol{\beta}),$$

respectively, where

$$\mathbf{W} = \boldsymbol{\Sigma}^{-\frac{1}{2}}\mathbf{X} \quad \text{and} \quad \mathbf{v} = \boldsymbol{\Sigma}^{-\frac{1}{2}}\mathbf{y}.$$

Also

$$\hat{\sigma}^2 = \frac{1}{N - r(\mathbf{W})}(\mathbf{v} - \mathbf{W}\boldsymbol{\beta})'(\mathbf{v} - \mathbf{W}\boldsymbol{\beta})$$

$$\hat{\sigma}_\gamma^2 = \frac{1}{r(\mathbf{G})}\left(\boldsymbol{\gamma}'\mathbf{G}^{-1}\boldsymbol{\gamma} + \hat{\sigma}^2\mathrm{tr}(\mathbf{G}^{-1}\mathbf{C})\right)$$

with

$$\mathbf{C} = (\mathbf{Z}'\mathbf{M}\mathbf{Z} + \mathbf{G}^{-1})^{-1} \quad \text{and} \quad \mathbf{M} = \mathbf{I} - \mathbf{X}(\mathbf{X}'\mathbf{X})^{-1}\mathbf{X}.$$

The estimation procedure runs as follows: get a starting value for λ and iterate through these equations until convergence is reached.

Bootstrap. When $\boldsymbol{\beta}$ and λ are known, it follows from the model reduced under the null hypothesis that $E(\mathbf{v}) = \mathbf{W}\boldsymbol{\beta}$ and $\text{var}(\mathbf{v}) = \sigma^2\mathbf{I}$, thus the distribution of vector of residuals, $\boldsymbol{\varepsilon} = \mathbf{v} - \mathbf{W}\boldsymbol{\beta}$, is exchangeable, which means that a re-sampling procedure based upon the residuals will have good asymptotic properties. This suggests the following semi-parametric bootstrap procedure: i) given $\tilde{\lambda}$ and $\tilde{\boldsymbol{\beta}}$ obtained under the mixed model without a major gene, i.e., under the null hypothesis, compute $\tilde{\boldsymbol{\varepsilon}} = \mathbf{D}(\mathbf{v} - \mathbf{W}\tilde{\boldsymbol{\beta}})$ where $\mathbf{D}$ is a diagonal matrix with each of the non-zero elements given by $(1 - h_{ii})^{-1}$ and h_{ii} being the ith the leverage coefficient; ii) with replacement, re-sample from $\tilde{\boldsymbol{\varepsilon}}$ to obtain $\boldsymbol{\varepsilon}^*$ and construct the pseudo-observation as $\mathbf{v}^* = \mathbf{W}\tilde{\boldsymbol{\beta}} + \boldsymbol{\varepsilon}^*$.

Testing. Obtain the genome-wide corrected empirical p-values by the following procedure: i) at each marker position, fit the major gene model

$$\mathbf{v} = \begin{pmatrix} \mathbf{W} & \boldsymbol{\Sigma}^{-\frac{1}{2}} q_m \end{pmatrix} \begin{pmatrix} \boldsymbol{\beta} \\ \xi_m \end{pmatrix} + \boldsymbol{\varepsilon}$$

(of course, this model is completely equivalent to the one described in the text) and estimate the model parameters with the mixed model procedure outlined above; ii) compute the test statistic vector $\mathbf{t}_m$; iii) draw a pseudo-observation $\mathbf{v}^*$ by using the previous re-sampling scheme and fit the major gene model in (i) with $\mathbf{v}$ replaced by $\mathbf{v}^*$ to obtain a pseudo-statistic vector $\mathbf{t}_m^*$ as well as its associated critical value $t_c^* = \max \mathbf{t}_m^*$; iv) for each t_m in t_m, if $t_m \le t_c^*$, update the m-th rejection count by adding an unit. v) Repeat the steps (iii)-(iv) B times and compute the estimates of p-values by dividing the rejection count vector by B.

Evidence was considered significant for linkage when the test statistic associated to each marker had a p-value $P < 0.01$.

RESULTS

We determined the bacillary load of BCG strains Pasteur and Russia in the lungs and spleens of C57BL/6J and A/J mice following a low dose (~$3x10^3$ bacilli) intravenous injection of bacilli. Pulmonary counts of BCG Pasteur were below the limit of detectability (80 bacilli/lung) at weeks 1 and 6 post infection but showed a modest peak of approximately 100 bacilli/lung at week 3 (Figure 1). This suggested limited dispersion and growth of BCG Pasteur in the lungs. In addition, there was no detectable difference in the pulmonary load of BCG Pasteur between C57BL6/J and A/J mice. By contrast, we observed an increase of 1-1.5 log CFU in the spleens between weeks 1 and 3 post infection that was followed by a 1 log decrease at week 6. The splenic bacillary burden of BCG Pasteur was substantially higher in C57BL/6J mice at weeks 1 and 3. BCG Russia showed a constant increase of pulmonary CFU from week 1 to week 6. In the spleen, growth of BCG Russia lagged growth of Pasteur and did not show evidence for a peak at 3 weeks post infection, as was observed for Pasteur (Figure 1). Overall, the pattern of tissue CFU for BCG Pasteur strongly resembled the one described for BCG Montreal which has previously been shown to be under *Nramp1* control [35, 38]. The kinetics of lung and spleen bacillary counts of BCG Russia were distinct from the previously described BCG growth patterns.

To investigate the genetic control of *in-vivo* growth of BCG Russia and BCG Pasteur, mice from a panel of 35 AcB/BcA RC strains were intravenously challenged with a low dose (3-5 x 10^3 bacilli) of BCG Russia or BCG Pasteur. The number of colony forming units (CFU) in the spleen and lung was used as the phenotype for the genetic analysis. CFU were determined at 1 week and 6 weeks post infection since it is well established that at 3 weeks, the *Nramp1* gene dominates the host response to BCG Montreal [38], making it potentially more difficult to discern additional genetic control elements.

To best indicate the effect of genotype on CFU, all RCS were stratified according to genotype at each marker, i.e. AA for markers on chromosomal segments

derived from A/J or BB for chromosomal segments derived from C57BL/6J. Mice of all RCS with a given genotype were then used to obtain the mean and 95% confidence interval of their pulmonary and splenic CFU. This presentation allowed to graphically depict the effect of both marker genotype and of the general strain background on CFU. Results for the spleen and lung for both BCG strains are presented in Figures 2 and 3. A clear impact of strain background on susceptibility to BCG in the spleen at 1 week post infection was evidenced by the larger bacillary counts in mice of the BB genotype across most chromosomes (Figure 2). The strong strain background effect on splenic CFU was resolved by 6 weeks post infection, particularly for BCG Pasteur where differences in splenic bacillary burden appeared negligible across all markers (Figure 2). By contrast, CFU differences in BCG Russia were observed for several small chromosomal segments possibly suggesting the presence of specific genetic loci (Figure 2). As in the parental strains, pulmonary burdens were at the limit of detectability at week 1 for both Russia and Pasteur, and week 6 for Pasteur. However, at the 6-week endpoint, preferential replication of BCG Russia was observed in mice bearing specific A/J-derived chromosomal segments, particularly at the distal portion of chromosome 11 (Figure 3).

Markers where the mean CFU of the AA and BB genotype groups diverged were indicative of chromosomal regions that potentially harboured a BCG susceptibility locus. To confirm the potential linkage of these chromosomal segments to bacterial burden, a genetic analysis comparing mice of the AA to BB genotype was performed. The initial analysis compared genotype groups without taking into account the genetic background of the strain or the gender of the mouse (incomplete model). As expected, markers significantly linked to bacterial burden corresponded well with chromosomal regions where the two genotypes differed (Figures 2 to 6). From this analysis, the genetic control of BCG Pasteur and Russia splenic infection appeared to be highly multigenic at the early time point. Employing a very stringent level of significance ($P < 0.0003$), quantitative trait loci (QTL) were identified across 8 and 15 different chromosomes for BCG

Pasteur and Russia, respectively (Figure 4). At the 6 week endpoint, a locus was identified on chromosome 1 for splenic BCG Russia load whereas genetic effects were not detected for BCG Pasteur load (Figure 5). Pulmonary CFU of BCG Russia was controlled by a locus on chromosome 11 while for BCG Pasteur a locus was identified on chromosome 8 (Figure 6).

Visual inspection of CFU across genotypes suggested a strong impact of strain background on bacillary loads. To account for the potential impact of background genes on linkage peaks, we developed a main model that accounted for the genetic background and gender of the mice. The number of loci identified by the main model was reduced relative to the incomplete model, particularly at the 1 week time point (Figures 7 and 8, and Table 1). For lung CFU, the locus on chromosome 11 remained that impacted on bacillary load of BCG Russia at 6 weeks post infection (Figure 9). No genetic effect was detected for pulmonary load of BCG Pasteur which is consistent with the very limited growth of BCG Pasteur in the lungs of all mice (data not shown).

In contrast to the lung, the genetic control of splenic bacillary load remained largely multigenic even after correction for strain background effects. For BCG Russia at 1 week post infection, a single locus on chromosome 1 (36.9 cM - 48.8 cM) was found to control splenic load (Figure 7). At 6 weeks post infection, the genetic control of BCG Russia was multigenic (Figure 8). In addition to the chromosome 1 locus (32.8-55.1 cM), loci were detected on chromosome 6 (45.5-46.3 cM), chromosome 11 (47.67 cM), and chromosome 19 (51 cM). Splenic load of BCG Pasteur at 1 week post infection was controlled by loci on chromosome 2 (10-15 and 22.5-26.2 cM), chromosome 7 (63.5-65.6 cM), and the X chromosome (37-40.2 cM). Additional weaker effects were identified on chromosome 3 (33.7 and 58.8 cM), chromosome 6 (63.9 cM), chromosome 10 (3 cM), and chromosome 17 (23.2 cM). A major gene effect detected on chromosome 1 (17-58.5 cM) overlapped the chromosome 1 locus controlling BCG Russia infection (Figure 7, Table 1). Genetic control elements were not

detected in response to BCG Pasteur infection at the 6 week time point (data not shown). The inverse complexity of Pasteur (multigenic at 1 week; no genes at week 6) and Russia (a single gene at week 1, multigenic at week 6) reflects differences in the replication pattern of the bacteria: Russia showed a delayed onset of growth that continued at week 6 while Pasteur showed rapid initial growth with a strong decline of CFU at week 6 as compared to week 3.

The chromosome 1 locus significant for linkage early during BCG Pasteur infection and at the early and late phase of BCG Russia infection was indistinguishable from *Nramp1*. Employing what we termed the "conditional model," we determined whether the additional linkage peaks were conditional on the *Nramp1* gene. For this the main model was modified to adjust for the effect of *Nramp1* by adding a column with the BB genotype indicator at the *Nramp1* position to the matrix **X**. Chromosomal regions identified at the week 1 time point of both BCG Pasteur and BCG Russia infection were no longer significant for linkage following correction for the chromosome 1 locus (data not shown). Similarly, the genetic effects detected on chromosome 6 and 19 were no longer significant at the 6 week time point of BCG Russia infection. However, the linkage hit detected on chromosome 11 (47.67 cM) retained its significance. By contrast, a secondary peak detected only for splenic CFU immediately proximal to this locus did not reach significance. Finally, an additional locus was localized to chromosome 13 (73-75 cM) (Figure 10).

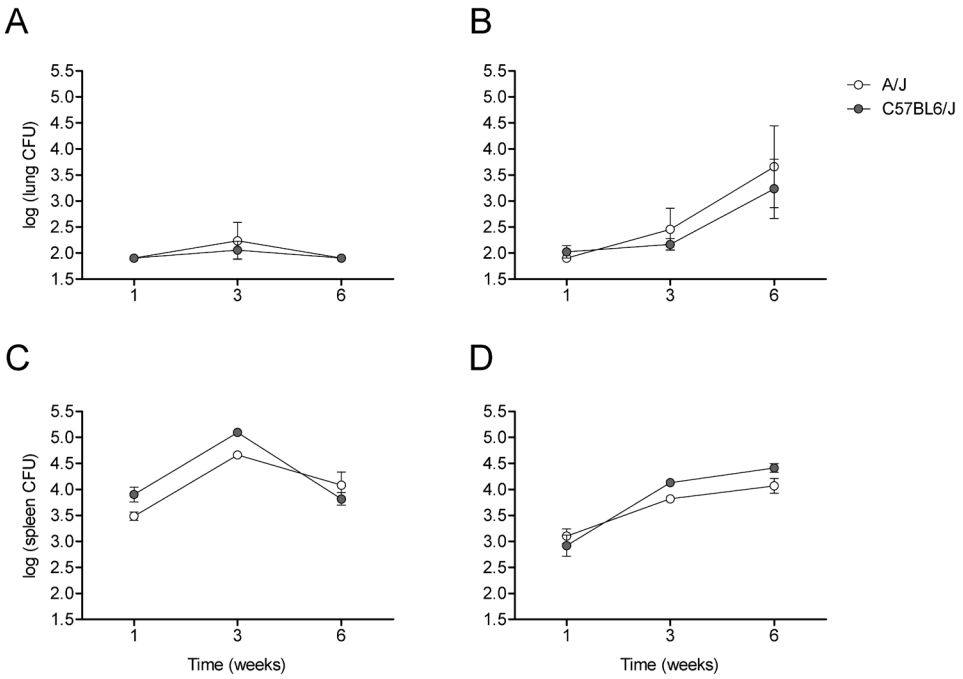

Figure 1. Replication of BCG in the lungs and spleen of A/J and C57BL/6J mice. A/J and C57BL/6J were intravenously infected with a low dose ($3\text{-}5 \times 10^3$) of either BCG Pasteur (A, C) or BCG Russia (B, D). The number of CFU in the lungs (A, B) and spleen (C, D) was determined at 1, 3, and 6 weeks post-infection. Bacterial counts of BCG Pasteur and BCG Russia were compared in A/J and C57BL/6J mice by two-way ANOVA. Differences in the pulmonary counts of BCG Pasteur and BCG Russia between A/J and C57BL/6J failed to reach significance. However, there was a significant difference in the splenic loads of BCG Pasteur ($P < 0.004$) and BCG Russia ($P < 0.0001$) between the two strains of mice. These results are representative of at least two experiments. Four to 13 mice were used at each time-point. Data at each time point are the mean $\log_{10}$ CFU and SD. White, A/J; grey, C57BL/6J.

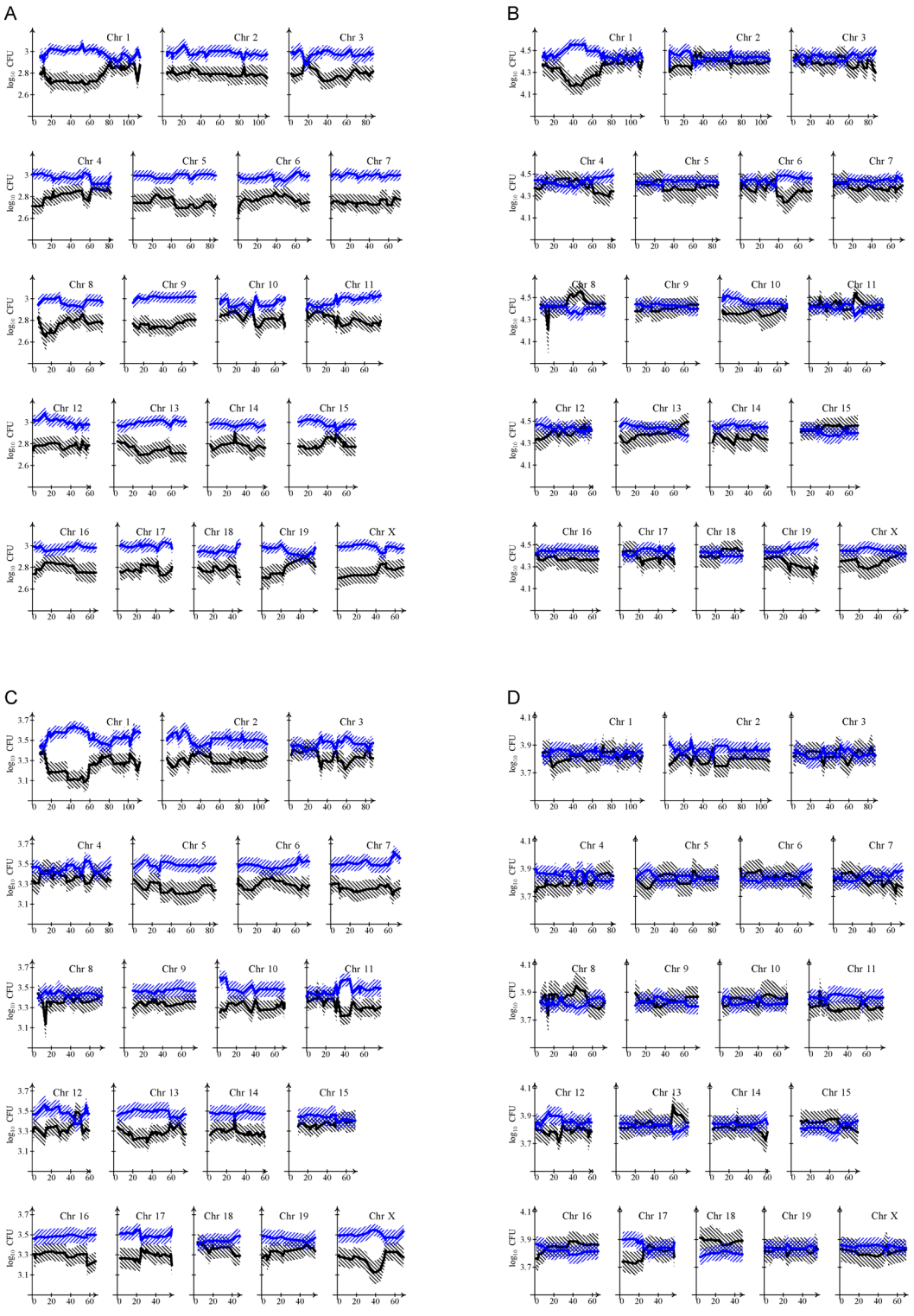
A
B
C
D
Chr 1
Chr 2
Chr 3
Chr 4
Chr 5
Chr 6
Chr 7
Chr 8
Chr 9
Chr 10
Chr 11
Chr 12
Chr 13
Chr 14
Chr 15
Chr 16
Chr 17
Chr 18
Chr 19
Chr X
log10 CFU

Figure 2. Spleen bacillary counts relative to A/J and C57BL/6J-derived chromosomal segments in RC mice. AcB and BcA mice were infected with BCG Russia (A, B) or BCG Pasteur (C, D) and spleen bacterial counts were determined at 1 week (A, C) and 6 weeks (B, D) post-infection. RC mice were stratified by genotype (AA in black or BB in blue) at each microsatellite marker and the mean $\log_{10}$ CFU (solid line) as well as twice the standard error confidence bounds (hatched area) were determined for the two groups of mice. Gaps between the mean CFU of the AA and BB genotype are indicative of markers where the two groups differed. Chromosomal positions are given in centimorgans (cM).

Figure 3. Lung bacillary counts relative to A/J and C57BL/6J-derived chromosomal segments in RC mice. Pulmonary bacterial loads in RC mice intravenously infected with BCG Russia (A, B) or BCG Pasteur (C, D) were determined at 1 week (A, C) and 6 weeks (B, D) post-infection. RC mice were stratified by genotype (AA in black or BB in blue) at each microsatellite marker and the mean $\log_{10}$ CFU (solid line) and confidence bounds (hatched area) were determined for the two groups of mice. A divergence in the mean CFU of the AA and BB genotype groups represent chromosomal regions where the two groups differed. Chromosomal positions are given in centimorgans (cM).

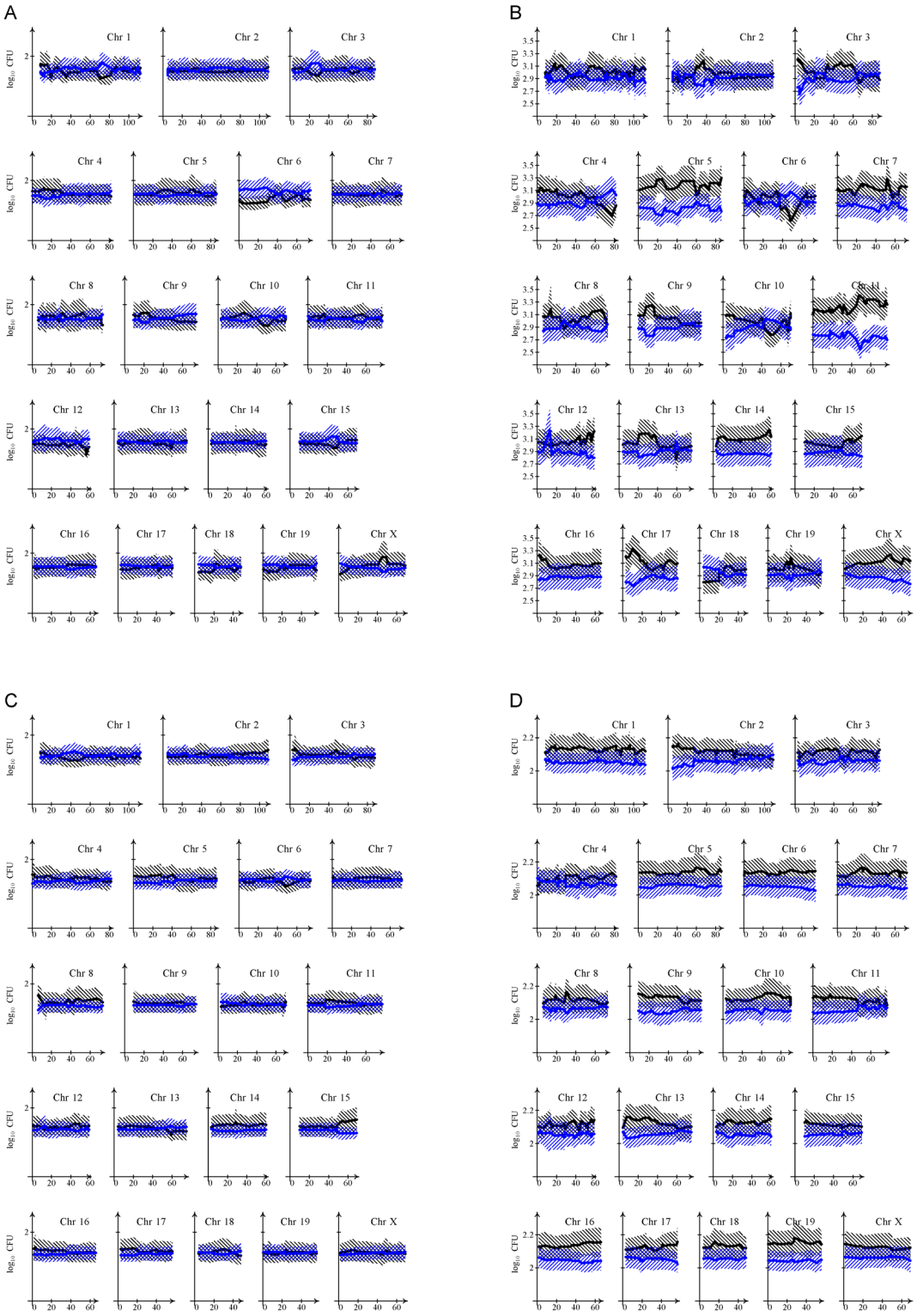
A
B
C
D
Chr 1
Chr 2
Chr 3
Chr 4
Chr 5
Chr 6
Chr 7
Chr 8
Chr 9
Chr 10
Chr 11
Chr 12
Chr 13
Chr 14
Chr 15
Chr 16
Chr 17
Chr 18
Chr 19
Chr X
log10 CFU

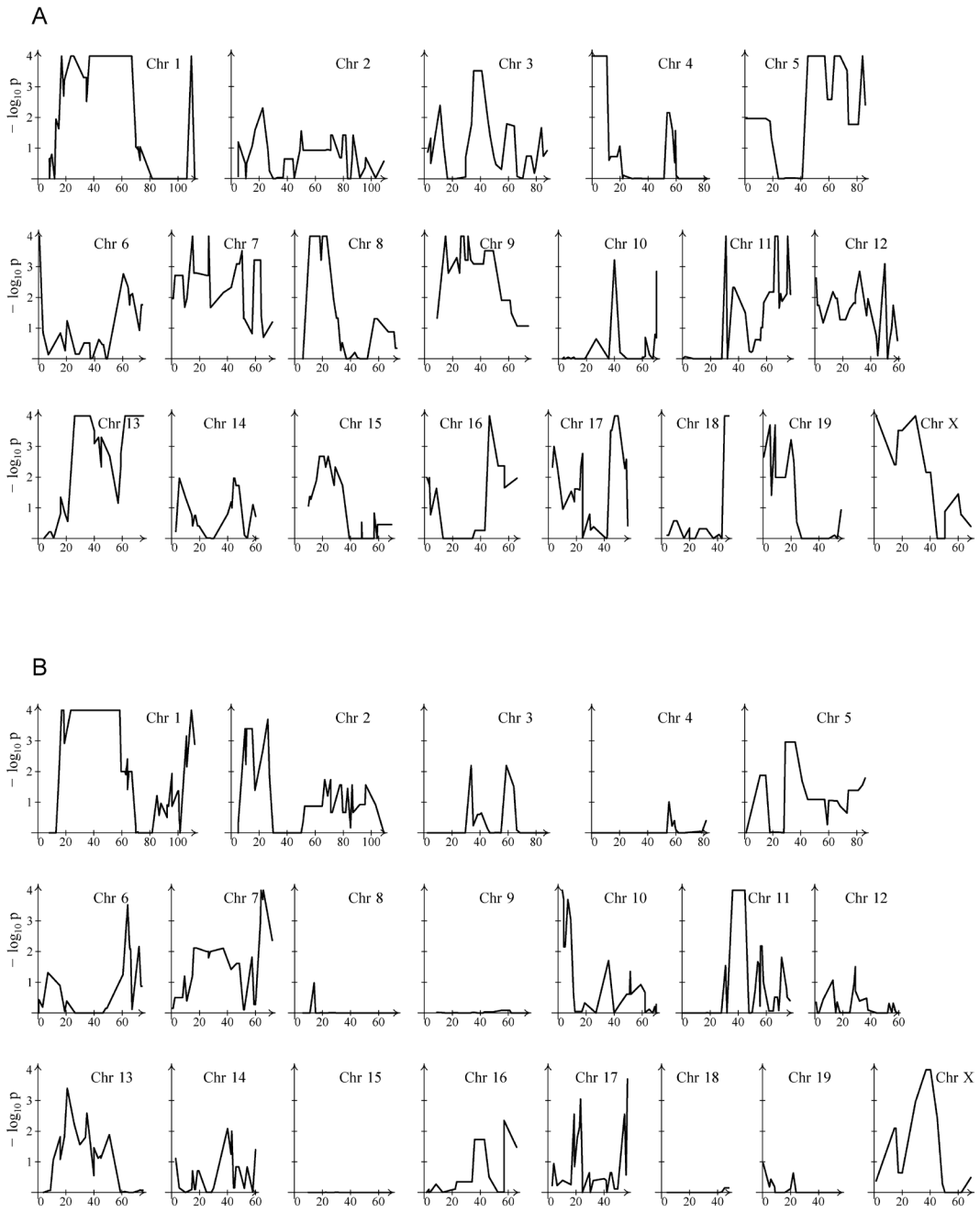

Figure 4. **Linkage analysis of early splenic counts independent of the genetic background.** Bacillary counts of BCG Russia and BCG Pasteur in the spleen of RC mice at the week 1 time point were used for QTL analysis. AA and BB genotype groups were analyzed without taking into account the gender or genetic background of the RC mice. Significant evidence for linkage was detected across 15 different chromosomes for BCG Russia (A) and across 8 different chromosomes for BCG Pasteur (B) at the week 1 time point. Chromosomal positions are given in centimorgans (cM).

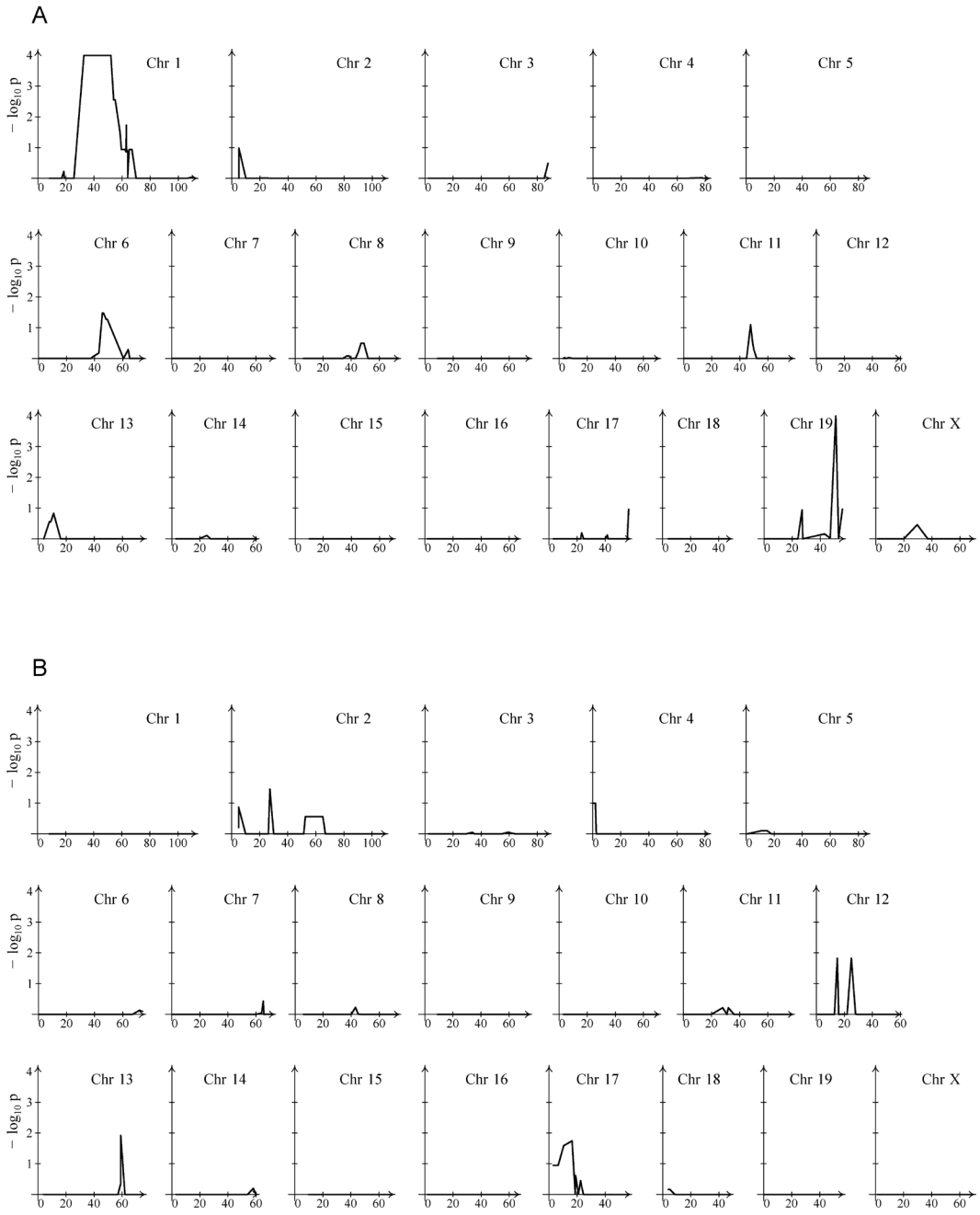

Figure 5. **Linkage analysis of late splenic counts independent of the genetic background.** Bacterial numbers of BCG Russia and BCG Pasteur in the spleen of RC mice at the week 6 time point were used for linkage analysis. Significant linkages were detected on chromosomes 1 and 19 for BCG Russia (A) whereas no significant evidence for linkage was detected for BCG Pasteur (B). Chromosomal positions are given in centimorgans (cM).

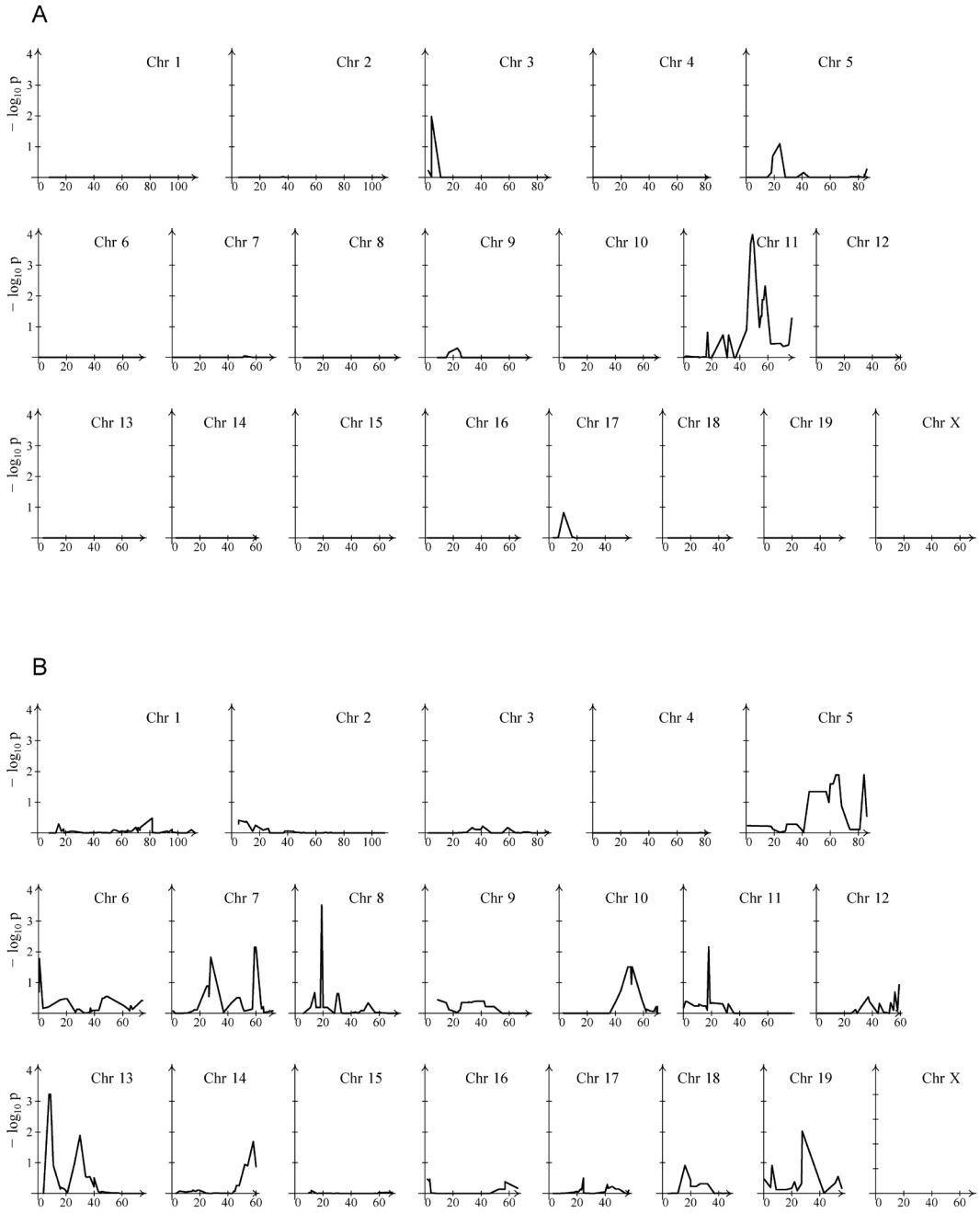

Figure 6. **Linkage analysis of late pulmonary counts independent of the genetic background.** QTL analysis was performed using pulmonary counts of BCG Russia and BCG Pasteur at the week 6 time point. Loci controlling pulmonary bacterial numbers were identified on chromosome 11 for BCG Russia (A) and chromosome 8 for BCG Pasteur (B). Chromosomal positions are given in centimorgans (cM).

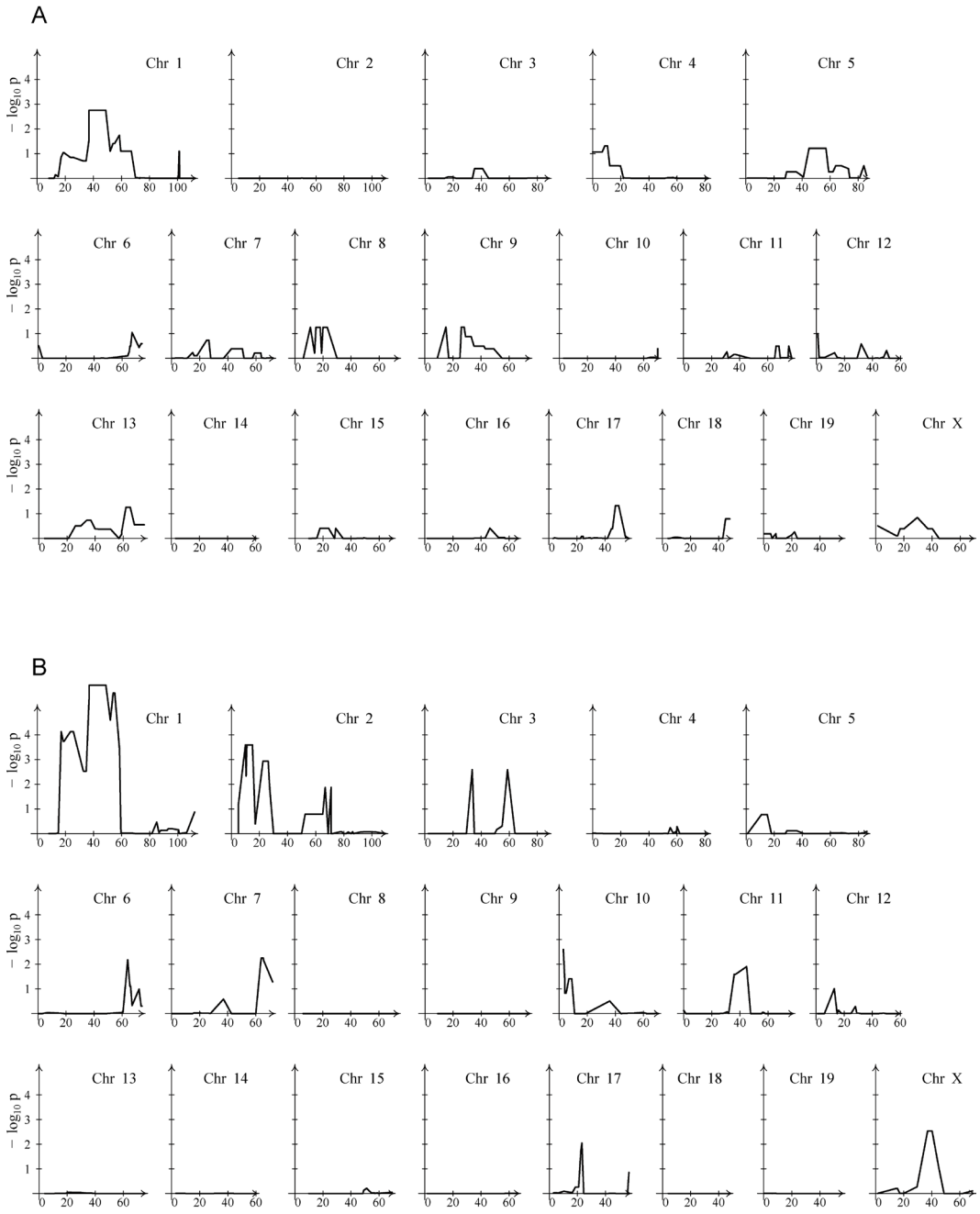

Figure 7. **Genetic control of early spleen bacillary counts of BCG Russia and BCG Pasteur.** Linkage analysis of splenic bacterial counts at the week 1 time point was performed with an adjustment for strain genetic background and gender. A single locus on chromosome 1 was identified in response to early BCG Russia infection (A). Loci linked to splenic BCG Pasteur counts were detected on chromosomes 1, 2, 3, 6, 7, 10, 17 and X at at the week 1 time point (B). Chromosomal positions are given in centimorgans (cM).

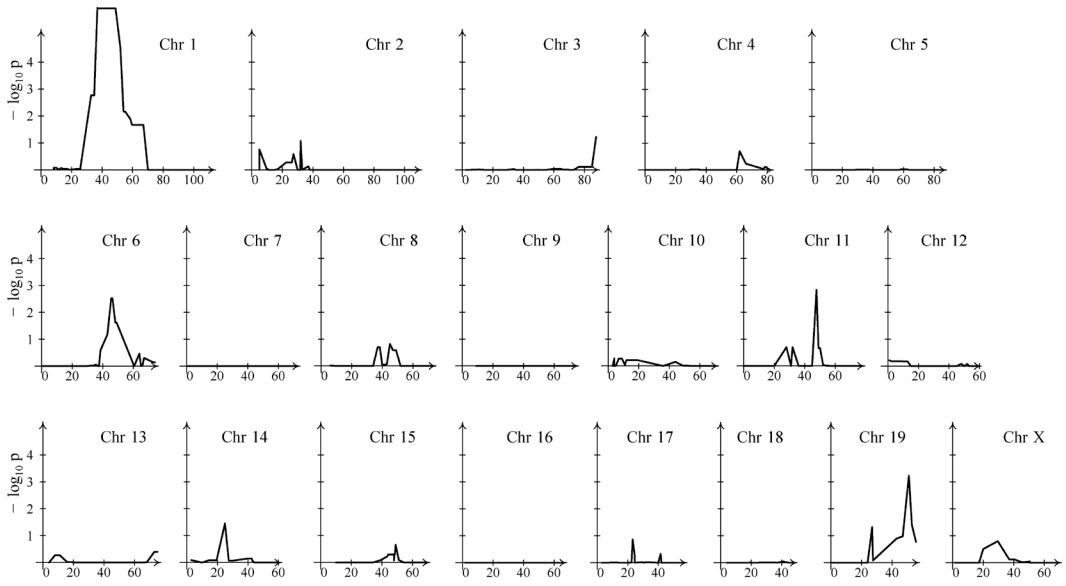

Figure 8. **Genetic control of late spleen bacillary counts following infection of the RC strains with BCG Russia.** Background- and gender-adjusted QTL analysis was performed using spleen counts of BCG Russia at the 6-week endpoint. A locus on chromosome 1 had a major effect on the bacterial numbers of BCG Russia. Additional loci were detected on chromosomes 6, 11, and 19 Chromosomal positions are given in centimorgans (cM).

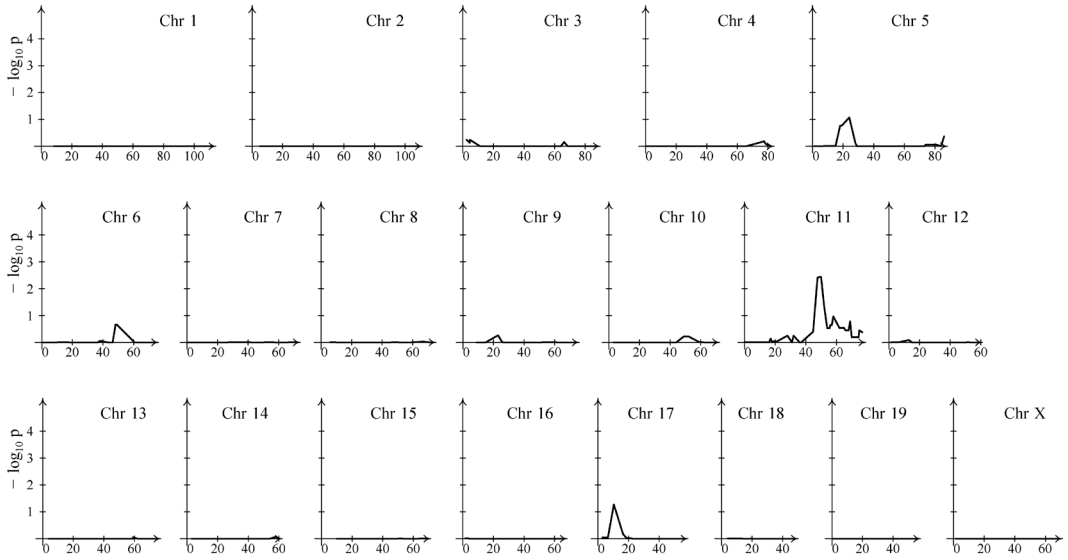

Figure 9. Genetic control of late pulmonary bacillary counts of BCG Russia. Linkage analysis of BCG Russia pulmonary counts at the 6-week time point was performed with background and gender-adjustment. A single locus controlling BCG Russia pulmonary counts was identified on chromosome 11. Chromosomal positions are given in centimorgans (cM).

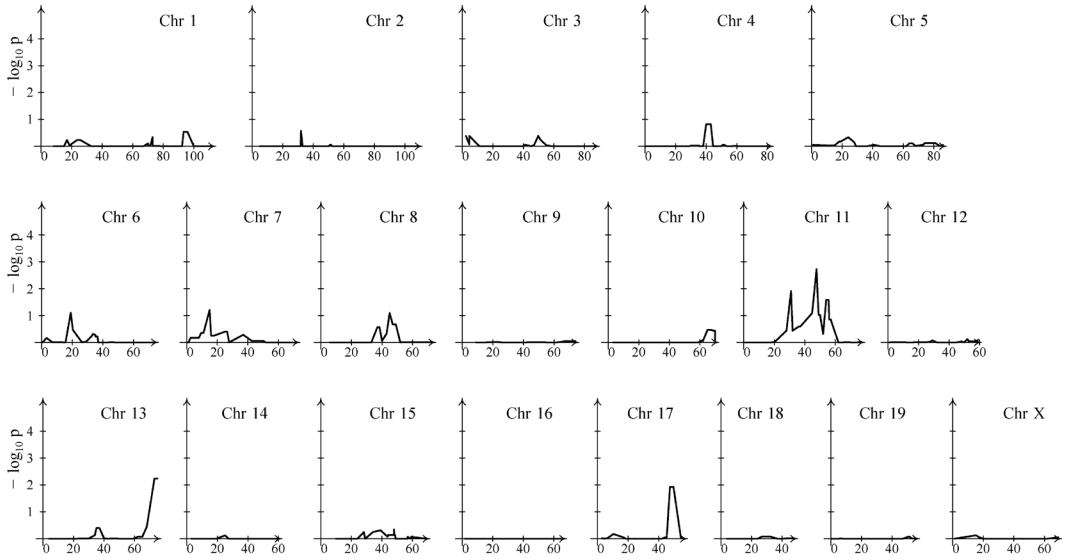

Figure 10. Linkage analysis of late spleen bacillary counts contingent on the chromosome 1 locus. Linkage analysis was performed with an adjustment for the locus on chromosome 1 which had a major effect on the splenic bacillary counts of BCG Russia at the 6-week time point. The loci identified on chromosomes 6 and 19 were conditional upon the chromosome 1 locus and lost their significance when adjusted. The genetic effect detected on chromosome 11 was independent of the chromosome 1 locus and maintained its significance. An additional locus was localized to chromosome 13. Chromosomal positions are given in centimorgans (cM).

Table 1. Summary of significant linkage peaks obtained using the main and conditional models.

Strain	Organ	Day	Main model	Conditional model
BCG Pasteur	Spleen	7	Chrs. 1, 2, 3, 6, 7, 10, 17, X	(Chr. 1)[a]
		42	-[b]	N/A
	Lung	7	-	N/A
		42	-	N/A
BCG Russia	Spleen	7	Chr. 1	(Chr. 1)
		42	Chrs. 1, 6, 11, 19	Chrs. (1), 11, 13
	Lung	7	-	N/A
		42	Chr. 11	N/A

Chr., chromosome; N/A, not applicable
[a] (Chr. 1), exclusion of markers on chromosome 1 to adjust for major genetic effect
[b] -, no significant genetic effects detected

DISCUSSION

RC strains are particularly useful to establish pathways of causality in complex read-outs such as immune reactivity and are well suited to track gene-gene interactions [33]. However, RC strains have also proven useful for positional identification of disease susceptibility loci by employing RC strains with extreme phenotypes in subsequent genetic crosses [39-41]. A third application of RC strains is the genome-wide identification of quantitative trait loci (QTL) in complex diseases. This feature of RC strains is particularly attractive since it allows the measurement of quantitative traits in many genetically identical mice belonging to the same strain which greatly increases the accuracy of trait determination. A genome-wide scan for the presence of QTL can then be conducted among the relatively limited number of RC strains in each panel. This is highly efficient compared to the breeding and genotyping of hundreds of mice in traditional backcross or F2 based genome-wide mapping studies. For example, a recent study used the AcB/BcA RC strain panel to localize a large number of asthma susceptibility loci across the genome [42]. A potential problem that is faced in these speedy genome-wide scans in RC strains is the confounding impact of strain background and of strong susceptibility loci on the overall pattern of QTLs mapped. We have developed a new analytical methodology that overcomes both of these potentially confounding limitations while conducting genome-wide QTL mapping in RC strains. Our results demonstrate the ease of genome-wide scanning in RC strains and the importance of adjusting especially on strain background to achieve reliable QTL identification.

Our ability to detect the *Nramp1* genomic region also served as an internal validation of the analytical approach. Another interesting observation was the loci that could only be detected in connection with *Nramp1*. Once the analysis was adjusted on the *Nramp1* gene, these loci were no longer significant for linkage. The most parsimonious explanation for this effect is that these loci are interacting with *Nramp1*. Why we would detect a large number of genes that interact with *Nramp1* in the genetic control of BCG Pasteur as compared to BCG

Russia is not known but may reflect the differences in pathogenesis between the two BCG strains. For BCG Pasteur, putatively interacting genes were detected at one week post infection while for BCG Russia such interacting loci were observed at the 6 week time point. At 3 weeks, BCG Pasteur shows a sharp peak of splenic bacillary burden while the growth of BCG Russia continues well past 6 weeks before a slow and gradual reduction of splenic burden becomes evident after 12 weeks of infection (data not shown). While the interpretation of our results as *Nramp1* interacting loci appears reasonable, it is important to realize that this conclusion needs further direct experimental validation. However, if correct, the mapping tools presented in this paper would provide a very powerful approach for the identification of interacting loci which is still a major obstacle in complex trait analysis in both human and model animals.

The study of the impact of strain variability of *M. tuberculosis* on disease expression is of considerable interest for the implementation of tuberculosis control measures. An increasing body of evidence suggests that different strains/lineages of *M. tuberculosis* display substantial differences in their pathogenic potential [8, 9]. In addition, evidence is emerging that genetic variability among BCG vaccine strains is a potent factor in modulating BCG induced anti-tuberculosis immunity [31]. This mycobacterial strain variability reflects an even greater divergence in host responsiveness to both BCG and *M. tuberculosis* that is largely under host genetic control (reviewed in [43]). These observations raise the question if host and mycobacterial variability are independent of each other. If independent, we would expect hosts to display a spectrum of responsiveness from highly resistant to highly susceptible irrespective of the infecting mycobacterial strain. Similarly, *M. tuberculosis* strains would vary from highly virulent to mildly virulent across all hosts. Alternatively, it is possible that "susceptibility" and "virulence" are not absolute but rather reflect specific combinations of mycobacterial strain and human host. The latter possibility is supported by recent observations of preferential associations of tuberculosis lineages with ethnic groups that may reflect co-adaptation of *M. tuberculosis* and its human host [10].

Moreover, a number of host genetic association studies have reported a preferential association of tuberculosis susceptibility variants with specific *M. tuberculosis* lineages [12-14]. The results of our study obtained in a highly controlled experimental setting support the hypothesis of host-pathogen specific genetic "fits." Hence, human susceptibility to tuberculosis may only become tractable by jointly considering host and pathogen genetic backgrounds.

By conducting a genome-wide mapping of loci that impact on the splenic and pulmonary burden following a low dose infection with two strains of BCG, we revealed a divergent pattern of susceptibility loci. An unexpected result was the pronounced dynamic of genetic loci impacting on bacillary counts. This observation demonstrated how different genetic control elements came into play as the BCG infection advanced and further emphasized the intimate interplay between host genetics and pathogenesis. Perhaps less surprising was the large difference in the number of loci involved in the control of splenic vs pulmonary bacillary counts. BCG Pasteur shows little dissemination and growth in the lungs of infected mice and the absence of susceptibility loci was therefore expected. However, BCG Russia reaches bacillary counts in the lungs that are similar to those in the spleen. Yet, only one susceptibility locus on chromosome 11 was detected to impact on pulmonary counts while splenic counts are under more complex control. It is interesting that a locus on chromosome 1 which is indistinguishable from the *Nramp1* gene had by far the strongest impact on bacillary burden in both Pasteur and Russia, but this effect was limited to splenic counts. By contrast, the chromosome 11 locus was detected for BCG Russia only but in both the spleens and lungs. The results therefore indicate that host genetic control is characterized by very strong common control elements that act in a tissue-specific manner and by somewhat weaker BCG strain specific susceptibility genes that are not tissue specific. Together these data indicate that host genetic control of mycobacterial replication is sensitive to the particular strains but also to differences in disease manifestations (here, lung vs spleen). Interestingly, the strongest genetic effect ever found in human studies was found

in an outbreak of tuberculosis in Northern Canada [44]. During this outbreak, all cases had been infected from a single index case, i.e. a single bacterial strain [45]. A fine tuned host genetic response to mycobacteria might explain why it has been difficult to reproducibly detect strong host genetic effects in human tuberculosis. Consequently, future genetic studies of tuberculosis susceptibility might need to be adjusted on the detailed clinical picture and infecting *M. tuberculosi*s strain.

ACKNOWLEDGEMENTS

We thank Dr. Kenneth Morgan for helpful advice. The RCS genotypes were kindly provided by Emerillon Therapeutics.

References

1. Ng VH, Cox JS, Sousa AO, MacMicking JD, McKinney JD. Role of KatG catalase-peroxidase in mycobacterial pathogenesis: countering the phagocyte oxidative burst. *Mol Microbiol.* Jun 2004;52(5):1291-1302.

2. Darwin KH, Ehrt S, Gutierrez-Ramos JC, Weich N, Nathan CF. The proteasome of Mycobacterium tuberculosis is required for resistance to nitric oxide. *Science.* Dec 12 2003;302(5652):1963-1966.

3. Tobin DM, Vary JC, Jr., Ray JP, et al. The lta4h locus modulates susceptibility to mycobacterial infection in zebrafish and humans. *Cell.* Mar 5 2010;140(5):717-730.

4. Divangahi M, Chen M, Gan H, et al. Mycobacterium tuberculosis evades macrophage defenses by inhibiting plasma membrane repair. *Nat Immunol.* Aug 2009;10(8):899-906.

5. Gan H, Lee J, Ren F, Chen M, Kornfeld H, Remold HG. Mycobacterium tuberculosis blocks crosslinking of annexin-1 and apoptotic envelope formation on infected macrophages to maintain virulence. *Nat Immunol.* Oct 2008;9(10):1189-1197.

6. Chen M, Divangahi M, Gan H, et al. Lipid mediators in innate immunity against tuberculosis: opposing roles of PGE2 and LXA4 in the induction of macrophage death. *J Exp Med.* Nov 24 2008;205(12):2791-2801.

7. Behr M, Schurr E, Gros P. TB: screening for responses to a vile visitor. *Cell.* Mar 5 2010;140(5):615-618.

8. Gagneux S, Small PM. Global phylogeography of Mycobacterium tuberculosis and implications for tuberculosis product development. *Lancet Infect Dis.* May 2007;7(5):328-337.

9. Nicol MP, Wilkinson RJ. The clinical consequences of strain diversity in Mycobacterium tuberculosis. *Trans R Soc Trop Med Hyg.* Oct 2008;102(10):955-965.

10. Gagneux S, DeRiemer K, Van T, et al. Variable host-pathogen compatibility in Mycobacterium tuberculosis. *Proc Natl Acad Sci U S A.* Feb 21 2006;103(8):2869-2873.

11. Reed MB, Pichler VK, McIntosh F, et al. Major Mycobacterium tuberculosis lineages associate with patient country of origin. *J Clin Microbiol.* Apr 2009;47(4):1119-1128.

12. Caws M, Thwaites G, Dunstan S, et al. The influence of host and bacterial genotype on the development of disseminated disease with Mycobacterium tuberculosis. *PLoS Pathog.* Mar 2008;4(3):e1000034.

13. Herb F, Thye T, Niemann S, et al. ALOX5 variants associated with susceptibility to human pulmonary tuberculosis. *Hum Mol Genet.* Apr 1 2008;17(7):1052-1060.

14. Intemann CD, Thye T, Niemann S, et al. Autophagy gene variant IRGM -261T contributes to protection from tuberculosis caused by Mycobacterium tuberculosis but not by M. africanum strains. *PLoS Pathog.* Sep 2009;5(9):e1000577.

15. Behr MA, Small PM. A historical and molecular phylogeny of BCG strains. *Vaccine.* Feb 26 1999;17(7-8):915-922.

16. Calmette A, Guérin C, Breton M. Contribution à l'étude de la tuberculose expérimentale du cobaye. *Ann Inst Pasteur.* 1907(21):401-416.

17. Oettinger T, Jorgensen M, Ladefoged A, Haslov K, Andersen P. Development of the Mycobacterium bovis BCG vaccine: review of the historical and biochemical evidence for a genealogical tree. *Tuber Lung Dis.* 1999;79(4):243-250.

18. Lewis KN, Liao R, Guinn KM, et al. Deletion of RD1 from Mycobacterium tuberculosis mimics bacille Calmette-Guerin attenuation. *J Infect Dis.* Jan 1 2003;187(1):117-123.

19. Pym AS, Brodin P, Brosch R, Huerre M, Cole ST. Loss of RD1 contributed to the attenuation of the live tuberculosis vaccines Mycobacterium bovis BCG and Mycobacterium microti. *Mol Microbiol.* Nov 2002;46(3):709-717.

20. Mostowy S, Tsolaki AG, Small PM, Behr MA. The in vitro evolution of BCG vaccines. *Vaccine.* Oct 1 2003;21(27-30):4270-4274.

21. Keller PM, Bottger EC, Sander P. Tuberculosis vaccine strain Mycobacterium bovis BCG Russia is a natural recA mutant. *BMC Microbiol.* 2008;8:120.

22. Brosch R, Gordon SV, Garnier T, et al. Genome plasticity of BCG and impact on vaccine efficacy. *Proc Natl Acad Sci U S A.* Mar 27 2007;104(13):5596-5601.

23. Behr MA, Schroeder BG, Brinkman JN, Slayden RA, Barry CE, 3rd. A point mutation in the mma3 gene is responsible for impaired methoxymycolic acid production in Mycobacterium bovis BCG strains obtained after 1927. *J Bacteriol.* Jun 2000;182(12):3394-3399.

24. Mahairas GG, Sabo PJ, Hickey MJ, Singh DC, Stover CK. Molecular analysis of genetic differences between Mycobacterium bovis BCG and virulent M. bovis. *J Bacteriol.* Mar 1996;178(5):1274-1282.

25. Salamon H, Kato-Maeda M, Small PM, Drenkow J, Gingeras TR. Detection of deleted genomic DNA using a semiautomated computational analysis of GeneChip data. *Genome Res.* Dec 2000;10(12):2044-2054.

26. Charlet D, Mostowy S, Alexander D, Sit L, Wiker HG, Behr MA. Reduced expression of antigenic proteins MPB70 and MPB83 in Mycobacterium bovis BCG strains due to a start codon mutation in sigK. *Mol Microbiol.* Jun 2005;56(5):1302-1313.

27. Spreadbury CL, Pallen MJ, Overton T, et al. Point mutations in the DNA- and cNMP-binding domains of the homologue of the cAMP receptor protein (CRP) in Mycobacterium bovis BCG: implications for the inactivation of a global regulator and strain attenuation. *Microbiology.* Feb 2005;151(Pt 2):547-556.

28. Black GF, Weir RE, Floyd S, et al. BCG-induced increase in interferon-gamma response to mycobacterial antigens and efficacy of BCG vaccination in Malawi and the UK: two randomised controlled studies. *Lancet.* Apr 20 2002;359(9315):1393-1401.

29. Lalor MK, Ben-Smith A, Gorak-Stolinska P, et al. Population Differences in Immune Responses to Bacille Calmette-Guerin Vaccination in Infancy. *J Infect Dis.* Feb 1 2009;199(3):795–800.

30. Wu B, Huang C, Garcia L, et al. Unique gene expression profiles in infants vaccinated with different strains of Mycobacterium bovis bacille Calmette-Guerin. *Infect Immun.* Jul 2007;75(7):3658-3664.

31. Liu J, Tran V, Leung AS, Alexander DC, Zhu B. BCG vaccines: their mechanisms of attenuation and impact on safety and protective efficacy. *Hum Vaccin.* Feb 2009;5(2):70-78.

32. Trunz BB, Fine P, Dye C. Effect of BCG vaccination on childhood tuberculous meningitis and miliary tuberculosis worldwide: a meta-analysis and assessment of cost-effectiveness. *Lancet.* Apr 8 2006;367(9517):1173-1180.

33. Demant P, Hart AA. Recombinant congenic strains--a new tool for analyzing genetic traits determined by more than one gene. *Immunogenetics.* 1986;24(6):416-422.

34. Fortin A, Diez E, Rochefort D, et al. Recombinant congenic strains derived from A/J and C57BL/6J: a tool for genetic dissection of complex traits. *Genomics.* May 15 2001;74(1):21-35.

35. Gros P, Skamene E, Forget A. Genetic control of natural resistance to Mycobacterium bovis (BCG) in mice. *J Immunol.* Dec 1981;127(6):2417-2421.

36. Belley A, Alexander D, Di Pietrantonio T, et al. Impact of methoxymycolic acid production by Mycobacterium bovis BCG vaccines. *Infect Immun.* May 2004;72(5):2803-2809.

37. Mouse Genome Database (MGD) at the Mouse Genome Informatics website TJL, Bar Harbor, Maine. http://www.informatics.jax.org. Accessed December 2009.

38. Vidal SM, Malo D, Vogan K, Skamene E, Gros P. Natural resistance to infection with intracellular parasites: isolation of a candidate for Bcg. *Cell.* May 7 1993;73(3):469-485.

39. Mullerova J, Hozak P. Use of recombinant congenic strains in mapping disease-modifying genes. *News Physiol Sci.* Jun 2004;19:105-109.

40. Min-Oo G, Fortin A, Tam MF, Nantel A, Stevenson MM, Gros P. Pyruvate kinase deficiency in mice protects against malaria. *Nat Genet.* Dec 2003;35(4):357-362.

41. Roy MF, Riendeau N, Bedard C, et al. Pyruvate kinase deficiency confers susceptibility to Salmonella typhimurium infection in mice. *J Exp Med.* Nov 26 2007;204(12):2949-2961.

42. Camateros P, Marino R, Fortin A, et al. Identification of novel chromosomal regions associated with airway hyperresponsiveness in recombinant congenic strains of mice. *Mamm Genome.* Feb 2010;21(1-2):28-38.

43. Schurr E, Kramnik I. Genetic control of host susceptibility to tuberculosis. In: Kaufmann S, Britten W, eds. *Handbook of Tuberculosis*. Weinheim, Germany: Wiley-VCH; 2008:305-346.

44. Greenwood CM, Fujiwara TM, Boothroyd LJ, et al. Linkage of tuberculosis to chromosome 2q35 loci, including NRAMP1, in a large aboriginal Canadian family. *Am J Hum Genet.* Aug 2000;67(2):405-416.

45. Schurr E. Is susceptibility to tuberculosis acquired or inherited? *J Intern Med.* Feb 2007;261(2):106-111.

Preface to Chapter 4

The results presented in Chapter 3 showed that bacterial counts of two closely related strains of BCG are under the control of general as well as BCG-specific genetic elements. As part of our efforts to compare patterns of host genetic control across different mycobacteria, we expanded this analysis to also include *M. tuberculosis*. We reasoned that some genetic control elements could affect both the extent of BCG replication and survival to *M. tuberculosis* infection while others would be specific to the mycobacterial strain. Chapter 4 describes the genetic analysis of the AcB and BcA strains infected with *M. tuberculosis*.

CHAPTER 4
Susceptibility to *Mycobacterium tuberculosis* in the AcB and BcA Recombinant Congenic Strains is Under Control of One Fully Penetrant and Additional Incompletely Penetrant Loci

---

Tania Di Pietrantonio[1,2,3], Carmen Hernandez[1], Marcel A. Behr[1,3], J Concepción Loredo-Osti[4*] and Erwin Schurr[1,2,3*]

[1] McGill Centre for the Study of Host Resistance, Research Institute of the McGill University Health Centre, Montreal, Quebec, Canada

[2]Department of Human Genetics and [3]Department of Medicine, McGill University, Montreal, Quebec, Canada

[3]Department of Medicine, McGill University, Montreal, Quebec, Canada

[4] Department of Mathematics and Statistics, Memorial University of Newfoundland, St Johns, Newfoundland and Labrador, Canada

* Share senior authorship.

ABSTRACT

Susceptibility to *Mycobacterium tuberculosis* infection is under complex genetic control in the mouse. To identify novel genetic effects involved in the host response to tuberculosis, we performed a genetic analysis in a panel of AcB/BcA recombinant congenic (RC) strains derived from "susceptible" A/J and "resistant" C57BL/6J progenitors. Three hypersusceptible strains, AcB51, AcB52, and AcB54, were identified during phenotypic characterization of the RC panel. These strains presented with large pulmonary bacterial burdens, had extensive lung pathology, and succumbed early following infection with *M. tuberculosis*. Among the BcA strains, BcA78 had the shortest duration of survival. Using survival time following *M. tuberculosis* infection as a measure of susceptibility, a major genetic effect was detected on chromosome 10 that accounted for the extreme susceptibility of mice of the AcB51, AcB52, and AcB54 RC strains. This locus, designated "hypersusceptibility to mycobacterium tuberculosis 1" (*Hsmtb1*), was fully penetrant, with rapid mortality occurring in all the AcB strains that inherited a C57BL/6-derived chromosome 10 segment. Linkage analysis conditional on the chromosome 10 marker with the strongest effect, D10Mit42, identified three additional loci on chromosomes 2, 4, and 13. The locus on chromosome 13, termed "susceptibility to mycobacterium tuberculosis 1" (*Smtb1*), explained the variation of the BcA78 strain, with a penetrance of 67%. The estimated penetrances of the loci on chromosomes 2 (*Smtb2*) and 4 (*Smtb3*) were 21% and 38%, respectively. These results demonstrate the complexity of the host genetic control of *M. tuberculosis* infection.

INTRODUCTION

Tuberculosis, primarily caused by the human pathogen *Mycobacterium tuberculosis*, remains a global health emergency that claims an estimated 1.8 million lives each year [1]. The disease is characterized by a large variability in susceptibility to both infection and clinical disease. Approximately 50% to 70% of those exposed to *M. tuberculosi*s will become infected and there is strong evidence that such susceptibility to infection is under host genetic control [2,3]. Among those infected, only approximately 10% will develop clinical tuberculosis disease and there is strong epidemiological evidence that host genetic factors contribute to susceptibility [4]. Despite the strong evidence for a role of host genetic factors and despite the use of genome-wide-linkage (GWL) and genome-wide-association (GWA) studies, only few genetic tuberculosis susceptibility factors have been discovered and validated in independent studies [5]. This suggests that currently used study designs lack precision and/or sensitivity to detect critical host genetic factors of tuberculosis susceptibility. By contrast, genetic studies in model animals-while not necessarily representing all aspect of the human disease-can more easily identify genes within critical pathways of the host-*M. tuberculosi*s interplay. The genes identified will not only result in more focused human genetic studies but will also help to identify tuberculosis sub-phenotypes that could be preferentially used in the corresponding human studies.

The A/J and C57BL/6J inbred mouse strains vary extensively in their susceptibility to tuberculosis. Mice of the susceptible A/J strain develop a progressive interstitial pneumonitis that causes early death following infection with *M. tuberculosis* [6,7]. A/J mice do not form functional granulomas, resulting in diffuse cellular infiltration and bacterial dissemination within the lung [8]. Although infection is also lethal in C57BL/6J mice, this strain can survive for extensive periods [7]. The extended survival of C57BL/6J mice is associated with granuloma formation and corresponding bacterial containment [6,8]. Increased susceptibility in the A/J mouse strain has been attributed in part to a deficiency in the C5 component of the complement pathway [7]. Additional mechanisms

underlying differences in the host response to *M. tuberculosis* between the A/J and C57BL/6J strains have yet to be uncovered.

We exploited the differential susceptibility of A/J and C57BL/6J mice to *M. tuberculosi*s for susceptibility gene mapping using a panel of AcB and BcA recombinant congenic (RC) strains. The AcB and BcA strains were derived from A/J and C57BL/6J progenitors by inbreeding pairs of double backcross mice [AcB: (F1 × A/J) × A/J and BcA: (F1 × C57BL/6J) × C57BL/6J] [9]. Each AcB and BcA strain contains a unique genome, with a different set of randomly distributed chromosomal segments from the donor genome (~13%), fixed on the recipient genetic background (~85%, 2% unknown). Individual AcB and BcA strains are genetically well characterized, with known genome boundaries of donor segments. A significant advantage of quantitative trait locus (QTL) mapping with RC strains is that multiple measurements of a phenotype can be implemented in genetically identical mice of a strain, minimizing phenotypic noise. This is in contrast to conventional mouse crosses, where phenotypic estimates by necessity are based on single animals. More importantly, discordant strains identified within the panel can be used for additional mapping studies or to generate congenic lines for phenotypic analysis. This allows for rapid determination and validation of causative genetic effects.

In the present study, we infected mice of the AcB/BcA strains with *M. tuberculosis* H3Rv and determined the survival times of individual mice. By using survival analysis, we identified a locus on distal chromosome 10 that controlled hypersusceptibility to *M. tuberculosis*. When the genetic analysis was adjusted for the presence of the chromosome 10 locus, three additional loci were identified that impacted on survival time.

MATERIALS AND METHODS

Animals

Male A/J and C57BL/6J mice were purchased from the Jackson Laboratory (Bar Harbor, Maine). Thirty-one RC strains originally derived from a reciprocal double backcross between the A/J and C57BL/6J progenitors [9] were purchased from Emerillon Therapeutics Inc. (Montreal, QC.). All animal experiments were performed under conditions specified by the Canadian Council on Animal Care and approved by the McGill University Animal Care Committee.

M. tuberculosis Infection

M. tuberculosis H37Rv (Pasteur) was growth in Middlebrook 7H9 broth (Difco Laboratories, Detroit, MI) containing 0.05% Tween 80 (Sigma-Aldrich, St. Louis, MO) and 10% albumin-dextrose-catalase (ADC) supplement (Becton Dickinson and Co., Sparks, MD). Liquid cultures were adjusted to an OD_{650} nm of 0.4 and stored at -80°C as 25% glycerol stocks. Prior to infection, stocks were thawed and diluted to 3×10^6 colony-forming units (CFU)/ml in PBS/Tween 80 (0.05%). Mice were infected for 10 minutes in an inhalation exposure system (In-Tox Products, Moriaty, NM). For each RC strain, 4 to 12 mice (male and female) were infected. The infectious dose was verified one day post-infection; lungs were homogenized in 2 ml of 0.025% Saponin-PBS using large tissue grinders (TYCO Healthcare Group, Mansfield, MA) and 200 μL was plated on Middlebrook 7H10 agar (Difco Laboratories, Detroit, MI) supplemented with oleic acid-albumin-dextrose-catalase (OADC) enrichment and BACTEC PANTA PLUS (Becton Dickinson and Co., Sparks, MD). Mice were monitored daily and severely moribund animals were sacrificed by CO2 asphyxiation. Survival times were recorded and used for statistical analysis.

Genotyping

All RC strains were previously genotyped using a panel of 625 microsatellite markers [9]. Based on Build 36.1, markers with reassigned positions were removed from the current analysis [10].

Pulmonary load of *M. tuberculosis*

The bacterial load in the lungs of moribund mice was determined by homogenizing the tissue in 4 ml of 0.025% Saponin-PBS using large tissue grinders (TYCO Healthcare Group, Mansfield, MA). Lung homogenates were serially diluted tenfold and plated on Middlebrook 7H10 agar (Difco Laboratories, Detroit, MI) containing OADC enrichment and BACTEC PANTA PLUS (Becton Dickinson and Co., Sparks, MD). Bacterial enumeration was performed after 3 weeks at 37°C.

Histopathology

Lungs were harvested from moribund mice. Tissues were fixed in 10% buffered formalin, embedded in paraffin, sectioned, and stained with haematoxylin and eosin.

Genetic analysis

Survival data were analyzed through the Cox's proportional hazards regression analysis. One by one, each marker was included in the model in addition to a factor accounting for the genetic background (i.e. each RC strain was labelled as being of the "A" or "B" background for each marker and those labels were used as a factor-the RC strain labels themselves could not be used because the method is very sensitive to numerical convergence problem when the number of individuals per factor is low). To avoid the possibility of inflated significance of linkage signals, we also used the background as a frailty (i.e. as a random effect instead of as fixed effect). However, this approach resulted in a procedure that was numerically unstable for many markers. Hence, the analysis that was performed is a compromise between the need to account for genetic background and the numerical feasibility of the estimation. For the conditional analysis, the D10Mit42 marker was added as the explanatory variable to the model and the model was fitted accordingly. The p-values were obtained by bootstrap (10,000 re-samples) with the particularity that the time-to-death was re-sampled and

nested into the background. Once the significant peaks were identified they were 'validated' through an exhaustive inspection for association with the early time-to-death observations as well as check for redundancy in the strain distribution pattern (SDP). Peaks that did not meet these consistency requirements were discarded regardless of their estimated p-value.

RESULTS

Mice of the A/J and C57BL/6J strains were infected by aerosol with ~400 CFU of virulent *M. tuberculosis* H3Rv. Infected mice were monitored daily and moribund animals were sacrificed. Survival times were recorded for individual A/J and C57BL/6J mice and are presented in Figure 1. A/J animals succumbed to infection between days 31 and 157, with a corresponding median survival time (MST) of 137 days. C57BL/6J mice survived between 143 and 218 days, with a MST of 187.5 days.

To investigate the genetic control of survival to *M. tuberculosis* infection, we infected 31 AcB and BcA strains with ~450 CFU of *M. tuberculosis* H3Rv by aerosol. The survival time of mice from the RC strains is shown in Figure 2. Strains were ranked based on the number of mice that died early (<50 days). The AcB51, AcB52 and AcB54 strains ranked highest in susceptibility to *M. tuberculosis* infection [AcB51: MST=29 (range: 28-38 days), AcB52: MST=29 (range: 26-31 days), AcB54: MST=27 (range: 26-28 days)] and had high bacterial burdens in the lungs at the time of death (AcB51: mean $\log_{10}$CFU= 9.86; AcB52: mean $\log_{10}$CFU= 9.99; AcB54: mean $\log_{10}$CFU= 9.67). The BcA78 strain exhibited the greatest susceptibility among the BcA strains and ranked fourth within the panel [MST=30 (range: 23-134 days)]. The bacterial load (mean $\log_{10}$CFU=8.50) at time of death of BcA78 mice was lower compared to mice of the AcB51, AcB52 and AcB54 strains.

Gross and histological evaluation of the lungs of mice from the AcB51, AcB52 and AcB54 strains at the time of death identified marked differences in pathology relative to the other RC strains. The lungs of mice from these three strains were edematous and had large lesions on their surface. Microscopic examination of the lesions in AcB51 showed a central region of caseous necrosis surrounded by a wall of lymphocytes (Figure 3) that resembled tuberculous granulomas in human lungs. For comparison, we examined the lungs of mice of the long-surviving AcB58 strain. Upon visual inspection of gross lung anatomy, there were fewer

and smaller lesions on the surface of the lungs of AcB58 mice relative to the AcB51, AcB52 and AcB54 strains (Figure 3). By histopathology, individual lesions could not be distinguished since there was little lymphocytic organization and cellular infiltration was diffuse. Rafts of polymorphonuclear cells (PMNs) were often associated with degenerating macrophages and multinucleated giant cells. Cholesterol clefts, crystal-like structures resulting from the release of cholesterol from necrotized cells [11], were visible within small foci throughout the lungs of AcB58 mice (Figure 3). These observations are consistent with the suggestion that the pathogenesis of tuberculosis differs between hypersusceptible mice of the AcB51, AcB52 and AcB54 strains compared to mice of strains with longer MSTs.

Prior to genetic linkage analysis, we examined the impact of sex and genetic background on survival times. While differences in sex were not detected, there was a large effect of genetic strain background (Figure 2; data not shown) which highlighted the necessity to adjust on this variable in subsequent genetic analyses. Strain background adjusted analysis of survival times identified potential linkages across 6 different chromosomes (Figure 4) using a very stringent level of significance ($P < 0.0003$). A strong effect was detected in the distal region of chromosome 10 in an 18 cM interval flanked by the markers D10Mit42 (χ^2= 83.801, P=0.0001) and D10Mit233 (χ^2= 30.087, P=0.0001). This locus was termed hypersusceptibility to mycobacterium tuberculosis 1 (*Hsmtb1*). A locus was also identified on chromosome 6 between markers D6Mit86 and D6Mit166 (χ^2=35.735, P=0.0001 for both). Two loci were detected on the proximal portion of chromosome 18. One locus was defined by the markers D18Mit110 and D18Mit20 (χ^2=34.417, P=0.0001 for both) while the second locus was between the markers D18Mit120 and D18Mit17 (χ^2=31.727, P=0.0001 and χ^2=34.878, P=0.0001, respectively). Single marker effects were detected on chromosome 1 at marker D1Mit211 (χ^2= 30.176, P=0.0001), on chromosome 6 at marker D6Mit340 (χ^2= 30.821, P=0.0001), on chromosome 19 at marker D19Mit68 (χ^2=

35.735, *P*=0.0001) and on the X chromosome at marker DXMit55 (χ^2= 35.735, *P*=0.0001).

Next, we conducted a haplotype analysis of the *Hsmtb1* locus that is delineated by the markers D10Mit42 and D10Mit233. The *Hsmtb1* locus is only expressed in mice of an A/J background that inherited the chromosome 10 segment from the C57BL/6J progenitor. To estimate the strength of *Hsmtb1* on extreme susceptibility to *M. tuberculosis*, we defined the penetrance of a locus as the ratio of mice with a given genotype on a given genetic background that died within 50 days of infection relative to the total number of infected mice having that particular combination of genotype and genetic background. With this definition, the *Hsmtb1* locus was fully penetrant with early death occurring in all RC strains carrying a C57BL/6J segment on an A/J background for the chromosome 10 region. Specifically, penetrance was 100% for all markers within the chromosome 10 interval in the three informative AcB strains (26 mice/26 mice for the markers D10Mit42, D10Mit230, D10Mit264, D10Mit10, D10Mit68 and D10Mit231; 17/17 for the markers D10Mit133 and D10Mit70 and 8/8 for the marker D10Mit233). Hence, the chromosomal interval to which *Hsmtb1* can be assigned spans from D10Mit42 to D10Mit231 corresponding to a genetic distance of 7.5 cM (Figure 5).

The SDP for survival was compared to the genotypes of the markers on chromosomes 1, 6, 10, 18, 19, and X with the largest χ^2 statistic (D1Mit211, D6Mit340, D10Mit42, D18Mit20, D19Mit68, and DXMit68, respectively). Examination of the SDP in the AcB strains, particularly in AcB51, AcB52, and AcB54, suggested that the D1Mit211, D6Mit340, D18Mit20, D19Mit68, and DXMit68 markers were partial proxies for D10Mit42. Indeed, these loci were no longer significant for linkage when the analysis was adjusted for the D10Mit42 marker (Figure 6). Importantly, the analysis conditional on D10Mit42 identified additional loci on chromosomes 2, 4, 7, and 13. The locus identified on chromosome 13 spans the markers D13Mit59, D13Mit266, and D13Mit117

(χ^2=23.038, *P*=0.0002 for the three markers) and was termed susceptibility to mycobacterium tuberculosis 1 (*Smtb1*). *Smtb1* plausibly explains the increased susceptibility of the BcA78 strains with a penetrance that ranges from 44% (4/9) to 67% (2/3). A single marker effect was also identified on chromosome 7 (D7Mit66: χ^2=25.252, *P*<0.0001). The SDP for the D7Mit66 marker was similar to that of D13Mit117, suggesting one of the effects was an artefact. The lower penetrance of D7Mit66 (42% or 3/7) compared to D13Mit117 suggested it was acting as a proxy for D13Mit117, although confirmation would require additional mouse crosses. A locus on chromosome 2 included two adjacent markers, D2Mit311 (χ^2=23.216, *P*=0.0002) and D2Mit500 (χ^2=26.549, *P*<0.0001) as well as two single marker effects, D2Mit345 and D2Mit113 (χ^2=23.216, *P*=0.0002 for both). In mice with a C57BL/6J genetic background, A/J genotypes at these markers were associated with increased susceptibility to infection, as seen with the BcA76, BcA77 and BcA82 strains [penetrance 21% (7/33)] and this locus was termed *Smtb2*. The locus detected on chromosome 4 spans two markers, D4Mit172 and D4Mit41 (χ^2=23.549, *P*=0.0002 for both). At this locus, susceptibility was associated with a C57BL/6J-derived segment on the A/J genetic background. This region fully explains the variation observed in the AcB62 AcB65 and AcB57 strains [estimated penetrance 38% (5/13)] and the locus was termed *Smtb3*.

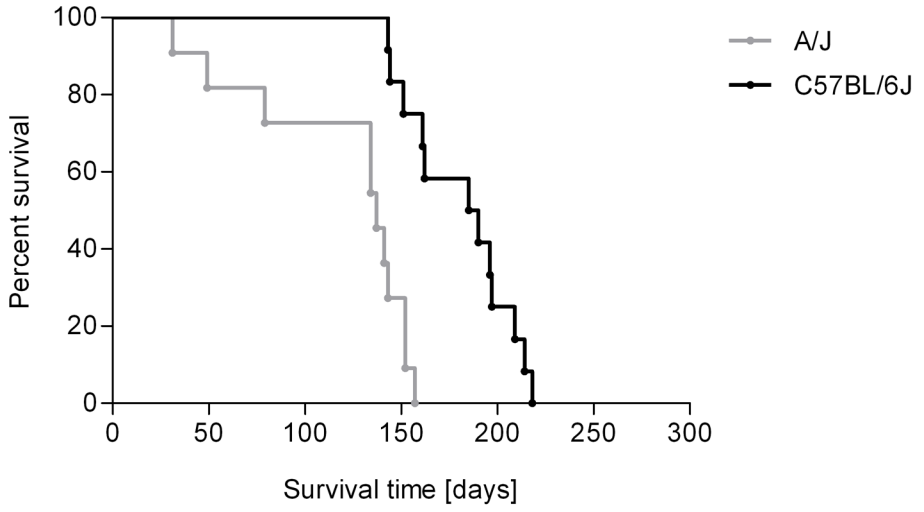

Figure 1. Survival time of the A/J and C57BL/6J mouse strains following aerosol infection with *M. tuberculosis*. Twelve A/J and C57BL/6J mice were aerogenically infected with a moderate dose of *M. tuberculosis* H37Rv (~400 CFU) and survival times were recorded. The percent survival is plotted as a function of time. Experiments were repeated twice with similar results. Grey, A/J; black, C57BL/6J.

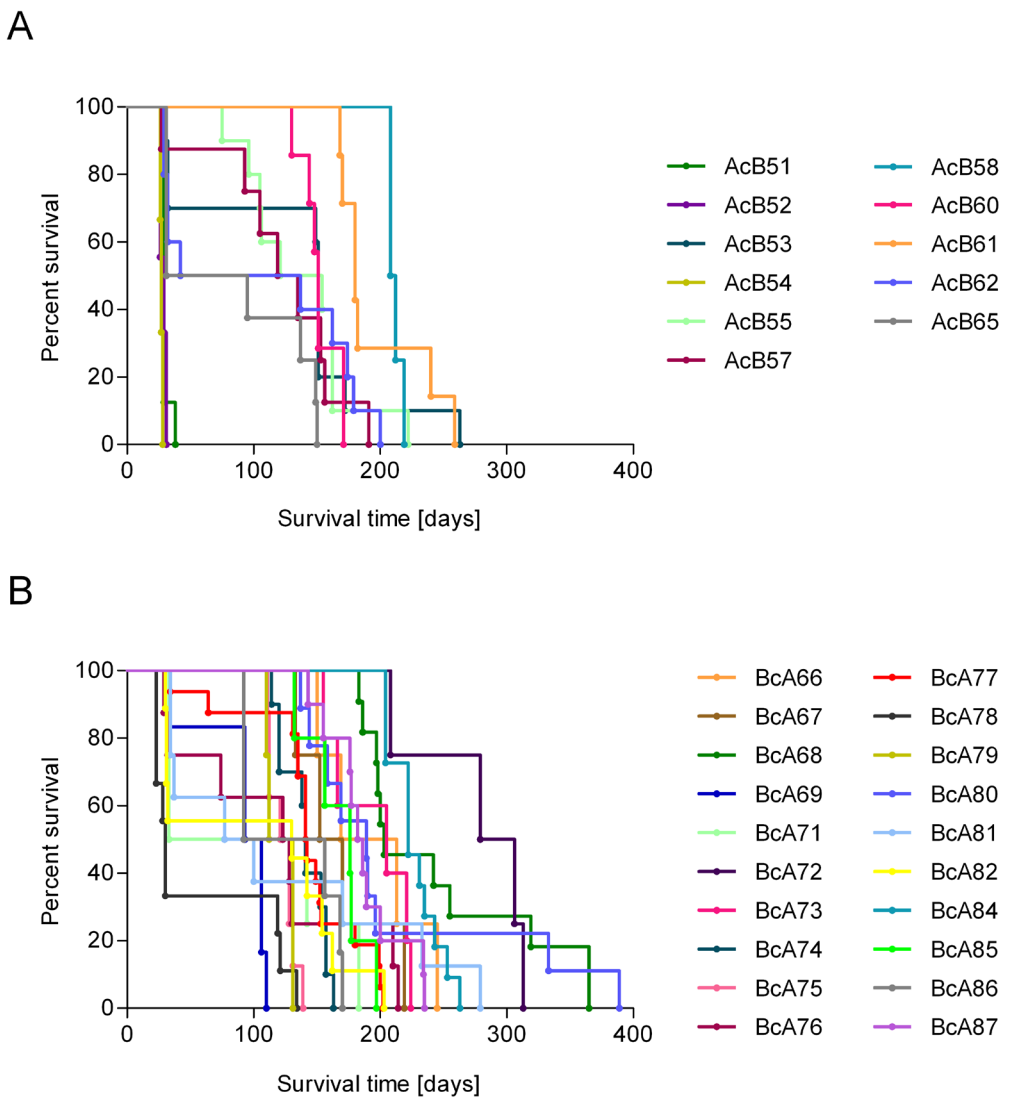

Figure 2. Survival in the AcB and BcA strains infected with *M. tuberculosis*. The RC strains were infected by aerosol with a moderate dose of *M. tuberculosis* H37Rv (~450 CFU) and the duration of survival was measured. (A) The percent survival of mice from 11 AcB strains was plotted across time. The AcB51 (olive), AcB52 (purple), and AcB54 (green) strains were extremely susceptible to infection with *M. tuberculosis* (survival <40 days) whereas the AcB58 (teal) and AcB61 (coral) were among the most resistant [AcB58: MST=210 (range: 208-219 days); AcB61: MST=180 (range: 168-259 days)]. (B) The percentage of surviving mice was plotted against time for 20 BcA strains. Based on median survival time, the BcA78 strain (grey) displayed the greatest susceptibility to *M. tuberculosis* infection while the BcA72 strain [indigo, MST=292.5 (range: 208-313 days)] was the most resistant. Four to 11 mice were infected per RC strain.

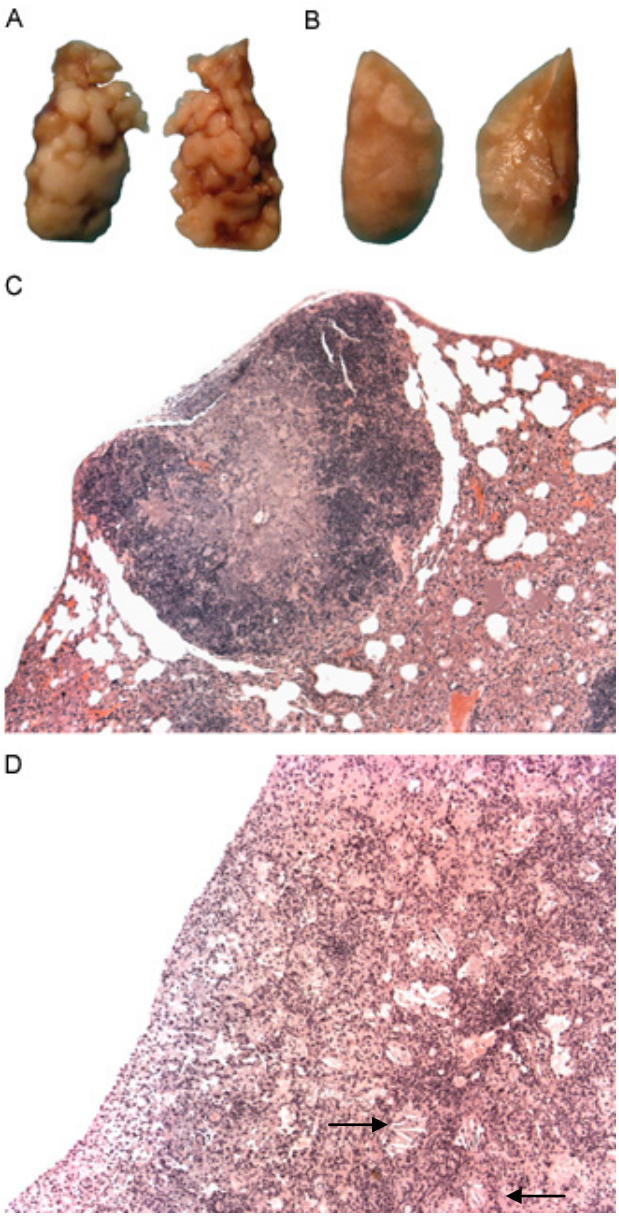

Figure 3. Pulmonary lesions in AcB51 and AcB58 mice infected with *M. tuberculosis*. Lungs from mice of the susceptible AcB51 and the more resistant AcB58 strain were compared at the time of death following *M. tuberculosis* infection. Differences between the two strains were observed both macroscopically (A and B) and microscopically (C and D). Lesions were larger and more numerous in AcB51 (A) relative to AcB58 (B). Ventral aspect of the lung, left; dorsal aspect, right. Lung sections from AcB51 (C) and AcB58 (D) were stained with hematoxylin and eosin. Arrows point to cholesterol clefts resulting from the destruction of macrophages. Representative photomicrographs of four mice are shown, magnification 5×.

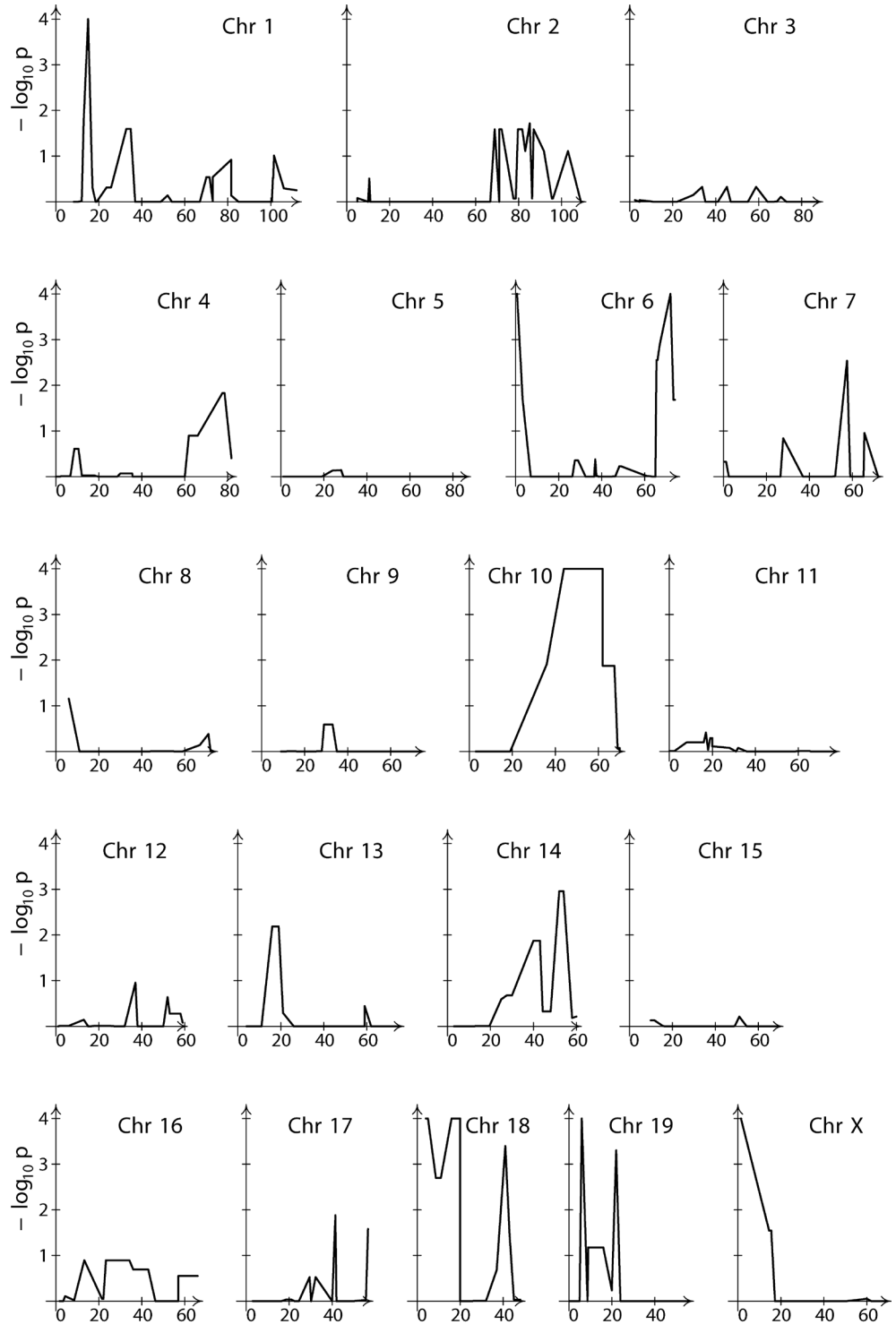

Figure 4. Linkage analysis of susceptibility to infection with *M. tuberculosis* in the RC strains. The survival times of AcB and BcA strains infected with aerosolized *M. tuberculosis* H37Rv were used for linkage analysis. The –logP plots for all chromosomes are shown. Significant evidence for linkage (–logP > 3.5) was detected on chromosomes 1, 6, 10, 18, 19, and X. Chromosomal positions are given in centimorgans (cM).

A

Marker	D10Mit42	D10Mit230	D10Mit264	D10Mit10	D10Mit68	D10Mit231	D10Mit133	D10Mit70	D10Mit233
Position (cM)	44.00	49.00	50.00	51.00	51.50	52.00	59.00	59.00	62.00
χ^2	83.801	81.801	81.801	81.801	81.801	81.801	43.409	43.409	30.087
P-value	0.0001	0.0001	0.0001	0.0001	0.0001	0.0001	0.0001	0.0001	0.0001

Strain	Rank									
AcB51	1	b	b	b	b	b	b	b	b	b
AcB52	1	b	b	b	b	b	b	b	b	a
AcB54	1	b	b	b	b	b	b	a	a	a
AcB53	10	a	a	a	a	a	a	a	a	a
AcB55	15	a	a	a	a	a	a	a	a	a
AcB57	13	a	a	a	a	a	a	a	a	a
AcB58	15	a	a	a	a	a	a	a	a	a
AcB60	15	a	a	a	a	a	a	a	a	a
AcB61	15	a	a	a	a	a	a	a	a	a
AcB62	5	a	a	a	a	a	a	a	a	a
AcB65	5	a	a	a	a	a	a	a	a	a
BcA66	15	b	b	b	b	b	b	b	b	b
BcA67	15	b	b	b	b	b	b	b	b	b
BcA68	15	b	b	b	b	b	b	b	b	a
BcA69	12	b	b	b	b	b	b	b	b	b
BcA70	15	b	b	b	b	b	b	b	b	b
BcA71	5	b	b	b	b	0	b	b	b	b
BcA72	15	0	a	a	a	a	a	a	a	a
BcA73	15	b	b	b	b	b	b	b	b	b
BcA74	15	b	b	b	b	b	b	b	b	b
BcA75	15	b	b	b	b	b	b	b	b	b
BcA76	11	b	b	b	b	b	b	b	b	b
BcA77	14	b	b	b	b	b	b	b	b	b
BcA78	4	b	b	b	b	b	b	b	b	b
BcA79	15	b	b	b	b	b	b	b	b	b
BcA80	15	b	b	b	b	b	b	b	b	b
BcA81	15	b	b	b	b	b	b	b	b	b
BcA82	9	0	b	b	b	b	b	b	b	b
BcA83	15	b	b	b	b	b	b	b	b	b
BcA84	15	b	b	b	b	b	b	b	b	b
BcA85	15	b	b	b	b	b	b	b	b	b
BcA86	15	b	b	b	b	b	b	b	b	b
BcA87	15	b	b	b	b	b	b	b	b	b

B

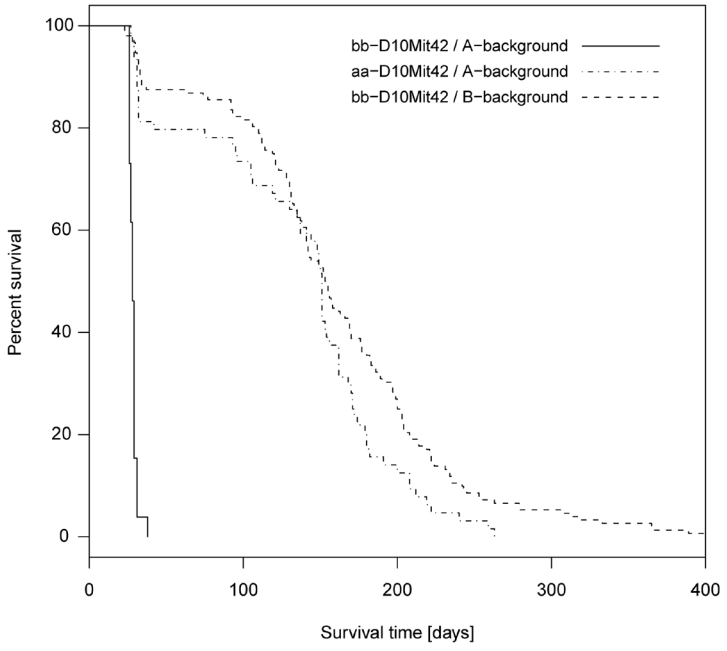

Figure 5. The Chromosome 10 interval. (A) The locus on chromosome 10 spans from marker D10Mit42 to D10Mit233. RC strains were ranked from 1 to 15 based on their survival following *M. tuberculosis* infection. "1" represents strains that are highly susceptible (all mice died before day 50) and "15" represents strains where all mice survived past day 50. Most BcA strains contain a C57BL/6J-derived genotype (b, grey) at the chromosome 10 interval. The BcA72 strain has an undetermined genotype at D10Mit42 (identified as "0") and A/J-derived genotypes (a, white) for all other markers within the interval. The BcA68 strain contains an A/J-derived genotype at marker D10Mit233. Among the AcB strains, the AcB51, AcB52, and AcB54 strains (boxed, rank 1) contain a C57BL/6J-derived segment for the interval defined by markers D10Mit42 and D10Mit232. For each marker, the chromosomal position in centiMorgans (cM) as well as the χ^2 statistic and P-value from the linkage analysis are given. (B) Survival of the RC mice to *M. tuberculosis* infection according to their background and genotype at marker D10Mit42. The majority of BcA mice contain a C57BL/6J-derived D10Mit42 genotype on a C57BL/6J background (bb-D10Mit42/B-background) while most AcB mice have an A/J-derived D10Mit42 genotype on an A/J background (aa-D10Mit42/A-background). Mice with a C57BL/6J-derived D10Mit42 genotype on an A/J background (bb-D10Mit42/A-background) are highly susceptible to *M. tuberculosis*. The percentage of surviving mice is plotted against time.

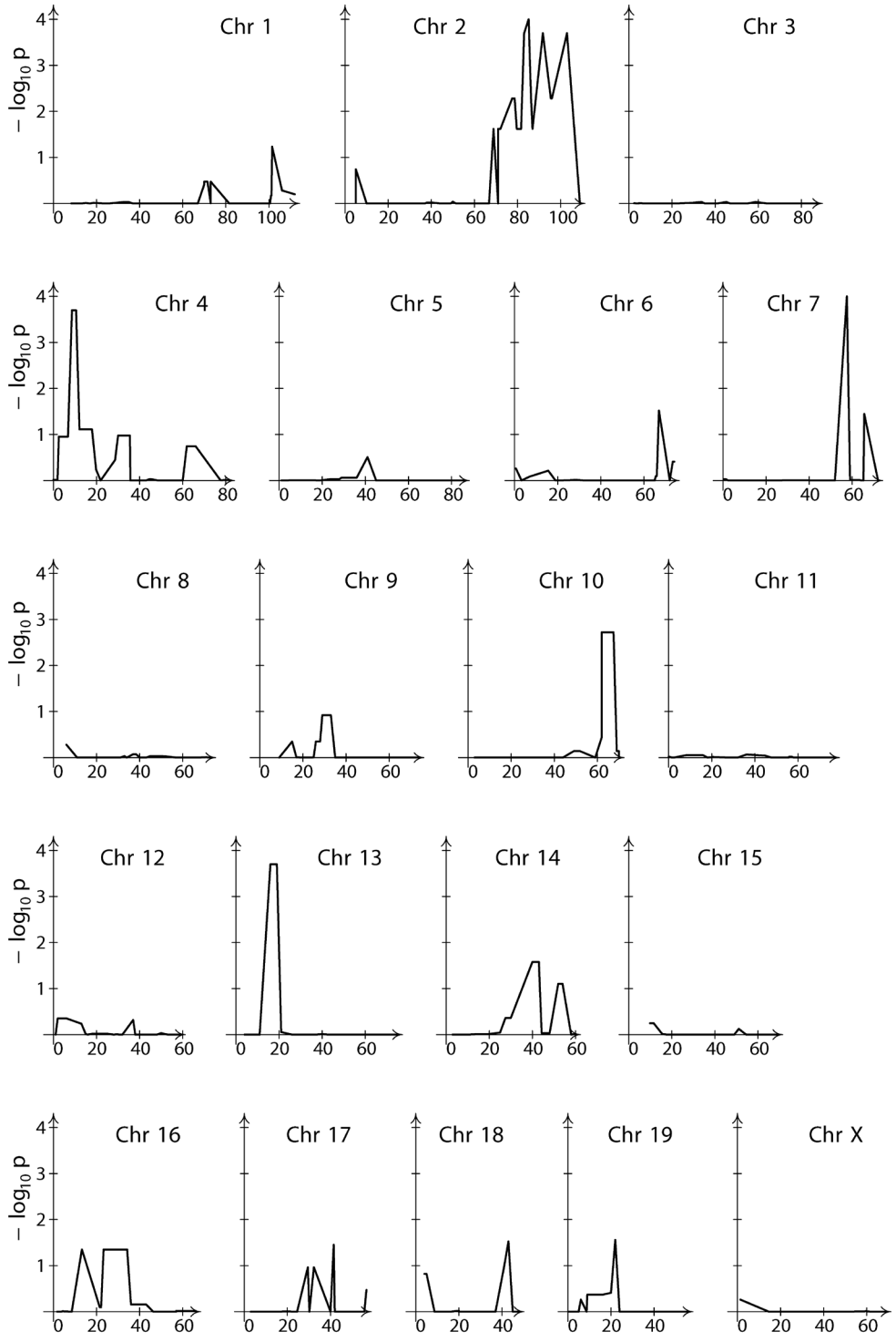

Figure 6: Linkage analysis of susceptibility to *M. tuberculosis* infection contingent on the D10Mit42 marker. Linkage analysis conditional on D10Mit42 identified loci on chromosomes 2, 4, 7, and 13 controlling survival to aerosol infection with *M. tuberculosis* H37Rv. The –logP plots are shown for all chromosomes. Chromosomal positions are given in centimorgans (cM).

DISCUSSION

In the present study, we identified the *Hsmtb1* locus that confers hypersusceptibility to infection with *M. tuberculosis* on distal chromosome 10. A previous genetic study employing "weight loss following *M. tuberculosis* infection" as a measure of susceptibility had found suggestive evidence for a susceptibility locus in the vicinity of *Hsmtb1* in male mice only [12]. While the phenotype described in the present study is substantially more extreme, it is possible that a different more benign allele occurring in I/St mice was detected in the weight loss study. Apart from this report there was no further overlap of the loci detected in previous mouse studies and those described in the present study. The above mentioned study involving a backcross of *M. tuberculosis* susceptible I/St and resistant A/Sn mice identified two major loci on chromosomes 3 and 9 and two suggestive loci on chromosomes 8 and 17 that controlled *M. tuberculosis*-triggered weight loss in female mice [12]. A validation study in an F2 population confirmed the locus that mapped to chromosome 3 and showed that the loci on chromosomes 9 and 17 affect both post-infection body weight loss and survival following *M. tuberculosis* infection [13]. A coding mutation in the tumor necrosis factor α (*Tnfa*) gene was responsible for the effect localized to chromosome 17 [14]. In linkage studies of F2 mice from susceptible C3HeB/FeJ and resistant C57BL/6J mice, a locus designated susceptibility to tuberculosis 1 (*sst1*) was identified on chromosome 1 [15]. The gene underlying *sst1* was later confirmed as the intracellular pathogen resistance 1 (*Ipr1*) gene, which encodes the IFN-induced protein 75 (Ifi75) [16]. Homozygosity for the resistant allele of *sst1* did not fully restore resistance in mice of a C3HeB/FeJ background, suggesting the presence of additional susceptibility loci in this strain. Adjustment for the resistant allele of *sst1* identified loci on chromosomes 7, 12, 15, and 17 [17] while crosses fixed for the susceptibility allele of *sst1* confirmed the locus detected on chromosome 7 [18]. The locus on chromosome 7 was also identified in genetic studies of susceptible DBA/2J and resistant C57BL/6J mice. This locus controlled both the extent of pulmonary replication following aerosol infection and survival to an intravenous dose of *M. tuberculosis* [19]. Additional loci

identified in genetic studies involving the DBA/2J and C57BL/6J strain combination were phenotype specific. A locus on chromosome 19 was shown to affect the *M. tuberculosis* replication in the lung whereas loci on chromosomes 1 and 3 controlled the length of survival following infection [20]. The limited overlap of susceptibility loci in our study with previously identified loci is not surprising since the genetic control of *M. tuberculosis* infection depends on the infectious dose, the route of infection, and the genetic background of the mice used for the study [19].

RC strains have proven particularly useful for the study of gene-gene interactions. The hypersusceptibility phenotype of the AcB51, AcB52, and AcB54 strains extends beyond that of either parental inbred line, suggesting the effect of *Hsmtb1* is due to epistasis. Hypersusceptibility attributed to *Hsmtb1* likely results from the transfer of a C57BL/6J-derived genome sequence onto an A/J genetic background. The minimum region on distal chromosome 10 harbouring the *Hsmtb1* locus extends from 36 cM to 59 cM which corresponds approximately to 67.7Mb to 103.5 Mb on the sequence map. Within this 35.8 Mb segment a total of 501 genes and open reading frames have been assigned [10]. A substantial proportion of these genes encode proteins that could conceivably be involved in extreme susceptibility to *M. tuberculosis* infection. Among these are a number of solute carrier family member genes (e.g. *Slc5a4a*, *Slc5a4b*, *Slc19a1*, and *Slc1a6*). Two members of this large group of genes have been implicated in susceptibility to infection by *M. tuberculosis* and susceptibility to clinical tuberculosis [3,21]. Another candidate is matrix metallopeptidase 11 (*Mmp11*) encoding a protein that is involved in tissue remodelling. Similarly, *Timp3* encodes a metalloprotease inhibitor that is involved in tumor-necrosis factor α (TNF-α) metabolism by inhibiting TNF-α-converting enzyme (Tace, also called Adam17). This inhibitor is a critical regulator of the pro-inflammatory cytokine TNF [22], which is involved in tuberculosis susceptibility in both humans and mice [23,24]. In addition, the segment includes a number of genes that encode proteins involved in signal transduction (e.g. *Stk11*, *Mknk2*, *Map2k2*, and *Pip5k1c*) that might impact on the

quality of intracellular signalling in *M. tuberculosis* infected cells. Given this large number of candidates the most efficient approach is a systematic sequence and expression analysis of all genes in the critical interval.

By using the AcB/BcA RC strain panel we have been able to map one fully penetrant and three incompletely penetrant susceptibility loci to well delineated chromosomal regions in the mouse genome. These results provide a genome-wide overview of the host genetic control system of *M. tuberculosis* H37Rv infection. Since all mice of a given RC strain are genetic replicas, this genetic control system can now be compared among different *M. tuberculosis* strains and clinical isolates. A currently unresolved question of the host genetics of tuberculosis susceptibility is if and to what extent host genetic control is strain-specific. For example, genetic association studies in human populations have detected preferential associations between a Toll-like receptor 2 (*TLR2*) polymorphism and tuberculosis meningitis caused by Beijing strains [25]. Likewise, 5'-lipoxygenase (*ALOX5*) was associated with pulmonary tuberculosis caused by *M. africanum*, but not *M. tuberculosis* [26] while the immunity-related GTPase M (*IRGM*) was associated with protection only from pulmonary tuberculosis caused by Euro-American strains of *M. tuberculosis* [27]. While the human studies lack replication, by employing the AcB/BcA RC strain panel we recently confirmed strain-specific genetic control of the Russia and Pasteur substrains of the widely used BCG tuberculosis vaccine [28]. From these experiments we can already conclude a certain level of specificity of the *Hsmtb1* locus since none of the three hypersusceptible strains displayed hypersusceptibility to the two BCG strains used in our study. If the *Hsmtb1* locus is acting in a *M. tuberculosi*s isolate-specific fashion, this would provide a reasonable explanation why genetic association studies in human populations that fail to account for the *M. tuberculosis* isolate either fail or detect only weak evidence for association.

ACKNOWLEDGEMENTS

We gratefully acknowledge the technical assistance of Fiona McIntosh and Vlad Kamenski. We also thank Pilar Domenech for providing the *M. tuberculosis* H37Rv (Pasteur) and for helpful advice.

References

1. WHO. *Global tuberculosis control: a short update to the 2009 report*2009.

2. Cobat A, Gallant CJ, Simkin L, et al. High heritability of antimycobacterial immunity in an area of hyperendemicity for tuberculosis disease. *J Infect Dis.* Jan 1 2010;201(1):15-19.

3. Cobat A, Gallant CJ, Simkin L, et al. Two loci control tuberculin skin test reactivity in an area hyperendemic for tuberculosis. *J Exp Med.* Nov 23 2009;206(12):2583-2591.

4. Casanova JL, Abel L. Genetic dissection of immunity to mycobacteria: the human model. *Annu Rev Immunol.* 2002;20:581-620.

5. Schurr E, Kramnik I. Genetic control of host susceptibility to tuberculosis. In: Kaufmann S, Britten W, eds. *Handbook of Tuberculosis*. Weinheim, Germany: Wiley-VCH; 2008:305-346.

6. Actor JK, Olsen M, Jagannath C, Hunter RL. Relationship of survival, organism containment, and granuloma formation in acute murine tuberculosis. *J Interferon Cytokine Res.* Oct 1999;19(10):1183-1193.

7. Jagannath C, Hoffmann H, Sepulveda E, Actor JK, Wetsel RA, Hunter RL. Hypersusceptibility of A/J mice to tuberculosis is in part due to a deficiency of the fifth complement component (C5). *Scand J Immunol.* Oct 2000;52(4):369-379.

8. Watson VE, Hill LL, Owen-Schaub LB, et al. Apoptosis in mycobacterium tuberculosis infection in mice exhibiting varied immunopathology. *J Pathol.* Feb 2000;190(2):211-220.

9. Fortin A, Diez E, Rochefort D, et al. Recombinant congenic strains derived from A/J and C57BL/6J: a tool for genetic dissection of complex traits. *Genomics.* May 15 2001;74(1):21-35.

10. Mouse Genome Database (MGD) at the Mouse Genome Informatics website TJL, Bar Harbor, Maine. http://www.informatics.jax.org. Accessed December 2009.

11. Rhoades ER, Frank AA, Orme IM. Progression of chronic pulmonary tuberculosis in mice aerogenically infected with virulent Mycobacterium tuberculosis. *Tuber Lung Dis.* 1997;78(1):57-66.

12. Lavebratt C, Apt AS, Nikonenko BV, Schalling M, Schurr E. Severity of tuberculosis in mice is linked to distal chromosome 3 and proximal chromosome 9. *J Infect Dis.* Jul 1999;180(1):150-155.

13. Sanchez F, Radaeva TV, Nikonenko BV, et al. Multigenic control of disease severity after virulent Mycobacterium tuberculosis infection in mice. *Infect Immun.* Jan 2003;71(1):126-131.

14. Kahler AK, Persson AS, Sanchez F, et al. A new coding mutation in the Tnf-alpha leader sequence in tuberculosis-sensitive I/St mice causes higher secretion levels of soluble TNF-alpha. *Genes Immun.* Oct 2005;6(7):620-627.

15. Kramnik I, Dietrich WF, Demant P, Bloom BR. Genetic control of resistance to experimental infection with virulent Mycobacterium tuberculosis. *Proc Natl Acad Sci U S A.* Jul 18 2000;97(15):8560-8565.

16. Pan H, Yan BS, Rojas M, et al. Ipr1 gene mediates innate immunity to tuberculosis. *Nature.* Apr 7 2005;434(7034):767-772.

17. Yan BS, Kirby A, Shebzukhov YV, Daly MJ, Kramnik I. Genetic architecture of tuberculosis resistance in a mouse model of infection. *Genes Immun.* Apr 2006;7(3):201-210.

18. Sissons J, Yan BS, Pichugin AV, Kirby A, Daly MJ, Kramnik I. Multigenic control of tuberculosis resistance: analysis of a QTL on mouse chromosome 7 and its synergism with sst1. *Genes Immun.* Jan 2009;10(1):37-46.

19. Mitsos LM, Cardon LR, Ryan L, LaCourse R, North RJ, Gros P. Susceptibility to tuberculosis: a locus on mouse chromosome 19 (Trl-4) regulates Mycobacterium tuberculosis replication in the lungs. *Proc Natl Acad Sci U S A.* May 27 2003;100(11):6610-6615.

20. Mitsos LM, Cardon LR, Fortin A, et al. Genetic control of susceptibility to infection with Mycobacterium tuberculosis in mice. *Genes Immun.* Dec 2000;1(8):467-477.

21. Greenwood CM, Fujiwara TM, Boothroyd LJ, et al. Linkage of tuberculosis to chromosome 2q35 loci, including NRAMP1, in a large aboriginal Canadian family. *Am J Hum Genet.* Aug 2000;67(2):405-416.

22. Mohammed FF, Smookler DS, Taylor SE, et al. Abnormal TNF activity in Timp3-/- mice leads to chronic hepatic inflammation and failure of liver regeneration. *Nat Genet.* Sep 2004;36(9):969-977.

23. Bean AG, Roach DR, Briscoe H, et al. Structural deficiencies in granuloma formation in TNF gene-targeted mice underlie the heightened susceptibility to aerosol Mycobacterium tuberculosis infection, which is not compensated for by lymphotoxin. *J Immunol.* Mar 15 1999;162(6):3504-3511.

24. Flynn JL, Goldstein MM, Chan J, et al. Tumor necrosis factor-alpha is required in the protective immune response against Mycobacterium tuberculosis in mice. *Immunity.* Jun 1995;2(6):561-572.

25. Caws M, Thwaites G, Dunstan S, et al. The influence of host and bacterial genotype on the development of disseminated disease with Mycobacterium tuberculosis. *PLoS Pathog.* Mar 2008;4(3):e1000034.

26. Herb F, Thye T, Niemann S, et al. ALOX5 variants associated with susceptibility to human pulmonary tuberculosis. *Hum Mol Genet.* Apr 1 2008;17(7):1052-1060.

27. Intemann CD, Thye T, Niemann S, et al. Autophagy gene variant IRGM -261T contributes to protection from tuberculosis caused by Mycobacterium tuberculosis but not by M. africanum strains. *PLoS Pathog.* Sep 2009;5(9):e1000577.

28. Di Pietrantonio T, Hernandez C, Girard M, et al. Strain-specific differences in the genetic control of two closely related mycobacteria. *PLoS Pathog.* 2010;6(10):e1001169.

CHAPTER 5
Discussion and Future Directions

5.1 Overview

In the mid-20th century, James V. Neel, a pioneer in the field of human genetics, proposed that infectious diseases were the result of a complex interaction between environmental, microbial and host factors [284]. Consistent with Neel's theory, host genetic factors have long been known to contribute to the outcome of *M. tuberculosis* infection. More recent studies have also confirmed that *M. tuberculosis* isolates are more genetically diverse than originally assumed, raising questions about the contribution of bacterial factors to disease pathogenesis. The results presented in this thesis provide evidence for a joint effect of host and pathogen on the host response to mycobacterial infection. The combined impact of host and pathogen was detectable at both the phenotypic and genetic level.

In Chapter 2, the effect of host and pathogen genetic variation on biological and mechanistic phenotypes was concurrently investigated in the A/J and C57BL/6J mouse strains infected with BCG Russia, BCG Pasteur, or *M. tuberculosis*. The impact of the mycobacterial strain was much greater compared to the host genetic effect. Bacterial-related differences were observed for biological phenotypes (pulmonary replication, lung histopathology) and mechanistic phenotypes (pulmonary transcription of *Ifng*, *Il12b*, *Il4* and chemokine genes). However, differences in pulmonary replication, lung pathology, and chemokine induction across the mycobacteria were pronounced in the A/J mouse strain, suggesting a role for the host strain in modulating the magnitude of the response. These findings showed that the host response to mycobacteria reflects a genetically controlled, joint effect, of both host and pathogen.

A comparative genetic analysis was performed in AcB and BcA strains infected with BCG Russia or BCG Pasteur as described in Chapter 3. A novel analytical method was developed to overcome the confounding impact of the strain genetic background when performing genome-wide linkage analyses using the RC strains. Mapping under this model identified 11 shared as well as tissue- and BCG-

specific susceptibility loci controlling bacterial counts in the lung and spleen. A locus indistinguishable from *Nramp1* on chromosome 1 was shown to control early BCG Pasteur and early and late BCG Russia infection in a spleen-specific manner. To ensure that this locus would not mask additional QTL, the analysis was modified to adjust for the effect of *Nramp1*. Loci impacting on late BCG Russia but not BCG Pasteur infection in the spleen were identified on chromosomes 11 and 13. The locus on chromosome 11 also controlled the pulmonary counts of BCG Russia but not BCG Pasteur. These results demonstrated that phenotypic differences in the RC strains are the result of a tissue-specific interplay between host and bacterial genes.

The AcB and BcA strains were infected with *M. tuberculosis* as part of our efforts to compare patterns of host genetic control across different mycobacteria. The genetic analysis described in Chapter 4 identified linkage between the mid-distal portion of chromosome 10 and survival following *M. tuberculosis* infection. This locus was fully penetrant, with rapid death occurring in all AcB strains that contained a congenic C57BL/6J-derived chromosome 10 segment. Among the markers within the chromosome 10 interval, the D10Mit42 marker showed the strongest genetic effect. Linkage analysis conditional on this marker identified additional genetic effects on chromosomes 2, 4, and 13. Neither of these loci, including the hit on chromosome 13, overlapped loci controlling susceptibility to BCG Pasteur and BCG Russia infection as measured by bacillary counts. While differences in the route of infection and in the phenotypic measure of susceptibility may have contributed to the lack of overlap, these results are consistent with the notion that host genetic control of mycobacterial infection is dependent on bacterial-related factors.

5.2 *Nramp1* and Susceptibility to Mycobacterial Infection

Susceptibility to BCG in mice is genetically controlled by the *Nramp1* gene. *Nramp1* is known to regulate the splenic replication of BCG Montreal at the early phase of infection (0-3 weeks) but not at the late phase (3-6 weeks) [60]. Genetic

analysis of the bacterial counts of BCG Russia or Pasteur in the RC strains identified a locus on chromosome 1 indistinguishable from *Nramp1*. The *Nramp1*-containing locus was shown to control early BCG Pasteur infection in a spleen-specific manner. An overlap in the host genetic control of BCG Montreal and BCG Pasteur has been suggested [285] and was expected, considering the phylogenetic relatedness and similar replication patterns of the two BCG strains. A second interesting observation was the involvement of the *Nramp1*-containing locus in the control of the early as well as late phase of BCG Russia infection in the spleen. An effect for *Nramp1* in late BCG Russia infection was not surprising, given that the kinetics of BCG Russia infection is strikingly different from that of BCG Montreal, with persistent splenic replication occurring until at least 18 weeks post-infection (data not shown). These results confirm the central role of *Nramp1* in the host control of BCG infection. By contrast, the *Nramp1* region was not shown to control survival following infection with *M. tuberculosis.* This finding is consistent with a number of previous reports showing that resistance to *M. tuberculosis* infection is independent of *Nramp1* [74,75,286,287]. This suggests the impact of *Nramp1* depends on specific pathogen-encoded factors and provides further evidence for a joint contribution of host and pathogen in mycobacterial susceptibility.

5.3 Strain-Specific Host Genetic Control of Tuberculosis

Until recently, *M. tuberculosis* strains were thought to exhibit low genetic variation [127,288]. Increasing evidence now suggests that *M. tuberculosis* isolates are more genetically diverse than originally assumed, and that this diversity may be linked to the pathogenic potential of the strain [19,20] and the clinical manifestation of disease [278]. A largely unknown aspect of this bacterial variability is how it impacts on the host genetic control of infection. This would have important implications in human genetic studies of tuberculosis susceptibility, especially considering that most genetic studies do not account for the infecting *M. tuberculosis* strain. The comparative genetic analysis described in Chapter 3 outlined the importance of accounting for the mycobacterial strain when

performing genetic studies. The observation that only a minority of genetic control elements were shared between the two closely related strains of BCG suggests that strains of *M. tuberculosis* are also under heterogenous genetic control. Infection of the RC strain set with *M. tuberculosis* H37Rv did not detect an overlap in the host genetic control with either of the two BCG strains. We anticipate that infection of the RC strains with other strains of *M. tuberculosis* would also be under different host genetic control. This may explain why population-based genetic studies identify weak and poorly reproducible genetic effects. To date, the strongest association between a human gene and adult tuberculosis was obtained with *NRAMP1*, the human orthologue of the mouse *Nramp1* gene. A major genetic effect for *NRAMP1* [logarithm of odds (LOD) =3.81; relative risk (RR) = 10] was detected in a study involving a tuberculosis outbreak in an extended Aboriginal Canadian family. In this study, all cases had been infected from a single index case, i.e. a single bacterial strain [281]. However, in population-based studies of *NRAMP1* where disease is caused by different strains of *M. tuberculosis*, more modest genetic effects (odds ratio <4) have been reported [289,290]. The importance of *M. tuberculosis* strain variability in the genetic control of infection has also been demonstrated in studies of interacting host-pathogen genotypes. For example, a variant in the *TLR2* gene was associated with tuberculosis meningitis caused by Beijing strains in a Vietnamese cohort [278]. In a Ghanian population, a preferential association was noted between a variant of *ALOX5* and pulmonary tuberculosis caused by the *M. africanum* West-African 2 lineage [279], while in the same population, a polymorphism in the *IRGM* gene was protective against the Euro-American subgroup of *M. tuberculosis* but not *M. africanum* [280]. As in all human studies, these results may be confounded by unrecognized factors. Even in the *NRAMP1* study centered on a single family, liability classes (age, purified protein derivative, and vaccination status) had to be specified to obtain significant evidence for linkage [281]. A major advantage of our studies was the use of mouse models which allow for control of extraneous variables. Under highly regulated experimental conditions, these results strongly suggest that pathogenesis is host-pathogen specific and indicates that future

genetic studies should pay closer attention to the strains of *M. tuberculosis* that circulate in the study population.

5.4 The High Dose Aerosol Model of Tuberculosis

Most studies of tuberculosis in the mouse are typically performed using a low dose aerosol infection protocol (~100 *M. tuberculosis* organisms), since this model appears to most closely approximate infection in humans. This is the case in developed countries, where a low dose exposure in non-immunized individuals can cause disease. However, Rook *et al.* [291] recently put forward a compelling argument that, in developing countries with a high disease burden, mouse models infected with a high-dose challenge may best represent the course of disease. Unlike in northern developed countries, overcrowding and delayed diagnosis of contagious individuals invariably results in prolonged exposure to infectious family members sharing the same dwelling. In addition, most individuals living in developing countries are partially protected by vaccination with BCG and/or exposure to environmental mycobacteria [292]. In these individuals, higher doses of *M. tuberculosis* are likely required to overcome partial immunity and progress to disease.

While a high dose infection mouse model may best mimic disease in high burden countries, there are both advantages and limitations to using a high dose challenge for genetic studies in the mouse. An obvious advantage of the high dose model is the shortened survival, which reduces the length of the experiment and the cost of maintaining mice. For genetic analysis, a disadvantage of the high dose model is the decrease in differential susceptibility between the two mouse strains being studied. This was nicely demonstrated by Medina *et al.* using the DBA/2J (susceptible) and BALB/c (resistant) mouse strains [156]. Increasing the intravenous dose from 10^5 to 10^6 bacilli diminished the differential susceptibility of the strains. A dose of 10^7 bacteria completely abolished the superior resistance of BALB/c over DBA/2J mice, with both mouse strains having a survival time of 40 days. For genetic studies with the RC strains, the progenitors do not need to differ

significantly in the phenotype of interest, as we demonstrated in Chapter 3. This highlights another major advantage of using the RC strains for genetic mapping. We did however, test different aerosol doses to determine the dose most suitable for our approach (data not shown). At a dose of ~400 bacilli, the difference in median survival between A/J and C57BL/6J mice was approximately 50 days, with the last mouse dying at 218 days. This dose was high enough to minimize the length of the experiment, but it also showed good discriminant ability.

5.5 Future Directions

5.5.1 Characterization of the Chromosome 11 Locus

Linkage analysis using the RC strains detected a locus on chromosome 11 controlling BCG Russia replication in the lung (47.67-50 cM, P=0.0037) and spleen (47.67 cM, P=0.0019) at 6 weeks post-infection. Preferential replication of BCG Russia in both organs was associated with the A/J-derived segment of chromosome 11. From public assemblies of the mouse genome [Mouse Genome Informatics (MGI)], the overlapping region of significance (47.67 ± 2 cM) is predicted to contain 63 annotated genes [293]. Positional candidates include the chemokine (C-C motif) ligands 1-9 and 11-12. As a first step, we compared the chemokine expression levels for the lungs of A/J and C7BL/6J progenitors collected as part of real-time experiments described in Chapter 2. Among the aforementioned chemokines, *Ccl2* transcription levels were 2.3 times greater (95% CI: 1.2-4.4) in C57BL/6J mice relative to A/J mice at the 6 week time-point of BCG Russia infection. These results provide support for *Ccl2* as a candidate for the chromosome 11 locus. Additional evidence could be obtained from profiling *Ccl2* expression levels in the organs of RC mice. These experiments are highly feasible since pulmonary and splenic RNA from mice infected with BCG Russia have already been collected for 17 of the 35 RC strains. Because the genotypes of markers within the chromosome 11 interval are known for all RC strains, a possible correlation between the A/J-derived segment, gene expression, and susceptibility to BCG Russia can be readily established.

5.5.2 Complex Genetic Control of Susceptibility to M. tuberculosis

The conventional approach to search for susceptibility loci in deviant RC strains is to backcross the informative strain to its background progenitor and perform a limited genome scan using markers informative for the known congenic fragments. This strategy contributed to the identification of a role for the pantetheinase enzyme in the host response to malaria [294]. Alternatively, informative F2 populations can be generated by intercrossing the RC strains to an unrelated inbred strain. Ideally, the strain selected for intercross bears a phenotype opposite to the RC strain of interest. This strategy presents several advantages over backcrossing to the progenitor strain. First, the presence of small congenic segments may have gone undetected during the initial genotyping of the RC strain and would be missed in the limited genome scan. Second, polymorphisms introduced by crossing to a new strain increase the likelihood of identifying the QTL. Finally, if the phenotype was caused by a mutation that arose during the original derivation of the RC strains, it would be more difficult to identify using a conventional backcross, unless the mutation occurred within or close to a congenic segment. This approach led to the identification of a role for the pyruvate kinase (*Pklr*) gene in susceptibility to malaria [295] and salmonella infection [296].

Phenotyping of the AcB/BcA panel for susceptibility to tuberculosis identified strains AcB51, AcB52 and AcB54 as hypersusceptible. These strains show rapid and uncontrolled replication of *M. tuberculosis* in the lungs ($>10^{10}$ bacteria) and have extremely short survival times (survival time<40 days). We identified a locus on chromosome 10 which explained 100% of the variation of these strains. Exome sequencing of genes within the linkage interval and/or expression profiling could help identify positional candidates. To confirm causality, the susceptibility locus can be introgressed onto an A/J background to establish a congenic line that can be tested for increased susceptibility. Although unlikely, it is possible that the causative effect lies outside the chromosome 10 region and

consequently, outside a C57BL/6J-derived congenic segment. In this instance, identification of the susceptibility locus would require additional mapping studies in an intercross population. The BALB/c mouse strain is best suited for the proposed experiments since it is ranked among the strains most resistant to *M. tuberculosis* [156]. Linkage studies in informative (AcB51/AcB52/AcB54 x BALB/c) F2 populations using survival time as the quantitative trait would localize the QTL responsible for the increased susceptibility of these strains.

A major criticism of using mice to model tuberculosis is that they develop a pathology which does not reflect the human disease. Granulomas in the mouse are generally described as cellular infiltrates lacking structural organization with no central necrosis. These observations were derived from C57BL/6J and BALB/c mice, two relatively resistant mouse strains. In humans with tuberculosis (susceptible humans), granulomas appear as caseous necrotic lesions surrounded by a well-structured ring of lymphocytes. Thus, the pathological manifestations considered to be characteristic of murine and human tuberculosis are remarkably different, since they are representative of resistant mice and susceptible humans, respectively. Apt and Kramnik recently presented the case that susceptible mouse strains are better suited to study the pathological aspects of human tuberculosis [297]. A number of susceptible strains have been identified that recapitulate the lung pathology observed in humans. In the C3HeB/FeJ mouse strain described in section 1.3.3, necrotizing granulomas of the lung were determined to be a specific effect of the *sst1* locus [172,298]. The AcB51 mouse strain identified as hypersusceptible in our studies also develops well-organized, necrotic lung granulomas following infection with *M. tuberculosis*. This strain could be useful to dissect the immunological and genetic aspects of pulmonary necrosis induced by *M. tuberculosis*.

5.6 Conclusion

Human studies have provided evidence for host-pathogen specificity in susceptibility to mycobacterial diseases. Although intriguing, these studies cannot

rule out the potentially confounding impact of sociological, epidemiological, and environmental factors. To overcome this issue, we have used a mouse model of infection. Under highly controlled experimental conditions, the research presented in this thesis constitutes strong evidence for a joint effect of host and pathogen when considering mycobacterial infection and disease. Together, our results strongly suggest that a proper understanding of the flow of mycobacteria through exposed populations needs to consider not only isolated genetically-controlled host and pathogen factors but also an interaction between pathogen virulence and host susceptibility factors.

ORIGINAL CONTRIBUTIONS TO KNOWLEDGE

1. Host and pathogen factors jointly impact on common biological and mechanistic read-outs.

2. The host genetic control of mycobacterial infection is pathogen-specific.

3. A locus identified on chromosome 11 controls the bacterial counts of BCG Russia in the lung and spleen while a locus on chromosome 13 is spleen-specific.

4. Hypersusceptibility to *M. tuberculosis* infection in the AcB51, AcB52, and AcB54 strains is linked to a locus on chromosome 10 (*Hsmtb1*).

5. Loci on chromosomes 13 (*Smtb1*), 2 (*Smtb2*) and 4 (*Smtb3*) impact on survival to *M. tuberculosis* infection.

References

1. WHO. *Global tuberculosis control: a short update to the 2009 report*2009.

2. Colditz GA, Berkey CS, Mosteller F, et al. The efficacy of bacillus Calmette-Guerin vaccination of newborns and infants in the prevention of tuberculosis: meta-analyses of the published literature. *Pediatrics.* Jul 1995;96(1 Pt 1):29-35.

3. Trunz BB, Fine P, Dye C. Effect of BCG vaccination on childhood tuberculous meningitis and miliary tuberculosis worldwide: a meta-analysis and assessment of cost-effectiveness. *Lancet.* Apr 8 2006;367(9517):1173-1180.

4. Fine PE. Variation in protection by BCG: implications of and for heterologous immunity. *Lancet.* Nov 18 1995;346(8986):1339-1345.

5. Bloom BR, Fine PEM. The BCG Experience: Implications for Future Vaccines against Tuberculosis. In: Bloom BR, ed. *Tuberculosis: Pathogenesis, Protection, and Control*. Washington, DC: Am Soc Microbiol; 1994:531-557.

6. Chan J, Xing Y, Magliozzo RS, Bloom BR. Killing of virulent Mycobacterium tuberculosis by reactive nitrogen intermediates produced by activated murine macrophages. *J Exp Med.* Apr 1 1992;175(4):1111-1122.

7. Wolf AJ, Desvignes L, Linas B, et al. Initiation of the adaptive immune response to Mycobacterium tuberculosis depends on antigen production in the local lymph node, not the lungs. *J Exp Med.* Jan 21 2008;205(1):105-115.

8. Wolf AJ, Linas B, Trevejo-Nunez GJ, et al. Mycobacterium tuberculosis infects dendritic cells with high frequency and impairs their function in vivo. *J Immunol.* Aug 15 2007;179(4):2509-2519.

9. Reiley WW, Calayag MD, Wittmer ST, et al. ESAT-6-specific CD4 T cell responses to aerosol Mycobacterium tuberculosis infection are initiated in the mediastinal lymph nodes. *Proc Natl Acad Sci U S A.* Aug 5 2008;105(31):10961-10966.

10. Sharma SK, Mohan A, Sharma A, Mitra DK. Miliary tuberculosis: new insights into an old disease. *Lancet Infect Dis.* Jul 2005;5(7):415-430.

11. Marais BJ, Gie RP, Schaaf HS, et al. The natural history of childhood intra-thoracic tuberculosis: a critical review of literature from the pre-chemotherapy era. *Int J Tuberc Lung Dis.* Apr 2004;8(4):392-402.

12. Donald PR, Schoeman JF. Tuberculous meningitis. *N Engl J Med.* Oct 21 2004;351(17):1719-1720.

13. Kaufmann SH. How can immunology contribute to the control of tuberculosis? *Nat Rev Immunol.* Oct 2001;1(1):20-30.

14. Stead WW. Genetics and resistance to tuberculosis. Could resistance be enhanced by genetic engineering? *Ann Intern Med.* Jun 1 1992;116(11):937-941.

15. Stead WW, Senner JW, Reddick WT, Lofgren JP. Racial differences in susceptibility to infection by Mycobacterium tuberculosis. *N Engl J Med.* Feb 15 1990;322(7):422-427.

16. Comstock GW. Tuberculosis in twins: a re-analysis of the Prophit survey. *Am Rev Respir Dis.* Apr 1978;117(4):621-624.

17. Casanova JL, Abel L. Genetic dissection of immunity to mycobacteria: the human model. *Annu Rev Immunol.* 2002;20:581-620.

18. Fortin A, Abel L, Casanova JL, Gros P. Host genetics of mycobacterial diseases in mice and men: forward genetic studies of BCG-osis and tuberculosis. *Annu Rev Genomics Hum Genet.* 2007;8:163-192.

19. Nicol MP, Wilkinson RJ. The clinical consequences of strain diversity in Mycobacterium tuberculosis. *Trans R Soc Trop Med Hyg.* Oct 2008;102(10):955-965.

20. Gagneux S, Small PM. Global phylogeography of Mycobacterium tuberculosis and implications for tuberculosis product development. *Lancet Infect Dis.* May 2007;7(5):328-337.

21. Onyebujoh P, Rook GA. Tuberculosis. *Nat Rev Microbiol.* Dec 2004;2(12):930-932.

22. Koch R. Die aetiologie der tuberculose. *Berl Klin Wochenschr.* 1882;15:221-230.

23. North RJ, Jung YJ. Immunity to tuberculosis. *Annu Rev Immunol.* 2004;22:599-623.

24. Buer J, Balling R. Mice, microbes and models of infection. *Nat Rev Genet.* Mar 2003;4(3):195-205.

25. Fisler JS, Warden CH. Mapping of mouse obesity genes: A generic approach to a complex trait. *J Nutr.* Sep 1997;127(9):1909S-1916S.

26. Boyse EA. The increasing value of congenic mice in biomedical research. *Lab Anim Sci.* Oct 1977;27(5 Pt 2):771-781.

27. Wakeland E, Morel L, Achey K, Yui M, Longmate J. Speed congenics: a classic technique in the fast lane (relatively speaking). *Immunol Today.* Oct 1997;18(10):472-477.

28. Bailey DW. Recombinant-inbred strains. An aid to finding identity, linkage, and function of histocompatibility and other genes. *Transplantation.* Mar 1971;11(3):325-327.

29. Demant P, Hart AA. Recombinant congenic strains--a new tool for analyzing genetic traits determined by more than one gene. *Immunogenetics.* 1986;24(6):416-422.

30. Mullerova J, Hozak P. Use of recombinant congenic strains in mapping disease-modifying genes. *News Physiol Sci.* Jun 2004;19:105-109.

31. Fortin A, Diez E, Rochefort D, et al. Recombinant congenic strains derived from A/J and C57BL/6J: a tool for genetic dissection of complex traits. *Genomics.* May 15 2001;74(1):21-35.

32. Calmette A, Guérin C, Breton M. Contribution à l'étude de la tuberculose expérimentale du cobaye. *Ann Inst Pasteur.* 1907(21):401-416.

33. Calmette A, Guérin C. Recherches expérimentales sur la défense de l'organisme contre l'infection tuberculeuse. *Ann Inst Pasteur.* 1911(25):625–641.

34. Calmette A, Boquet A, Negre L. Contribution a l'etude du bacille tuberculeux bilie. *Ann Inst Pasteur.* 1921;35:561–570.

35. Weill-Hallé B, Turpin R. Premiers essais de vaccination antituberculeuse de l'enfant par le Bacille Calmette-Guérin. *Bull Mem Soc Med l'Hosp de Paris.* 1925(49):1589-1601.

36. Boe J. Variations in the virulence of BCG. *Acta Tuberc Scand.* 1948;22(1-2):125-133.

37. Osborn TW. Changes in BCG strains. *Tubercle.* Mar 1983;64(1):1-13.

38. Mahairas GG, Sabo PJ, Hickey MJ, Singh DC, Stover CK. Molecular analysis of genetic differences between Mycobacterium bovis BCG and virulent M. bovis. *J Bacteriol.* Mar 1996;178(5):1274-1282.

39. Behr MA, Wilson MA, Gill WP, et al. Comparative genomics of BCG vaccines by whole-genome DNA microarray. *Science.* May 28 1999;284(5419):1520-1523.

40. Pym AS, Brodin P, Brosch R, Huerre M, Cole ST. Loss of RD1 contributed to the attenuation of the live tuberculosis vaccines Mycobacterium bovis BCG and Mycobacterium microti. *Mol Microbiol.* Nov 2002;46(3):709-717.

41. Berthet FX, Rasmussen PB, Rosenkrands I, Andersen P, Gicquel B. A Mycobacterium tuberculosis operon encoding ESAT-6 and a novel low-molecular-mass culture filtrate protein (CFP-10). *Microbiology.* Nov 1998;144 (Pt 11):3195-3203.

42. Sorensen AL, Nagai S, Houen G, Andersen P, Andersen AB. Purification and characterization of a low-molecular-mass T-cell antigen secreted by Mycobacterium tuberculosis. *Infect Immun.* May 1995;63(5):1710-1717.

43. Brodin P, Rosenkrands I, Andersen P, Cole ST, Brosch R. ESAT-6 proteins: protective antigens and virulence factors? *Trends Microbiol.* Nov 2004;12(11):500-508.

44. Pym AS, Brodin P, Majlessi L, et al. Recombinant BCG exporting ESAT-6 confers enhanced protection against tuberculosis. *Nat Med.* May 2003;9(5):533-539.

45. Lewis KN, Liao R, Guinn KM, et al. Deletion of RD1 from Mycobacterium tuberculosis mimics bacille Calmette-Guerin attenuation. *J Infect Dis.* Jan 1 2003;187(1):117-123.

46. Brosch R, Gordon SV, Garnier T, et al. Genome plasticity of BCG and impact on vaccine efficacy. *Proc Natl Acad Sci U S A.* Mar 27 2007;104(13):5596-5601.

47. Behr MA, Small PM. A historical and molecular phylogeny of BCG strains. *Vaccine.* Feb 26 1999;17(7-8):915-922.

48. Mostowy S, Tsolaki AG, Small PM, Behr MA. The in vitro evolution of BCG vaccines. *Vaccine.* Oct 1 2003;21(27-30):4270-4274.

49. Keller PM, Bottger EC, Sander P. Tuberculosis vaccine strain Mycobacterium bovis BCG Russia is a natural recA mutant. *BMC Microbiol.* 2008;8:120.

50. Fomukong NG, Dale JW, Osborn TW, Grange JM. Use of gene probes based on the insertion sequence IS986 to differentiate between BCG vaccine strains. *J Appl Bacteriol.* Feb 1992;72(2):126-133.

51. Gonzalo Asensio J, Maia C, Ferrer NL, et al. The virulence-associated two-component PhoP-PhoR system controls the biosynthesis of polyketide-derived lipids in Mycobacterium tuberculosis. *J Biol Chem.* Jan 20 2006;281(3):1313-1316.

52. Perez E, Samper S, Bordas Y, Guilhot C, Gicquel B, Martin C. An essential role for phoP in Mycobacterium tuberculosis virulence. *Mol Microbiol.* Jul 2001;41(1):179-187.

53. Leung AS, Tran V, Wu Z, et al. Novel genome polymorphisms in BCG vaccine strains and impact on efficacy. *BMC Genomics.* 2008;9:413.

54. Oettinger T, Andersen AB. Cloning and B-cell-epitope mapping of MPT64 from Mycobacterium tuberculosis H37Rv. *Infect Immun.* May 1994;62(5):2058-2064.

55. Charlet D, Mostowy S, Alexander D, Sit L, Wiker HG, Behr MA. Reduced expression of antigenic proteins MPB70 and MPB83 in Mycobacterium bovis BCG strains due to a start codon mutation in sigK. *Mol Microbiol.* Jun 2005;56(5):1302-1313.

56. Behr MA, Schroeder BG, Brinkman JN, Slayden RA, Barry CE, 3rd. A point mutation in the mma3 gene is responsible for impaired methoxymycolic acid production in Mycobacterium bovis BCG strains obtained after 1927. *J Bacteriol.* Jun 2000;182(12):3394-3399.

57. Spreadbury CL, Pallen MJ, Overton T, et al. Point mutations in the DNA- and cNMP-binding domains of the homologue of the cAMP receptor protein (CRP) in Mycobacterium bovis BCG: implications for the inactivation of a global regulator and strain attenuation. *Microbiology.* Feb 2005;151(Pt 2):547-556.

58. Salamon H, Kato-Maeda M, Small PM, Drenkow J, Gingeras TR. Detection of deleted genomic DNA using a semiautomated computational analysis of GeneChip data. *Genome Res.* Dec 2000;10(12):2044-2054.

59. Forget A, Skamene E, Gros P, Miailhe AC, Turcotte R. Differences in response among inbred mouse strains to infection with small doses of Mycobacterium bovis BCG. *Infect Immun.* Apr 1981;32(1):42-47.

60. Gros P, Skamene E, Forget A. Genetic control of natural resistance to Mycobacterium bovis (BCG) in mice. *J Immunol.* Dec 1981;127(6):2417-2421.

61. Malo D, Vidal SM, Hu J, Skamene E, Gros P. High-resolution linkage map in the vicinity of the host resistance locus Bcg. *Genomics.* Jun 1993;16(3):655-663.

62. Skamene E, Gros P, Forget A, Kongshavn PA, St Charles C, Taylor BA. Genetic regulation of resistance to intracellular pathogens. *Nature.* Jun 10 1982;297(5866):506-509.

63. O'Brien AD, Rosenstreich DL, Taylor BA. Control of natural resistance to Salmonella typhimurium and Leishmania donovani in mice by closely linked but distinct genetic loci. *Nature.* Oct 2 1980;287(5781):440-442.

64. Forbes JR, Gros P. Divalent-metal transport by NRAMP proteins at the interface of host-pathogen interactions. *Trends Microbiol.* Aug 2001;9(8):397-403.

65. Vidal SM, Malo D, Vogan K, Skamene E, Gros P. Natural resistance to infection with intracellular parasites: isolation of a candidate for Bcg. *Cell.* May 7 1993;73(3):469-485.

66. Vidal SM, Pinner E, Lepage P, Gauthier S, Gros P. Natural resistance to intracellular infections: Nramp1 encodes a membrane phosphoglycoprotein absent in macrophages from susceptible (Nramp1 D169) mouse strains. *J Immunol.* Oct 15 1996;157(8):3559-3568.

67. Vidal S, Tremblay ML, Govoni G, et al. The Ity/Lsh/Bcg locus: natural resistance to infection with intracellular parasites is abrogated by disruption of the Nramp1 gene. *J Exp Med.* Sep 1 1995;182(3):655-666.

68. Govoni G, Vidal S, Gauthier S, Skamene E, Malo D, Gros P. The Bcg/Ity/Lsh locus: genetic transfer of resistance to infections in C57BL/6J mice transgenic for the Nramp1 Gly169 allele. *Infect Immun.* Aug 1996;64(8):2923-2929.

69. Roupie V, Rosseels V, Piersoel V, Zinniel DK, Barletta RG, Huygen K. Genetic resistance of mice to Mycobacterium paratuberculosis is influenced by Slc11a1 at the early but not at the late stage of infection. *Infect Immun.* May 2008;76(5):2099-2105.

70. de Chastellier C, Frehel C, Offredo C, Skamene E. Implication of phagosome-lysosome fusion in restriction of Mycobacterium avium growth in bone marrow macrophages from genetically resistant mice. *Infect Immun.* Sep 1993;61(9):3775-3784.

71. Goto Y, Buschman E, Skamene E. Regulation of host resistance to Mycobacterium intracellulare in vivo and in vitro by the Bcg gene. *Immunogenetics.* 1989;30(3):218-221.

72. Denis M, Forget A, Pelletier M, Gervais F, Skamene E. Killing of Mycobacterium smegmatis by macrophages from genetically susceptible and resistant mice. *J Leukoc Biol.* Jan 1990;47(1):25-30.

73. Skamene E, Gros P, Forget A, Patel PJ, Nesbitt MN. Regulation of resistance to leprosy by chromosome 1 locus in the mouse. *Immunogenetics.* 1984;19(2):117-124.

74. Medina E, North RJ. Evidence inconsistent with a role for the Bcg gene (Nramp1) in resistance of mice to infection with virulent Mycobacterium tuberculosis. *J Exp Med.* Mar 1 1996;183(3):1045-1051.

75. North RJ, LaCourse R, Ryan L, Gros P. Consequence of Nramp1 deletion to Mycobacterium tuberculosis infection in mice. *Infect Immun.* Nov 1999;67(11):5811-5814.

76. Canonne-Hergaux F, Calafat J, Richer E, et al. Expression and subcellular localization of NRAMP1 in human neutrophil granules. *Blood.* Jul 1 2002;100(1):268-275.

77. Gruenheid S, Pinner E, Desjardins M, Gros P. Natural resistance to infection with intracellular pathogens: the Nramp1 protein is recruited to the membrane of the phagosome. *J Exp Med.* Feb 17 1997;185(4):717-730.

78. Forbes JR, Gros P. Iron, manganese, and cobalt transport by Nramp1 (Slc11a1) and Nramp2 (Slc11a2) expressed at the plasma membrane. *Blood.* Sep 1 2003;102(5):1884-1892.

79. Jabado N, Jankowski A, Dougaparsad S, Picard V, Grinstein S, Gros P. Natural resistance to intracellular infections: natural resistance-associated macrophage protein 1 (Nramp1) functions as a pH-dependent manganese transporter at the phagosomal membrane. *J Exp Med.* Nov 6 2000;192(9):1237-1248.

80. Hackam DJ, Rotstein OD, Zhang W, Gruenheid S, Gros P, Grinstein S. Host resistance to intracellular infection: mutation of natural resistance-associated macrophage protein 1 (Nramp1) impairs phagosomal acidification. *J Exp Med.* Jul 20 1998;188(2):351-364.

81. Malo D, Vogan K, Vidal S, et al. Haplotype mapping and sequence analysis of the mouse Nramp gene predict susceptibility to infection with intracellular parasites. *Genomics.* Sep 1 1994;23(1):51-61.

82. Turcotte K, Gauthier S, Mitsos LM, et al. Genetic control of myeloproliferation in BXH-2 mice. *Blood.* Mar 15 2004;103(6):2343-2350.

83. Turcotte K, Gauthier S, Tuite A, Mullick A, Malo D, Gros P. A mutation in the Icsbp1 gene causes susceptibility to infection and a chronic myeloid leukemia-like syndrome in BXH-2 mice. *J Exp Med.* Mar 21 2005;201(6):881-890.

84. Marquis JF, LaCourse R, Ryan L, North RJ, Gros P. Disseminated and rapidly fatal tuberculosis in mice bearing a defective allele at IFN regulatory factor 8. *J Immunol.* Mar 1 2009;182(5):3008-3015.

85. Dejager L, Libert C, Montagutelli X. Thirty years of Mus spretus: a promising future. *Trends Genet.* May 2009;25(5):234-241.

86. Turcotte K, Loredo-Osti JC, Fortin P, Schurr E, Morgan K, Gros P. Complex genetic control of susceptibility to Mycobacterium bovis (Bacille Calmette-Guerin) infection in wild-derived Mus spretus mice. *Genes Immun.* Dec 2006;7(8):684-687.

87. Pelletier M, Forget A, Bourassa D, Gros P, Skamene E. Immunopathology of BCG infection in genetically resistant and susceptible mouse strains. *J Immunol.* Nov 1982;129(5):2179-2185.

88. Ladel CH, Hess J, Daugelat S, Mombaerts P, Tonegawa S, Kaufmann SH. Contribution of alpha/beta and gamma/delta T lymphocytes to immunity against Mycobacterium bovis bacillus Calmette Guerin: studies with T cell receptor-deficient mutant mice. *Eur J Immunol.* Mar 1995;25(3):838-846.

89. Fitch FW, McKisic MD, Lancki DW, Gajewski TF. Differential regulation of murine T lymphocyte subsets. *Annu Rev Immunol.* 1993;11:29-48.

90. Mombaerts P, Clarke AR, Rudnicki MA, et al. Mutations in T-cell antigen receptor genes alpha and beta block thymocyte development at different stages. *Nature.* Nov 19 1992;360(6401):225-231.

91. Janeway CA, Jr. The T cell receptor as a multicomponent signalling machine: CD4/CD8 coreceptors and CD45 in T cell activation. *Annu Rev Immunol.* 1992;10:645-674.

92. Ladel CH, Daugelat S, Kaufmann SH. Immune response to Mycobacterium bovis bacille Calmette Guerin infection in major histocompatibility complex class I- and II-deficient knock-out mice: contribution of CD4 and CD8 T cells to acquired resistance. *Eur J Immunol.* Feb 1995;25(2):377-384.

93. Bank I, DePinho RA, Brenner MB, Cassimeris J, Alt FW, Chess L. A functional T3 molecule associated with a novel heterodimer on the surface of immature human thymocytes. *Nature.* Jul 10-16 1986;322(6075):179-181.

94. Brenner MB, McLean J, Dialynas DP, et al. Identification of a putative second T-cell receptor. *Nature.* Jul 10-16 1986;322(6075):145-149.

95. Lanier LL, Federspiel NA, Ruitenberg JJ, et al. The T cell antigen receptor complex expressed on normal peripheral blood CD4-, CD8- T lymphocytes. A CD3-associated disulfide-linked gamma chain heterodimer. *J Exp Med.* Apr 1 1987;165(4):1076-1094.

96. Seder RA, Paul WE. Acquisition of lymphokine-producing phenotype by CD4+ T cells. *Annu Rev Immunol.* 1994;12:635-673.

97. Erb KJ, Kirman J, Delahunt B, Chen W, Le Gros G. IL-4, IL-5 and IL-10 are not required for the control of M. bovis-BCG infection in mice. *Immunol Cell Biol.* Feb 1998;76(1):41-46.

98. Kaufmann SH. Immunity to intracellular bacteria. *Annu Rev Immunol.* 1993;11:129-163.

99. Lazarevic V, Flynn J. CD8+ T cells in tuberculosis. *Am J Respir Crit Care Med.* Oct 15 2002;166(8):1116-1121.

100. Dalton DK, Pitts-Meek S, Keshav S, Figari IS, Bradley A, Stewart TA. Multiple defects of immune cell function in mice with disrupted interferon-gamma genes. *Science.* Mar 19 1993;259(5102):1739-1742.

101. Kamijo R, Le J, Shapiro D, et al. Mice that lack the interferon-gamma receptor have profoundly altered responses to infection with Bacillus Calmette-Guerin and subsequent challenge with lipopolysaccharide. *J Exp Med.* Oct 1 1993;178(4):1435-1440.

102. Jacobs M, Marino MW, Brown N, et al. Correction of defective host response to Mycobacterium bovis BCG infection in TNF-deficient mice by bone marrow transplantation. *Lab Invest.* Jun 2000;80(6):901-914.

103. Hsieh CS, Macatonia SE, Tripp CS, Wolf SF, O'Garra A, Murphy KM. Development of TH1 CD4+ T cells through IL-12 produced by Listeria-induced macrophages. *Science.* Apr 23 1993;260(5107):547-549.

104. Kobayashi M, Fitz L, Ryan M, et al. Identification and purification of natural killer cell stimulatory factor (NKSF), a cytokine with multiple biologic effects on human lymphocytes. *J Exp Med.* Sep 1 1989;170(3):827-845.

105. Oppmann B, Lesley R, Blom B, et al. Novel p19 protein engages IL-12p40 to form a cytokine, IL-23, with biological activities similar as well as distinct from IL-12. *Immunity.* Nov 2000;13(5):715-725.

106. Chackerian AA, Chen SJ, Brodie SJ, et al. Neutralization or absence of the interleukin-23 pathway does not compromise immunity to mycobacterial infection. *Infect Immun.* Nov 2006;74(11):6092-6099.

107. Holscher C, Atkinson RA, Arendse B, et al. A protective and agonistic function of IL-12p40 in mycobacterial infection. *J Immunol.* Dec 15 2001;167(12):6957-6966.

108. Wakeham J, Wang J, Magram J, et al. Lack of both types 1 and 2 cytokines, tissue inflammatory responses, and immune protection during pulmonary infection by Mycobacterium bovis bacille Calmette-Guerin in IL-12-deficient mice. *J Immunol.* Jun 15 1998;160(12):6101-6111.

109. Brosch R, Gordon SV, Marmiesse M, et al. A new evolutionary scenario for the Mycobacterium tuberculosis complex. *Proc Natl Acad Sci U S A.* Mar 19 2002;99(6):3684-3689.

110. Tsukamura M, Mizuno S, Toyama H. Taxonomic studies on the Mycobacterium tuberculosis series. *Microbiol Immunol.* 1985;29(4):285-299.

111. van Soolingen D, Hoogenboezem T, de Haas PE, et al. A novel pathogenic taxon of the Mycobacterium tuberculosis complex, Canetti: characterization of an exceptional isolate from Africa. *Int J Syst Bacteriol.* Oct 1997;47(4):1236-1245.

112. Brosch R, Gordon SV, Pym A, Eiglmeier K, Garnier T, Cole ST. Comparative genomics of the mycobacteria. *Int J Med Microbiol.* May 2000;290(2):143-152.

113. Mostowy S, Cousins D, Brinkman J, Aranaz A, Behr MA. Genomic deletions suggest a phylogeny for the Mycobacterium tuberculosis complex. *J Infect Dis.* Jul 1 2002;186(1):74-80.

114. Mostowy S, Behr MA. The origin and evolution of Mycobacterium tuberculosis. *Clin Chest Med.* Jun 2005;26(2):207-216, v-vi.

115. Gagneux S, DeRiemer K, Van T, et al. Variable host-pathogen compatibility in Mycobacterium tuberculosis. *Proc Natl Acad Sci U S A.* Feb 21 2006;103(8):2869-2873.

116. Anh DD, Borgdorff MW, Van LN, et al. Mycobacterium tuberculosis Beijing genotype emerging in Vietnam. *Emerg Infect Dis.* May-Jun 2000;6(3):302-305.

117. Chan MY, Borgdorff M, Yip CW, et al. Seventy percent of the Mycobacterium tuberculosis isolates in Hong Kong represent the Beijing genotype. *Epidemiol Infect.* Aug 2001;127(1):169-171.

118. Prodinger WM, Bunyaratvej P, Prachaktam R, Pavlic M. Mycobacterium tuberculosis isolates of Beijing genotype in Thailand. *Emerg Infect Dis.* May-Jun 2001;7(3):483-484.

119. van Crevel R, Nelwan RH, de Lenne W, et al. Mycobacterium tuberculosis Beijing genotype strains associated with febrile response to treatment. *Emerg Infect Dis.* Sep-Oct 2001;7(5):880-883.

120. Drobniewski F, Balabanova Y, Nikolayevsky V, et al. Drug-resistant tuberculosis, clinical virulence, and the dominance of the Beijing strain family in Russia. *JAMA.* Jun 8 2005;293(22):2726-2731.

121. Toungoussova OS, Mariandyshev A, Bjune G, Sandven P, Caugant DA. Molecular epidemiology and drug resistance of Mycobacterium tuberculosis isolates in the Archangel prison in Russia: predominance of the W-Beijing clone family. *Clin Infect Dis.* Sep 1 2003;37(5):665-672.

122. Thwaites G, Caws M, Chau TT, et al. Relationship between Mycobacterium tuberculosis genotype and the clinical phenotype of pulmonary and meningeal tuberculosis. *J Clin Microbiol.* Apr 2008;46(4):1363-1368.

123. Buu TN, Huyen MN, Lan NT, et al. The Beijing genotype is associated with young age and multidrug-resistant tuberculosis in rural Vietnam. *Int J Tuberc Lung Dis.* Jul 2009;13(7):900-906.

124. Glynn JR, Whiteley J, Bifani PJ, Kremer K, van Soolingen D. Worldwide occurrence of Beijing/W strains of Mycobacterium tuberculosis: a systematic review. *Emerg Infect Dis.* Aug 2002;8(8):843-849.

125. Mostowy S, Onipede A, Gagneux S, et al. Genomic analysis distinguishes Mycobacterium africanum. *J Clin Microbiol.* Aug 2004;42(8):3594-3599.

126. Hershberg R, Lipatov M, Small PM, et al. High functional diversity in Mycobacterium tuberculosis driven by genetic drift and human demography. *PLoS Biol.* Dec 16 2008;6(12):e311.

127. Sreevatsan S, Pan X, Stockbauer KE, et al. Restricted structural gene polymorphism in the Mycobacterium tuberculosis complex indicates evolutionarily recent global dissemination. *Proc Natl Acad Sci U S A.* Sep 2 1997;94(18):9869-9874.

128. Brosch R, Philipp WJ, Stavropoulos E, Colston MJ, Cole ST, Gordon SV. Genomic analysis reveals variation between Mycobacterium tuberculosis H37Rv and the attenuated M. tuberculosis H37Ra strain. *Infect Immun.* Nov 1999;67(11):5768-5774.

129. McMurray DN. Disease model: pulmonary tuberculosis. *Trends Mol Med.* Mar 2001;7(3):135-137.

130. North RJ. Mycobacterium tuberculosis is strikingly more virulent for mice when given via the respiratory than via the intravenous route. *J Infect Dis.* Dec 1995;172(6):1550-1553.

131. Algood HM, Chan J, Flynn JL. Chemokines and tuberculosis. *Cytokine Growth Factor Rev.* Dec 2003;14(6):467-477.

132. Hickman SP, Chan J, Salgame P. Mycobacterium tuberculosis induces differential cytokine production from dendritic cells and macrophages with divergent effects on naive T cell polarization. *J Immunol.* May 1 2002;168(9):4636-4642.

133. Barry CE, 3rd, Boshoff HI, Dartois V, et al. The spectrum of latent tuberculosis: rethinking the biology and intervention strategies. *Nat Rev Microbiol.* Dec 2009;7(12):845-855.

134. Gan H, Lee J, Ren F, Chen M, Kornfeld H, Remold HG. Mycobacterium tuberculosis blocks crosslinking of annexin-1 and apoptotic envelope formation on infected macrophages to maintain virulence. *Nat Immunol.* Oct 2008;9(10):1189-1197.

135. Chen M, Divangahi M, Gan H, et al. Lipid mediators in innate immunity against tuberculosis: opposing roles of PGE2 and LXA4 in the induction of macrophage death. *J Exp Med.* Nov 24 2008;205(12):2791-2801.

136. Bafica A, Scanga CA, Serhan C, et al. Host control of Mycobacterium tuberculosis is regulated by 5-lipoxygenase-dependent lipoxin production. *J Clin Invest.* Jun 2005;115(6):1601-1606.

137. Divangahi M, Desjardins D, Nunes-Alves C, Remold HG, Behar SM. Eicosanoid pathways regulate adaptive immunity to Mycobacterium tuberculosis. *Nat Immunol.* Aug 2010;11(8):751-758.

138. Divangahi M, Chen M, Gan H, et al. Mycobacterium tuberculosis evades macrophage defenses by inhibiting plasma membrane repair. *Nat Immunol.* Aug 2009;10(8):899-906.

139. Levine B, Deretic V. Unveiling the roles of autophagy in innate and adaptive immunity. *Nat Rev Immunol.* Oct 2007;7(10):767-777.

140. Schmid D, Munz C. Innate and adaptive immunity through autophagy. *Immunity.* Jul 2007;27(1):11-21.

141. Schmid D, Munz C. Immune surveillance via self digestion. *Autophagy.* Mar-Apr 2007;3(2):133-135.

142. van der Wel N, Hava D, Houben D, et al. M. tuberculosis and M. leprae translocate from the phagolysosome to the cytosol in myeloid cells. *Cell.* Jun 29 2007;129(7):1287-1298.

143. Flannagan RS, Cosio G, Grinstein S. Antimicrobial mechanisms of phagocytes and bacterial evasion strategies. *Nat Rev Microbiol.* May 2009;7(5):355-366.

144. Gutierrez MG, Master SS, Singh SB, Taylor GA, Colombo MI, Deretic V. Autophagy is a defense mechanism inhibiting BCG and Mycobacterium tuberculosis survival in infected macrophages. *Cell.* Dec 17 2004;119(6):753-766.

145. Tiwari S, Choi HP, Matsuzawa T, Pypaert M, MacMicking JD. Targeting of the GTPase Irgm1 to the phagosomal membrane via PtdIns(3,4)P(2) and PtdIns(3,4,5)P(3) promotes immunity to mycobacteria. *Nat Immunol.* Aug 2009;10(8):907-917.

146. Xu Y, Jagannath C, Liu XD, Sharafkhaneh A, Kolodziejska KE, Eissa NT. Toll-like receptor 4 is a sensor for autophagy associated with innate immunity. *Immunity.* Jul 2007;27(1):135-144.

147. Harris J, De Haro SA, Master SS, et al. T helper 2 cytokines inhibit autophagic control of intracellular Mycobacterium tuberculosis. *Immunity.* Sep 2007;27(3):505-517.

148. Long ER, Vogt AB. Relation of sex to the course of experimental tuberculosis in mice. *Amer Rev Tuberc.* 1941;44:196.

149. Gray DF, Graham-Smith H, Noble JL. Variations in natural resistance to tuberculosis. *J Hyg (Lond).* Jun 1960;58:215-227.

150. Gray DF, Mattinson MW. Detection of small numbers of tubercle bacilli from dispersed cultures, using mice, guinea pigs, and artificial media. *Am Rev Tuberc.* May 1952;65(5):572-588.

151. Grumbach F. Contribution à l' étude du terrain dans la tuberculose expérimentale: influence de la constitution héréditaire et de l'âge des souris. *Proc Intern Congr Microbiol 6tk Rome.* 1953;4:331.

152. Pierce C, Dubos RJ, Middlebrook G. Infection of Mice with Mammalian Tubercle Bacilli Grown in Tween-Albumin Liquid Medium. *J Exp Med.* Jul 31 1947;86(2):159-174.

153. Lynch CJ, Pierce-Chase CH, Dubos R. A Genetic Study of Susceptibility to Experimental Tuberculosis in Mice Infected with Mammalian Tubercle Bacilli. *J Exp Med.* Jun 1 1965;121:1051-1070.

154. Chackerian AA, Behar SM. Susceptibility to Mycobacterium tuberculosis: lessons from inbred strains of mice. *Tuberculosis (Edinb).* 2003;83(5):279-285.

155. Actor JK, Olsen M, Jagannath C, Hunter RL. Relationship of survival, organism containment, and granuloma formation in acute murine tuberculosis. *J Interferon Cytokine Res.* Oct 1999;19(10):1183-1193.

156. Medina E, North RJ. Resistance ranking of some common inbred mouse strains to Mycobacterium tuberculosis and relationship to major histocompatibility complex haplotype and Nramp1 genotype. *Immunology.* Feb 1998;93(2):270-274.

157. Nikonenko BV, Averbakh MM, Jr., Lavebratt C, Schurr E, Apt AS. Comparative analysis of mycobacterial infections in susceptible I/St and resistant A/Sn inbred mice. *Tuber Lung Dis.* 2000;80(1):15-25.

158. Jagannath C, Hoffmann H, Sepulveda E, Actor JK, Wetsel RA, Hunter RL. Hypersusceptibility of A/J mice to tuberculosis is in part due to a deficiency of the fifth complement component (C5). *Scand J Immunol.* Oct 2000;52(4):369-379.

159. Mitsos LM, Cardon LR, Ryan L, LaCourse R, North RJ, Gros P. Susceptibility to tuberculosis: a locus on mouse chromosome 19 (Trl-4) regulates Mycobacterium tuberculosis replication in the lungs. *Proc Natl Acad Sci U S A.* May 27 2003;100(11):6610-6615.

160. Turner J, Gonzalez-Juarrero M, Saunders BM, et al. Immunological basis for reactivation of tuberculosis in mice. *Infect Immun.* May 2001;69(5):3264-3270.

161. Chackerian AA, Perera TV, Behar SM. Gamma interferon-producing CD4+ T lymphocytes in the lung correlate with resistance to infection with Mycobacterium tuberculosis. *Infect Immun.* Apr 2001;69(4):2666-2674.

162. Medina E, North RJ. Genetically susceptible mice remain proportionally more susceptible to tuberculosis after vaccination. *Immunology.* Jan 1999;96(1):16-21.

163. Orme IM. The immunopathogenesis of tuberculosis: a new working hypothesis. *Trends Microbiol.* Mar 1998;6(3):94-97.

164. Watson VE, Hill LL, Owen-Schaub LB, et al. Apoptosis in mycobacterium tuberculosis infection in mice exhibiting varied immunopathology. *J Pathol.* Feb 2000;190(2):211-220.

165. Lavebratt C, Apt AS, Nikonenko BV, Schalling M, Schurr E. Severity of tuberculosis in mice is linked to distal chromosome 3 and proximal chromosome 9. *J Infect Dis.* Jul 1999;180(1):150-155.

166. Sanchez F, Radaeva TV, Nikonenko BV, et al. Multigenic control of disease severity after virulent Mycobacterium tuberculosis infection in mice. *Infect Immun.* Jan 2003;71(1):126-131.

167. Kahler AK, Persson AS, Sanchez F, et al. A new coding mutation in the Tnf-alpha leader sequence in tuberculosis-sensitive I/St mice causes

higher secretion levels of soluble TNF-alpha. *Genes Immun.* Oct 2005;6(7):620-627.

168. Kramnik I, Demant P, Bloom BB. Susceptibility to tuberculosis as a complex genetic trait: analysis using recombinant congenic strains of mice. *Novartis Found Symp.* 1998;217:120-131; discussion 132-127.

169. Pan H, Yan BS, Rojas M, et al. Ipr1 gene mediates innate immunity to tuberculosis. *Nature.* Apr 7 2005;434(7034):767-772.

170. Kramnik I, Dietrich WF, Demant P, Bloom BR. Genetic control of resistance to experimental infection with virulent Mycobacterium tuberculosis. *Proc Natl Acad Sci U S A.* Jul 18 2000;97(15):8560-8565.

171. Yan BS, Kirby A, Shebzukhov YV, Daly MJ, Kramnik I. Genetic architecture of tuberculosis resistance in a mouse model of infection. *Genes Immun.* Apr 2006;7(3):201-210.

172. Sissons J, Yan BS, Pichugin AV, Kirby A, Daly MJ, Kramnik I. Multigenic control of tuberculosis resistance: analysis of a QTL on mouse chromosome 7 and its synergism with sst1. *Genes Immun.* Jan 2009;10(1):37-46.

173. Mitsos LM, Cardon LR, Fortin A, et al. Genetic control of susceptibility to infection with Mycobacterium tuberculosis in mice. *Genes Immun.* Dec 2000;1(8):467-477.

174. Marquis JF, Lacourse R, Ryan L, North RJ, Gros P. Genetic and functional characterization of the mouse Trl3 locus in defense against tuberculosis. *J Immunol.* Mar 15 2009;182(6):3757-3767.

175. Gonzalez-Juarrero M, Turner OC, Turner J, Marietta P, Brooks JV, Orme IM. Temporal and spatial arrangement of lymphocytes within lung granulomas induced by aerosol infection with Mycobacterium tuberculosis. *Infect Immun.* Mar 2001;69(3):1722-1728.

176. Bosio CM, Gardner D, Elkins KL. Infection of B cell-deficient mice with CDC 1551, a clinical isolate of Mycobacterium tuberculosis: delay in dissemination and development of lung pathology. *J Immunol.* Jun 15 2000;164(12):6417-6425.

177. Johnson CM, Cooper AM, Frank AA, Bonorino CB, Wysoki LJ, Orme IM. Mycobacterium tuberculosis aerogenic rechallenge infections in B cell-deficient mice. *Tuber Lung Dis.* 1997;78(5-6):257-261.

178. Maglione PJ, Xu J, Chan J. B cells moderate inflammatory progression and enhance bacterial containment upon pulmonary challenge with Mycobacterium tuberculosis. *J Immunol.* Jun 1 2007;178(11):7222-7234.

179. Vordermeier HM, Venkataprasad N, Harris DP, Ivanyi J. Increase of tuberculous infection in the organs of B cell-deficient mice. *Clin Exp Immunol.* Nov 1996;106(2):312-316.

180. Kondratieva TK, Rubakova EI, Linge IA, Evstifeev VV, Majorov KB, Apt AS. B cells delay neutrophil migration toward the site of stimulus: tardiness critical for effective bacillus Calmette-Guerin vaccination against tuberculosis infection in mice. *J Immunol.* Feb 1 2010;184(3):1227-1234.

181. Caruso AM, Serbina N, Klein E, Triebold K, Bloom BR, Flynn JL. Mice deficient in CD4 T cells have only transiently diminished levels of IFN-gamma, yet succumb to tuberculosis. *J Immunol.* May 1 1999;162(9):5407-5416.

182. Mogues T, Goodrich ME, Ryan L, LaCourse R, North RJ. The relative importance of T cell subsets in immunity and immunopathology of airborne Mycobacterium tuberculosis infection in mice. *J Exp Med.* Feb 5 2001;193(3):271-280.

183. Flynn JL, Goldstein MM, Triebold KJ, Koller B, Bloom BR. Major histocompatibility complex class I-restricted T cells are required for resistance to Mycobacterium tuberculosis infection. *Proc Natl Acad Sci U S A.* Dec 15 1992;89(24):12013-12017.

184. Sousa AO, Mazzaccaro RJ, Russell RG, et al. Relative contributions of distinct MHC class I-dependent cell populations in protection to tuberculosis infection in mice. *Proc Natl Acad Sci U S A.* Apr 11 2000;97(8):4204-4208.

185. Schaible UE, Collins HL, Priem F, Kaufmann SH. Correction of the iron overload defect in beta-2-microglobulin knockout mice by lactoferrin abolishes their increased susceptibility to tuberculosis. *J Exp Med.* Dec 2 2002;196(11):1507-1513.

186. Ladel CH, Blum C, Dreher A, Reifenberg K, Kaufmann SH. Protective role of gamma/delta T cells and alpha/beta T cells in tuberculosis. *Eur J Immunol.* Oct 1995;25(10):2877-2881.

187. D'Souza CD, Cooper AM, Frank AA, Mazzaccaro RJ, Bloom BR, Orme IM. An anti-inflammatory role for gamma delta T lymphocytes in acquired immunity to Mycobacterium tuberculosis. *J Immunol.* Feb 1 1997;158(3):1217-1221.

188. Flynn JL, Chan J, Triebold KJ, Dalton DK, Stewart TA, Bloom BR. An essential role for interferon gamma in resistance to Mycobacterium tuberculosis infection. *J Exp Med.* Dec 1 1993;178(6):2249-2254.

189. MacMicking JD, Taylor GA, McKinney JD. Immune control of tuberculosis by IFN-gamma-inducible LRG-47. *Science.* Oct 24 2003;302(5645):654-659.

190. Cooper AM, Kipnis A, Turner J, Magram J, Ferrante J, Orme IM. Mice lacking bioactive IL-12 can generate protective, antigen-specific cellular responses to mycobacterial infection only if the IL-12 p40 subunit is present. *J Immunol.* Feb 1 2002;168(3):1322-1327.

191. Cooper AM, Magram J, Ferrante J, Orme IM. Interleukin 12 (IL-12) is crucial to the development of protective immunity in mice intravenously infected with mycobacterium tuberculosis. *J Exp Med.* Jul 7 1997;186(1):39-45.

192. Khader SA, Partida-Sanchez S, Bell G, et al. Interleukin 12p40 is required for dendritic cell migration and T cell priming after Mycobacterium tuberculosis infection. *J Exp Med.* Jul 10 2006;203(7):1805-1815.

193. Khader SA, Pearl JE, Sakamoto K, et al. IL-23 compensates for the absence of IL-12p70 and is essential for the IL-17 response during tuberculosis but is dispensable for protection and antigen-specific IFN-gamma responses if IL-12p70 is available. *J Immunol.* Jul 15 2005;175(2):788-795.

194. Kaplan MH, Grusby MJ. Regulation of T helper cell differentiation by STAT molecules. *J Leukoc Biol.* Jul 1998;64(1):2-5.

195. Szabo SJ, Glimcher LH, Ho IC. Genes that regulate interleukin-4 expression in T cells. *Curr Opin Immunol.* Dec 1997;9(6):776-781.

196. Orme IM, Roberts AD, Griffin JP, Abrams JS. Cytokine secretion by CD4 T lymphocytes acquired in response to Mycobacterium tuberculosis infection. *J Immunol.* Jul 1 1993;151(1):518-525.

197. Hernandez-Pando R, Orozcoe H, Sampieri A, et al. Correlation between the kinetics of Th1, Th2 cells and pathology in a murine model of experimental pulmonary tuberculosis. *Immunology.* Sep 1996;89(1):26-33.

198. North RJ. Mice incapable of making IL-4 or IL-10 display normal resistance to infection with Mycobacterium tuberculosis. *Clin Exp Immunol.* Jul 1998;113(1):55-58.

199. Saunders BM, Frank AA, Orme IM, Cooper AM. Interleukin-6 induces early gamma interferon production in the infected lung but is not required for generation of specific immunity to Mycobacterium tuberculosis infection. *Infect Immun.* Jun 2000;68(6):3322-3326.

200. Jung YJ, LaCourse R, Ryan L, North RJ. Evidence inconsistent with a negative influence of T helper 2 cells on protection afforded by a dominant T helper 1 response against Mycobacterium tuberculosis lung infection in mice. *Infect Immun.* Nov 2002;70(11):6436-6443.

201. Buccheri S, Reljic R, Caccamo N, et al. IL-4 depletion enhances host resistance and passive IgA protection against tuberculosis infection in BALB/c mice. *Eur J Immunol.* Mar 2007;37(3):729-737.

202. Hernandez-Pando R, Aguilar D, Hernandez ML, Orozco H, Rook G. Pulmonary tuberculosis in BALB/c mice with non-functional IL-4 genes: changes in the inflammatory effects of TNF-alpha and in the regulation of fibrosis. *Eur J Immunol.* Jan 2004;34(1):174-183.

203. Bean AG, Roach DR, Briscoe H, et al. Structural deficiencies in granuloma formation in TNF gene-targeted mice underlie the heightened susceptibility to aerosol Mycobacterium tuberculosis infection, which is not compensated for by lymphotoxin. *J Immunol.* Mar 15 1999;162(6):3504-3511.

204. Flynn JL, Goldstein MM, Chan J, et al. Tumor necrosis factor-alpha is required in the protective immune response against Mycobacterium tuberculosis in mice. *Immunity.* Jun 1995;2(6):561-572.

205. Smith S, Liggitt D, Jeromsky E, Tan X, Skerrett SJ, Wilson CB. Local role for tumor necrosis factor alpha in the pulmonary inflammatory response to Mycobacterium tuberculosis infection. *Infect Immun.* Apr 2002;70(4):2082-2089.

206. Ding AH, Nathan CF, Stuehr DJ. Release of reactive nitrogen intermediates and reactive oxygen intermediates from mouse peritoneal macrophages. Comparison of activating cytokines and evidence for independent production. *J Immunol.* Oct 1 1988;141(7):2407-2412.

207. Flesch IE, Kaufmann SH. Activation of tuberculostatic macrophage functions by gamma interferon, interleukin-4, and tumor necrosis factor. *Infect Immun.* Aug 1990;58(8):2675-2677.

208. Liew FY, Li Y, Millott S. Tumor necrosis factor-alpha synergizes with IFN-gamma in mediating killing of Leishmania major through the induction of nitric oxide. *J Immunol.* Dec 15 1990;145(12):4306-4310.

209. Roach DR, Bean AG, Demangel C, France MP, Briscoe H, Britton WJ. TNF regulates chemokine induction essential for cell recruitment, granuloma formation, and clearance of mycobacterial infection. *J Immunol.* May 1 2002;168(9):4620-4627.

210. Murdoch C, Finn A. Chemokine receptors and their role in inflammation and infectious diseases. *Blood.* May 15 2000;95(10):3032-3043.

211. Cyster JG. Chemokines, sphingosine-1-phosphate, and cell migration in secondary lymphoid organs. *Annu Rev Immunol.* 2005;23:127-159.

212. Allavena P, Sica A, Vecchi A, Locati M, Sozzani S, Mantovani A. The chemokine receptor switch paradigm and dendritic cell migration: its significance in tumor tissues. *Immunol Rev.* Oct 2000;177:141-149.

213. Sallusto F, Mackay CR, Lanzavecchia A. The role of chemokine receptors in primary, effector, and memory immune responses. *Annu Rev Immunol.* 2000;18:593-620.

214. Boring L, Gosling J, Chensue SW, et al. Impaired monocyte migration and reduced type 1 (Th1) cytokine responses in C-C chemokine receptor 2 knockout mice. *J Clin Invest.* Nov 15 1997;100(10):2552-2561.

215. Kurth I, Willimann K, Schaerli P, Hunziker T, Clark-Lewis I, Moser B. Monocyte selectivity and tissue localization suggests a role for breast and kidney-expressed chemokine (BRAK) in macrophage development. *J Exp Med.* Sep 17 2001;194(6):855-861.

216. Gunn MD, Kyuwa S, Tam C, et al. Mice lacking expression of secondary lymphoid organ chemokine have defects in lymphocyte homing and dendritic cell localization. *J Exp Med.* Feb 1 1999;189(3):451-460.

217. Gunn MD, Tangemann K, Tam C, Cyster JG, Rosen SD, Williams LT. A chemokine expressed in lymphoid high endothelial venules promotes the adhesion and chemotaxis of naive T lymphocytes. *Proc Natl Acad Sci U S A.* Jan 6 1998;95(1):258-263.

218. Saeki H, Moore AM, Brown MJ, Hwang ST. Cutting edge: secondary lymphoid-tissue chemokine (SLC) and CC chemokine receptor 7 (CCR7) participate in the emigration pathway of mature dendritic cells from the skin to regional lymph nodes. *J Immunol.* Mar 1 1999;162(5):2472-2475.

219. Kahnert A, Hopken UE, Stein M, Bandermann S, Lipp M, Kaufmann SH. Mycobacterium tuberculosis triggers formation of lymphoid structure in murine lungs. *J Infect Dis.* Jan 1 2007;195(1):46-54.

220. Olmos S, Stukes S, Ernst JD. Ectopic activation of Mycobacterium tuberculosis-specific CD4+ T cells in lungs of CCR7-/- mice. *J Immunol.* Jan 15 2010;184(2):895-901.

221. Khader SA, Rangel-Moreno J, Fountain JJ, et al. In a murine tuberculosis model, the absence of homeostatic chemokines delays granuloma

formation and protective immunity. *J Immunol.* Dec 15 2009;183(12):8004-8014.

222. Legler DF, Loetscher M, Roos RS, Clark-Lewis I, Baggiolini M, Moser B. B cell-attracting chemokine 1, a human CXC chemokine expressed in lymphoid tissues, selectively attracts B lymphocytes via BLR1/CXCR5. *J Exp Med.* Feb 16 1998;187(4):655-660.

223. Ansel KM, Harris RB, Cyster JG. CXCL13 is required for B1 cell homing, natural antibody production, and body cavity immunity. *Immunity.* Jan 2002;16(1):67-76.

224. Ebisuno Y, Tanaka T, Kanemitsu N, et al. Cutting edge: the B cell chemokine CXC chemokine ligand 13/B lymphocyte chemoattractant is expressed in the high endothelial venules of lymph nodes and Peyer's patches and affects B cell trafficking across high endothelial venules. *J Immunol.* Aug 15 2003;171(4):1642-1646.

225. Ansel KM, Ngo VN, Hyman PL, et al. A chemokine-driven positive feedback loop organizes lymphoid follicles. *Nature.* Jul 20 2000;406(6793):309-314.

226. Peters W, Scott HM, Chambers HF, Flynn JL, Charo IF, Ernst JD. Chemokine receptor 2 serves an early and essential role in resistance to Mycobacterium tuberculosis. *Proc Natl Acad Sci U S A.* Jul 3 2001;98(14):7958-7963.

227. Rhoades ER, Cooper AM, Orme IM. Chemokine response in mice infected with Mycobacterium tuberculosis. *Infect Immun.* Oct 1995;63(10):3871-3877.

228. Scott HM, Flynn JL. Mycobacterium tuberculosis in chemokine receptor 2-deficient mice: influence of dose on disease progression. *Infect Immun.* Nov 2002;70(11):5946-5954.

229. Matsukawa A, Lukacs NW, Hogaboam CM, Chensue SW, Kunkel SL. III. Chemokines and other mediators, 8. Chemokines and their receptors in cell-mediated immune responses in the lung. *Microsc Res Tech.* May 15 2001;53(4):298-306.

230. Saunders BM, Britton WJ. Life and death in the granuloma: immunopathology of tuberculosis. *Immunol Cell Biol.* Feb-Mar 2007;85(2):103-111.

231. Fraziano M, Cappelli G, Santucci M, et al. Expression of CCR5 is increased in human monocyte-derived macrophages and alveolar macrophages in the course of in vivo and in vitro Mycobacterium

tuberculosis infection. *AIDS Res Hum Retroviruses.* Jul 1 1999;15(10):869-874.

232. Mack M, Cihak J, Simonis C, et al. Expression and characterization of the chemokine receptors CCR2 and CCR5 in mice. *J Immunol.* Apr 1 2001;166(7):4697-4704.

233. Badewa AP, Quinton LJ, Shellito JE, Mason CM. Chemokine receptor 5 and its ligands in the immune response to murine tuberculosis. *Tuberculosis (Edinb).* May 2005;85(3):185-195.

234. Algood HM, Flynn JL. CCR5-deficient mice control Mycobacterium tuberculosis infection despite increased pulmonary lymphocytic infiltration. *J Immunol.* Sep 1 2004;173(5):3287-3296.

235. Vesosky B, Rottinghaus EK, Stromberg P, Turner J, Beamer G. CCL5 participates in early protection against Mycobacterium tuberculosis. *J Leukoc Biol.* Apr 6 2010.

236. Rot A, von Andrian UH. Chemokines in innate and adaptive host defense: basic chemokinese grammar for immune cells. *Annu Rev Immunol.* 2004;22:891-928.

237. Charo IF, Myers SJ, Herman A, Franci C, Connolly AJ, Coughlin SR. Molecular cloning and functional expression of two monocyte chemoattractant protein 1 receptors reveals alternative splicing of the carboxyl-terminal tails. *Proc Natl Acad Sci U S A.* Mar 29 1994;91(7):2752-2756.

238. Combadiere C, Ahuja SK, Van Damme J, Tiffany HL, Gao JL, Murphy PM. Monocyte chemoattractant protein-3 is a functional ligand for CC chemokine receptors 1 and 2B. *J Biol Chem.* Dec 15 1995;270(50):29671-29675.

239. Franci C, Wong LM, Van Damme J, Proost P, Charo IF. Monocyte chemoattractant protein-3, but not monocyte chemoattractant protein-2, is a functional ligand of the human monocyte chemoattractant protein-1 receptor. *J Immunol.* Jun 15 1995;154(12):6511-6517.

240. Gong X, Gong W, Kuhns DB, Ben-Baruch A, Howard OM, Wang JM. Monocyte chemotactic protein-2 (MCP-2) uses CCR1 and CCR2B as its functional receptors. *J Biol Chem.* May 2 1997;272(18):11682-11685.

241. Sarafi MN, Garcia-Zepeda EA, MacLean JA, Charo IF, Luster AD. Murine monocyte chemoattractant protein (MCP)-5: a novel CC chemokine that is a structural and functional homologue of human MCP-1. *J Exp Med.* Jan 6 1997;185(1):99-109.

242. Garcia-Zepeda EA, Combadiere C, Rothenberg ME, et al. Human monocyte chemoattractant protein (MCP)-4 is a novel CC chemokine with activities on monocytes, eosinophils, and basophils induced in allergic and nonallergic inflammation that signals through the CC chemokine receptors (CCR)-2 and -3. *J Immunol.* Dec 15 1996;157(12):5613-5626.

243. Stellato C, Collins P, Ponath PD, et al. Production of the novel C-C chemokine MCP-4 by airway cells and comparison of its biological activity to other C-C chemokines. *J Clin Invest.* Mar 1 1997;99(5):926-936.

244. Carr MW, Roth SJ, Luther E, Rose SS, Springer TA. Monocyte chemoattractant protein 1 acts as a T-lymphocyte chemoattractant. *Proc Natl Acad Sci U S A.* Apr 26 1994;91(9):3652-3656.

245. Kurihara T, Warr G, Loy J, Bravo R. Defects in macrophage recruitment and host defense in mice lacking the CCR2 chemokine receptor. *J Exp Med.* Nov 17 1997;186(10):1757-1762.

246. Kuziel WA, Morgan SJ, Dawson TC, et al. Severe reduction in leukocyte adhesion and monocyte extravasation in mice deficient in CC chemokine receptor 2. *Proc Natl Acad Sci U S A.* Oct 28 1997;94(22):12053-12058.

247. Sozzani S, Luini W, Borsatti A, et al. Receptor expression and responsiveness of human dendritic cells to a defined set of CC and CXC chemokines. *J Immunol.* Aug 15 1997;159(4):1993-2000.

248. Rutledge BJ, Rayburn H, Rosenberg R, et al. High level monocyte chemoattractant protein-1 expression in transgenic mice increases their susceptibility to intracellular pathogens. *J Immunol.* Nov 15 1995;155(10):4838-4843.

249. Kipnis A, Basaraba RJ, Orme IM, Cooper AM. Role of chemokine ligand 2 in the protective response to early murine pulmonary tuberculosis. *Immunology.* Aug 2003;109(4):547-551.

250. Lu B, Rutledge BJ, Gu L, et al. Abnormalities in monocyte recruitment and cytokine expression in monocyte chemoattractant protein 1-deficient mice. *J Exp Med.* Feb 16 1998;187(4):601-608.

251. Algood HM, Lin PL, Yankura D, Jones A, Chan J, Flynn JL. TNF influences chemokine expression of macrophages in vitro and that of CD11b+ cells in vivo during Mycobacterium tuberculosis infection. *J Immunol.* Jun 1 2004;172(11):6846-6857.

252. Qin S, Rottman JB, Myers P, et al. The chemokine receptors CXCR3 and CCR5 mark subsets of T cells associated with certain inflammatory reactions. *J Clin Invest.* Feb 15 1998;101(4):746-754.

253. Syrbe U, Siveke J, Hamann A. Th1/Th2 subsets: distinct differences in homing and chemokine receptor expression? *Springer Semin Immunopathol.* 1999;21(3):263-285.

254. Seiler P, Aichele P, Bandermann S, et al. Early granuloma formation after aerosol Mycobacterium tuberculosis infection is regulated by neutrophils via CXCR3-signaling chemokines. *Eur J Immunol.* Oct 2003;33(10):2676-2686.

255. Chakravarty SD, Xu J, Lu B, Gerard C, Flynn J, Chan J. The chemokine receptor CXCR3 attenuates the control of chronic Mycobacterium tuberculosis infection in BALB/c mice. *J Immunol.* Feb 1 2007;178(3):1723-1735.

256. Bazan JF, Bacon KB, Hardiman G, et al. A new class of membrane-bound chemokine with a CX3C motif. *Nature.* Feb 13 1997;385(6617):640-644.

257. Hall JD, Kurtz SL, Rigel NW, et al. The impact of chemokine receptor CX3CR1 deficiency during respiratory infections with Mycobacterium tuberculosis or Francisella tularensis. *Clin Exp Immunol.* May 2009;156(2):278-284.

258. Dormans J, Burger M, Aguilar D, et al. Correlation of virulence, lung pathology, bacterial load and delayed type hypersensitivity responses after infection with different Mycobacterium tuberculosis genotypes in a BALB/c mouse model. *Clin Exp Immunol.* Sep 2004;137(3):460-468.

259. Lopez B, Aguilar D, Orozco H, et al. A marked difference in pathogenesis and immune response induced by different Mycobacterium tuberculosis genotypes. *Clin Exp Immunol.* Jul 2003;133(1):30-37.

260. Manca C, Tsenova L, Barry CE, 3rd, et al. Mycobacterium tuberculosis CDC1551 induces a more vigorous host response in vivo and in vitro, but is not more virulent than other clinical isolates. *J Immunol.* Jun 1 1999;162(11):6740-6746.

261. Manca C, Reed MB, Freeman S, et al. Differential monocyte activation underlies strain-specific Mycobacterium tuberculosis pathogenesis. *Infect Immun.* Sep 2004;72(9):5511-5514.

262. Manca C, Tsenova L, Bergtold A, et al. Virulence of a Mycobacterium tuberculosis clinical isolate in mice is determined by failure to induce Th1 type immunity and is associated with induction of IFN-alpha /beta. *Proc Natl Acad Sci U S A.* May 8 2001;98(10):5752-5757.

263. Manca C, Tsenova L, Freeman S, et al. Hypervirulent M. tuberculosis W/Beijing strains upregulate type I IFNs and increase expression of

negative regulators of the Jak-Stat pathway. *J Interferon Cytokine Res.* Nov 2005;25(11):694-701.

264. Reed MB, Domenech P, Manca C, et al. A glycolipid of hypervirulent tuberculosis strains that inhibits the innate immune response. *Nature.* Sep 2 2004;431(7004):84-87.

265. Constant P, Perez E, Malaga W, et al. Role of the pks15/1 gene in the biosynthesis of phenolglycolipids in the Mycobacterium tuberculosis complex. Evidence that all strains synthesize glycosylated p-hydroxybenzoic methyl esters and that strains devoid of phenolglycolipids harbor a frameshift mutation in the pks15/1 gene. *J Biol Chem.* Oct 11 2002;277(41):38148-38158.

266. Marmiesse M, Brodin P, Buchrieser C, et al. Macro-array and bioinformatic analyses reveal mycobacterial 'core' genes, variation in the ESAT-6 gene family and new phylogenetic markers for the Mycobacterium tuberculosis complex. *Microbiology.* Feb 2004;150(Pt 2):483-496.

267. Rajakumar K, Shafi J, Smith RJ, et al. Use of genome level-informed PCR as a new investigational approach for analysis of outbreak-associated Mycobacterium tuberculosis isolates. *J Clin Microbiol.* May 2004;42(5):1890-1896.

268. Newton SM, Smith RJ, Wilkinson KA, et al. A deletion defining a common Asian lineage of Mycobacterium tuberculosis associates with immune subversion. *Proc Natl Acad Sci U S A.* Oct 17 2006;103(42):15594-15598.

269. Ng VH, Cox JS, Sousa AO, MacMicking JD, McKinney JD. Role of KatG catalase-peroxidase in mycobacterial pathogenesis: countering the phagocyte oxidative burst. *Mol Microbiol.* Jun 2004;52(5):1291-1302.

270. Adams LB, Dinauer MC, Morgenstern DE, Krahenbuhl JL. Comparison of the roles of reactive oxygen and nitrogen intermediates in the host response to Mycobacterium tuberculosis using transgenic mice. *Tuber Lung Dis.* 1997;78(5-6):237-246.

271. Jung YJ, LaCourse R, Ryan L, North RJ. Virulent but not avirulent Mycobacterium tuberculosis can evade the growth inhibitory action of a T helper 1-dependent, nitric oxide Synthase 2-independent defense in mice. *J Exp Med.* Oct 7 2002;196(7):991-998.

272. Darwin KH, Ehrt S, Gutierrez-Ramos JC, Weich N, Nathan CF. The proteasome of Mycobacterium tuberculosis is required for resistance to nitric oxide. *Science.* Dec 12 2003;302(5652):1963-1966.

273. Beisiegel M, Kursar M, Koch M, et al. Combination of host susceptibility and virulence of Mycobacterium tuberculosis determines dual role of nitric oxide in the protection and control of inflammation. *J Infect Dis.* Apr 15 2009;199(8):1222-1232.

274. Reed MB, Pichler VK, McIntosh F, et al. Major Mycobacterium tuberculosis lineages associate with patient country of origin. *J Clin Microbiol.* Apr 2009;47(4):1119-1128.

275. Hirsh AE, Tsolaki AG, DeRiemer K, Feldman MW, Small PM. Stable association between strains of Mycobacterium tuberculosis and their human host populations. *Proc Natl Acad Sci U S A.* Apr 6 2004;101(14):4871-4876.

276. Woolhouse ME, Webster JP, Domingo E, Charlesworth B, Levin BR. Biological and biomedical implications of the co-evolution of pathogens and their hosts. *Nat Genet.* Dec 2002;32(4):569-577.

277. Colditz GA, Brewer TF, Berkey CS, et al. Efficacy of BCG vaccine in the prevention of tuberculosis. Meta-analysis of the published literature. *JAMA.* Mar 2 1994;271(9):698-702.

278. Caws M, Thwaites G, Dunstan S, et al. The influence of host and bacterial genotype on the development of disseminated disease with Mycobacterium tuberculosis. *PLoS Pathog.* Mar 2008;4(3):e1000034.

279. Herb F, Thye T, Niemann S, et al. ALOX5 variants associated with susceptibility to human pulmonary tuberculosis. *Hum Mol Genet.* Apr 1 2008;17(7):1052-1060.

280. Intemann CD, Thye T, Niemann S, et al. Autophagy gene variant IRGM -261T contributes to protection from tuberculosis caused by Mycobacterium tuberculosis but not by M. africanum strains. *PLoS Pathog.* Sep 2009;5(9):e1000577.

281. Greenwood CM, Fujiwara TM, Boothroyd LJ, et al. Linkage of tuberculosis to chromosome 2q35 loci, including NRAMP1, in a large aboriginal Canadian family. *Am J Hum Genet.* Aug 2000;67(2):405-416.

282. Di Pietrantonio T, Schurr E. Mouse models for the genetic study of tuberculosis susceptibility. *Brief Funct Genomic Proteomic.* Nov 2005;4(3):277-292.

283. Zlotnik A, Yoshie O. Chemokines: a new classification system and their role in immunity. *Immunity.* Feb 2000;12(2):121-127.

284. Neel JV, Schull WJ. Human heredity. *Am J Phys Anthropol.* . 1954;12(4):636–638.

285. Denis M, Forget A, Pelletier M, Turcotte R, Skamene E. Control of the Bcg gene of early resistance in mice to infections with BCG substrains and atypical mycobacteria. *Clin Exp Immunol.* Mar 1986;63(3):517-525.

286. Medina E, Rogerson BJ, North RJ. The Nramp1 antimicrobial resistance gene segregates independently of resistance to virulent Mycobacterium tuberculosis. *Immunology.* Aug 1996;88(4):479-481.

287. North RJ, Medina E. Significance of the antimicrobial resistance gene, Nramp1, in resistance to virulent Mycobacterium tuberculosis infection. *Res Immunol.* Oct-Dec 1996;147(8-9):493-499.

288. Musser JM, Amin A, Ramaswamy S. Negligible genetic diversity of mycobacterium tuberculosis host immune system protein targets: evidence of limited selective pressure. *Genetics.* May 2000;155(1):7-16.

289. Bellamy R, Ruwende C, Corrah T, McAdam KP, Whittle HC, Hill AV. Variations in the NRAMP1 gene and susceptibility to tuberculosis in West Africans. *N Engl J Med.* Mar 5 1998;338(10):640-644.

290. Li HT, Zhang TT, Zhou YQ, Huang QH, Huang J. SLC11A1 (formerly NRAMP1) gene polymorphisms and tuberculosis susceptibility: a meta-analysis. *Int J Tuberc Lung Dis.* Jan 2006;10(1):3-12.

291. Rook GA, Hernandez-Pando R, Zumla A. Tuberculosis due to high-dose challenge in partially immune individuals: a problem for vaccination? *J Infect Dis.* Mar 1 2009;199(5):613-618.

292. Narayanan PR. Influence of sex, age & nontuberculous infection at intake on the efficacy of BCG: re-analysis of 15-year data from a double-blind randomized control trial in South India. *Indian J Med Res.* Feb 2006;123(2):119-124.

293. Mouse Genome Database (MGD) at the Mouse Genome Informatics website TJL, Bar Harbor, Maine. http://www.informatics.jax.org. Accessed December 2009.

294. Min-Oo G, Fortin A, Pitari G, Tam M, Stevenson MM, Gros P. Complex genetic control of susceptibility to malaria: positional cloning of the Char9 locus. *J Exp Med.* Mar 19 2007;204(3):511-524.

295. Min-Oo G, Fortin A, Tam MF, Nantel A, Stevenson MM, Gros P. Pyruvate kinase deficiency in mice protects against malaria. *Nat Genet.* Dec 2003;35(4):357-362.

296. Roy MF, Riendeau N, Bedard C, et al. Pyruvate kinase deficiency confers susceptibility to Salmonella typhimurium infection in mice. *J Exp Med.* Nov 26 2007;204(12):2949-2961.

297. Apt A, Kramnik I. Man and mouse TB: contradictions and solutions. *Tuberculosis (Edinb).* May 2009;89(3):195-198.

298. Pichugin AV, Yan BS, Sloutsky A, Kobzik L, Kramnik I. Dominant role of the sst1 locus in pathogenesis of necrotizing lung granulomas during chronic tuberculosis infection and reactivation in genetically resistant hosts. *Am J Pathol.* Jun 2009;174(6):2190-2201.

APPENDIX I
Modifed version of Chapter 2 submitted for review

Joint effects of host genetic background and mycobacterial pathogen on susceptibility to infection

Tania Di Pietrantonio[1,2,3], José A. Correa[4], Marianna Orlova[1,2] , Marcel A. Behr[1,3], and Erwin Schurr[1,2,3*]

[1] McGill Centre for the Study of Host Resistance, Research Institute of the McGill University Health Centre, Montreal, Quebec, Canada

[2] Department of Human Genetics, McGill University, Montreal, Quebec, Canada

[3] Department of Medicine, McGill University, Montreal, Quebec, Canada

[4] Department of Mathematics and Statistics, McGill University, Montreal, Quebec, Canada

Running Title: Host, pathogen and measures of susceptibility

*Corresponding author:
E. Schurr
Research Institute of the McGill University Health Centre,
1650 Cedar Avenue, L1-413
Montreal, H3G 1A4, QC, Canada
erwin.schurr@mcgill.ca
Tel: +1 (514) 934-1934 ext 44513
Fax: +1 (514) 934-8238

ABSTRACT

The present study examined the differential contribution of host genetic background and mycobacterial pathogen variability on biological and mechanistic phenotypes of infection. For this purpose, A/J and C57BL/6J mice were infected intravenously with a low dose of *Mycobacterium tuberculosis* or the Russia, Japan, and Pasteur substrains of *Mycobacterium bovis* Bacille Calmette Guérin (BCG). The pulmonary bacterial counts (CFU) and transcript levels of select cytokines (e.g. *Ifng*, *Il12b*, *Il4*) at 1, 3 and 6 weeks post-infection were measured as biological and mechanistic phenotypes, respectively. The individual and combined impact of the host and mycobacteria on these phenotypes was assessed using three-way ANOVA, which partitions phenotypic variation into host, pathogen, time, and interaction effects. All phenotypes, except pulmonary *Il4* transcript levels, displayed evidence for host-mycobacteria specificity by means of significant interaction terms. Pulmonary expression profiling of 34 chemokines and chemokine-related genes was compared across host and mycobacteria. The differences in induction of these immune messenger genes between A/J and C57BL/6J mice were modest and generally failed to reach significance. By contrast, the mycobacteria induced significant variance in a subset of the immune messenger genes that was more evident in A/J relative to C57BL/6J mice. Overall, the results demonstrated the importance of considering the joint effects of the mycobacteria and host genetic background in susceptibility to mycobacterial infections.

INTRODUCTION

Exposure of humans to *Mycobacterium tuberculosis*, the cause of tuberculosis, induces a highly variable response. Among persons exposed to *M. tuberculosis*, only 30-50% become infected during an outbreak, and of those infected only approximately 10% develop clinical disease. There is now clear evidence for the important impact of host genetic factors on this variable response (3, 11, 12). Evidence for an equally important role of *M. tuberculosis* strain variability is emerging (reviewed in 18, 35). However, it is not known if susceptibility to infection and disease is the result of host and pathogen factors acting independently or if it results from joint effects between host genes and the *M. tuberculosis* strain. Although studies have examined the impact of host background and mycobacterial type separately, strategies that focus on the simultaneous analysis of host and mycobacteria in disease expression have been lacking. We addressed the question of interdependence of host genetics and mycobacterial pathogen on expression of host susceptibility using an animal model. We selected well characterized biological and mechanistic phenotypes of mycobacterial infection in mice to determine the individual and combined impact of pathogen and host genetic variability on phenotype variance.

As mycobacterial pathogens, we employed the H37Rv reference strain of *M. tuberculosis* and three strains of *M. bovis* Bacille Calmette Guerin (BCG): BCG Russia, BCG Japan, and BCG Pasteur. The most notable genetic differences between *M. tuberculosis* and BCG strains are chromosomal deletions, such as the region of difference 1 (RD1) (29, 42). In addition to RD1, BCG Russia is characterized by the deletion of Rv3698 (RD Russia) (41). BCG Japan contains a 22 base pair deletion within the *Rv3405c* gene (4) which renders it incapable of synthesizing phenolic glycolipids (PGLs), cell wall lipids with established roles in virulence (10). In both BCG Japan and BCG Russia, the promoter region of the *phoP* gene contains an IS*6110* element

(8) which may also have implications for virulence. BCG Pasteur lacks this insertion, resulting in a lower expression of *phoP* (8). Compared to the BCG Russia and Japan strains, BCG Pasteur has deleted three additional chromosomal segments: RD2, n-RD18 and RD14 (6, 34, 45) and has a number of point mutations that lead to loss-of-function phenotypes (5, 8, 9, 48).

As hosts, we employed the A/J and C57BL6/J inbred mouse strains. Mice of these strains differ in their response to mycobacterial infection. Following aerosol or intravenous infection with *M. tuberculosis*, susceptible A/J mice succumb more rapidly compared to C57BL/6J mice (1, 22). The early death of A/J animals is caused by a progressive interstitial pneumonitis characterized by widespread tissue necrosis and an inability to form cohesive granulomas. In contrast, C57BL/6J mice form functional granulomas and survive for extended periods. Despite these differences, early pulmonary *M. tuberculosis* replication is similar between C57BL/6J and A/J mice (1, 51). A/J and C57BL6/J mice also differ in their innate susceptibility to low dose infection with BCG Montreal (20, 50). Interestingly, *M. tuberculosis*-resistant C57BL/6J mice are permissive to BCG Montreal and BCG Pasteur replication in the mononuclear phagocyte system organs whereas *M. tuberculosis*-susceptible A/J mice are resistant to low dose BCG infection (13, 20). The shift in host susceptibility in response to pathogenic *M. tuberculosis* and avirulent BCG strains has also been observed in other mouse strains (37, 38) and prompted the inclusion of *M. tuberculosis* in this study. Although the host genetic control of *M. tuberculosis* infection is complex, the differential susceptibility in early growth of BCG Montreal has been shown to be due to two allelic forms of the *Nramp1* gene (50). We have recently demonstrated that bacterial counts of both BCG Pasteur and BCG Russia in the spleen are under the control of a locus indistinguishable from *Nramp1* (14). In our experimental setting, the effect of *Nramp1* in the lung was modest and could not be detected by genetic analysis. We therefore focused our

analysis on pulmonary responses which are less impacted by *Nramp1* in comparison to the spleen (14).

In the present study, the A/J and C57BL/6J mouse strains were infected with a low dose of BCG Russia, BCG Japan, BCG Pasteur or *M. tuberculosis* H37Rv and a set of host response phenotypes was characterized in the lungs of both mouse strains in a time-dependent manner. This design permitted the simultaneous investigation of the host and pathogen genetic background on the magnitude and variance of widely used host response phenotypes.

MATERIALS AND METHODS

Animals. A/J and C57BL/6J mice were purchased from the Jackson Laboratory (Bar Harbor, ME) and housed in the rodent facility of the Montreal General Hospital. All animal procedures were performed in accordance with the guidelines outlined by the Canadian Council on Animal Care and approved by the Animal Care Committee of McGill University.

Infection of mice. BCG Russia (ATCC 35740) and BCG Pasteur (ATCC 35734) were transformed with a Hygromycin resistance vector (7) to allow for growth on Hygromycin-containing media and minimize the risk of contamination following isolation from mice. Prior to infection, recombinant BCG Russia, recombinant BCG Pasteur, BCG Japan and *M. tuberculosis* H37Rv (Pasteur) were grown on a rotating platform at 37°C in Middlebrook 7H9 medium (Difco Laboratories, Detroit, MI) containing 0.05% Tween 80 (Sigma-Aldrich, St. Louis, MO) and 10% albumin-dextrose-catalase (ADC) supplement (Becton Dickinson and Co., Sparks, MD). At early logarithmic phase (OD_{600} = 0.4-0.5), bacterial cultures were sonicated to disperse clumps and were diluted accordingly. For intravenous infection, mice were injected with ~3×10^3 CFU of *M. tuberculosis* or BCG in the lateral tail vein. Inoculum doses were verified by serial dilution plating on Middlebrook 7H10 agar (Difco Laboratories, Detroit, MI) supplemented with oleic acid-albumin-dextrose-catalase (OADC) enrichment (Becton Dickinson and Co., Sparks, MD). For aerosol infection, BCG Russia and BCG Pasteur cultures were grown to an OD_{600} nm of 0.4 and diluted to 3.5×10^7 CFU/ml. Mice were infected for 10 minutes in an inhalation exposure system (In-Tox Products, Moriaty, NM). At one day post-infection, infectious doses of ~2×10^3 were confirmed by homogenizing lungs in 2 ml of 0.025% Saponin-PBS using large tissue grinders (TYCO Healthcare Group, Mansfield, MA). 200 μL of the homogenate was plated on

Middlebrook 7H10 agar (Difco Laboratories, Detroit, MI) supplemented OADC enrichment (Becton Dickinson and Co., Sparks, MD) and BACTEC PANTA PLUS (Becton Dickinson and Co., Sparks, MD).

Pulmonary BCG growth. Infected mice were sacrificed by CO_2 inhalation at 1, 3 and 6 weeks post-infection. Lungs were aseptically removed and placed in 0.025% Saponin-PBS. BCG-infected lungs were homogenized mechanically using a Polytron PT 2100 homogenizer (Brinkman Instruments, Westbury, NY) and lungs infected with H37Rv were disrupted using large tissue grinders (TYCO Healthcare Group, Mansfield, MA). Homogenates were serially diluted tenfold and plated on Middlebrook 7H10 agar containing OADC enrichment and Hygromycin B (Wisent Inc., St.-Bruno, QC) or BACTEC PANTA PLUS (Becton Dickinson and Co., Sparks, MD) with our modifications. Bacterial enumeration was performed after a 3 or 6-week incubation at 37°C.

RNA isolation. For the isolation of total cellular RNA, lungs were harvested from control and BCG Pasteur-, Japan-, Russia-, or H37Rv-infected mice at 1, 3 or 6 weeks post-infection and stored in RNA later (QIAGEN, Mississauga, ON). Lungs were mechanically disrupted and RNA was purified using the RNeasy Mini Kit (QIAGEN, Mississauga, ON) according to the manufacturer's instructions. Genomic DNA was removed during the RNA extraction process using the RNase-free, DNase kit (QIAGEN, Mississauga, ON). The concentration and integrity of all RNA samples was assessed using the NanoDrop ND-1000 spectrophotometer (NanoDrop Technologies, Wilmington, DE) and the Agilent Bioanalyzer 2100 (Agilent Technologies, Palo Alto, CA).

Gene quantification studies. Synthesis of first-strand cDNA was performed with 0.5 μg of total RNA using the QuantiTect Reverse Transcription Kit (QIAGEN, Mississauga, ON) as recommended by the manufacturer. QuantiTect Gene Expression Assays for *Ifng*, *Il12b*, *Il4* and the *Gapdh* endogenous control gene were purchased from QIAGEN (QIAGEN, Mississauga, ON). cDNA was amplified using Quantitect reagents on the Rotor-Gene 3000 (Corbett Research, Sydney, Australia) as specified.

For multi-gene expression profiling, samples were reverse transcribed with the RT² First Strand Kit (SuperArray Bioscience Corporation, Frederick, MD). cDNA was amplified on the ABI Prism® 7500 (Applied Biosystems, Foster City, CA) using either the Mouse Inflammatory Cytokines and Receptors RT² Profiler PCR Array (APMM-011A) or the Mouse Chemokines & Receptors PCR Array (PAMM-022A) in combination with the RT² Real-Time PCR SYBR Green/ROX Master Mix (SuperArray Bioscience Corporation, Frederick, MD). Of the 84 genes, 34 met our inclusion criteria. These genes were included in both sets of arrays and dissociation assays did not show evidence of cross-hybridization. Using the NormFinder (2) and geNorm (49) algorithms, *Gusb*, *Hprt*, *Hspcb*, *Gapdh*, and *Actb* were determined to be a suitable set of endogenous control genes for normalization.

Statistical methods. A three-way Analysis of Variance (ANOVA) was performed to investigate differences in replication across bacteria, mouse strain and time following intravenous infection. An analysis of residuals for this model detected violations of the

assumptions of normality and heterogeneity of variance of errors across groups for ANOVA. Thus, CFU values were log-transformed (natural logarithm) and an ANOVA model with unequal variances with residual variances for each combination of bacteria, mouse strain, and time was considered (30). We used the procedure PROC MIXED available in SAS, version 9.2 (SAS Institute Inc., Cary, NC) to fit the model. Degrees of freedom were adjusted using the Kenward-Roger correction (23) because the groups were unbalanced in the sense that groups did not have the same number of subjects. Pair-wise post-hoc comparisons of means between bacterial strains at each time were performed, where warranted, and p-values were adjusted for multiple testing with the simulation-based adjustment for multiple testing implemented in the SAS %SimTests macro (52) to ensure an overall family-wise error rate (fwer). Also, for each bacterial strain separately, we performed a two-way ANOVA to investigate differences in bacterial replication across mouse strain and time. Differences in the log-transformed pulmonary loads following aerosol infection were statistically examined with the Student's t test for unequal variances. $P<0.05$ indicates statistical significance.

Fold changes of transcript levels between infected and control samples were determined by the $\Delta\Delta C_T$ calculation (32). Data are presented as the mean fold difference ± SEM on a logarithm dualis ($\log_2$) scale, which assumes an optimum PCR efficiency (E) of 2. When applicable, confidence intervals (CI) of 95% were computed with a lower limit $2^{-\Delta\Delta C_T - Z_{1.960}\,SEM}$ and an upper limit $2^{-\Delta\Delta C_T + Z_{1.960}\,SEM}$, where $-\Delta\Delta C_T \pm Z_{1.960}$ SEM denotes the upper and lower confidence limits of the change $\Delta\Delta C_T$, SEM is the standard error of the mean change $-\Delta\Delta C_T$, and $Z_{1.960}$ is the 95th-percentile of the standard normal distribution (16). Differences in *Ifng*, *Il12b*, and *Il4* expression were analyzed by a three-way ANOVA model with unequal variances. Residual variances for

each combination of mouse strain, bacterial strain, and time were considered (30). We used the procedure PROC MIXED available in SAS, version 9.2 (SAS Institute Inc., Cary, NC) to fit the model. Real-time Superarray data were statistically examined using ANOVA for unequal variances with a Benjamini and Hochberg multiple test correction (GeneSpring GX software, Agilent Technologies, Palo Alto, CA).

RESULTS

To analyze the extent to which the mycobacterial and host genetic background contribute to the variance of common measures of susceptibility, we used C57BL/6J and A/J mice and *M. tuberculosis*, BCG Russia, BCG Japan and BCG Pasteur as host and mycobacterial variants, respectively. Mice were intravenously infected with a low dose of bacteria (~3 $\times 10^3$) and phenotypic traits of infection were measured at 1, 3, and 6 weeks, which are time points classically used to decipher susceptibility to BCG infection. Since the ability of mycobacteria to replicate in the lungs is a critical predictor of morbidity and mortality, pulmonary bacterial loads were compared in mice of both strains by three-way ANOVA analysis. This type of analysis partitions phenotypic variation into host-, pathogen-, and time-related effects. Importantly, it provides a measure of host-pathogen specificity through its interaction term (26). The kinetics of lung CFU were significantly different for *M. tuberculosis*, BCG Russia, BCG Pasteur and BCG Japan in both A/J and C57BL/6J mice (Figure 1). As expected, *M. tuberculosis* had the largest bacillary burdens across all time points and in both mouse strains. The highest bacterial count among the BCG substrains was observed for BCG Russia, which increased progressively in mice of both strains. At the six week time point, BCG Russia counts were similar on average to those of *M. tuberculosis* in the C57BL/6J strain, although they were lower on average than *M. tuberculosis* in the A/J strain. BCG Japan was unrecoverable from the lung and counts of BCG Pasteur remained low throughout the experiment. As would be expected, these striking differences in bacterial growth resulted in a very strong impact of mycobacterial variant on the CFU phenotype, with differences in pulmonary burdens across the mycobacteria more pronounced in A/J than C57BL/6J mice (Figure 1). When the host component in the contribution to lung CFU was analysed, the strongest effect was observed for *M. tuberculosis*, where the pulmonary loads of *M. tuberculosis* were significantly larger in A/J mice (least square mean [LSM] of $\log_{10}$CFU=3.96, standard error [SE]=0.14) relative to C57BL/6J animals (LSM of

$\log_{10}$CFU=3.13, SE=0.20) (*P*=0.002). These results indicated that although the host genetic background impacted on bacterial replication, the mycobacteria had a dominant effect (Figure 1).

In contrast to BCG Russia and *M. tuberculosis*, BCG Pasteur and BCG Japan were consistently associated with low bacillary counts in the lungs of both mouse strains. Unlike BCG Japan which failed to grow in the spleen (data not shown), BCG Pasteur thrives in the spleen (14, 25). This raised the question if the low pulmonary burden of BCG Pasteur reflected the inability of BCG Pasteur to home to the lung following intravenous infection, or if BCG Pasteur had a general limited capacity to multiply in lungs. To test the ability of Pasteur to replicate in the lung, bacilli were directly implanted into the lung by aerosol. Using a high dose infection model (~2 $x10^3$ bacilli), the counts of BCG Pasteur and BCG Russia were compared at the 6 week time point. BCG Pasteur still had smaller pulmonary burdens in both the A/J (*P*= 0.001) and C57BL/6J (*P*= 5.7 x 10^{-5}) mice (Figure 2), suggesting that the observed differences were not due to spread to the lung, but rather to a decreased capacity of BCG Pasteur to replicate in the lung. In addition, a difference in BCG Russia pulmonary loads was observed between the mouse strains (*P*= 0.009) with C57BL6/J mice displaying higher CFUs. This was in contrast to *M. tuberculosi*s which reached higher bacterial counts in the lungs of A/J mice following intravenous infection (Figure 1). These results demonstrated that differences in pulmonary bacterial counts reflect a different ability of the three mycobacteria to grow in lungs, and this difference depended on the mouse strain.

Next, we determined the pulmonary transcript levels of the interferon gamma (*Ifng)* cytokine in A/J or C57BL/6J mice intravenously infected with the mycobacterial pathogens (Figure 3). *M. tuberculosis* consistently induced the largest transcript levels of *Ifng*, followed by BCG

Pasteur. Induction of *Ifng* by BCG Russia was delayed, particularly in the A/J mouse strain. Three-way ANOVA showed a significant effect of the mycobacteria [$F(3,20.6) = 123.7$, $P<0.001$] and of time [$F(2,26.7) = 74.1$, $P<0.001$] on *Ifng* transcription with a significant interaction between the two effects [$F(6,16) = 16.2$, $P<0.001$]. The interaction between the host strain and time was not significant [$F(2,26.7) = 2.6$, $P=0.1$] and a triple interaction between host, pathogen and time was not detected [$F(6,16) = 1.3$, $P=0.3$]. Although the effect of the host strain was not significant [$F(1,40.7) = 2.9$, $P=0.1$], there was a significant interaction between the host and bacteria [$F(3,20.6) = 10.7$, $P<0.001$] reflective of significant host-pathogen specificity in *Ifng* induction.

The pulmonary transcript levels of interleukin 12b (*Il12b*) and interleukin 4 (*Il4*) were next measured. Bacteria-related differences in *Il12b* induction were observed in both A/J and C57BL/6J mice (Figure 4), with *M. tuberculosis* inducing significantly more *Il12b* than the three BCG strains. Three-way ANOVA testing identified a significant effect of the mycobacteria [$F(3,25.8) = 190.5$, $P<0.001$] and mouse strain [$F(1,46.8) = 8.8$, $P=0.005$] on *Il12b* transcription. There was a significant interaction between the two effects [$F(3,25.8) = 6.1$, $P=0.003$], indicating specificity of host- pathogen interaction on *Il12b* induction. The effect of time was also significant [$F(2,30.5) = 4.1$, $P=0.03$] and there was a significant interaction between the bacterial strain and time [$F(6,19) = 4.9$, $P=0.004$], but not between the mouse strain and time [$F(2,30.5) = 1.9$, $P=0.2$]. A triple interaction was not detected between the effects [$F(6,19) = 1.1$, $P=0.4$]. Unlike *Il12b*, pulmonary *Il4* expression was negatively correlated with infection by all four mycobacteria (Figure 5). Three-way ANOVA testing showed a significant effect of the mycobacteria [$F(3,24.8) = 8.7$, $P<0.001$], mouse strain [$F(1,33.3) = 8.3$, $P=0.01$] and time [$F(2,24) = 6.7$, $P=0.005$] on *Il4* transcription. The interaction between the host and bacteria was not significant [$F(3,24.8) = 2.7$, $P=0.07$], indicating that mycobacterial variation and host genetics

act independently on *Il4* induction. There was a significant interaction between the effects of bacteria and time [$F(6,20.1) = 3.0$, $P=0.03$] and between the host strain and time [$F(2,24) = 6.8$, $P=0.005$]. A triple interaction was not observed [$F(6,20.1) = 0.8$, $P=0.6$]. Thus, our analysis detected evidence for host-pathogen specificity in the induction of *Ifng* and *Il12b* but not in the induction of *Il4*.

Transcriptional levels of 34 cytokines, chemokines, and chemokine-related genes were profiled by real time PCR in response to *M. tuberculosis*, BCG Russia and BCG Pasteur in A/J and C57BL/6J mice at 3 and 6 weeks post-infection. Due to the low variability of BCG Japan-induced host responses, this strain was not included in this analysis. Moreover, given the large number of chemokines studied, a three-way ANOVA analysis was not performed. Instead, one-way ANOVA analyses comparing the two mouse strains were performed for each mycobacterium and at each time point. Unexpectedly, significant differences in cytokine and chemokine transcript levels were not detected between A/J and C57BL/6J mice. Hence, subsequent ANOVA analyses were focused on the extent of differential gene expression across the three species of mycobacteria in mice of each strain at each time point. The magnitude of the transcriptional response was shown to be the largest during *M. tuberculosis* infection, while BCG Russia had a lagged expression for most of the genes tested. Expression differences across the three mycobacteria were more pronounced in the A/J mouse strain. Among the genes that were significantly up- or down-regulated, 15 and 11 genes were differentially expressed across bacteria at 3 and 6 weeks, respectively (Tables 1 and 2 and Supplemental Tables 1 and 2). In C57BL6/J mice, differences in induction related to the mycobacteria were observed for 9 genes at 3 weeks and for 3 genes at 6 weeks (Tables 1 and 2 and Supplemental Tables 3 and 4). These results demonstrated that the magnitude of differences in cytokine and chemokine levels following mycobacterial infection was critically dependent on the host background.

DISCUSSION

Analysis of functional host phenotypes in the mouse has demonstrated that bacteria of different *M. tuberculosis* lineages cause a range of immunological and pathological effects (15, 33). Specifically, the Euro-American group of strains is unable to produce a PGL-tb molecule that has been associated with subversion of innate immune responses and increased mortality in mice (43). Differences in the magnitude of the inflammatory response have also been observed in response to infection with BCG substrains (21). Moreover, different strains of BCG induce different levels of protective tuberculosis immunity in mice and vary in the incidence of adverse effects in human studies (28, 31). These studies show an association between mycobacterial genetic variation and host immune responses. On the other hand, it has been clearly established that genetically distinct inbred mice and humans differ dramatically in their susceptibility to mycobacterial infections. In humans, it has recently been shown that susceptibility to infection with *M. tuberculosis* is under genetic control and strongly impacted by a locus on chromosome 11 (11, 12). A number of additional genes modulate the risk of developing clinical tuberculosis of infected persons, including the *NRAMP1* gene (19, 36). The mouse orthologue of the latter gene was previously identified as the major determinant of innate susceptibility to infection in the spleen with several BCG strains (14, 50). In addition, variable susceptibility of inbred strains of mice to *M. tuberculosis* has been linked to a number of loci (24, 27, 39, 40, 46, 47, 53). Taken together, these data establish that genetic variability of both the mycobacterial pathogen and murine or human hosts strongly impact on different aspects of host susceptibility to mycobacterial infection. However, there is a lack of studies that have systematically analysed, in parallel, the joint contribution of both the host and mycobacteria on host responses.

A consistent finding of our experiments was that all infectious phenotypes were more sensitive to variation of the mycobacterial pathogen than host background. Given the very small number of mycobacteria and host strains, this may be at least partly a result of the larger genetic variability among the four types of mycobacteria as compared to the more related A/J and C57BL/6J mice. By including wild-derived mice or mice with known genetic defects in such comparisons, by studying a later phase of infection, or by changing the mode and dose of infection, the relative impact of host genetic background vs bacterial pathogen may well have changed. Despite such limitations, our data are consistent with the view that the major effect on host responses is due to the type of mycobacteria while the host genetic background is the modulator of responsiveness. Yet, even in our study with a dominant impact of the mycobacterial pathogen on the studied phenotypes, it became clear that a comparison of the mycobacteria for both pulmonary CFU burden and mechanistic phenotypes (*Ifng* and chemokine transcript levels) had more discriminatory power in A/J mice as compared to C57BL/6J mice. This highlights problems that can be encountered when studies employing the same mycobacterial strain are compared in different hosts. Above all, the analysis of common host responses to mycobacteria in this model system provided proof-of-principle for host-pathogen joint effects on phenotype variance. This is an important extension of our previous observation of BCG strain-specific genetic control of BCG Russia and BCG Pasteur replication (14).

The detection of significant interactions of host and pathogen on phenotype expression by necessity invokes differences in the pathogenesis, either quantitative or qualitative, between different host- pathogen strain combinations. Given that both lung CFU and the wide array of mechanistic phenotypes studied showed evidence for significant joint mycobacteria-host effects, it seems likely that similar effects are also seen in human populations. This opens the question if the search for protective correlates of tuberculosis should be focused on mechanistic phenotypes

that show little sensitivity to host-pathogen variability or if different host-pathogen combinations invoke different protective correlates. Similarly, if a large number of persons are exposed to an array of *M. tuberculosis* strains, it is possible that among the persons who develop tuberculosis, some are susceptible to all strains while others are susceptible to specific subsets of *M. tuberculosis* strains. Such a hypothetical scenario would provide a straightforward biological explanation why *M. tuberculosis* strains are preferentially associated with distinct human populations (17, 44). To judge the relevance of the above considerations will require a more accurate estimate of the relative importance of pathogen, host and joint effects on phenotype expression. This in turn will require much larger comparative studies covering a larger range of phenotypes as well as hosts and pathogens.

ACKNOWLEDGEMENTS

We gratefully acknowledge the technical assistance of Manon Girard, Fiona McIntosh, Vlad Kamenski and Annie Verville. We also thank Adam Belley for providing the BCG Russia and BCG Pasteur, David Alexander for providing the BCG Japan, and Pilar Domenech for providing the *M. tuberculosis* H37Rv (Pasteur).

This work was supported by grant HL68533 from the National Institutes of Health (NIH) and a grant from the Canadian Institutes of Health Research (CIHR) to E.S. E.S. is a Chercheur National du Fonds de la Recherche en Santé du Québec and an International Research Scholar of the Howard Hughes Medical Institute.

References

1. **Actor, J. K., M. Olsen, C. Jagannath, and R. L. Hunter.** 1999. Relationship of survival, organism containment, and granuloma formation in acute murine tuberculosis. J Interferon Cytokine Res **19:**1183-1193.

2. **Andersen, C. L., J. L. Jensen, and T. F. Orntoft.** 2004. Normalization of real-time quantitative reverse transcription-PCR data: a model-based variance estimation approach to identify genes suited for normalization, applied to bladder and colon cancer data sets. Cancer Res **64:**5245-5250.

3. **Baghdadi, J. E., M. Orlova, A. Alter, B. Ranque, M. Chentoufi, F. Lazrak, M. I. Archane, J. L. Casanova, A. Benslimane, E. Schurr, and L. Abel.** 2006. An autosomal dominant major gene confers predisposition to pulmonary tuberculosis in adults. J Exp Med **203:**1679-1684.

4. **Bedwell, J., S. K. Kairo, M. A. Behr, and J. A. Bygraves.** 2001. Identification of substrains of BCG vaccine using multiplex PCR. Vaccine **19:**2146-2151.

5. **Behr, M. A., B. G. Schroeder, J. N. Brinkman, R. A. Slayden, and C. E. Barry, 3rd.** 2000. A point mutation in the *mma3* gene is responsible for impaired methoxymycolic acid production in *Mycobacterium bovis* BCG strains obtained after 1927. J Bacteriol **182:**3394-3399.

6. **Behr, M. A., M. A. Wilson, W. P. Gill, H. Salamon, G. K. Schoolnik, S. Rane, and P. M. Small.** 1999. Comparative genomics of BCG vaccines by whole-genome DNA microarray. Science **284:**1520-1523.

7. **Belley, A., D. Alexander, T. Di Pietrantonio, M. Girard, J. Jones, E. Schurr, J. Liu, D. R. Sherman, and M. A. Behr.** 2004. Impact of methoxymycolic acid production by *Mycobacterium bovis* BCG vaccines. Infect Immun **72:**2803-2809.

8. **Brosch, R., S. V. Gordon, T. Garnier, K. Eiglmeier, W. Frigui, P. Valenti, S. Dos Santos, S. Duthoy, C. Lacroix, C. Garcia-Pelayo, J. K. Inwald, P. Golby, J. N. Garcia, R. G. Hewinson, M. A. Behr, M. A. Quail, C. Churcher, B. G. Barrell, J. Parkhill, and S. T. Cole.** 2007. Genome plasticity of BCG and impact on vaccine efficacy. Proc Natl Acad Sci U S A **104:**5596-5601.

9. **Charlet, D., S. Mostowy, D. Alexander, L. Sit, H. G. Wiker, and M. A. Behr.** 2005. Reduced expression of antigenic proteins MPB70 and MPB83 in *Mycobacterium bovis* BCG strains due to a start codon mutation in *sigK*. Mol Microbiol **56:**1302-1313.

10. **Chen, J. M., S. T. Islam, H. Ren, and J. Liu.** 2007. Differential productions of lipid virulence factors among BCG vaccine strains and implications on BCG safety. Vaccine **25:**8114-8122.

11. **Cobat, A., C. J. Gallant, L. Simkin, G. F. Black, K. Stanley, J. Hughes, T. M. Doherty, W. A. Hanekom, B. Eley, N. Beyers, J. P. Jais, P. van Helden, L. Abel, E. G. Hoal, A. Alcais, and E. Schurr.** 2010. High heritability of antimycobacterial immunity in an area of hyperendemicity for tuberculosis disease. J Infect Dis **201:**15-19.

12. **Cobat, A., C. J. Gallant, L. Simkin, G. F. Black, K. Stanley, J. Hughes, T. M. Doherty, W. A. Hanekom, B. Eley, J. P. Jais, A. Boland-Auge, P. van Helden, J. L. Casanova, L. Abel, E. G. Hoal, E. Schurr, and A. Alcais.** 2009. Two loci control tuberculin skin test reactivity in an area hyperendemic for tuberculosis. J Exp Med **206:**2583-2591.

13. **Denis, M., A. Forget, M. Pelletier, R. Turcotte, and E. Skamene.** 1986. Control of the Bcg gene of early resistance in mice to infections with BCG substrains and atypical mycobacteria. Clin Exp Immunol **63:**517-525.

14. **Di Pietrantonio, T., C. Hernandez, M. Girard, A. Verville, M. Orlova, A. Belley, M. A. Behr, J. C. Loredo-Osti, and E. Schurr.** 2010. Strain-specific differences in the genetic control of two closely related mycobacteria. PLoS Pathog **6:**e1001169.

15. **Dormans, J., M. Burger, D. Aguilar, R. Hernandez-Pando, K. Kremer, P. Roholl, S. M. Arend, and D. van Soolingen.** 2004. Correlation of virulence, lung pathology, bacterial load and delayed type hypersensitivity responses after infection with different *Mycobacterium tuberculosis* genotypes in a BALB/c mouse model. Clin Exp Immunol **137:**460-468.

16. **Fu, W. J., J. Hu, T. Spencer, R. Carroll, and G. Wu.** 2006. Statistical models in assessing fold change of gene expression in real-time RT-PCR experiments. Comput Biol Chem **30:**21-26.

17. **Gagneux, S., K. DeRiemer, T. Van, M. Kato-Maeda, B. C. de Jong, S. Narayanan, M. Nicol, S. Niemann, K. Kremer, M. C. Gutierrez, M. Hilty, P. C. Hopewell, and P. M. Small.** 2006. Variable host-pathogen compatibility in *Mycobacterium tuberculosis*. Proc Natl Acad Sci U S A **103:**2869-2873.

18. **Gagneux, S., and P. M. Small.** 2007. Global phylogeography of *Mycobacterium tuberculosis* and implications for tuberculosis product development. Lancet Infect Dis **7:**328-337.

19. **Greenwood, C. M., T. M. Fujiwara, L. J. Boothroyd, M. A. Miller, D. Frappier, E. A. Fanning, E. Schurr, and K. Morgan.** 2000. Linkage of tuberculosis to chromosome

2q35 loci, including *NRAMP1*, in a large aboriginal Canadian family. Am J Hum Genet **67:**405-416.

20. **Gros, P., E. Skamene, and A. Forget.** 1981. Genetic control of natural resistance to *Mycobacterium bovis* (BCG) in mice. J Immunol **127:**2417-2421.

21. **Irwin, S. M., A. Goodyear, A. Keyser, R. Christensen, J. M. Troudt, J. L. Taylor, A. Bohsali, V. Briken, and A. A. Izzo.** 2008. Immune response induced by three *Mycobacterium bovis* BCG substrains with diverse regions of deletion in a C57BL/6 mouse model. Clin Vaccine Immunol **15:**750-756.

22. **Jagannath, C., H. Hoffmann, E. Sepulveda, J. K. Actor, R. A. Wetsel, and R. L. Hunter.** 2000. Hypersusceptibility of A/J mice to tuberculosis is in part due to a deficiency of the fifth complement component (C5). Scand J Immunol **52:**369-379.

23. **Kowalchuk, R. K., H. J. Keselman, J. Algina, and R. D. Wolfinger.** 2004. The Analysis of Repeated Measurements with Mixed-Model Adjusted F Tests. Educ Psychol Meas **64:**224-242.

24. **Kramnik, I., W. F. Dietrich, P. Demant, and B. R. Bloom.** 2000. Genetic control of resistance to experimental infection with virulent *Mycobacterium tuberculosis*. Proc Natl Acad Sci U S A **97:**8560-8565.

25. **Lagranderie, M. R., A. M. Balazuc, E. Deriaud, C. D. Leclerc, and M. Gheorghiu.** 1996. Comparison of immune responses of mice immunized with five different Mycobacterium bovis BCG vaccine strains. Infect Immun **64:**1-9.

26. **Lambrechts, L.** 2010. Dissecting the genetic architecture of host-pathogen specificity. PLoS Pathog **6e:**e1001019.

27. **Lavebratt, C., A. S. Apt, B. V. Nikonenko, M. Schalling, and E. Schurr.** 1999. Severity of tuberculosis in mice is linked to distal chromosome 3 and proximal chromosome 9. J Infect Dis **180:**150-155.

28. **Leung, A. S., V. Tran, Z. Wu, X. Yu, D. C. Alexander, G. F. Gao, B. Zhu, and J. Liu.** 2008. Novel genome polymorphisms in BCG vaccine strains and impact on efficacy. BMC Genomics **9:**413.

29. **Lewis, K. N., R. Liao, K. M. Guinn, M. J. Hickey, S. Smith, M. A. Behr, and D. R. Sherman.** 2003. Deletion of RD1 from *Mycobacterium tuberculosis* mimics bacille Calmette-Guerin attenuation. J Infect Dis **187:**117-123.

30. **Littell, R. C., G. A. Milliken, W. W. Stroup, R. D. Wolfinger, and O. Schabenberger.** 2006. SAS® for Mixed Models, Second Edition. SAS Institute Inc., Cary, NC, USA.

31. **Liu, J., V. Tran, A. S. Leung, D. C. Alexander, and B. Zhu.** 2009. BCG vaccines: their mechanisms of attenuation and impact on safety and protective efficacy. Hum Vaccin **5:**70-78.

32. **Livak, K. J., and T. D. Schmittgen.** 2001. Analysis of relative gene expression data using real-time quantitative PCR and the $2^{-\Delta\Delta CT}$ Method. Methods **25:**402-408.

33. **Lopez, B., D. Aguilar, H. Orozco, M. Burger, C. Espitia, V. Ritacco, L. Barrera, K. Kremer, R. Hernandez-Pando, K. Huygen, and D. van Soolingen.** 2003. A marked difference in pathogenesis and immune response induced by different *Mycobacterium tuberculosis* genotypes. Clin Exp Immunol **133:**30-37.

34. **Mahairas, G. G., P. J. Sabo, M. J. Hickey, D. C. Singh, and C. K. Stover.** 1996. Molecular analysis of genetic differences between *Mycobacterium bovis* BCG and virulent *M. bovis*. J Bacteriol **178:**1274-1282.

35. **Malik, A. N., and P. Godfrey-Faussett.** 2005. Effects of genetic variability of *Mycobacterium tuberculosis* strains on the presentation of disease. Lancet Infect Dis **5:**174-183.

36. **Malik, S., L. Abel, H. Tooker, A. Poon, L. Simkin, M. Girard, G. J. Adams, J. R. Starke, K. C. Smith, E. A. Graviss, J. M. Musser, and E. Schurr.** 2005. Alleles of the *NRAMP1* gene are risk factors for pediatric tuberculosis disease. Proc Natl Acad Sci U S A **102:**12183-12188.

37. **Medina, E., and R. J. North.** 1996. Evidence inconsistent with a role for the Bcg gene (Nramp1) in resistance of mice to infection with virulent Mycobacterium tuberculosis. J Exp Med **183:**1045-1051.

38. **Medina, E., and R. J. North.** 1998. Resistance ranking of some common inbred mouse strains to Mycobacterium tuberculosis and relationship to major histocompatibility complex haplotype and Nramp1 genotype. Immunology **93:**270-274.

39. **Mitsos, L. M., L. R. Cardon, A. Fortin, L. Ryan, R. LaCourse, R. J. North, and P. Gros.** 2000. Genetic control of susceptibility to infection with *Mycobacterium tuberculosis* in mice. Genes Immun **1:**467-477.

40. **Mitsos, L. M., L. R. Cardon, L. Ryan, R. LaCourse, R. J. North, and P. Gros.** 2003. Susceptibility to tuberculosis: a locus on mouse chromosome 19 (*Trl-4*) regulates *Mycobacterium tuberculosis* replication in the lungs. Proc Natl Acad Sci U S A **100:**6610-6615.

41. **Mostowy, S., A. G. Tsolaki, P. M. Small, and M. A. Behr.** 2003. The in vitro evolution of BCG vaccines. Vaccine **21:**4270-4274.

42. **Pym, A. S., P. Brodin, R. Brosch, M. Huerre, and S. T. Cole.** 2002. Loss of RD1 contributed to the attenuation of the live tuberculosis vaccines *Mycobacterium bovis* BCG and *Mycobacterium microti*. Mol Microbiol **46:**709-717.

43. **Reed, M. B., P. Domenech, C. Manca, H. Su, A. K. Barczak, B. N. Kreiswirth, G. Kaplan, and C. E. Barry, 3rd.** 2004. A glycolipid of hypervirulent tuberculosis strains that inhibits the innate immune response. Nature **431:**84-87.

44. **Reed, M. B., V. K. Pichler, F. McIntosh, A. Mattia, A. Fallow, S. Masala, P. Domenech, A. Zwerling, L. Thibert, D. Menzies, K. Schwartzman, and M. A. Behr.** 2009. Major *Mycobacterium tuberculosis* lineages associate with patient country of origin. J Clin Microbiol **47:**1119-1128.

45. **Salamon, H., M. Kato-Maeda, P. M. Small, J. Drenkow, and T. R. Gingeras.** 2000. Detection of deleted genomic DNA using a semiautomated computational analysis of GeneChip data. Genome Res **10:**2044-2054.

46. **Sanchez, F., T. V. Radaeva, B. V. Nikonenko, A. S. Persson, S. Sengul, M. Schalling, E. Schurr, A. S. Apt, and C. Lavebratt.** 2003. Multigenic control of disease severity after virulent *Mycobacterium tuberculosis* infection in mice. Infect Immun **71:**126-131.

47. **Sissons, J., B. S. Yan, A. V. Pichugin, A. Kirby, M. J. Daly, and I. Kramnik.** 2009. Multigenic control of tuberculosis resistance: analysis of a QTL on mouse chromosome 7 and its synergism with sst1. Genes Immun **10:**37-46.

48. **Spreadbury, C. L., M. J. Pallen, T. Overton, M. A. Behr, S. Mostowy, S. Spiro, S. J. Busby, and J. A. Cole.** 2005. Point mutations in the DNA- and cNMP-binding domains of the homologue of the cAMP receptor protein (CRP) in *Mycobacterium bovis* BCG: implications for the inactivation of a global regulator and strain attenuation. Microbiology **151:**547-556.

49. **Vandesompele, J., K. De Preter, F. Pattyn, B. Poppe, N. Van Roy, A. De Paepe, and F. Speleman.** 2002. Accurate normalization of real-time quantitative RT-PCR data by geometric averaging of multiple internal control genes. Genome Biol **3:**RESEARCH0034.

50. **Vidal, S. M., D. Malo, K. Vogan, E. Skamene, and P. Gros.** 1993. Natural resistance to infection with intracellular parasites: isolation of a candidate for *Bcg*. Cell **73:**469-485.

51. **Watson, V. E., L. L. Hill, L. B. Owen-Schaub, D. W. Davis, D. J. McConkey, C. Jagannath, R. L. Hunter, Jr., and J. K. Actor.** 2000. Apoptosis in *Mycobacterium tuberculosis* infection in mice exhibiting varied immunopathology. J Pathol **190:**211-220.

52. **Westfall, P. H.** 1997. Multiple testing of general contrasts using logical constraints and correlations. J Am Stat Assoc **92::**299–306.

53. **Yan, B. S., A. Kirby, Y. V. Shebzukhov, M. J. Daly, and I. Kramnik.** 2006. Genetic architecture of tuberculosis resistance in a mouse model of infection. Genes Immun **7:**201-210.

Table 1: Genes differentially expressed across mycobacteria at week 3

	Adjusted p-value	
	A/J	C57BL/6J
Genes identified in A/J and C57BL/6J		
Ccl20	0.037	0.048
Ccl4	0.006	0.021
Ccl5	0.006	0.021
Cxcl10	0.006	0.021
Genes specific to A/J		
Ccl1	0.013	-[a]
Ccl12	0.006	-
Ccl2	0.033	-
Ccl7	0.020	-
Ccl8	0.009	-
Ccr5	0.020	-
Cx3cl1	0.007	-
Cxcl11	0.029	-
Cxcl9	0.006	-
Cxcr3	0.011	-
Tnf	0.011	-
Genes specific to C57BL/6J		
Ccl11	-	0.048
Ccl19	-	0.032
Ccr9	-	0.048
Cxcl5	-	0.048
Il18	-	0.039

[a] non-significant

Ccl, chemokine (C-C motif) ligand; *Ccr*, chemokine (C-C motif) receptor; *Cx3cl1*, chemokine (C-X3-C motif) ligand 1; *Cxcl*, chemokine (C-X-C motif) ligand; *Cxcr*, chemokine (C-X-C motif) receptor; *Tnf*, tumor necrosis factor; *Il18,* interleukin 18.

Table 2: Genes differentially expressed across mycobacteria at week 6

	Adjusted p-value	
	A/J	C57BL/6J
Genes identified in A/J and C57BL/6J		
Ccr1	0.037	0.007
Ccr2	0.034	0.023
Genes specific to A/J		
Ccl5	0.048	-[a]
Ccl8	0.040	-
Ccr5	0.040	-
Ccr9	0.034	-
Cxcl10	0.040	-
Cxcl15	0.034	-
Cxcl5	0.048	-
Cxcl9	0.040	-
Cxcr3	0.008	-
Genes specific to C57BL/6J		
Ccl19	-	0.018

[a] non-significant

Ccl, chemokine (C-C motif) ligand; *Ccr*, chemokine (C-C motif) receptor; *Cxcl*, chemokine (C-X-C motif) ligand; *Cxcr*, chemokine (C-X-C motif) receptor.

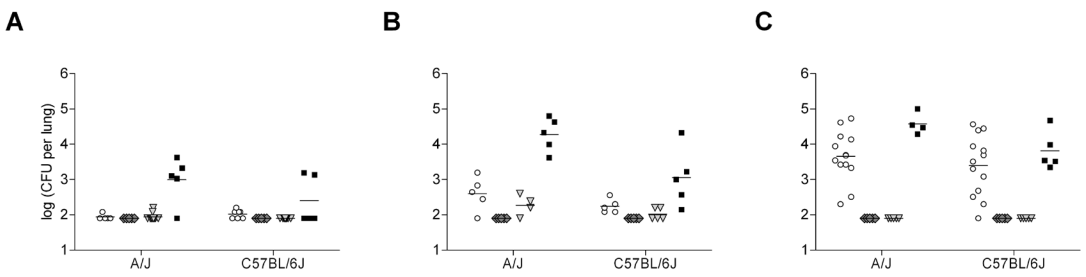

Figure 1. Pulmonary bacterial counts of BCG and *M. tuberculosis* in the A/J and C57BL/6J mouse strains. The number of bacteria (log_{10}CFU) in the lungs of individual A/J and C57BL/6J mice was quantified at 1 week (A), 3 weeks (B), and 6 weeks (C) following intravenous infection with a low dose (~3×10^3 bacilli) of BCG Russia, BCG Japan, BCG Pasteur or *M. tuberculosis*. Mycobacterial counts in A/J and C57BL/6J mice were compared across time by three-way ANOVA. BCG Japan was excluded from the analysis because bacteria were unrecoverable in all mice tested and the lack of variance precluded the use of ANOVA. Three way ANOVA showed a significant effect of bacteria [$F(2,30.9) = 118.3$, $P<0.001$], mouse strain [$F(1,34.3) = 18.6$, $P<0.001$], and time [$F(2,23) = 49.2$, $P<0.001$] on bacterial counts. Significant interaction effects were detected between the bacteria and mouse strain [$F(2, 30.9)=5.5$, $P=0.01$], providing evidence of host-pathogen specificity. A significant interaction was also detected between the bacteria and time [$F(4, 21.6) = 31.1$, $P<0.001$] but not between the mouse strain and time [$F(2, 23) = 1.8$, $P=0.2$]. A triple interaction between the effects was not detected $F(4, 21.6) = 0.6$, $P=0.7$]. Limit of detectability was 80 bacilli/lung. Bars indicate the mean log_{10}CFU for the group. BCG Russia, white circle; BCG Japan, grey diamond; BCG Pasteur, light grey triangle; *M. tuberculosis*, black square.

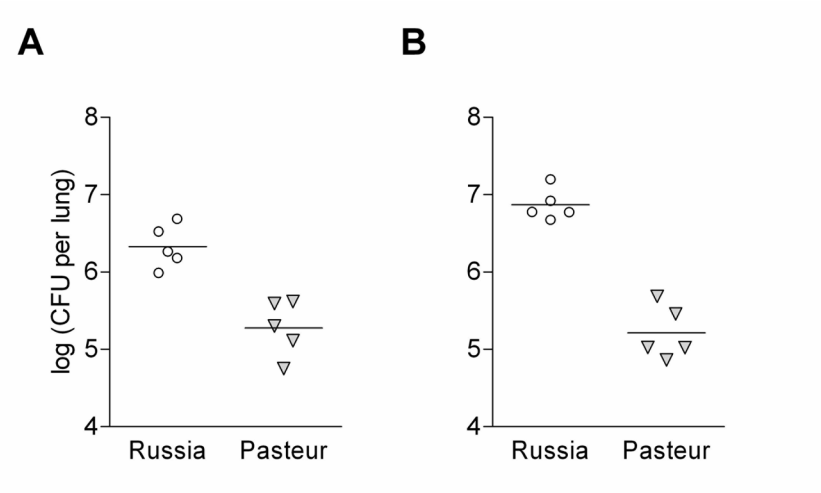

Figure 2. Pulmonary load of BCG Pasteur and BCG Russia in A/J and C57BL/6J mice following a high dose aerosol infection. The bacterial counts (log_{10}CFU) of BCG Russia (white circle) or BCG Pasteur (grey square) were determined in the lungs of A/J (A) and C57BL/6J (B) mice at 6 weeks following a high dose (~3×10^3 bacilli) aerosol infection. Bars are representative of the mean log_{10}CFU for the group.

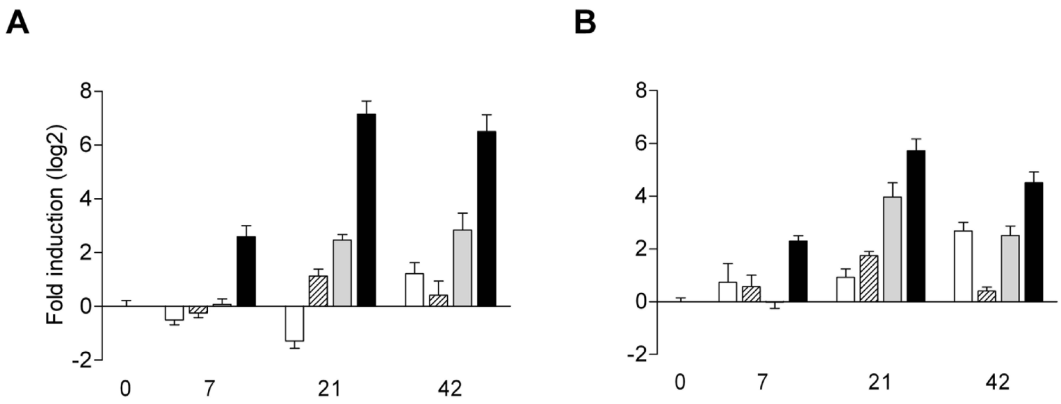

Figure 3. Pulmonary *Ifng* transcript levels in the A/J and C57BL/6J mouse strains following mycobacterial infection. Induction of *Ifng* transcription by BCG Russia (white), BCG Japan (hatched), BCG Pasteur (grey) and *M. tuberculosis* (black) was compared in the A/J (A) and C57BL/6J (B) mouse strains at 1, 3, and 6 weeks following a low dose intravenous infection. Fold induction (log_2) is the ratio of *Ifng* expression in infected mice (n=4) relative to uninfected mice (n=4). Error bars represent SEM.

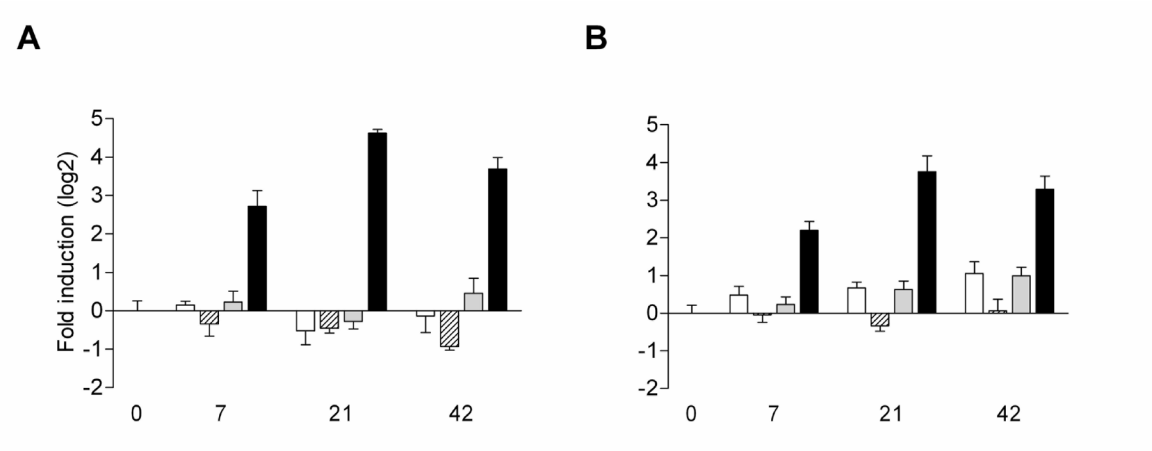

Figure 4. Pulmonary transcription of *Il12b* in the A/J and C57BL/6J mouse strains infected with BCG or *M. tuberculosis*. Induction of *Il12b* during a low dose intravenous infection with BCG Russia, BCG Japan, BCG Pasteur or *M. tuberculosis* was compared in A/J (A) and C57BL/6J (B) mice at 1, 3, and 6 weeks. Data represent the fold change (log_2) of *Il12b* transcription in infected (n=4) relative to uninfected (n=4) mice + SEM. BCG Russia, white; BCG Japan, hatched; BCG Pasteur, grey; *M. tuberculosis*, black.

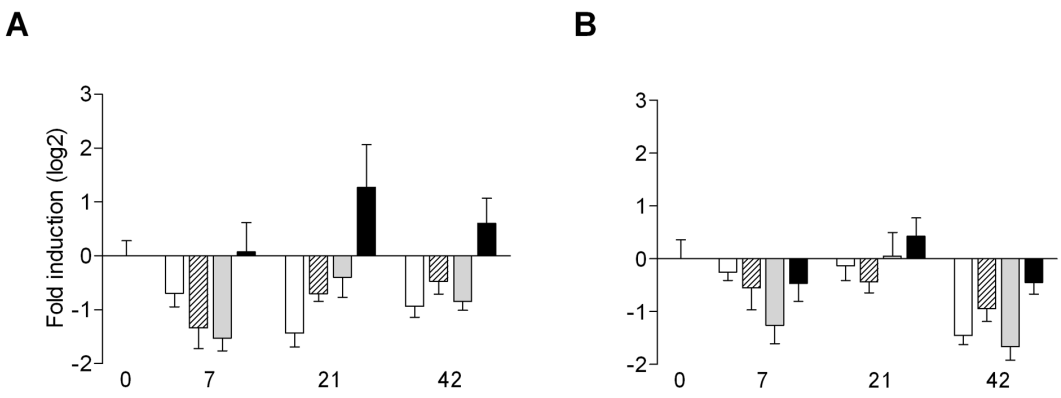

Figure 5. Transcript levels of *Il4* in the lungs of A/J and C57BL/6J mice following infection with BCG or *M. tuberculosis*. The extent of pulmonary *Il4* transcription was determined at 1, 3, and 6 weeks following a low dose intravenous infection with BCG Russia, BCG Japan, BCG Pasteur or *M. tuberculosis*. . Data are presented as a fold change of *Il4* transcription in infected (n=4) relative to uninfected (n=4) mice + SEM. BCG Russia, white; BCG Japan, hatched; BCG Pasteur, grey; *M. tuberculosis*, black.

APPENDIX II
Article Reprint

OPEN ACCESS Freely available online

PLoS PATHOGENS

Strain-Specific Differences in the Genetic Control of Two Closely Related Mycobacteria

Tania Di Pietrantonio[1,2,3], Carmen Hernandez[1], Manon Girard[1], Annie Verville[1], Marianna Orlova[1,2], Adam Belley[1], Marcel A. Behr[1,3], J. Concepción Loredo-Osti[4]*¶, Erwin Schurr[1,2,3]*¶

1 McGill Centre for the Study of Host Resistance, Research Institute of the McGill University Health Centre, Montreal, Quebec, Canada, **2** Department of Human Genetics, McGill University, Montreal, Quebec, Canada, **3** Department of Medicine, McGill University, Montreal, Quebec, Canada, **4** Department of Mathematics and Statistics, Memorial University of Newfoundland, St Johns, Newfoundland and Labrador, Canada

Abstract

The host response to mycobacterial infection depends on host and pathogen genetic factors. Recent studies in human populations suggest a strain specific genetic control of tuberculosis. To test for mycobacterial-strain specific genetic control of susceptibility to infection under highly controlled experimental conditions, we performed a comparative genetic analysis using the A/J- and C57BL/6J-derived recombinant congenic (RC) mouse panel infected with the Russia and Pasteur strains of *Mycobacterium bovis* Bacille Calmette Guérin (BCG). Bacillary counts in the lung and spleen at weeks 1 and 6 post infection were used as a measure of susceptibility. By performing genome-wide linkage analyses of loci that impact on tissue-specific bacillary burden, we were able to show the importance of correcting for strain background effects in the RC panel. When linkage analysis was adjusted on strain background, we detected a single locus on chromosome 11 that impacted on pulmonary counts of BCG Russia but not Pasteur. The same locus also controlled the splenic counts of BCG Russia but not Pasteur. By contrast, a locus on chromosome 1 which was indistinguishable from *Nramp1* impacted on splenic bacillary counts of both BCG Russia and Pasteur. Additionally, dependent upon BCG strain, tissue and time post infection, we detected 9 distinct loci associated with bacillary counts. Hence, the ensemble of genetic loci impacting on BCG infection revealed a highly dynamic picture of genetic control that reflected both the course of infection and the infecting strain. This high degree of adaptation of host genetics to strain-specific pathogenesis is expected to provide a suitable framework for the selection of specific host-mycobacteria combinations during co-evolution of mycobacteria with humans.

Citation: Di Pietrantonio T, Hernandez C, Girard M, Verville A, Orlova M, et al. (2010) Strain-Specific Differences in the Genetic Control of Two Closely Related Mycobacteria. PLoS Pathog 6(10): e1001169. doi:10.1371/journal.ppat.1001169

Editor: Eric J. Rubin, Harvard School of Public Health, United States of America

Received July 20, 2010; **Accepted** September 29, 2010; **Published** October 28, 2010

Funding: Funding for this research was provided by the Canadian Institutes of Health Research (CIHR) and the National Institutes of Health (NIH), grant #HL68533. The funders had no role in study design, data collection and analysis, decision to publish, or preparation of the manuscript.

Competing Interests: The authors have declared that no competing interests exist.

* E-mail: erwin.schurr@mcgill.ca (ES); jcloredoosti@mun.ca (JCLO)

¶ These authors share senior authorship.

Introduction

The primary cause of tuberculosis is the human pathogenic bacterium *Mycobacterium tuberculosis*. The host cells of *M. tuberculosis* are macrophages and the bacilli have developed numerous adaptations to survive within these powerful immune effector cells. For example, human pathogenic strains of *M. tuberculosis* inactivate microbicidal superoxide via katalase [1], avoid the detrimental effects of iNOS products [2], skew the anti-mycobacterial response in macrophages towards production of anti-inflammatory molecules [3,4], and favour necrosis over apoptosis [5,6,7]. Interestingly, circulating strains of *M. tuberculosis* may differ in their pathogenic potential [8,9]. Since humans and *M. tuberculosis* have co-evolved over millennia, a question remains if and to what extent *M. tuberculosis* has adapted to genetically distinct hosts. Indeed, two studies conducted in ethnically mixed samples detected a non-random association of *M. tuberculosis* strains with distinct ethnic populations [10,11]. These observations are supported by the results of several genetic association studies that detected preferential associations between a Toll-like receptor 2 (*TLR2*) polymorphism and tuberculosis meningitis caused by Beijing strains [12], as well as between variants of 5′-lipoxygenase (*ALOX5*) and pulmonary tuberculosis caused by *M. africanum*, but not *M. tuberculosis* [13]. In addition, variants of the immunity-related GTPase M (*IRGM*) were associated with protection from pulmonary tuberculosis due to Euro-American strains of *M. tuberculosis* [14]. Due to the complex interactions of *M. tuberculosis* and humans in exposed populations, it is possible that those results may have been confounded by unrecognized factors. In the absence of independent replication studies, the question of strain specific genetic effects as a consequence of *M. tuberculosis* human co-evolution still awaits testing under carefully controlled conditions.

M. bovis Bacille Calmette-Guerin (BCG) strains are phylogenetic descendants of an ancestral BCG stock originally derived from virulent *M. bovis* through *in vitro* propagation [15,16,17]. Attenuation of the original BCG stock occurred as a result of deletions in the *M. bovis* genome, specifically the region of difference 1 (RD1) [18,19]. Loss of RD1 is common across all BCG strains, although additional genetic alterations have been identified for each strain. BCG Russia and BCG Pasteur are among the most phylogenetically distant BCG strains [15].

Author Summary

Susceptibility to mycobacterial infection results from a complex interaction between host and bacterial genetic factors. To examine the effect of host and pathogen genetic variability on the control of mycobacterial infection, we infected a panel of genetically related recombinant congenic (RC) mouse strains with two closely related strains of *Mycobacterium bovis* BCG. Bacterial counts of BCG Russia and BCG Pasteur were determined in the lung and spleen at 1 and 6 weeks following infection and used for genetic analysis. A novel analytical approach was developed to perform genome-wide linkage analyses using the RC strains. Comparative linkage analysis using this model identified a strong genetic effect on chromosome 1 controlling counts of BCG Pasteur at 1 week and of BCG Russia at 1 week and 6 weeks in the spleen. A locus impacting on late BCG Russia counts in the lung and spleen was identified on chromosome 11. Nine additional loci were shown to control bacterial counts in a tissue-, time-, and BCG strain-specific manner. Our findings suggest that the host genetic control of mycobacterial infection is highly dynamic and adapted to the stage of pathogenesis and to the infecting strain. Such a high degree of genetic plasticity in the host-pathogen interplay is expected to favour evolutionary co-adaptation in mycobacterial disease.

Genetic events identified in BCG Russia include the deletion of RD Russia (Rv3698) [20], an insertion mutation in the *recA* gene (recA_D140*) [21], and the presence of an IS*6110* element in the promoter region of the *phoP* gene [15,22]. BCG Pasteur is characterized by the loss of RD2, nRD18, and RD14 [23,24,25] as well as a number of single point mutations and duplication events [22,23,26,27]. Phenotypic differences between BCG Pasteur and BCG Russia can therefore be tentatively linked to these known changes in gene content and an unknown number of point mutations. A number of unresolved questions surround the BCG host interplay which is characterized by highly variable host responsiveness. For example, the immunogenicity of the same strain of BCG given to vaccinees of different genetic background can vary tremendously [28,29] while host responses triggered by different strains of BCG are equally divergent [30]. On a population scale, BCG strains differ in the adverse reactions they trigger [31] and there is evidence that the protective effect of BCG vaccination against tuberculosis meningitis varies among ethnically divergent population groups [32]. Taken together, these data suggest that, similar to tuberculosis susceptibility, host responsiveness may reflect specific host-BCG strain interactions. To test this possibility, we compared the genetic control of closely related strains of BCG in a mouse model of infection.

Recombinant congenic (RC) strains are a set of genetically related inbred strains. In RC strains, discrete chromosomal segments of donor genome (12.5%) are transferred onto a recipient genetic background (87.5%) through a double backcross and corresponding strains are derived by subsequent inbreeding [33]. The AcB/BcA panel used in the present study was derived from a reciprocal double backcross between C57BL/6J and A/J [34], two mouse strains known to differ in their susceptibility to *M. bovis* BCG strain Montreal [35]. Each RC strain is genetically distinct with its own unique genome. The genomes of all RC strains have been mapped extensively and represent frozen replicas of recombinant progenitor genomes with known genomic boundaries of chromosomal segments derived from the two progenitor strains. A major advantage of RC strains over conventional crosses is that any phenotype can be measured repeatedly in genetically identical mice of a RC strain, greatly improving the accuracy of the phenotypic estimates.

In the present study, 35 distinct AcB/BcA strains were infected with a low dose of either BCG Pasteur or BCG Russia. A genetic analysis of the bacillary counts in the spleen and lungs of these strains identified general, as well as tissue- and BCG strain-specific susceptibility loci for BCG infection. These results demonstrated that the host response to mycobacteria reflects a genetically controlled, joint effect of both host and pathogen. Our findings established strain specific effects of the host-mycobacteria interplay in the absence of selective pressure and, therefore, argue in favour of additional host-mycobacterial adaptation during the co-evolution of humans and mycobacteria.

Materials and Methods

Mice and ethics statement

A/J and C57BL/6J mice were purchased from the Jackson Laboratory (Bar Harbor, Maine). Thirty-five independent RC strains originally derived from a reciprocal double backcross between the A/J and C57BL/6J progenitors [34] were purchased from Emerillon Therapeutics Inc. (Montreal, Qc.). All mice were housed in the rodent facility of the Montreal General Hospital. Animal use protocols were approved by the Animal Care Committee of McGill University and are in direct accordance with the guidelines outlined by the Canadian Council on Animal Care.

Bacterial strains

Recombinant BCG Russia (ATCC 35740) and Pasteur (ATCC 35734), were transformed with pGH1, an integrating vector that inserts into the attB site of the mycobacterial genome and that combines a firefly luciferase lux gene cassette, an integrase [int] gene, a MOP promoter, and a hygromycin resistance [Hyg] gene [31]. The pGH1 vector allows for growth on antibiotic-containing media to reduce risk of contamination [36].

Infection of mice

BCG strains were grown on a rotating platform at 37°C in Middlebrook 7H9 medium (Difco Laboratories, Detroit, Mich.) containing 0.05% Tween 80 (Sigma-Aldrich, St. Louis, Mo.) and 10% albumin-dextrose-catalase (ADC) supplement (Becton Dickinson and Co., Sparks, Md.). At an optical density (OD_{600}) of 0.4 to 0.5, bacteria were diluted in phosphate buffered saline (PBS) to 10^5 colony forming units (CFU)/ml. Mice were injected intravenously with 10^3 to 10^4 CFU of BCG in 100 µL of PBS. Inoculum doses were confirmed by plating on Middlebrook 7H10 agar (Difco Laboratories, Detroit, Mich.) supplemented with oleic acid-albumin-dextrose-catalase (OADC) enrichment (Becton Dickinson and Co., Sparks, Md.).

BCG load in target organs

Infected mice were sacrificed by CO_2 inhalation after 1 and 6 weeks post-infection. Lungs and spleens were aseptically removed, placed in 0.025% Saponin-PBS, and homogenized mechanically using a Polytron PT 2100 homogenizer (Brinkman Instruments, Westbury, NY). Homogenates were serially diluted tenfold and plated on Middlebrook 7H10 agar supplemented with OADC enrichment and containing hygromycin B (Wisent Inc., St.-Bruno, Qc.). Bacterial enumeration was performed following a six-week incubation at 37°C. For BCG Pasteur infection, a total of 221 and 175 mice were used at the week 1 and 6 time points, respectively.

A total of 145 and 189 mice, respectively, were used at 1 and 6 weeks for BCG Russia infection.

Genotyping

Strains of the AcB/BcA panel were genotyped for 625 microsatellite markers spanning the entire genome with an average distance of 2.6 cM [34]. Based on Build 36.1 of Mouse Genome Informatics (MGI) Mouse Genome Database, six markers with reassigned positions were removed from the current analysis [37].

Statistical analysis

The first QTL model was the linear model

$$\mathbf{y} = \mathbf{Xb} + \mathbf{q}_m g_m + \mathbf{e}$$

where y represents a vector with the individual total count of bacteria ($\log_{10}$CFU); $\mathbf{q}_m$ is a vector with each entry being an indicator variable of the genotype BB at the marker position m with g_m being its associated effect (major gene effect); $\mathbf{X}$ is a matrix of fixed covariates (a constant and gender in our main model) and its corresponding parameter vector $\mathbf{b}$; $\mathbf{e}$ is a vector of independent and identically distributed random variables representing the error term with $E(\mathbf{e})=\mathbf{0}$ and $\mathrm{Var}(\mathbf{e})=s^2\mathbf{I}$. At each marker position m, M-estimates of the parameters and a t-statistic were computed. The genome-wide corrected p-values were obtained by bootstrap under the hypothesis that there is no major gene, i.e., re-sampling under the reduced model

$$\mathbf{y} = \mathbf{Xb} + \mathbf{e}$$

Mean confidence bounds at each marker were defined as twice the standard error around the marker's group mean without considering gender effect in the model.

In order to account for the genetic background, a second linear model of the form

$$\mathbf{y} = \mathbf{Xb} + \mathbf{Zu} + \mathbf{q}_m g_m + \mathbf{e}$$

was employed, i.e., our second model was the mixed model resulting from adding a random component, $\mathbf{Zu}$, to our original model, where $\mathbf{u}$ is a random vector associated to the genetic background of each RCS and $\mathbf{Z}$ is the design matrix associating the RCS effect to the phenotype $\mathbf{y}$. The assumptions for this model component were $\mathrm{E}(\mathbf{u})=\mathbf{0}$ and $\mathrm{Var}(\mathbf{u})=s_u^2\mathbf{G}$, with $s_u^2>0$ being an unknown constant and $\mathbf{G}$ a positive definite-matrix (in fact, a background correlation matrix which is a function of length of the segments identical by descent shared amongst strains) assumed to be known, although a genomic estimate of it was previously obtained. At each marker position m, iteratively, estimates of fixed effect parameters and the variance components were obtained under this model and a t-statistic of the same form as before was computed. The genome-wide corrected p-values were obtained by bootstrap under the hypothesis that there is no major gene, i.e., re-sampling under the reduced model

$$\mathbf{y}=\mathbf{Xb}+\mathbf{Zu}+\mathbf{e}.$$

More details of estimation and testing are given in Methods S1. Evidence was considered significant for linkage when single-point regression analysis at the markers was $P<0.01$.

Results

We determined the bacillary load of BCG strains Pasteur and Russia in the lungs and spleens of C57BL/6J and A/J mice following a low dose ($\sim 3\times10^3$ bacilli) intravenous injection of bacilli. Pulmonary counts of BCG Pasteur were below the limit of detectability (80 bacilli/lung) at weeks 1 and 6 post infection but showed a modest peak of approximately 100 bacilli/lung at week 3 (Figure 1). This suggested limited dispersion and growth of BCG Pasteur in the lungs. In addition, there was no detectable difference in the pulmonary load of BCG Pasteur between C57BL6/J and A/J mice. By contrast, we observed an increase of 1–1.5 log CFU in the spleens between weeks 1 and 3 post infection that was followed by a 1 log decrease at week 6. The splenic bacillary burden of BCG Pasteur was substantially higher in C57BL/6J mice at weeks 1 and 3. BCG Russia showed a constant increase of pulmonary CFU from week 1 to week 6. In the spleen, growth of BCG Russia lagged growth of Pasteur and did not show evidence for a peak at 3 weeks post infection, as was observed for Pasteur (Figure 1). Overall, the pattern of tissue CFU for BCG Pasteur strongly resembled the one described for BCG Montreal which has previously been shown to be under *Nramp1* control [35,38]. The kinetics of lung and spleen bacillary counts of BCG Russia were distinct from the previously described BCG growth patterns.

To investigate the genetic control of *in-vivo* growth of BCG Russia and BCG Pasteur, mice from a panel of 35 AcB/BcA RC strains were intravenously challenged with a low dose ($3–5\times10^3$ bacilli) of BCG Russia or BCG Pasteur. The number of colony forming units (CFU) in the spleen and lung was used as the phenotype for the genetic analysis. CFU were determined at 1 week and 6 weeks post infection since it is well established that at 3 weeks, the *Nramp1* gene dominates the host response to BCG Montreal [38], making it potentially more difficult to discern additional genetic control elements.

To best indicate the effect of genotype on CFU, all RCS were stratified according to genotype at each marker, i. e. AA for markers on chromosomal segments derived from A/J or BB for chromosomal segments derived from C57BL/6J. Mice of all RCS with a given genotype were then used to obtain the mean and 95% confidence interval of their pulmonary and splenic CFU. This presentation allowed to graphically depict the effect of both marker genotype and of the general strain background on CFU. Results for the spleen and lung for both BCG strains are presented in Figures 2 and 3. A clear impact of strain background on susceptibility to BCG in the spleen at 1 week post infection was evidenced by the larger bacillary counts in mice of the BB genotype across most chromosomes (Figure 2). The strong strain background effect on splenic CFU was resolved by 6 weeks post infection, particularly for BCG Pasteur where differences in splenic bacillary burden appeared negligible across all markers (Figure 2). By contrast, CFU differences in BCG Russia were observed for several small chromosomal segments possibly suggesting the presence of specific genetic loci (Figure 2). As in the parental strains, pulmonary burdens were at the limit of detectability at week 1 for both Russia and Pasteur, and week 6 for Pasteur. However, at the 6-week endpoint, preferential replication of BCG Russia was observed in mice bearing specific A/J-derived chromosomal segments, particularly at the distal portion of chromosome 11 (Figure 3).

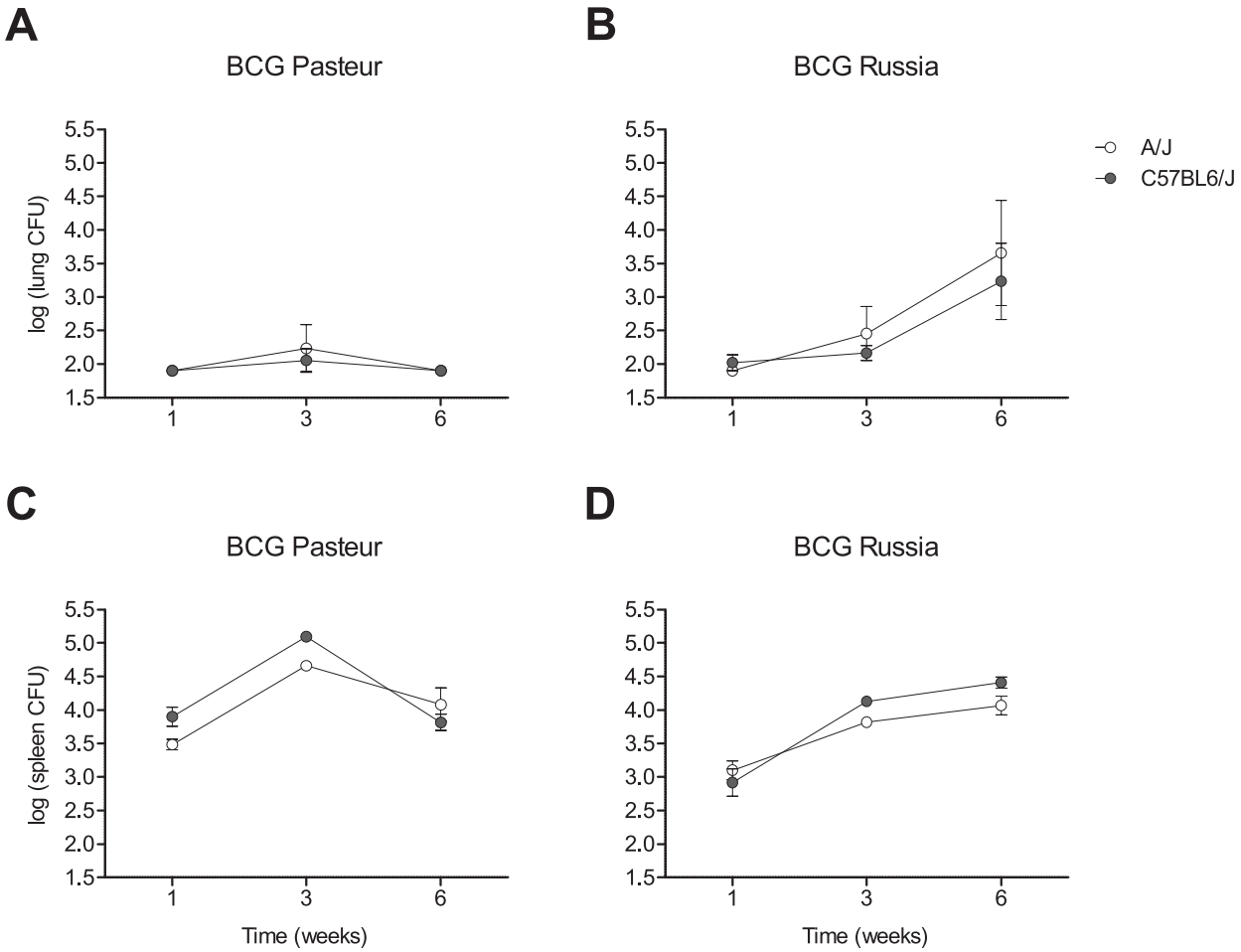

Figure 1. Replication of BCG in the lungs and spleen of A/J and C57BL/6J mice. A/J and C57BL/6J were intravenously infected with a low dose (3–5×10^3) of either BCG Pasteur (A, C) or BCG Russia (B, D). The number of CFU in the lungs (A, B) and spleen (C, D) was determined at 1, 3, and 6 weeks post-infection. Bacterial counts of BCG Pasteur and BCG Russia were compared in A/J and C57BL/6J mice by two-way ANOVA. Differences in the pulmonary counts of BCG Pasteur and BCG Russia between A/J and C57BL/6J failed to reach significance. However, there was a significant difference in the splenic loads of BCG Pasteur ($P<0.004$) and BCG Russia ($P<0.0001$) between the two strains of mice. These results are representative of at least two experiments. Four to 13 mice were used at each time-point. Data at each time point are the mean $\log_{10}$CFU and SD. White, A/J; grey, C57BL/6J.
doi:10.1371/journal.ppat.1001169.g001

Markers where the mean CFU of the AA and BB genotype groups diverged were indicative of chromosomal regions that potentially harboured a BCG susceptibility locus. To confirm the potential linkage of these chromosomal segments to bacterial burden, a genetic analysis comparing mice of the AA to BB genotype was performed. The initial analysis compared genotype groups without taking into account the genetic background of the strain or the gender of the mouse (incomplete model). As expected, markers significantly linked to bacterial burden corresponded well with chromosomal regions where the two genotypes differed (Figures 2 and 3; Figures S1 to S3). From this analysis, the genetic control of BCG Pasteur and Russia splenic infection appeared to be highly multigenic at the early time point. Employing a very stringent level of significance ($P<0.0003$), quantitative trait loci (QTL) were identified across 8 and 15 different chromosomes for BCG Pasteur and Russia, respectively (Figure S1). At the 6 week endpoint, a locus was identified on chromosome 1 for splenic BCG Russia load whereas genetic effects were not detected for BCG Pasteur load (Figure S2). Pulmonary CFU of BCG Russia was controlled by a locus on chromosome 11 while for BCG Pasteur a locus was identified on chromosome 8 (Figure S3).

Visual inspection of CFU across genotypes suggested a strong impact of strain background on bacillary loads. To account for the potential impact of background genes on linkage peaks, we developed a main model that accounted for the genetic background and gender of the mice. The number of loci identified by the main model was reduced relative to the incomplete model, particularly at the 1 week time point (Figures S4 and S5, and Table 1). For lung CFU, the locus on chromosome 11 remained that impacted on bacillary load of BCG Russia at 6 weeks post infection (Figure 4). No genetic effect was detected for pulmonary load of BCG Pasteur which is consistent with the very limited growth of BCG Pasteur in the lungs of all mice (data not shown).

In contrast to the lung, the genetic control of splenic bacillary load remained largely multigenic even after correction for strain background effects. For BCG Russia at 1 week post infection, a single locus on chromosome 1 (36.9 cM–48.8 cM) was found to control splenic load (Figure S4). At 6 weeks post infection, the genetic control of BCG Russia was multigenic (Figure S5). In

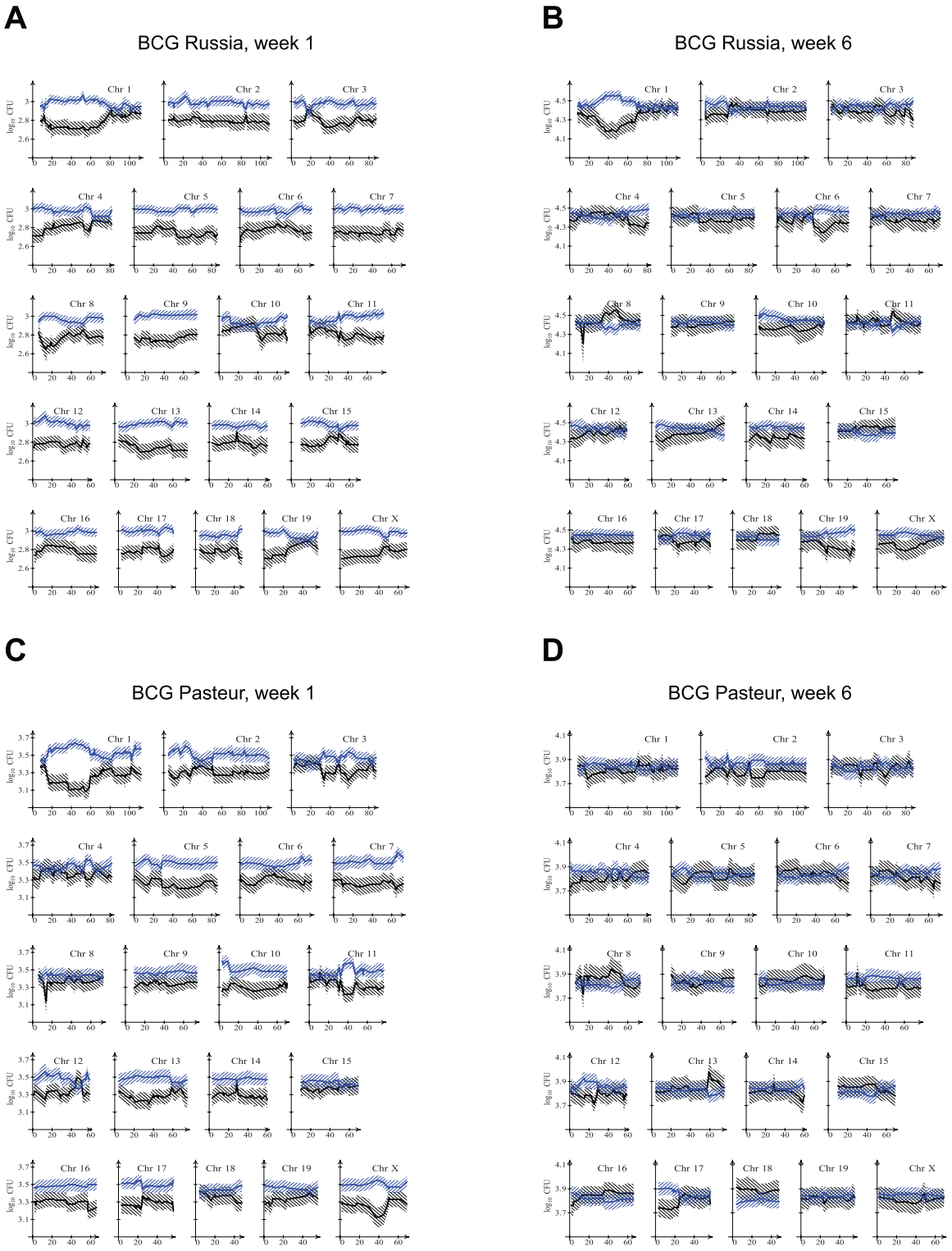

Figure 2. Spleen bacillary counts relative to A/J and C57BL/6J-derived chromosomal segments in RC mice. AcB and BcA mice were infected with BCG Russia (A, B) or BCG Pasteur (C, D) and spleen bacterial counts were determined at 1 week (A, C) and 6 weeks (B, D) post-infection. RC mice were stratified by genotype (AA in black or BB in blue) at each microsatellite marker and the mean $\log_{10}$CFU (solid line) as well as twice the standard error confidence bounds (hatched area) were determined for the two groups of mice. Gaps between the mean CFU of the AA and BB genotype are indicative of markers where the two groups differed. Chromosomal positions are given in centimorgans (cM).
doi:10.1371/journal.ppat.1001169.g002

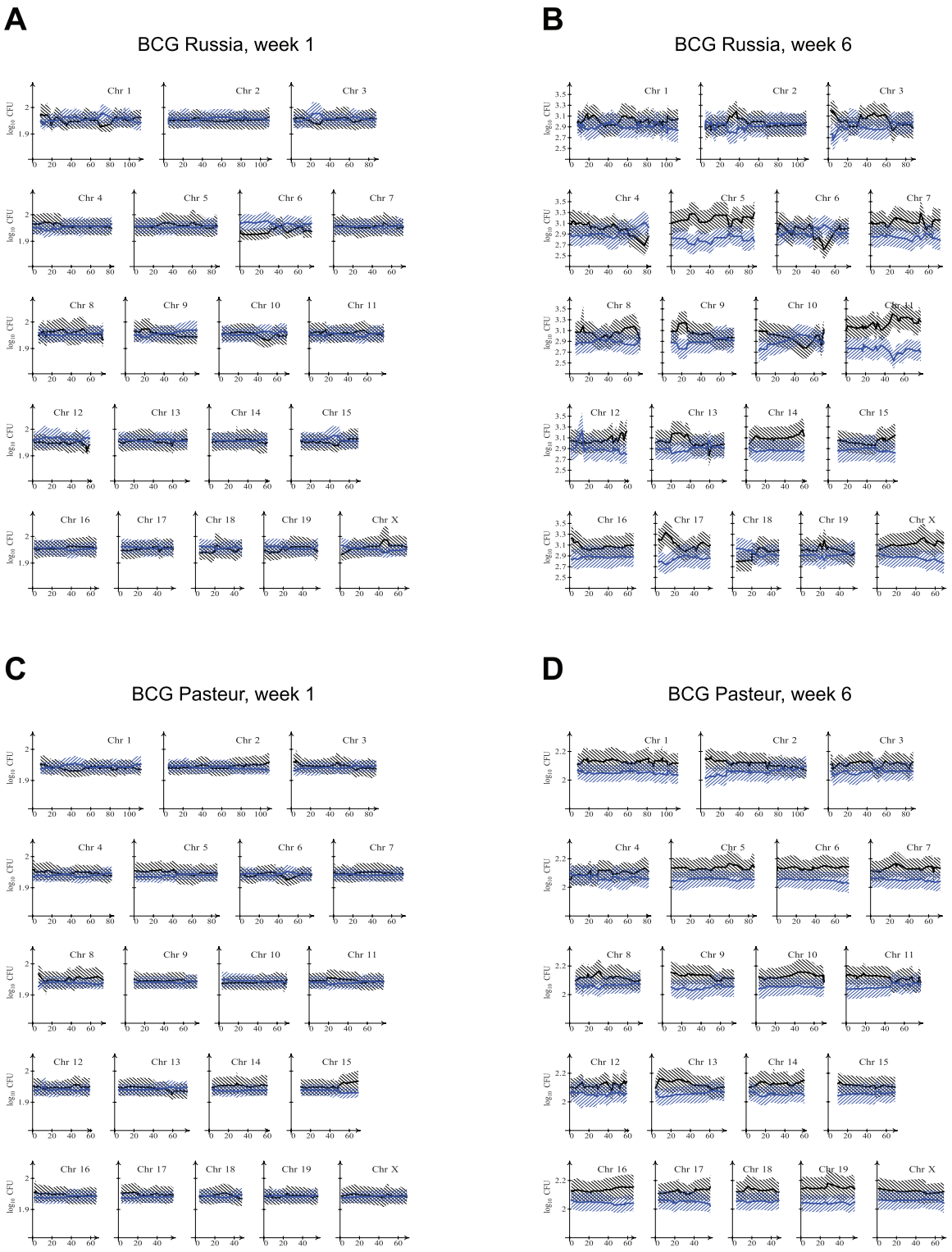

Figure 3. Lung bacillary counts relative to A/J and C57BL/6J-derived chromosomal segments in RC mice. Pulmonary bacterial loads in RC mice intravenously infected with BCG Russia (A, B) or BCG Pasteur (C, D) were determined at 1 week (A, C) and 6 weeks (B, D) post-infection. RC mice were stratified by genotype (AA in black or BB in blue) at each microsatellite marker and the mean $\log_{10}$CFU (solid line) and confidence bounds (hatched area) were determined for the two groups of mice. A divergence in the mean CFU of the AA and BB genotype groups represent chromosomal regions where the two groups differed. Chromosomal positions are given in centimorgans (cM).
doi:10.1371/journal.ppat.1001169.g003

Table 1. Summary of significant linkage peaks obtained using the main and conditional models.

Strain	Organ	Day	Main model	Conditional model
BCG Pasteur	Spleen	7	Chrs. 1, 2, 3, 6, 7, 10, 17, X	(Chr. 1)[a]
		42	-[b]	N/A
	Lung	7	-	N/A
		42	-	N/A
BCG Russia	Spleen	7	Chr. 1	(Chr. 1)
		42	Chrs. 1, 6, 11, 19	Chrs. (1), 11, 13
	Lung	7	-	N/A
		42	Chr. 11	N/A

Chr., chromosome; N/A, not applicable.
[a](Chr. 1), exclusion of markers on chromosome 1 to adjust for major genetic effect.
[b]-, no significant genetic effects detected.
doi:10.1371/journal.ppat.1001169.t001

addition to the chromosome 1 locus (32.8–55.1 cM), loci were detected on chromosome 6 (45.5–46.3 cM), chromosome 11 (47.67 cM) and chromosome 19 (51 cM). Splenic load of BCG Pasteur at 1 week post infection was controlled by loci on chromosome 2 (10–15 and 22.5–26.2 cM), chromosome 7 (63.5–65.6 cM) and the X chromosome (37–40.2 cM). Additional weaker effects were identified on chromosome 3 (33.7 and 58.8 cM), chromosome 6 (63.9 cM), chromosome 10 (3 cM), and chromosome 17 (23.2 cM). A major gene effect detected on chromosome 1 (17–58.5 cM) overlapped the chromosome 1 locus controlling BCG Russia infection (Figure S4, Table 1). Genetic control elements were not detected in response to BCG Pasteur infection at the 6 week time point (data not shown). The inverse complexity of BCG Pasteur (multigenic at 1 week; no genes at week 6) and BCG Russia (a single gene at week 1, multigenic at week 6) reflects differences in the replication pattern of the bacteria: BCG Russia showed a delayed onset of growth that continued at week 6 while BCG Pasteur showed rapid initial growth with a strong decline of CFU at week 6 as compared to week 3.

The chromosome 1 locus significant for linkage early during BCG Pasteur infection and at the early and late phase of BCG Russia infection was indistinguishable from *Nramp1*. Employing what we termed the "conditional model," we determined whether the additional linkage peaks were conditional on the *Nramp1* gene. For this the main model was modified to adjust for the effect of *Nramp1* by adding a column with the BB genotype indicator at the *Nramp1* position to the matrix $\mathbf{X}$. Chromosomal regions identified at the week 1 time point of both BCG Pasteur and BCG Russia infection were no longer significant for linkage following correction for the chromosome 1 locus (data not shown). Similarly, the genetic effects detected on chromosome 6 and 19 were no longer significant at the 6 week time point of BCG Russia infection. However, the linkage hit detected on chromosome 11 (47.67 cM) retained its significance. By contrast, a secondary peak detected only for splenic CFU immediately proximal to this locus did not reach significance (Figure 5). Finally, an additional locus was localized to chromosome 13 (73–75 cM) (Figure 5).

Discussion

RC strains are particularly useful to establish pathways of causality in complex read-outs such as immune reactivity and are well suited to track gene-gene interactions [33]. However, RC strains have also proven useful for positional identification of disease susceptibility loci by employing RC strains with extreme phenotypes in subsequent genetic crosses [39,40,41]. A third application of RC strains is the genome-wide identification of quantitative trait loci (QTL) in complex diseases. This feature of RC stains is particularly attractive since it allows the measurement

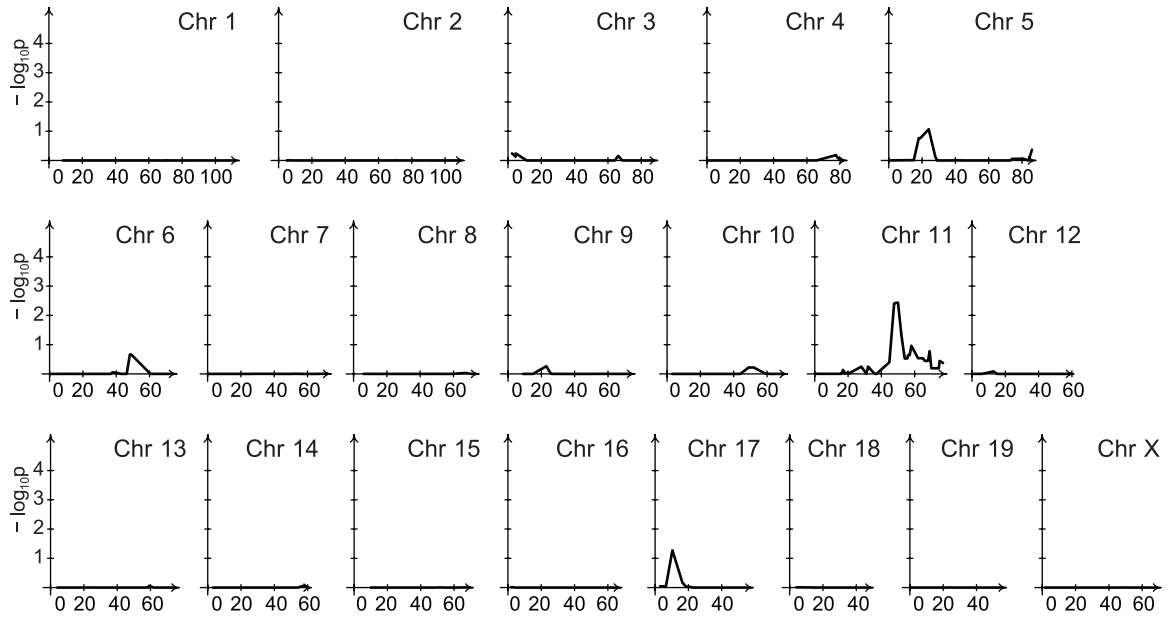

Figure 4. Genetic control of late pulmonary bacillary counts of BCG Russia. Linkage analysis of BCG Russia pulmonary counts at the 6-week time point was performed with background and gender-adjustment. A single locus controlling BCG Russia pulmonary counts was identified on chromosome 11. Chromosomal positions are given in centimorgans (cM).
doi:10.1371/journal.ppat.1001169.g004

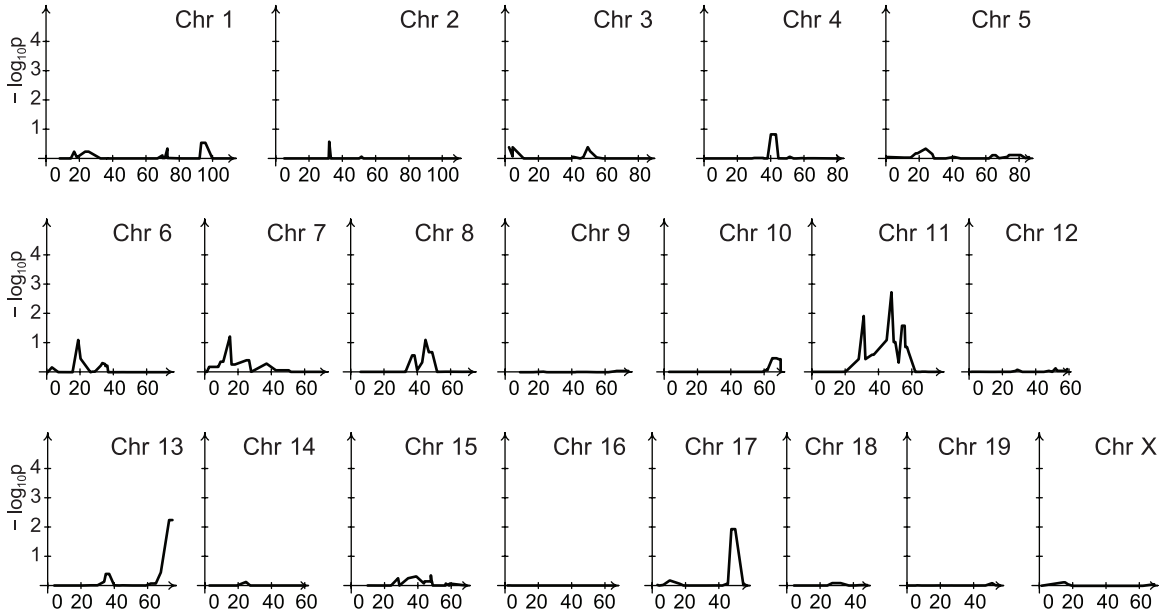

Figure 5. Linkage analysis of late spleen bacillary counts contingent on the chromosome 1 locus. Linkage analysis was performed with an adjustment for the locus on chromosome 1 which had a major effect on the splenic bacillary counts of BCG Russia at the 6-week time point. The loci identified on chromosomes 6 and 19 were conditional upon the chromosome 1 locus and lost their significance when adjusted. The genetic effect detected on chromosome 11 was independent of the chromosome 1 locus and maintained its significance. An additional locus was localized to chromosome 13. Chromosomal positions are given in centimorgans (cM).
doi:10.1371/journal.ppat.1001169.g005

of quantitative traits in many genetically identical mice belonging to the same strain which greatly increases the accuracy of trait determination. A genome-wide scan for the presence of QTL can then be conducted among the relatively limited number of RC strains in each panel. This is highly efficient compared to the breeding and genotyping of hundreds of mice in traditional backcross or F2 based genome-wide mapping studies. For example, a recent study used the AcB/BcA RC strain panel to localize a large number of asthma susceptibility loci across the genome [42]. A potential problem that is faced in these speedy genome-wide scans in RC strains is the confounding impact of strain background and of strong susceptibility loci on the overall pattern of QTLs mapped. We have developed a new analytical methodology that overcomes both of these potentially confounding limitations while conducting genome-wide QTL mapping in RC strains. Our results demonstrate the ease of genome-wide scanning in RC strains and the importance of adjusting especially on strain background to achieve reliable QTL identification.

Our ability to detect the *Nramp1* genomic region also served as an internal validation of the analytical approach. Another interesting observation was the loci that could only be detected in connection with *Nramp1*. Once the analysis was adjusted on the *Nramp1* gene, these loci were no longer significant for linkage. The most parsimonious explanation for this effect is that these loci are interacting with *Nramp1*. Why we would detect a large number of genes that interact with *Nramp1* in the genetic control of BCG Pasteur as compared to BCG Russia is not known but may reflect the differences in pathogenesis between the two BCG strains. For BCG Pasteur, putatively interacting genes were detected at 3 weeks post infection while for BCG Russia such interacting loci were observed at the 6 week time point. At 3 weeks, BCG Pasteur shows a sharp peak of splenic bacillary burden while the growth of BCG Russia continues well past 6 weeks before a slow and gradual reduction of splenic burden becomes evident after 12 weeks of infection (data not shown). While the interpretation of our results as *Nramp1* interacting loci appears reasonable, it is important to realize that this conclusion needs further direct experimental validation. However, if correct, the mapping tools presented in this paper would provide a very powerful approach for the identification of interacting loci which is still a major obstacle in complex trait analysis in both human and model animals.

The study of the impact of strain variability of *M tuberculosis* on disease expression is of considerable interest for the implementation of tuberculosis control measures. An increasing body of evidence suggests that different strains/lineages of *M. tuberculosis* display substantial differences in their pathogenic potential [8,9]. In addition, evidence is emerging that genetic variability among BCG vaccine strains is a potent factor in modulating BCG induced anti-tuberculosis immunity [31]. This mycobacterial strain variability reflects an even greater divergence in host responsiveness to both BCG and *M. tuberculosis* that is largely under host genetic control (reviewed in [43]). These observations raise the question if host and mycobacterial variability are independent of each other. If independent, we would expect hosts to display a spectrum of responsiveness from highly resistant to highly susceptible irrespective of the infecting mycobacterial strain. Similarly, *M. tuberculosis* strains would vary from highly virulent to mildly virulent across all hosts. Alternatively, it is possible that "susceptibility" and "virulence" are not absolute but rather reflect specific combinations of mycobacterial strain and human host. The latter possibility is supported by recent observations of preferential associations of tuberculosis lineages with ethnic groups that may reflect co-adaptation of *M. tuberculosis* and its human host [10]. Moreover, a number of host genetic association studies have reported a preferential association of tuberculosis susceptibility variants with specific *M. tuberculosis* lineages [12,13,14]. The results of our study obtained in a highly controlled experimental setting support the hypothesis of host – pathogen specific genetic "fits." Hence,

human susceptibility to tuberculosis may only become tractable by jointly considering host and pathogen genetic backgrounds.

By conducting a genome-wide mapping of loci that impact on the splenic and pulmonary burden following a low dose infection with two strains of BCG, we revealed a divergent pattern of susceptibility loci. An unexpected result was the pronounced dynamic of genetic loci impacting on bacillary counts. This observation demonstrated how different genetic control elements came into play as the BCG infection advanced and further emphasized the intimate interplay between host genetics and pathogenesis. Perhaps less surprising was the large difference in the number of loci involved in the control of splenic vs pulmonary bacillary counts. BCG Pasteur shows little dissemination and growth in the lungs of infected mice and the absence of susceptibility loci was therefore expected. However, BCG Russia reaches bacillary counts in the lungs that are similar to those in the spleen. Yet, only one susceptibility locus on chromosome 11 was detected to impact on pulmonary counts while splenic counts are under more complex control. It is interesting that a locus on chromosome 1 which is indistinguishable from the *Nramp1* gene had by far the strongest impact on bacillary burden in both BCG Pasteur and Russia, but this effect was limited to splenic counts. By contrast, the chromosome 11 locus was detected only for BCG Russia but in both the spleens and lungs. The results therefore indicate that host genetic control is characterized by very strong common control elements that act in a tissue –specific manner, and by somewhat weaker BCG strain specific susceptibility genes that are not tissue specific. Together these data indicate that host genetic control of mycobacterial replication is sensitive to the particular strains but also to differences in disease manifestations (here, lung vs spleen). Interestingly, the strongest genetic effect ever found in human studies was found in an outbreak of tuberculosis in Northern Canada [44]. During this outbreak, all cases had been infected from a single index case, i.e. a single bacterial strain [45]. A fine tuned host genetic response to mycobacteria might explain why it has been difficult to reproducibly detect strong host genetic effects in human tuberculosis. Consequently, future genetic studies of tuberculosis susceptibility might need to be adjusted on the detailed clinical picture and infecting *M. tuberculosi*s strain.

Supporting Information

Methods S1 Details of estimation, bootstrap and testing.
Found at: doi:10.1371/journal.ppat.1001169.s001 (0.05 MB PDF)

Figure S1 Linkage analysis of early splenic counts independent of the genetic background. Bacillary counts of BCG Russia and BCG Pasteur in the spleen of RC mice at the week 1 time point were used for QTL analysis. AA and BB genotype groups were analyzed without taking into account the gender or genetic background of the RC mice. Significant evidence for linkage was detected across 15 different chromosomes for BCG Russia (A) and across 8 different chromosomes for BCG Pasteur (B) at the week 1 time point. Chromosomal positions are given in centimorgans (cM).
Found at: doi:10.1371/journal.ppat.1001169.s002 (1.83 MB TIF)

Figure S2 Linkage analysis of late splenic counts independent of the genetic background. Bacterial numbers of BCG Russia and BCG Pasteur in the spleen of RC mice at the week 6 time point were used for linkage analysis. Significant linkages were detected on chromosomes 1 and 19 for BCG Russia (A) whereas no significant evidence for linkage was detected for BCG Pasteur (B). Chromosomal positions are given in centimorgans (cM).
Found at: doi:10.1371/journal.ppat.1001169.s003 (1.59 MB TIF)

Figure S3 Linkage analysis of late pulmonary counts independent of the genetic background. QTL analysis was performed using pulmonary counts of BCG Russia and BCG Pasteur at the week 6 time point. Loci controlling pulmonary bacterial numbers were identified on chromosome 11 for BCG Russia (A) and chromosome 8 for BCG Pasteur (B). Chromosomal positions are given in centimorgans (cM).
Found at: doi:10.1371/journal.ppat.1001169.s004 (1.61 MB TIF)

Figure S4 Genetic control of early spleen bacillary counts of BCG Russia and BCG Pasteur. Linkage analysis of splenic bacterial counts at the week 1 time point was performed with an adjustment for strain genetic background and gender. A single locus on chromosome 1 was identified in response to early BCG Russia infection (A). Loci linked to splenic BCG Pasteur counts were detected on chromosomes 1, 2, 3, 6, 7, 10, 17 and X at the week 1 time point (B). Chromosomal positions are given in centimorgans (cM).
Found at: doi:10.1371/journal.ppat.1001169.s005 (1.69 MB TIF)

Figure S5 Genetic control of late spleen bacillary counts following infection of the RC strains with BCG Russia. Background- and gender-adjusted QTL analysis was performed using spleen counts of BCG Russia at the 6-week endpoint. A locus on chromosome 1 had a major effect on the bacterial numbers of BCG Russia. Additional loci were detected on chromosomes 6, 11, and 19. Chromosomal positions are given in centimorgans (cM).
Found at: doi:10.1371/journal.ppat.1001169.s006 (0.73 MB TIF)

Acknowledgments

We thank Dr. Kenneth Morgan for helpful advice. The RCS genotypes were kindly provided by Emerillon Therapeutics. E.S. is a Chercheur National du Fonds de la Recherche en Santé du Québec and an International Research Scholar of the Howard Hughes Medical Institute.

Author Contributions

Conceived and designed the experiments: TDP JCLO ES. Performed the experiments: TDP MG AV MO. Analyzed the data: TDP CH JCLO ES. Contributed reagents/materials/analysis tools: AB MAB. Wrote the paper: TDP JCLO ES.

References

1. Ng VH, Cox JS, Sousa AO, MacMicking JD, McKinney JD (2004) Role of KatG catalase-peroxidase in mycobacterial pathogenesis: countering the phagocyte oxidative burst. Mol Microbiol 52: 1291–1302.
2. Darwin KH, Ehrt S, Gutierrez-Ramos JC, Weich N, Nathan CF (2003) The proteasome of *Mycobacterium tuberculosis* is required for resistance to nitric oxide. Science 302: 1963–1966.
3. Tobin DM, Vary JC, Jr., Ray JP, Walsh GS, Dunstan SJ, et al. (2010) The *lta4h* locus modulates susceptibility to mycobacterial infection in zebrafish and humans. Cell 140: 717–730.
4. Divangahi M, Chen M, Gan H, Desjardins D, Hickman TT, et al. (2009) *Mycobacterium tuberculosis* evades macrophage defenses by inhibiting plasma membrane repair. Nat Immunol 10: 899–906.
5. Gan H, Lee J, Ren F, Chen M, Kornfeld H, et al. (2008) *Mycobacterium tuberculosis* blocks crosslinking of annexin-1 and apoptotic envelope formation on infected macrophages to maintain virulence. Nat Immunol 9: 1189–1197.
6. Chen M, Divangahi M, Gan H, Shin DS, Hong S, et al. (2008) Lipid mediators in innate immunity against tuberculosis: opposing roles of PGE2 and LXA4 in the induction of macrophage death. J Exp Med 205: 2791–2801.
7. Behr M, Schurr E, Gros P (2010) TB: screening for responses to a vile visitor. Cell 140: 615–618.
8. Gagneux S, Small PM (2007) Global phylogeography of *Mycobacterium tuberculosis* and implications for tuberculosis product development. Lancet Infect Dis 7: 328–337.
9. Nicol MP, Wilkinson RJ (2008) The clinical consequences of strain diversity in *Mycobacterium tuberculosis*. Trans R Soc Trop Med Hyg 102: 955–965.

10. Gagneux S, DeRiemer K, Van T, Kato-Maeda M, de Jong BC, et al. (2006) Variable host-pathogen compatibility in *Mycobacterium tuberculosis*. Proc Natl Acad Sci U S A 103: 2869–2873.
11. Reed MB, Pichler VK, McIntosh F, Mattia A, Fallow A, et al. (2009) Major *Mycobacterium tuberculosis* lineages associate with patient country of origin. J Clin Microbiol 47: 1119–1128.
12. Caws M, Thwaites G, Dunstan S, Hawn TR, Lan NT, et al. (2008) The influence of host and bacterial genotype on the development of disseminated disease with *Mycobacterium tuberculosis*. PLoS Pathog 4: e1000034.
13. Herb F, Thye T, Niemann S, Browne EN, Chinbuah MA, et al. (2008) *ALOX5* variants associated with susceptibility to human pulmonary tuberculosis. Hum Mol Genet 17: 1052–1060.
14. Intemann CD, Thye T, Niemann S, Browne EN, Amanua Chinbuah M, et al. (2009) Autophagy gene variant *IRGM* -261T contributes to protection from tuberculosis caused by *Mycobacterium tuberculosis* but not by *M. africanum* strains. PLoS Pathog 5: e1000577.
15. Behr MA, Small PM (1999) A historical and molecular phylogeny of BCG strains. Vaccine 17: 915–922.
16. Calmette A, Guérin C, Breton M (1907) Contribution à l'étude de la tuberculose expérimentale du cobaye. Ann Inst Pasteur. pp 401–416.
17. Oettinger T, Jorgensen M, Ladefoged A, Haslov K, Andersen P (1999) Development of the *Mycobacterium bovis* BCG vaccine: review of the historical and biochemical evidence for a genealogical tree. Tuber Lung Dis 79: 243–250.
18. Lewis KN, Liao R, Guinn KM, Hickey MJ, Smith S, et al. (2003) Deletion of RD1 from *Mycobacterium tuberculosis* mimics bacille Calmette-Guerin attenuation. J Infect Dis 187: 117–123.
19. Pym AS, Brodin P, Brosch R, Huerre M, Cole ST (2002) Loss of RD1 contributed to the attenuation of the live tuberculosis vaccines *Mycobacterium bovis* BCG and *Mycobacterium microti*. Mol Microbiol 46: 709–717.
20. Mostowy S, Tsolaki AG, Small PM, Behr MA (2003) The in vitro evolution of BCG vaccines. Vaccine 21: 4270–4274.
21. Keller PM, Bottger EC, Sander P (2008) Tuberculosis vaccine strain *Mycobacterium bovis* BCG Russia is a natural *recA* mutant. BMC Microbiol 8: 120.
22. Brosch R, Gordon SV, Garnier T, Eiglmeier K, Frigui W, et al. (2007) Genome plasticity of BCG and impact on vaccine efficacy. Proc Natl Acad Sci U S A 104: 5596–5601.
23. Behr MA, Schroeder BG, Brinkman JN, Slayden RA, Barry CE, 3rd (2000) A point mutation in the *mma3* gene is responsible for impaired methoxymycolic acid production in *Mycobacterium bovis* BCG strains obtained after 1927. J Bacteriol 182: 3394–3399.
24. Mahairas GG, Sabo PJ, Hickey MJ, Singh DC, Stover CK (1996) Molecular analysis of genetic differences between *Mycobacterium bovis* BCG and virulent *M. bovis*. J Bacteriol 178: 1274–1282.
25. Salamon H, Kato-Maeda M, Small PM, Drenkow J, Gingeras TR (2000) Detection of deleted genomic DNA using a semiautomated computational analysis of GeneChip data. Genome Res 10: 2044–2054.
26. Charlet D, Mostowy S, Alexander D, Sit L, Wiker HG, et al. (2005) Reduced expression of antigenic proteins MPB70 and MPB83 in *Mycobacterium bovis* BCG strains due to a start codon mutation in *sigK*. Mol Microbiol 56: 1302–1313.
27. Spreadbury CL, Pallen MJ, Overton T, Behr MA, Mostowy S, et al. (2005) Point mutations in the DNA- and cNMP-binding domains of the homologue of the cAMP receptor protein (CRP) in *Mycobacterium bovis* BCG: implications for the inactivation of a global regulator and strain attenuation. Microbiology 151: 547–556.
28. Black GF, Weir RE, Floyd S, Bliss L, Warndorff DK, et al. (2002) BCG-induced increase in interferon-gamma response to mycobacterial antigens and efficacy of BCG vaccination in Malawi and the UK: two randomised controlled studies. Lancet 359: 1393–1401.
29. Lalor MK, Ben-Smith A, Gorak-Stolinska P, Weir RE, Floyd S, et al. (2009) Population Differences in Immune Responses to Bacille Calmette-Guerin Vaccination in Infancy. J Infect Dis 199: 795–800.
30. Wu B, Huang C, Garcia L, Ponce de Leon A, Osornio JS, et al. (2007) Unique gene expression profiles in infants vaccinated with different strains of *Mycobacterium bovis* bacille Calmette-Guerin. Infect Immun 75: 3658–3664.
31. Liu J, Tran V, Leung AS, Alexander DC, Zhu B (2009) BCG vaccines: their mechanisms of attenuation and impact on safety and protective efficacy. Hum Vaccin 5: 70–78.
32. Trunz BB, Fine P, Dye C (2006) Effect of BCG vaccination on childhood tuberculous meningitis and miliary tuberculosis worldwide: a meta-analysis and assessment of cost-effectiveness. Lancet 367: 1173–1180.
33. Demant P, Hart AA (1986) Recombinant congenic strains—a new tool for analyzing genetic traits determined by more than one gene. Immunogenetics 24: 416–422.
34. Fortin A, Diez E, Rochefort D, Laroche L, Malo D, et al. (2001) Recombinant congenic strains derived from A/J and C57BL/6J: a tool for genetic dissection of complex traits. Genomics 74: 21–35.
35. Gros P, Skamene E, Forget A (1981) Genetic control of natural resistance to *Mycobacterium bovis* (BCG) in mice. J Immunol 127: 2417–2421.
36. Belley A, Alexander D, Di Pietrantonio T, Girard M, Jones J, et al. (2004) Impact of methoxymycolic acid production by *Mycobacterium bovis* BCG vaccines. Infect Immun 72: 2803–2809.
37. Mouse Genome Database (MGD) at the Mouse Genome Informatics website TJL, Bar Harbor, Maine.
38. Vidal SM, Malo D, Vogan K, Skamene E, Gros P (1993) Natural resistance to infection with intracellular parasites: isolation of a candidate for *Bcg*. Cell 73: 469–485.
39. Mullerova J, Hozak P (2004) Use of recombinant congenic strains in mapping disease-modifying genes. News Physiol Sci 19: 105–109.
40. Min-Oo G, Fortin A, Tam MF, Nantel A, Stevenson MM, et al. (2003) Pyruvate kinase deficiency in mice protects against malaria. Nat Genet 35: 357–362.
41. Roy MF, Riendeau N, Bedard C, Helie P, Min-Oo G, et al. (2007) Pyruvate kinase deficiency confers susceptibility to *Salmonella typhimurium* infection in mice. J Exp Med 204: 2949–2961.
42. Camateros P, Marino R, Fortin A, Martin JG, Skamene E, et al. (2010) Identification of novel chromosomal regions associated with airway hyperresponsiveness in recombinant congenic strains of mice. Mamm Genome 21: 28–38.
43. Schurr E, Kramnik I (2008) Genetic control of host susceptibility to tuberculosis. In: Kaufmann S, Britten W, eds. Handbook of Tuberculosis. Weinheim, Germany: Wiley-VCH. pp 305–346.
44. Greenwood CM, Fujiwara TM, Boothroyd LJ, Miller MA, Frappier D, et al. (2000) Linkage of tuberculosis to chromosome 2q35 loci, including *NRAMP1*, in a large aboriginal Canadian family. Am J Hum Genet 67: 405–416.
45. Schurr E (2007) Is susceptibility to tuberculosis acquired or inherited? J Intern Med 261: 106–111.